Title
Regulation of T cell activation and proliferation through cell-intrinsic cytoskeletal elements and cell-extrinsic cellular interactions

Author
Mujal, Adriana

Publication Date
2017

Peer reviewed|Thesis/dissertation

Regulation of T cell activation and proliferation through cell-intrinsic cytoskeletal elements and cell-extrinsic cellular interactions

by

Adriana M. Mujal

DISSERTATION

Submitted in partial satisfaction of the requirements for the degree of

DOCTOR OF PHILOSOPHY

in

Biomedical Sciences

in the

[redacted]

ACKNOWLEDGEMENTS

The work presented here is a product of the guidance and mentorship I was fortunate to receive in Max Krummel's lab. Working with Max has been an inspiring and rewarding training experience, and I have especially appreciated and grown from the atmosphere of excitement, creativity, curiosity, and rigor that Max has instilled within the lab's culture. I would like to also acknowledge lab members Audrey Gerard, Mark Headley, Edward Roberts, Mikhail Binnewies, and collaborator Josh Pollack for sharing their time and expertise, and would like to recognize their contributions both to the projects put forth here and my development as a scientist. Lastly, my thesis committee comprised of Art Weiss, Jason Cyster, and Mark Anderson has brought valuable feedback and direction as I completed this thesis work and graduate school here at UCSF.

The text and figures within Chapter 3 are adapted from Mujal AM, Gilden JK, Gerard A, Kinoshita M, Krummel MF. A septin requirement differentiates autonomous and contact-facilitated T cell proliferation. *Nat Immunol* **17,** 315-22 (2016). The text and figures within Chapter 5 were done in collaboration with Mikhail Binnewies and Josh Pollack with supervision by Max Krummel. Mikhail Binnewies contributed toward experimental design and execution. Josh Pollack computationally processed the single-cell RNA sequencing data and assisted with downstream analysis.

Regulation of T cell activation and proliferation through cell-intrinsic cytoskeletal elements and cell-extrinsic cellular interactions

Adriana Marie Mujal

ABSTRACT

An efficacious immune response requires both rapid clonal expansion of activated T cells and homeostatic turnover to maintain the T cell compartment. These various proliferative processes are driven by different stimuli such as T cell receptor signaling or cytokines that act independently or synergistically. Although it has been thought that these distinct cues result in similar use of cellular machinery to undergo cell division, we found that $CD8^+$ T cell division selectively requires the septin cytoskeleton depending on the stimulus condition. Septin-deficient $CD8^+$ T cells undergo robust proliferation when activated by antigen-presenting cells (APCs) that provide co-stimulatory PI3K signaling, but these T cells exhibit cytokinetic failure following cytokine-driven division. This differential requirement for septins reveals previously unrecognized complexity of T cell proliferation with the potential for therapeutic modulation of context-specific T cell expansion.

As specialized APCs, dendritic cells (DCs) play a central role in initiating and guiding antigen-specific T cells responses. For example, in the setting of cancer, a pro-stimulatory $CD103^+$ DC population has been identified as required for driving effector $CD8^+$ T cell activity. In addition to targeting $CD8^+$ T cells, therapeutic modulation of effector $CD4^+$ T cells may too have clinical benefit in augmenting anti-tumor responses. It has been unclear, however, which myeloid population is predominantly involved in initial priming of $CD4^+$ T cells. To address this diversity in DC populations that participate in anti-tumor responses, we have employed single-cell RNA-sequencing to investigate the heterogeneity present in the lymph node (LN) myeloid compartment and to better understand the migratory DC populations that traffic from the tumor

to the local draining LN. From this, we have used a combination of *in vivo* and *in vitro* assays to identify multiple tumor-antigen bearing $CD11b^{+}$ DCs subsets in the lymph nodes that can contribute to anti-tumor T cell response.

TABLE OF CONTENTS

LIST OF FIGURES

INTRODUCTION

I. INTERFACE BETWEEN INNATE AND ADAPTIVE IMMUNITY

The immune system relies on adaptive antigen-specific immune cells to coordinate responses that attack and eliminate foreign entities (e.g. pathogens) while preserving non-threatening self-expressing cells (e.g. host tissue cells). Burnet's original theory of clonal selection posited the role for antigen-specific lymphocytes that could be triggered to expand in a clonal fashion[1]. This model was first centered on antibody-producing B cells, but was later extended to T cells, and here we will focus exclusively on the T cell arm of the adaptive immune system. T cells ultimately posses the potential to directly lyse and kill other target cells and regulation of T cell activation must fundamentally balance the need for antigen-specific protection and the danger of off-target autoimmunity. Initiation of T cell activation thus requires a series of sequential biological processes summarized below, with the collective T cell response resulting from the integration of multicellular and environmental cues.

In brief, rearrangement of the variable domains of a given cellular clone's T cell receptor (TCR) endows lymphocytes with antigen-specific recognition and these receptor permutations allow for a polyclonal repertoire that equips the immune system with broad coverage and versatility in responding to unknown antigens that have not yet been introduced to the host system[2]. Positive and negative selection processes against self-antigens in thymus generates a polyclonal repertoire of mature $CD8^+$ and $CD4^+$ T cells that are both self-MHC restricted and responsive to foreign antigen[3]. These naïve T cells home to peripheral secondary lymphoid organs (SLO) such as the lymph node (LN) or the spleen. Upon entry in a SLO, T cells localize to the T cell zone through expression of CCR7[4] where they receive survival factors like IL-7 and tonic TCR signaling through self-peptide-MHC (-pMHC)[5]. These processes maintain a diverse set of quiescent T cells that is critical to both ensure immunological readiness against pathogens or tumor outgrowths and to protect the host against spontaneous autoimmunity.

Triggering of T cell immunity is controlled by the innate immune system, and this relationship allows for cellular communication regarding the nature and magnitude of the immunological challenge and results in a tailored and systemic response distal to the insulted tissue. Antigen-specific T cell activation is typically initiated by dendritic cells (DCs) of the myeloid lineage, which were first identified by Ralph Steinman based on their morphology[6]. This cell population was soon demonstrated as superior in stimulating T cells and supporting cytotoxic T lymphocyte (CTL) development in mixed leukocyte reactions (MLRs) *in vitro*[7,8]. In support of this critical role in T cell activation, depletion of DCs with a *Cd11c*-DTR model abrogated $CD8^+$ T cell priming in settings of bacterial and parasitic infections[9]. While this model results in broad ablation of *Cd11c*-expressing non-DC myeloid cells such as macrophages, more restricted depletion of DCs with *Zbtb46*-DTR mice again affirmed their key role in T cell priming[10,11]. Notably, DCs express both MHC-I and MHC-II and initiate T cell responses through TCR binding to cognate pMHC. Although DCs express both MHC-I and MHC-II, different DC subset populations specialize in guiding $CD8^+$ or $CD4^+$ T cell activation and coordination likely allows for refined tuning of cellular immunity[12,13].

As a critical link between innate and adaptive immunity, DCs are considered 'professional' APCs and process antigen to optimize for later loading on MHC molecules through multiple pathways[14]. As reviewed previously[15], endogenous or viral cytosolic proteins in the DC are targeted to the proteasome for degradation and shuttled into the ER via the transporter TAP for loading onto MHC-I loading. Secretory proteins can also feed into this process through retrotranslocation from the ER to cytosolic processing by the proteasome. In addition, exogenous proteins can be processed in certain DC subsets for cross-presentation whereby antigen is transported from a phagosome to the cytosol through the translocon protein Sec61 and reimported into endosomes or the ER for MHC-I binding[16]. This process allows for antigen presentation of exogenous antigens to $CD8^+$ T cells, which is especially critical during an ongoing viral or cancer response. Exogenous peptides that have been endocytosed are

similarly loaded on MHC-II, as are endogenous peptides processed within the endosomal network[17]. In addition, autophagy can shuttle cytosolic and extracellular antigens into lysosomes, which can enable loading on MHC-II, and may be especially relevant for viral responses and immune tolerance[18,19].

These antigen presentation pathways are in place to present both foreign- and self-peptides. Several models have thus been put forth to explain how the immune system discerns between the two. DCs express a number of pathogen recognition receptors (PRRs) that bind to pathogen associated molecular patterns (PAMPs) that are specific to foreign pathogens and not host cells. Charles Janeway proposed that these receptors signal the presence of pathogens and prompt DCs into action[20]. This model was later extended by Polly Matzinger to include damage associate molecular patterns (DAMPs), or signals generated from tissue damage and immunogenic cell death, as similarly stimulatory to DCs[21]. Indeed some of these DAMPs can signal through shared receptors as PAMPs. Although these models are not complete, they have served as a compelling framework for conceptualizing recognition of general tissue infection or damage. In these prototypical scenarios that pertain to a tissue or organ, ligation of surface or cytosolic PRRs triggers maturation of tissue-resident DCs. These activated DCs subsequently up-regulate CCR7 to migrate from peripheral tissue to draining LNs[22]. While immature DCs are relatively static in steady-state dermis, they become highly motile with activation and migrate toward lymphatic vessels where immobilized CCL21 has been observed at the basement membrane[23].

Upon arrival in the LN, DCs enter the subcapsular sinus region and descend along a CCL21 chemokine gradient through the floor to reach the parenchyma and T cell zone [24,25]. Here in the T cell zone naïve T cells are highly motile and guided by the fibroblastic reticular cell (FRC) network as they use a combination of cell-intrinsic and –extrinsic mechanisms to search for the rare cognate pMHC-bearing DCs[26]. For example, myosin 1G has been demonstrated to facilitate a meandering walk pattern that optimizes efficient discovery of antigen-loaded DCs[27].

In addition, chemotactic cues like CCL3 and CCL4 can attract naïve CD8 T cells to an ongoing response in the LN and increase the probability of successfully encountering a cognate pMHC-bearing DC[28]. Upon recognition of a cognate pMHC on a DC, T cells engage in stable contacts that persist for 12 hours, after which point they undergo rapid clonal expansion and swarm around the DCs[29]. Although sphingosine-1-phosphate (S1P) typically prompts T cells egress from the LN, activated T cells transcriptionally down-regulates *S1pr1* and also up-regulates CD69 which further inhibits of S1P1R1 activity[30]. This initial retention in the LN allows for localized expansion and differentiation, after which point effector T cells egress from the LN and migrate to the site of immunogenic challenge. $CD8^+$ T cells can differentiate into effector or memory cells and evidence suggests that programming of their fate can begin early during the activation process[31,32]. While $CD4^+$ T cells contribute to a memory pool as well, they notably differentiate into functionally distinct helper T cell subsets that are tailored toward fighting particular classes of pathogens[33].

T cells are potent effectors of an adaptive immune response as they can augment immune activity of other immune cells, directly lyse target cells in an antigen-specific manner, and contribute to memory recall responses. Their activation thus must be tightly regulated by the innate immune arm as well as by other adaptive immune cells to appropriately tune a response to a given stimulus and achieve the appropriate magnitude of response. As illustrated above, T cell activation and expansion arises from cell-intrinsic mechanisms like T cell receptor (TCR) signaling pathways and cell division, but also is a product of cell-extrinsic interactions and signals from other immune cells. Further elucidation of the mechanisms that contribute to T cell responses and how external multicellular cues affect cell-intrinsic programming will contribute to a better understanding of how activated T cells are regulated in normal settings and how processes go awry in disease settings.

CHAPTER 1: T CELL ACTIVATION AND MAINTENANCE

I. THE IMMUNOLOGICAL SYNAPSE AND T CELL RECEPTOR SIGNALING

Cellular interactions between cognate pMHC-bearing APCs and antigen-specific T cells result in polarization of T cell receptors (TCRs) as well as associated surface receptors and signaling complexes at the region of contact, and this APC-T cell interface has been designated as the immunological synapse (IS)[34,35,36]. In early experiments the receptor components recruited to this interface exhibited a radially symmetric arrangement. First observed by 3D visualization of APC-T cell conjugates, TCR-pMHC clusters are found in the center encircled by the integrin LFA-1 to form an archetypal bull's eye pattern[37]. These regions were defined as supramolecular activation complexes (SMACs) that include the central (c)SMAC of TCR and protein kinase C-θ, the peripheral (p)SMAC of LFA-1 and talin, and the distal (d)SMAC of CD45 and F-actin[38,39]. Experiments with supported lipid bilayers that incorporate APC ligands like pMHC and ICAM-1 mimic the formation of these organized SMACs within T cells and have been a useful tool for visualizing and studying dynamics of IS generation[40,41]. While the prototypical IS is symmetrical and represents stably arrested cells, the IS can also exhibit various patterns *in vitro* and *in vivo*[42,43,44]. This variability is echoed by the findings that T cell activation can occur prior to stable arrest on an APC. Often T cells can remain motile for many hours as they engage in serial interactions with APCs and undergo active signaling and calcium flux before decelerating or stably arresting on an APC[45,46,29,47]. Contact dynamics with APCs are highly regulated and dependent on strength of TCR signaling and T cell cytoskeletal remodeling[48,49,50]. These motile contacts can be observed on lipid bilayers as well, especially as antigen dose is lowered[51], and are referred to as "kinapses"[52]. Together these data suggest that IS dynamics and structure are flexible with a continuum of synapse formation structure as T cells accumulate signaling and eventually decelerate in velocity[53].

T cells are exquisitely sensitive whereby a single pMHC can trigger recognition and downstream signaling, though sustained signaling requires 2-10 complexes[54]. While the molecular mechanism of pMHC discrimination by a TCR is still a source of active discussion, it has been proposed that the critical dwell time for a TCR to bind to an agonist pMHC and initiate signaling is ~2s[39]. Upon activation TCRs form microclusters and these are now considered the hub for initial signaling[55]. Peripheral microclusters emerge prior to the cSMAC and flow into the cSMAC, which may represent a site of TCR internalization and down-regulation instead of a defining event for T cell activation as originally presumed[56]. The TCR complex does not possess intrinsic catalytic activity but instead relies on phosphorylation of cytoplasmic immunoreceptor tyrosine-based activation motifs (ITAMs) by Lck upon productive pMHC-TCR binding, as well as recruitment and activation of effector kinases like ZAP-70[57,58]. To limit non-antigen-specific TCR signaling, negative regulation of signaling can occur through the Src kinase Csk and phosphatase activity of CD45[55]. Once set in motion, productive TCR signaling leads to phosphorylation and recruitment of the adaptor LAT. Here LAT acts as a scaffold to organize and generate critical downstream signaling events like intracellular calcium flux, key transcriptional programs through NFAT and NF-κβ, and cytoskeletal rearrangement[59,55].

A number of mechanisms may regulate initiation of TCR signaling in order to guard against spurious T cell activation[60]. As reviewed previously, different models propose that TCR triggering relies primarily on aggregation of signaling elements, conformational changes, or kinetic exclusion of inhibitory molecules from the TCR complex[61]. Aggregation refers to the need for physical accumulation of signaling components as a means to reinforce robust uninterrupted downstream signaling[62]. Other groups meanwhile have posited that productive p-MHC binding results in conformational changes that prompt TCR signaling. There is not consensus on the mechanism for this process, but studies have proposed that conformational changes occur in TCRαβ[63] or the cytoplasmic tail of CD3[64,65,66]. Finally, the kinetic segregation model has proposed that sustained TCR signaling occurs due to the segregation of vital regulatory

molecules at the immunological synapse[67]. This model rests on the argument that CD45's relatively large and rigid extracellular domain may kinetically exclude it from the cSMAC where T-APC membranes are closely juxtaposed[68,69,70], although additional mechanisms may be at play as well[69]. While still an active area of research, these different models may not be mutually exclusive from one another but instead represent a series of regulatory mechanisms in place to prevent off-target TCR activation.

II. ROLE OF THE CYTOSKELETON IN EARLY T CELL ACTIVATION

The actin and microtubule cytoskeletal networks provide the underlying dynamic structure to organize processes fundamental to T cell activation: cellular polarity, immunological synapse formation, cell-cell adhesion, and directed secretion. While naïve T cells are highly motile in the LN, they must eventually transition from a migratory to arrested state as they form stable contacts with cognate antigen-bearing DCs and transfer signaling molecules through synaptic exchange. Naïve T cells migrate in a front-rear polarized fashion within the lymph node as they search for cognate antigen[46,71]. This high degree of motility, characterized by a meandering walk, allows the T cell ample but efficient opportunity to come across antigen-bearing APCs[27]. Motile T cells exhibit ameboid morphology with a leading edge driven by Rac and Cdc42 GTPase activity and actin nucleation and a trailing uropod[71]. Retrograde cortical flow toward the uropod occurs in T cells[72] and it is thought that myosin II motor proteins control this flow given their localization to the leading edge and subsequent retrograde flow toward the uropod as well[73]. This directional flow likely underlies the increased density of receptors like the TCR[74], CD2[75], CD43[76], and CD44[77] at the uropod. Subsequent antigen recognition, however, can lead to T cell arrest through Ca^{2+}-dependent and –independent mechanisms[48,78,79,80] whereby the T cell becomes spherical and absorbs its uropod[81]. It has been proposed that inactivation of myosin II executes this 'stop signal' as TCR signaling leads to changes in myosin II's phosphorylation state and re-localization from the uropod to the synapse[73]. In accordance

with this model, inhibition of myosin II results in a loss of morphological polarity and motility. Although arrested T cells appear spherical morphologically, surface receptor distribution remains highly polarized with the IS at the APC-T cell interface and establishment of a distal pole complex[82]. To achieve this arrangement, TCR signaling reduces cellular rigidity and initiates surface receptor reorganization and clustering at the T-APC interface through dephosphorylation of ERM proteins and cleavage of actin-binding proteins like talin[83,84,85]. In addition to facilitating the clustering of integrins like LFA-1 at the IS, TCR "inside-out signaling" also induces high-affinity conformational changes in LFA-1 that augment binding to ICAM-1 on the APC surface and mediate strong cell-cell adhesion[85,86]. Together these processes organize T cell morphological and surface receptor polarity and coordinate shifts between motility and long durations of stable adhesion to APCs.

Immunological synapse formation is dependent on F-actin dynamics[87,88,89] as actin retrograde flow drives TCR microcluster transport into the cSMAC and assembly of new microclusters[90,91]. TCR triggering results in localized actin-binding protein activity and actin polymerization at the IS. Although many actin regulators are involved in polarized actin nucleation[92], critical factors include the guanine exchange factor (GEF) VAV1 and downstream effector GTPases CDC42 and RAC1. CDC42 and RAC1 regulate ARP2/3-mediated F-actin nucleation via WAVE2 and the WIP-WASP complex, as well as formin-driven nucleation. Actin regulation is undoubtedly complex, and concurrent actin depolymerization occurs to allow for inward TCR microcluster flow and cSMAC formation[51], as reflected by the F-actin ring observed originally in the dSMAC. Although the complete regulatory mechanisms remain to be determined, TCR signaling also leads to polarization of the microtubule networks and centrosome, or, the microtubule-organizing center (MTOC)[35,93,94]. MTOC relocalization enables directed secretion of lytic granules through the synapse[95] and the concomitant clearance of cortical actin in the synapse may facilitate centrosome docking and vesicle delivery[96,97]. In

addition to lytic granules, T cells can release certain cytokines like interferon-γ (IFNγ) in a directional manner that is dependent on microtubules[98].

III. CLONAL EXPANSION OF ACTIVATED T CELLS

Robust proliferation of an antigen-specific T cell clone is critical to generate a pool of effector cells that can clear an immunological challenge as well as long-lived memory cells that can protect against future breaches. $CD8^+$ T cells can divide rapidly with doubling times of 2-4 hours[99,100,101] and can achieve up to 50,000-fold increase in antigen-specific cell number[102]. Overall a number of factors contribute to the eventual T cell 'burst size' and these include the number of pre-existing antigen-specific cells in the naïve repertoire, the binding affinity of the TCR-pMHC, and the antigen density and stability, as reviewed by Tscharke and colleagues[103]. Yet, TCR signaling alone results in weak proliferation and anergy, and co-stimulatory signaling acts as 'Signal 2' to ensure and modulate complete T cell activation and effector generation[104,105,106,107].

For example, co-stimulatory CD28 signaling promotes activation and proliferation of T cells through several signaling pathways. The proximal YMNM motif on its cytoplasmic tail recruits the p85 subunit of phosphatidylinositol 3-kinase (PI3K) that induces activation of AKT[108]. This in turn activates downstream processes that support survival and hearty proliferation through kinases like mTOR, transcription factors like NF-κβ and NFAT, and other pro-survival factors like BCL-XL, GLUT1, and IL-2. In addition to the YMNM motif, CD28 contains a distal PYAP motif that recruits Lck and GRB2, which in turn activate PKCθ and increase NFAT-mediated IL-2 production[109]. GRB2 can bind to both the YMNM and PYAP motifs and also activates c-Jun N-terminal kinases (JNKs) and extracellular signal-regulated kinases (ERKs)[109]. In terms of regulation, CD28 assembles in microclusters with the TCR where it initially recruits and activates PKCθ[110]. Following T cell activation, co-inhibitory molecules like CTLA-4 or PD-1 are also recruited and can increase the threshold for CD28 signaling by excluding it from the

cSMAC as well as dephosphorylating TCR signaling machinery like TCRζ, ZAP70, and PKCθ[111,112,113].

Although CD28 has become one the best characterized co-stimulatory receptors, a large number of additional co-stimulatory molecules have also been identified. CD28, along with receptors such as CD27, OX40, and 4-1BB can help to boost proliferation and effector T cell function[114,115,116,117]. Functionally opposing co-inhibitory receptors like CTLA-4 are also expressed, and together these co-signaling molecules represent a diverse array of receptors that are primarily from the immunoglobulin superfamily (IgSF) and the tumor necrosis receptor superfamily (TNFRSF)[118]. Unsurprisingly, dynamic regulation of the co-signaling receptors is complex, and is achieved through a number of regulatory mechanisms that include spatiotemporal expression that fits a 'tidal model' of co-signaling[119], interactions with multiple ligands, and binding competition to shared ligands[109].

Inflammatory cytokines such as IL-2, IFNγ, IL-12, and type I IFN notably serve as the 'Signal 3' that shapes the magnitude of expansion and survival of effector T cells. Activated T cells up-regulate surface expression of IL-2R components[120] and IL-2 signaling in turn supports T cell survival and proliferation following activation[121]. IFNγ too can regulate the expansion of activated $CD8^+$ T cells[122,123], though the effect of IFNγ can vary based on model studied[124,125]. Similarly, IL-12 is secreted by activated DCs and supports proliferation and CTL differentiation[126,127,128], as can IL-27[129,130] and IFN-αβ[131,132,133]. Although these cytokines can share similar functionality with potential redundancy, the role of a given one may depend on the nature of the immune challenge and ensuing inflammation[134].

It should be noted that differentiation between effector and memory T cells is also a crucial process in T cell expansion that begins early following activation[135]. Asymmetric division, perhaps a holdover from the established polarity of the synapse, may contribute to early determination of effector or memory fate[31], although this model is difficult to reconcile with other studies and may instead contribute alongside other processes[136]. Additional secondary cellular

interactions and delivery of cytokines like IL-2, IFNγ, or IL-7 may also influence the balance between effector and memory T cell generation[137,138,32,139].

IV. HOMEOSTATIC T CELL MAINTENANCE AND EXPANSION

Under homeostatic conditions both naïve and memory T cells must be maintained in a quiescent state such that they will be viable and responsive to antigen-specific activation when necessary. Upon exit from the thymus and prior to activation naïve T cells circulate through lymphoid organs where they receive the necessary survival signals of endogenous TCR-self-pMHC interactions and IL-7[5]. Although strongly self-reactive thymocytes are theoretically removed from the repertoire during negative selection, basal low-affinity recognition of self-pMHC occurs in peripheral naïve T cells as evidenced by partial phosphorylation of the TCR CD3ζ chain[140,141,142]. A number of studies have demonstrated the importance of self-pMHC-I in naïve $CD8^+$ T cell survival, although several of these initial studies are limited by the caveats of using lymphopenic conditions that can alter T cell homeostasis and proliferation dynamics[143,144,145]. There is evidence in non-lymphopenic settings, however, that self-pMHC-I and TCR signaling is required for naïve $CD8^+$ T cell homeostasis[146,147,148].

Self-pMHC may be presented to T cells on DCs as well as stromal cells like FRCs[149]. Studies with irradiated bone marrow chimeras suggest that each are sufficient to support $CD8^+$ T cell survival[144,146] but DCs appear to be critical in maintaining T cell responsiveness[150]. In contrast to CD8 T cells, however, there are conflicting findings regarding the role and requirements of self-pMHC-II in $CD4^+$ T cell survival[141,151,152,153,154,155,156,157]. Beyond survival, there is evidence that tonic self-p-MHC-II recognition can similarly tune $CD4^+$ T cell sensitivity to foreign antigen[150,158,159]. Again, however, there are discrepancies amongst studies with some reporting increased reactivity following loss of self-TCR signaling[159,160], and others observing decreased[158] or no change in TCR responsiveness[157]. These conflicting results may arise from

different behavior in response to antigen levels or affinity, or altered cellular behavior independent of TCR signaling.

While self-pMHC-TCR signaling can be required for survival, disparities in strength of this self-pMHC signaling also impart differential functional behavior upon a T cell's recognition of foreign antigen. Surface CD5 levels are correlated with strength of self-pMHC-TCR signaling and heterogeneity within the T cell compartment exists at baseline[146,160,161,162,163]. Interestingly, $CD8^+$ T cell clones with higher self-reactivity and CD5 expression are enhanced for genes associated with T cell effector generation and trafficking and are preferentially incorporated early in response to a pathogenic challenge[164]. Here the authors did not find the $CD5^{hi}$ and $CD5^{lo}$ clones to differ in affinity for foreign p-MHC-TCR binding based on tetramer binding. $CD4^+$ T cells with stronger self-reactivity also have been demonstrated to dominate in responses against foreign antigen, although in these studies self-pMHC affinity directly correlated with foreign-pMHC affinity[165]. While this relationship between TCR affinity to self- and foreign-pMHC may reflect differences in $CD8^+$ and $CD4^+$ T cells, this association has not been consistently observed in $CD4^+$ T cells[166,167] and may instead be specific to tested conditions. Lastly, there are conflicting reports in which $CD5^{lo}$ $CD4^+$ T cell clones outperform $CD5^{hi}$ clones in primary responses[166,167]. While more work is required to understand the underlying discrepancies, there may be immunological settings in which $CD5^{lo}$ T cells are better positioned to participate in a given response. What is clear from these collective studies, however, is that basal self-pMHC-TCR signaling endows heterogeneity in responsiveness within the T cell repertoire and this diversity may have implications for incorporation of self-reactive clones, especially in settings of autoimmunity.

In conjunction with TCR-self-pMHC signals, the cytokine IL-7 supports T cell survival through up-regulation of anti-apoptotic factors like BCL-2 and MCL-1 and down-regulation of apoptotic factors[168,169,170]. IL-7 also triggers PI3K-AKT signaling to induce mTOR and GLUT1 expression[171,172]. Naïve T cell survival is thus diminished with blockade or absence of IL-

7[163,173,174,175]. In line with this, IL-7 levels set a homeostatic limit on the T cell compartment size, and over-expression of IL-7 leads to an increase in T cell numbers[176]. This relationship may reflect competition that occurs at the basal state amongst T cell clones for both IL-7 and self-pMHC signals, which serves as a mechanism to optimize clonal diversity within the T cell repertoire[177,178,179,180]. Unlike cytokines that promote proliferation of activated T cells, exposure to basal levels of IL-7 does not induce cell division as naive T cells generally persist without proliferation following exit from the thymus. In settings of lymphopenia, however, IL-7 levels are in excess to the current lymphocyte compartment, and T cells undergo a slow rate of T cell proliferation in an IL-7 dependent manner[168,175,181]. High levels of other cytokines like IL-2 and IL-15 concurrent with self-pMHC can also drive T cell proliferation[182,183].

In contrast to naïve T cells, $CD4^+$ and $CD8^+$ memory T cells can survive and proliferate without pMHC interactions, and instead rely on a combination of IL-7 and IL-15 for homeostatic maintenance[184]. It is thought that while IL-7 is critical for survival, IL-15 predominantly drives the basal rates of $CD8^+$ T cell turnover that have been observed in non-lymphopenic settings[185]. The requirements for memory $CD4^+$ T cells are largely similar to those of $CD8^+$ T cells, though data supports a role for both IL-7 and IL-15 in homeostatic proliferation[186,187] . IL-15 too has multiple sources of delivery with expression in stromal cells[188] coupled by trans-presentation by IL-15Ra on DCs and macrophages[189]. Localization of T cells may also influence the balance of accessible IL-7 and IL-15 signals, as IL-15 appears to preferentially support $CCR7^-$ effector memory $CD8^+$ T cell turnover in non-lymphoid tissue (NLT) while IL-7 maintains the $CCR7^+$ pool[190].

CHAPTER 2: THE SEPTIN CYTOSKELETON

I. PROPERTIES OF SEPTIN COMPLEXES

Septins consist of a family of GTPase proteins that forms a novel cytoskeletal network and that takes on non-canonical functions that complement and cross-regulate other cytoskeletal networks of actin and microtubules. Septin family members form hetero-oligomeric complexes that can then assemble into higher-order structure such as rings, gauzes, cage-like structures, and filaments[191]. These diverse structures can serve as scaffolds for protein recruitment and signaling, diffusion barriers, and architectural bulwarks that can coordinate a number of cellular tasks such as mitosis, cytokinesis, autophagy, ciliogenesis, dendritic branching, and cell shape. Four septin family members (*cdc3, cdc10, cdc11, cdc12)* were first identified in budding yeast *Saccharomyces cerevisae*[192], with a fifth septin homolog *Shs1* identified later[193]. Although septins in *S. cerevisae* can implement some yeast-specific functionality, the family is highly conserved with representation across eukaryotic species. Septins share a central domain that contains a polybasic region through which they can bind directly to the plasma membrane, a GTP-binding domain, and an uncharacterized septin unique element (SUE)[194,195,196,197].

Although the number of septins in organisms can be variable, with humans having 13, septins can be categorized into four groups based on homology[191,198,199]. Complexes in different organisms may contain different numbers of septins, but these complexes are typically paired symmetrically. In *S. cerevisae*, septin complexes form octamers of Cdc11-Cdc12-Cdc3-Cdc10-Cdc10-Cdc3-Cdc12-Cdc11 or Shs1-Cdc12-Cdc3-Cdc10-Cdc10-Cdc3-Cdc12-Shs1[200,201]. These Cdc11-capped complexes, or rods, form short filaments *in vitro* with high salt (300mM), but can assemble into long end-to-end paired filaments under lower salt conditions (<50mM)[200,202]. Complexes with Shs1 at the end instead assemble laterally and form curved bundled structures like rings *in vitro*[201], which suggest that regulation of complex arrangement may impart

differential functionality. In contrast, human septins form hexameric complexes and the structure of SEPT7-SEPT6-SEPT2-SEPT2-SEPT6-SEPT7 has been solved[203]. Humans do have four groups of septins, however, which may allow for octamer complexes as well. Such structures with SEPT9 added at the end have been observed, but the role and regulation of hexamers versus octamers remain unclear[204,205,206]. Notably, SEPT7 is the one SEPT7 group member and is required for intact septin assembly. Although the mechanism remains unknown, there likely exists some form of 'quality check' for septin complexes as loss of SEPT7 is accompanied by reduced expression of other septin family members[207,208,209,210]. While SEPT7 is unique, other septins are likely exchangeable for those in their respective group. This level of optionality would allow for both functional diversification and a substantial degree of redundancy as noted by the emergence of substitute complexes or altered filaments with depletion of certain septin members in yeast[201,211,212,213].

II. SEPTIN FILAMENT ORGANIZATION AND INTERACTIONS WITH OTHER CYTOSKELETAL ELEMENTS

Together septin complexes can assemble in nonpolar filaments that carry out critical functions, as demonstrated in budding yeast[213]. Although septins fall under the superclass of phosphate-binding (P-loop) NTPases that also contains RAS-like proteins[214], septins are not canonical GTPases that convert between active GTP-bound and inactive GDP-bound forms. Rather, GTP hydrolysis occurs very slowly[215,216,217] and septins' GTP-binding capacity may instead contribute to filament organization. GTP hydrolysis results in conformational changes at the monomer interfaces[203,218], and some members preferentially have GDP in their active sites[198] whereas others like SEPT6 cannot even support GTP hydrolysis[203]. Once polymerized, filaments can assemble laterally and form bundles, which in turn can give rise to ring structures[200,201,218,219,220]. In contrast to actin or microtubule filaments, septin filaments are relatively stable since they are not subject to dynamic turnover[221].

Septins can interact with actin and microtubules and these interactions allow for cross-regulation. Actin can provide a template for septin filament formation, and inhibition of actin polymerization with cytochalasin D disrupts septin filaments and results in cytoplasmic rings[207]. Close proximity with actin allows for interactions with other key actin-binding factors like myosin II and annilin, and cooperation may mediate critical cellular functions like cell shape and migration[208,222], cell division[223,224,225,226], or bacterial caging[227]. Septins can also influence actin structural dynamics by inducing bundling and curvature of actin[228]. As with actin, septins interact with microtubules[229] and septin filaments are disrupted when microtubule polymerization is inhibited[229,230,231]. Conversely, use of taxol to stabilize microtubule filaments increases septin filament number and longevity[230,232]. Septins also regulate microtubule polymerization[232] and turnover, with loss of septins leading to hyper-acteylation and -stabilization of microtubules that can interfere with processes like dendrite and axon growth[209] and cytokinesis[210,233]. In these cases, septins may modulate microtubule stability by preventing the microtubule-associated protein MAP4 from binding and bundling microtubules[233] or by recruiting HDAC6 to deacetylate microtubules[209].

In addition to other cytoskeletal components, septins can also bind directly to membrane phospholipids through their polybasic domain[194,195,234,235]. For example, monolayers of phosphatidylinositol-4,5-biphosphate (PtdIns4,5P2) lipids can support septin filament formation and influence filament organization and architecture[234]. Annealing to the membrane may provide stability for the filaments and cellular proximity to enhance localized functionality at the cell cortex. Septins may even modulate membrane dynamics by inducing membrane tubulation[235]. It was also recently suggested that septins can recognize membrane curvature on a micron scale and that sensing does not require filament formation[236]. Given the association between regions of membrane curvature and septin ring function (i.e. cytokinetic furrow, sperm annulus, cilia, or phagocytic vesicle), it may be that detection of membrane curvature allows for subcellular localization of septins to carry out their functions[237].

III. ROLE OF SEPTINS IN CELL SHAPE AND MOTILITY

Septins localize to the cell cortex where they maintain cortical tension and membrane rigidity[208,222,238]. Loss of septins thus compromises cellular integrity, and defects are often linked to dysregulated cell shape and directional cell migration. SEPT2- and SEPT11-depleted HeLa cells manifest divergent phenotypes but each exhibit changes in overall cell morphology and membrane elasticity, with implications for surface receptor dynamics[239]. SEPT7-deficient T cells present with an increase in membrane blebbing and protrusion formation due to decreased membrane tension and retraction capacity[208,222]. In these cells, impaired cortical tension was accompanied with elongated uropods, although the functional consequences of such morphological change remain unclear. Persistent migration of septin-deficient T cells is also hindered, although surprisingly these cells exhibit an enhanced ability to migrate through small pores, perhaps to due increased cortical flexibility[208]. Similar phenotypes of blebbing have been observed in other cell types including *Xenopus laevis*, and septins regulate directional motility in *Xenopus laevis* embryos as well[240]. In sperm cells, septins form a membrane-associated ring, or annulus, that separates the sperm tail from the cell body. SEPT4-deficient sperm lose this annulus, and instead contain a structurally weak segment between the cell body and tail that lacks proper cortical organization and is susceptible to collapse. As with other cell types, septin-depleted sperm cells have impaired motility, and this defect may be attributed to disorganization of cortical elements that would otherwise be associated with the annulus, though further work is required to test this hypothesis[241].

IV. SEPTIN FUNCTION IN ESTABLISHING DIFFUSION BARRIERS AND SUBCELLULAR DOMAINS

One of the unique properties of septins is the creation of diffusion barriers that allows for specialized compartmentalization of membrane proteins to subcellular regions and enables

precise spatial regulation[242]. Septin diffusion barriers were first identified in dividing yeast[243], but are present in non-dividing yeast, as well as other cell types. Septin rings at the base of primary cilia in mammalian cells have been identified and here septins are thought to restrict membrane protein traffic from the cilia membrane[240,244]. Depletion of septins hinders ciliogenesis and increases diffusion of membrane proteins at the cilia[244]. Indeed septins appear to facilitate the generation of cilia-specific complexes that are critical for creation of a diffusion barrier and cilia identity[245]. In sperm cells, the septin-driven annulus ring separates the anterior and posterior portion of the sperm tail[241,246] and this structure allows for compartmentalization of cellular proteins[247]. Septins similarly assemble into rings at the base of dendritic spines in neurons and are critical for dendritic branch morphology and length[248,249], as well as restriction for membrane protein movement[250]. In addition to forming higher-order ring structures that enforce diffusion barriers, septins can establish signaling scaffolds within the plasma membrane by modulating surface receptor expression, localization, and internalization. For example, loss of septins limited the distribution of surface receptor MET and subsequent ligand-receptor interactions[239], and septins bind directly to transmembrane protein glutamate aspartate transporter (GLAST) to regulate its localization and internalization[251,252]. Septins may also organize membrane lipid microdomains that permit stable signaling like store-operated $Ca2^{+}$ entry in HeLa cells[253].

V. SEPTINS IN CELL DIVISION

Lee Hartwell first discovered septins in *S. cerevisiae* budding yeast by screening for 'cell division cycle' mutants and found that loss of septin homologs *cdc3*, *cdc10*, *cdc11*, and *cdc12* resulted in defective cytokinesis and multinucleated cells[192]. *Shs1*, which was identified later, also is required for productive cytokinesis[193]. In *S. cerevisiae* two additional septins are produced during sporulation to form meiosis-specific complexes that aid in sporulation processes[212,254,255,256,257], though here we will solely focus on mitotic septins. In early G1-phase, Cdc42 recruits septins to the destined bud site and the septins complexes that accrue form a

filamentous ring[258,259,260]. Once the bud initiates, the septin ring transitions into a highly stable hourglass collar that persists until mitosis[261,262]. At the onset of cytokinesis, the collar separates into two rings and the contractile actomyosin ring (AMR) forms between the septin rings to provide the constrictive force to facilitate membrane ingression and subsequent septum formation between mother-daughter cells[263,264,265,266,267].Throughout cell division septin assembly is pivotal to recruit proteins to the bud neck that establish the bud site[268,269], maintain polarity during bud growth[270], and allow for progression through septin-dependent cell cycle checkpoints[271,272,273]. To prepare for cytokinesis in particular, septins recruit factors that will mediate mother-daughter cell separation such as chitin synthases for cell wall deposition[274] and actomyosin ring elements[275,276,277,278]. Notably, septin-dependent establishment of a diffusion barrier helps to retain proteins at the bud site and maintain polarity during mitosis[279,243]. This barrier also prevents transfer of aging factors from the mother to daughter cell[280], which while not critical for cytokinesis itself, affects daughter cell longevity.

Beyond yeast, septin requirements for cell division appear to be highly conserved in eukaryotic cells. Loss of septins results in mitotic or cytokinetic defects in *Drosophila melanogaster*[281,282], *Caenorhabditis. elegans*[283], and mammalian cells[229,231,284]. Septins are often, though not exclusively, found assembled at the cleavage furrow[284,285,286]. They have been suggested to be essential in organizing the contractile ring by coordinating myosin motor proteins[223], and facilitating the transition from the contractile ring to the midbody ring[287]. As cytokinesis progresses, septins can remodel the membrane[287] and anchor the midbody ring structure to the membrane[225] as mother-daughter cell separation is resolved. In addition to mediating cytokinesis at the membrane, septins can be found in the cytosol as well, such as at the microtubule spindle during metaphase[231]. Septins at the mitotic midplane aid in centromere-associated protein E (CENP-E) orientation and are thus crucial for chromosomal alignment and segregation[288,289]. Septins also modulate microtubule stability and depletion of septins leads to hyper-stable microtubules and cytokinetic failure in murine fibroblasts[210]. Regulation of cell

division by septins is complex and different septin members may have disproportionate roles in a given cell division process, perhaps driven by differential localization during cytokinesis[290]. In HeLa cells specific loss of SEPT2, SEPT11, and SEPT7 led to impaired cleavage furrow ingression, but loss of SEPT9 led to later-stage failure in midbody abscission[286].

Although septins play a number of distinct roles during the course of mitosis and cytokinesis, several studies have revealed that some cells are able to divide independently of septins. Although septins localize to cytokinetic machinery in embryonic *C. elegans* and *Drosophila*, septin-deficient organisms undergo successful early embryogenesis with cell division defects emerging later in development and adulthood[291]. Different cell types appear to have distinct requirements in murine models as well. Septin-deficient fibroblasts undergo cytokinetic failure while deficient T cells and bone marrow-derived myeloid cells are competent in cell division, and the differential requirement observed was attributed to varied stathmin levels and microtubule stabilization[210]. Comparable proliferation in septin-deficient D10 cell lines[208] and Jurkat cells[204,210] have also been observed. Intriguingly, septin-dependency may also rely on context-specific uses within the same cell type. For example, neuroepithelial cells in *Drosophila* do not require septins for orthogonal cell division but do rely on septins for planar division in which septins mediate actomyosin contractility in order to overcome tension from neighboring cells and adhesion disengagement from adjacent cells[226].

VI. REGULATION OF SEPTINS

Given the diversity in septin members and cellular functions, a complex level of genetic and spatiotemporal regulation is required for septin expression, localization, assembly, and disassembly within the cell. In yeast a number of proteins and kinases such as Cdc42, Gic1, Gic2, and Elm1 organize proper localization of the septin ring at the bud neck[292,293,260]. Dynamics of septin filaments are likely regulated by post-translational modifications. For example, phosphorylation of septins in yeast is often regulated by cell cycle signaling such as

G1 cyclin-dependent kinases[294,295]. These and additional kinases like Cla4 and Gin4 enable stable filament assembly and maintenance at the bud neck, and phosphorylation is critical for successful cytokinesis[296,297,298]. As an example of even more refined regulation, phosphorylation of certain septin residues can influence the higher-order structure formed by the filaments, be it a ring or gauze structure[201]. In contrast, sumolyation promotes disassembly of septin ring structures as mutations in sumolyation sites lead to septin rings accruing at the bud neck[299,300]. Ubiquitylation also contributes to septin degradation[301] and may be relevant in some disease settings like Parkinson's disease[302]. Regulation of septins in mammalian cells, however, remains poorly characterized aside from the identification of a family of Cdc42 effectors, BORGs (binders of RHO GTPases) that can directly bind to septins and regulate their localization within the cell[303]. In addition to filament assembly, regulation of protein expression is also unclear although altered expression levels, isoform splicing, or post-translational modifications like methylation are observed in a number of human diseases including cancer[304,305].

CHAPTER 3: ROLE OF THE SEPTIN CYTOSKELETON IN T CELL ACTIVATION AND EXPANSION

I. INTRODUCTION

T cell proliferation rapidly expands the number of antigen-specific cells, which is necessary to control infection. Typically, this kind of cell division is initiated by a T cell interaction with its cognate antigen on an APC, and its magnitude is determined by the strength of the TCR recognition event in that cell-cell contact[306,307,308]. Antigen-specific T cell clonal expansion has been reported to occur in the lymph node where swarming T cells engage in cell-cell contacts with proximal APCs and other activated T cells[29,309], and this may represent a 'niche' for cell division. Yet, cell division can also be driven by high local cytokine concentrations in the environment, in the possible absence of such cell-cell interaction. This scenario is considered a possible hazard for autoimmunity, as when non-virus-specific 'bystander' cells experience high concentrations of cytokines produced by viral-specific T cells during an immune response in a lymph node[307,310]. Cytokine-driven cell division is also clearly important for homeostatic maintenance whereby cytokines such as IL-7 or IL-15, in conjunction with transient low-affinity p-MHC-TCR interactions, support turnover of clones[5]. While asymmetric cell division has been proposed to be a pathway that can influence the individuality of daughter cells[31], completion of cytokinesis has been considered invariant. To our knowledge, it has not previously been possible to clearly separate cytokine- versus TCR-driven cell division.

The physical event of cell division requires multiple processes, including the functions of specific kinases[311], specific cytoskeletal proteins such as myosins and, notably, septins[312,231,286,313]. Septins are a family of GTP-binding proteins that self-assemble into tetrameric, hexameric, or octameric quaternary structures and further into large filaments, rings, and gauzes *in vitro* and *in vivo*, and are assembled on the cell cortex[207,314,315].The mammalian septins, 13 in number, can be divided into four groups with one from each class required to form

a canonical complex. In mammals, Septin 7, the only one in its class, appears indispensable for the generation of filaments, and its depletion leads to loss of the other septin proteins[207,208,209,210], presumably as a result of quality control processes. Septins were originally identified as 'cell division cycle' (cdc) mutations[192] and are evolutionarily conserved in their critical role for cytokinesis. Similar to yeast, septins in mammals have been found to be essential for completion of cytokinesis[286,191]. Septins are usually, but not exclusively, found assembled as a ring at the cleavage furrow[286,222]. They previously have been suggested to be essential at the furrow to coordinate myosin motor proteins during cell abscission[312,223], to remodel the membrane as cytokinesis progresses[287], and to anchor the midbody ring structure to the membrane[225] as mother and daughter cell separation is resolved.

One exception to the requirement of septins for mammalian cytokinesis has been T cells; we showed that Septin 7 depletion in cell lines led to loss of the other septins, but resulted in near-normal cell division in response to cues driven by APCs[208]. T cell cytokinesis in the absence of septins was also recently confirmed in a *Sept7* genetic knockout model[210]. To investigate how T cells might evade this highly conserved requirement, we generated T cell-specific depletion of Septin 7 in mice and examined $CD8^+$ T cell activation and functions under a variety of conditions. We unexpectedly found that septins are required differentially for T cell division, depending on whether or not T cells engaged in cell contacts during the period of cytokinesis. This finding led us to examine how proliferation occurs in septin-null $CD8^+$ T cells so as to isolate the compensatory pathways. Our results provide a rare insight into the possibility of specifically attenuating cytokine-driven expansion while leaving antigen-driven expansion untouched.

II. RESULTS

Development of Septin-deficient T cells is Intact

T cells were engineered to lack all septins using a *Cd4*-Cre allele in a genetic background of *Sept7*$^{flox/flox}$ (*Sept7*cKO)[210]. These mice were subsequently crossed to the OT-I TCR-transgenic allele. Mice from both polyclonal or OT-I backgrounds demonstrated near-complete loss of Septin 7 in peripheral T cells with a small proportion (5–10%) of 'escapees' as assessed by flow cytometry (**Figure 3.1A**). To remove this contaminating population, we took care in all future analyses to eliminate these "escapees" from our experimental analysis when possible: either by detection of intracellular Septin 7 or use of mTmG mice[316] wherein Cre recombinase activity converts mTomato^{+} cells to mGFP^{+}. As predicted from shRNA studies in cell lines[208], genetic deletion of Septin 7 led to coordinate loss of other key T cell-expressed septin family members in peripheral T cells as assessed by immunoblotting (**Figure 3.1B**). The *Cd4*-Cre allele is expressed in a pre-DP phase of thymic development[317] and we observed initial onset of septin loss in DN thymocytes with maximal loss by the single-positive stage in *Sept7*cKO mice (**Figure 3.1C**). We observed comparable proportions of DN, DP, and SP thymocyte populations (**Figure 3.1D**), equivalent cellularity in secondary lymph node organs (**Figure 3.1E**), and similar frequency of CD4^{+} and CD8^{+} T cells within those organs (**Figure 3.1F**). Additionally, naïve resting septin-deficient CD8^{+} T cells maintained normal amounts of filamentous actin (**Figure 3.1G**) and septin-deficient OT-I T cells exhibited morphological defects that phenocopied previous findings with septin knockdown in T cell clones[208,222] (**Figure 3.1H**,**I**). Together this demonstrates that development of septin-deficient T cells in this mouse model is largely intact.

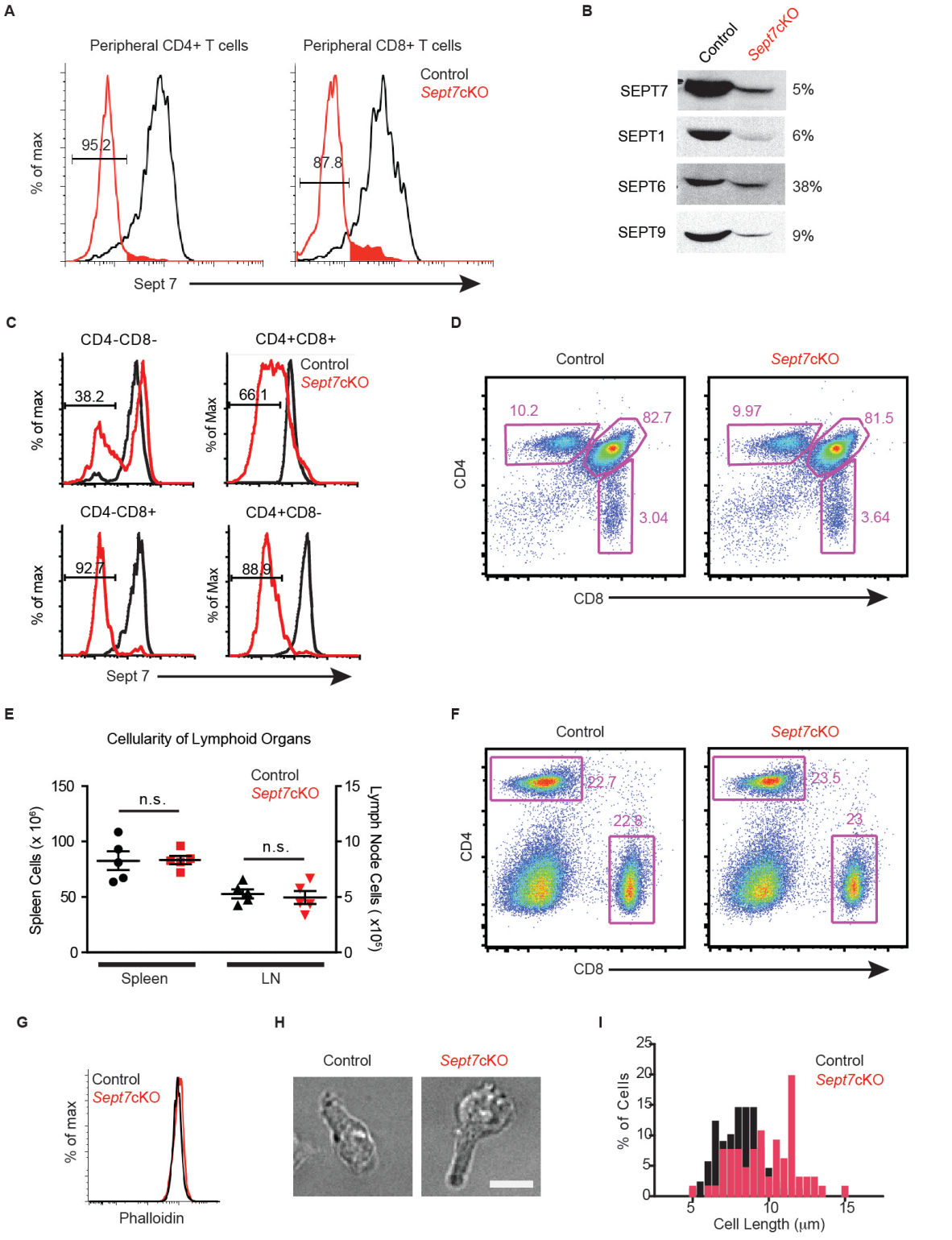
A
Peripheral CD4+ T cells
Peripheral CD8+ T cells
Control
Sept7cKO
% of max
95.2
87.8
Sept 7
B
Control
Sept7cKO
SEPT7
5%
SEPT1
6%
SEPT6
38%
SEPT9
9%
C
CD4-CD8-
CD4+CD8+
CD4-CD8+
CD4+CD8-
% of max
% of Max
38.2
66.1
92.7
88.9
Sept 7
D
Control
Sept7cKO
10.2
82.7
3.04
9.97
81.5
3.64
CD4
CD8
E
Cellularity of Lymphoid Organs
Control
Sept7cKO
n.s.
n.s.
Spleen Cells (x 10⁶)
Lymph Node Cells (x10⁵)
150
100
50
0
15
10
5
0
Spleen
LN
F
Control
Sept7cKO
22.7
22.8
23.5
23
CD4
CD8
G
Control
Sept7cKO
% of max
Phalloidin
H
Control
Sept7cKO
I
Control
Sept7cKO
% of Cells
25
20
15
10
5
0
5
10
15
Cell Length (μm)

Figure 3.1 Septin-deficient T cells develop comparably to wild-type T cells.
(**A**) Intracellular Septin 7 protein levels of polyclonal CD4+ and CD8+ T cells from Sept7cKO or control mouse spleen as assessed by flow cytometry. (**B**) Protein levels of septin family members determined by Western blots of isolated CD8+ T cells from Sept7cKO or control OT-I mouse spleens. (**C, D**) Intracellular septin 7 levels (**C**) and frequency (**D**) of thymocyte populations from the thymus of Sept7cKO or control mice. (**E, F**) Cellularity of secondary lymphoid organs (E) and frequency of peripheral lymphocytes in lymph nodes (**F**) of Sept7cKO or control mice. (**G**) Intracellular phalloidin levels of naïve polyclonal CD8+ Sept7cKO or control T cells as tested with flow cytometry. (**H, I**) Activated Sept7cKO and control OT-I cells were plated on ICAM-1-coated coverslips and imaged for morphological measurements. Images of control and Sept7cKO cells illustrating the elongated uropod of Sept7cKO cells (**H**). Quantification of measurements and population distribution of cell length (**I**). Data is representative of at least two (**H, I**), three (**A-C, E**), or five (**D, F**) independent experiments. Small horizontal bars denote the SEM. *P <0.05 with data analyzed with unpaired t-test (**E**).

Selective Proliferation Defects in Absence of Septins

We sought to examine T cell proliferation in the context of control or *Sept7*cKO $CD8^+$ T cells isolated from these mice. Although septins are required for cell division in various types of eukaryotic cells, we and others have found that T cells proficiently proliferate in the absence of Septin 7 and associated septin family members[208,222,210]. Consistent with this, we found that, when co-cultured *in vitro* with bone marrow-derived dendritic cells (BMDCs) pulsed with the OT-I peptide antigen SL8, $CD8^+$ OT-I T cells diluted CFSE (**Figure 3.2A**, **Figure 3.3A**), progressed in cell cycle, and expanded in numbers at a similar rate to wild-type cells (**Figure 3.2B**). Unexpectedly, however, when activated with plate-coated anti-TCR antibody or soluble phorbol myristate acetate (PMA) and ionomycin, septin-deficient OT-I T cells underwent fewer cell divisions as assessed by CFSE dilution (**Figure 3.2A, Figure 3.3A**) and by cell recovery (**Figure 3.2B**) after 72 h. Polyclonal $CD8^+$ *Sept7*cKO T cells exhibited these cell division defects as well (data not shown). Additionally, whereas stimulation with BMDCs generated largely conventional G1-S-G2/M cell cycle profiles, stimulation in the absence of APCs resulted in bi- and multi-nucleated cells, as detected by flow cytometry (**Figure 3.2A, Figure 3.3A**) and confocal microscopy (**Figure 3.2C**). This differential block in cell division was also observed in accumulation of septin-deficient forward-scatter^{hi} cells as compared to the septin-competent "escapees" from *Sept7*cKO OT-I mice in T cell cultures stimulated with anti-TCR or PMA and ionomycin (**Figure 3.3C**). Altogether, this data demonstrates that T cells are not intrinsically unique in not requiring septins for cytokinesis, as was recently proposed[210], but rather that only certain cytokinetic pathways are septin-independent. Moreover, in assessing how the generation of multinucleate cells relates to cell division, we observed that septin-deficient cells are susceptible to cytokinesis failure with every division, not simply the first (**Figure 3.2D**). This observation argues that failure to divide is a stochastic event with the limited expansion of *Sept7*cKO T cells to APC-independent stimuli resulting from a breakthrough event with each division.

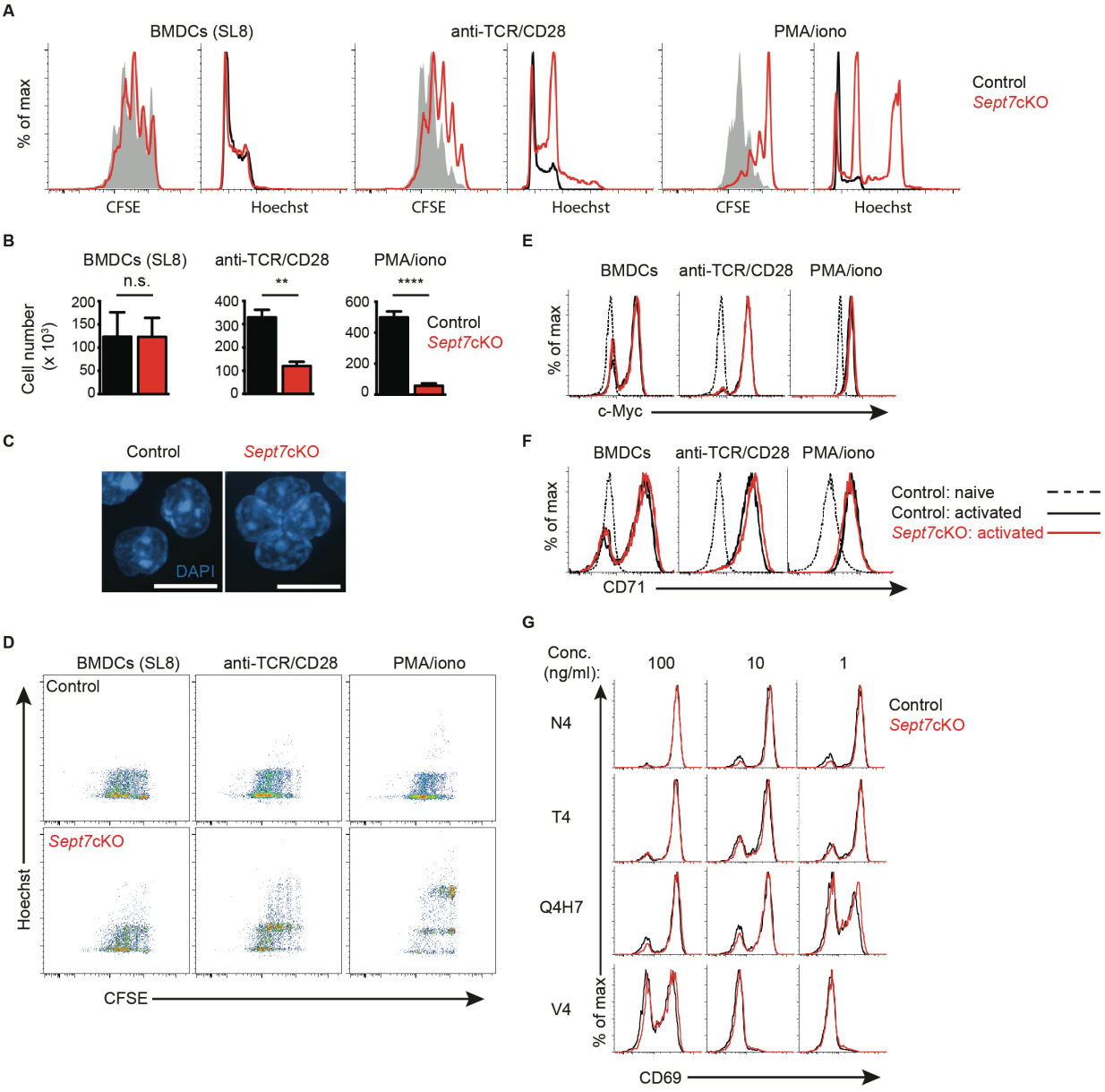
A
BMDCs (SL8)
anti-TCR/CD28
PMA/iono
% of max
CFSE
Hoechst
Control
Sept7cKO
B
BMDCs (SL8)
anti-TCR/CD28
PMA/iono
n.s.
**
****
Cell number (x 10³)
Control
Sept7cKO
C
Control
Sept7cKO
DAPI
D
BMDCs (SL8)
anti-TCR/CD28
PMA/iono
Control
Sept7cKO
Hoechst
CFSE
E
BMDCs
anti-TCR/CD28
PMA/iono
% of max
c-Myc
F
BMDCs
anti-TCR/CD28
PMA/iono
% of max
CD71
Control: naive
Control: activated
Sept7cKO: activated
G
Conc. (ng/ml):
100
10
1
N4
T4
Q4H7
V4
% of max
CD69
Control
Sept7cKO

Figure 3.2 Septin-deficient T cells exhibit selective cytokinetic defects upon APC-independent stimulation.
(**A-B**) Sept7cKO and control $CD8^+$ OT-I T cells were activated *in vitro* through co-culture with SL8-pulsed (100ng/ml) BMDCs, culture on plate-bound anti-TCR and soluble anti-CD28, or stimulation with PMA and ionomycin. Proliferation and cellular DNA content of live blasted cells were assessed by flow cytometry 72h later as indicated by CFSE dilution and Hoechst, respectively (**A**), along with cell number recovery (**B**). (**C**) Confocal images of fixed Sept7cKO and control $CD8^+$ polyclonal T cell nuclei stained with DAPI 48h after activation with PMA and ionomycin. Scale bar, 10mM. (**D**) Kinetics of OT-I multi-nucleation formation through comparison of CFSE and Hoechst content by flow cytometry 72h following a given activation condition. (**E, F**) Intracellular expression of c-myc (**E**) and cell surface expression of CD71 (F) expressed in naïve or activated live Sept7cKO and control $CD8^+$ OT-I T cells 24h after activation. (**G**) Cell surface CD69 levels expressed by live Sept7cKO and control $CD8^+$ OT-I T cells 24h after co-culture with BMDCs pulsed with a given OT-I peptide and concentration. Small horizontal lines denote the standard error of the mean (SEM). Data is representative of at least two (**C**) or three (**A, D-G**) independent experiments or pooled from the average values of technical triplicates from three independent experiments (**B**). *P < 0.05, **P < 0.01, ***P < 0.001, ****P < 0.0001 with data analyzed with unpaired *t*-test (**B**).

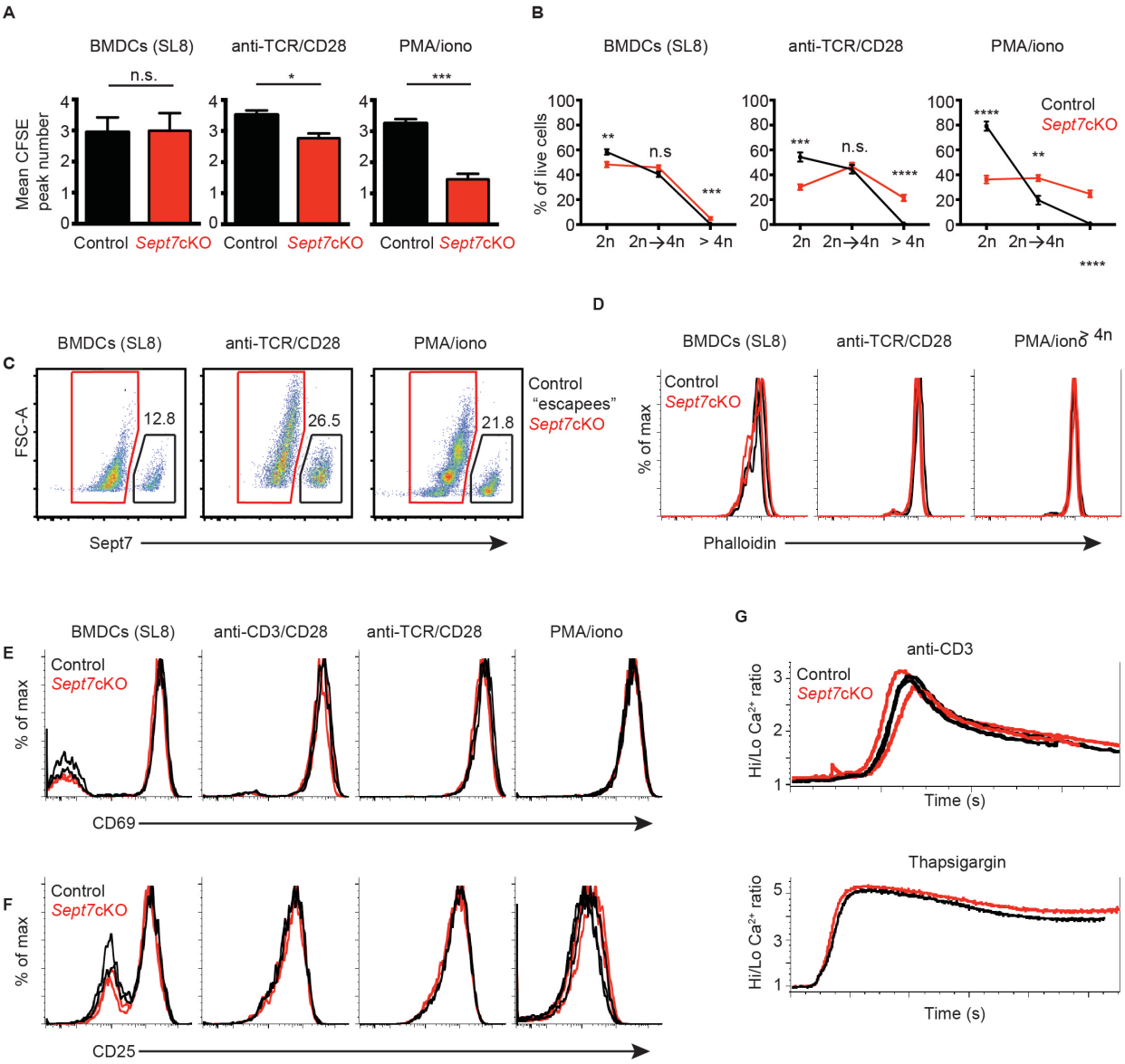
A
BMDCs (SL8)
anti-TCR/CD28
PMA/iono
n.s.
*
***
Mean CFSE peak number
Control
Sept7cKO
B
% of live cells
2n
2n→4n
> 4n
n.s
Control
Sept7cKO
C
FSC-A
12.8
26.5
21.8
Control "escapees" Sept7cKO
Sept7
D
% of max
Phalloidin
PMA/iono ≥ 4n
E
anti-CD3/CD28
CD69
F
CD25
G
anti-CD3
Hi/Lo Ca2+ ratio
Time (s)
Thapsigargin

Figure 3.3 Septin-deficient $CD8^+$ T cell multinucleated cell formation is associated with an increase in size despite similar initial F-actin levels and normal activation.
(**A-F**) Sept7cKO or control $CD8^+$ OT-I T cells were cultured *in vitro* with SL8-pulsed (100ng/ml) BMDCs, on plate-bound anti-CD3 or anti-TCR with soluble anti-CD28, or with PMA and ionomycin. Quantification of mean CFSE dilution peak number of live Sept7cKO and control OT-I T cells 72h after a designated *in vitro* condition (**A**). Frequency of live $CD8^+$ cells from Sept7cKO or control OT-I mice with a given DNA content level as assessed by Hoechst with flow cytometry 72h following *in vitro* activation (**B**). Comparison of cellular forward-scatter area and intracellular Septin 7 within $CD8^+$ T cells isolated from Sept7cKO OT-I lymph nodes 72h after *in vitro* activation. Gating delineates an "escapee" population of septin-competent T cells in Sept7cKO mice (**C**). F-actin levels in Sept7cKO and control $CD8^+$ OT-I T cells 24h following *in vitro* activation (**D**). Cell surface CD69 (**E**) and CD25 (**F**) levels expressed by $CD8^+$ OT-I T cells 24h after activation. (**G**) Calcium flux in isolated naïve $CD8^+$ OT-I T cells following stimulation by anti-CD3 clustering (**top**) or thapsigargin stimulation (**bottom**). The average of technical duplicate or triplicate samples for a given experiment and condition was calculated and graphed (**A, B**). Data is pooled from at least three (**A**) or six (**B**) independent experiments, or representative of at least three independent experiments (**C-G**). Small horizontal bars denote the SEM. *P <0.05, **P<0.01, ***P< 0.001, ****P< 0.0001 with data analyzed with unpaired *t*-test (**A, B**).

The division defect was not an obvious result of differential loss of filamentous actin with some stimuli and not others, as phalloidin staining at 24 h was identical between *Sept7*cKO and control OT-I cells (**Figure 3.3D**). Additionally, proximal signaling in response to all cues was unaffected by Septin 7 depletion. This was apparent in equivalent up-regulation of c-Myc and CD71 following all forms of stimulation (**Figure 3.2E,F**). Further, *Sept7*cKO OT-I cells stimulated by APC-dependent or -independent stimuli up-regulated CD69 and CD25 similarly (**Figure 3.3E,F**). Finally, *Sept7*cKO OT-I T cell calcium flux in response to anti-CD3 crosslinking or thapsigargin blockade of SERCA uptake was also equivalent to that of wild-type cells (**Figure 3.3G**). To determine whether the distinction amongst these stimuli related to strength-of-signal, we co-cultured T cells from control or *Sept7*cKO OT-I mice *in vitro* with BMDCs that had been pulsed with peptides differing in pMHC-OT-I-TCR affinity across a range of concentrations and measured CD69 up-regulation after 24 h (**Figure 3.2G**). Weak agonist peptides and lower doses induced less activation by this measure but *Sept7*cKO cells behaved identically to controls, demonstrating that *Sept7*cKO T cells sensed the density and identity of TCR signals similarly to wild-type cells. Thus, the differences we observed in *Sept7*cKO T cell proliferative capacity stimuli did not stem from defective TCR signaling or cell-cycle entry, but rather suggested that APCs contribute key cellular factors that facilitate division of *Sept7*cKO T cells.

*Sept7*cKO Division Defects with APC-independent Stimuli

Soluble cytokines also substantially drive T cell expansion and so we tested whether this stimulus would lead to cell division defects in septin-null T cells. We found that naïve septin-deficient $CD8^+$ OT-I T cells did not divide *in vitro* following exposure either to homeostatic cytokines IL-7 plus IL-15 or high concentrations of IL-2 (**Figure 3.4A, Figure 3.5A**)[318]. Again, defects in *in vitro* proliferation did not appear to result from dysfunctional signaling for *Sept7*cKO $CD8^+$ OT-I cells phosphorylated STAT5, a target of these cytokine receptors, to a similar extent as control T cells (**Figure 3.4B**). As with TCR-stimulation in the absence of APCs, soluble

cytokines induced multi-nucleated septin-deficient $CD8^+$ T cells (**Figure 3.4C**). The combination of APC-independent activation (PMA or anti-TCR) with addition of IL-2 also failed to rescue *in vitro* proliferation, suggesting that the defect observed did not result from inadequate cytokine production (**Figure 3.4D, Figure 3.5B**). Rather, we concluded that, in contrast to stimuli from BMDCs, cytokines alone fail to support cytokinesis of septin-null T cells.

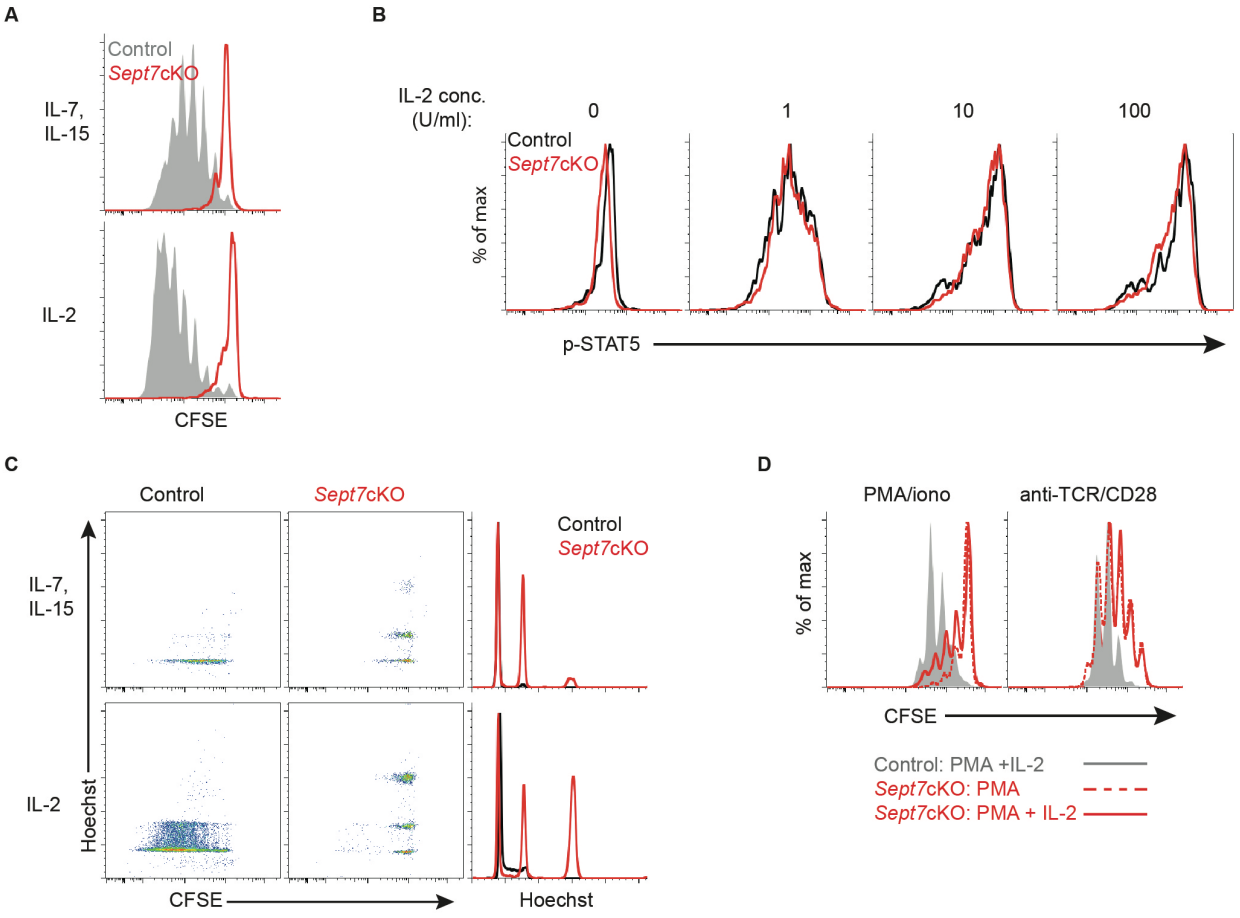
A
Control
Sept7cKO
IL-7,
IL-15
IL-2
CFSE
B
IL-2 conc.
(U/ml):
0
1
10
100
Control
Sept7cKO
% of max
p-STAT5
C
Control
Sept7cKO
IL-7,
IL-15
IL-2
Hoechst
CFSE
Control
Sept7cKO
Hoechst
D
PMA/iono
anti-TCR/CD28
% of max
CFSE
Control: PMA +IL-2
Sept7cKO: PMA
Sept7cKO: PMA + IL-2

Figure 3.4 Septin-deficient T cells undergo cytokinetic failure following cytokine exposure. (**A**) Proliferation as indicated by CFSE dilution of live naïve Sept7cKO and control $CD8^+$ OT-I T cells following *in vitro* culture with IL-7 (5ng/ml) and IL-15 (100ng/ml) (**top**), or IL-2 (5000U/ml) (bottom) for 5 days. (**B**) Intracellular levels of phosphorylated STAT5 in live control and Sept7cKO $CD8^+$ OT-I T cells following IL-2 exposure 24h after cells were stimulated with PMA and ionomycin. (**C**) CFSE dilution and Hoechst levels in live Sept7cKO and control $CD8^+$ OT-I T cells cultured *in vitro* with IL-7 and IL-15 (**top**) or IL-2 (**bottom**). (**D**) Proliferation of live Sept7cKO and control $CD8^+$ OT-I T cells 72h following *in vitro* activation as indicated with addition of IL-2 (10-20 U/ml) at initial plating. Data is representative of at least three independent experiments.

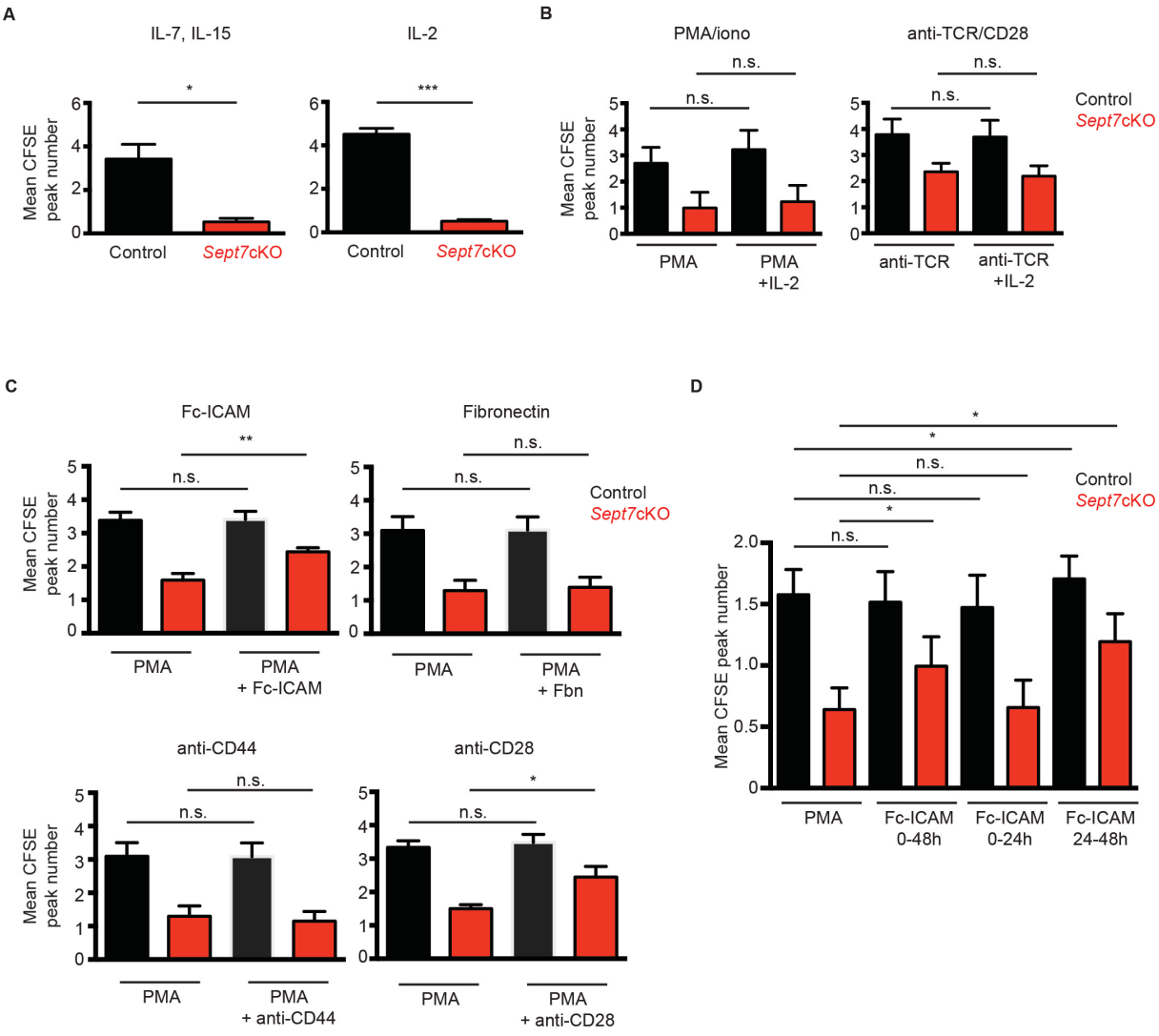
A
IL-7, IL-15
IL-2
Mean CFSE peak number
*
***
Control
Sept7cKO
B
PMA/iono
anti-TCR/CD28
n.s.
PMA
PMA +IL-2
anti-TCR
anti-TCR +IL-2
Control
Sept7cKO
C
Fc-ICAM
Fibronectin
anti-CD44
anti-CD28
**
PMA + Fc-ICAM
PMA + Fbn
PMA + anti-CD44
PMA + anti-CD28
D
Fc-ICAM 0-48h
Fc-ICAM 0-24h
Fc-ICAM 24-48h

Figure 3.5 Septin-null T cell division is enhanced by co-stimulatory but not cytokine signaling. (**A-D**) Sept7cKO and control OT-I T cells were stimulated *in vitro* and the mean CFSE peak number of live cells was quantified. Analysis of cell proliferation 5d after exposure *in vitro* to IL-7 (5ng/ml) and IL-15 (100ng/ml), or IL-2 (5000U/ml) (**A**), 72h after PMA/iono or anti-TCR activation with or without the presence of low-dose IL-2 (10-20U/ml) (**B**), 72h after PMA/iono activation in the presence of plate-bound Fc-ICAM, fibronectin anti-CD44, or anti-CD28 (**C**), or 48h following PMA/iono stimulation in conjunction with platebound Fc-ICAM for a designated temporal duration (**D**). The average of technical duplicate or triplicate samples was calculated and graphed. Small horizontal bars represent the SEM. Data is pooled from at least three independent experiments. *P< 0.05, **<P 0.01, ***P< 0.001 with data analyzed with unpaired (**A, C**), or paired (**B**) *t*-test, or a matched one-way ANOVA test with Fisher's LSD post-test (**D**).

Rescue of Defective Proliferation Through Cell Contacts

We next sought to determine whether BMDCs were providing additional signals that overcame a block in proliferation in *Sept7*cKO cells. To do so, we performed add-back *in vitro* experiments, using PMA and ionomycin as a base stimulus. Addition of peptide-pulsed BMDCs to these OT-I T cell cultures largely restored cell division as assessed by CFSE dilution (**Figure 3.6A, Figure 3.7A**)**.** This partial rescue was equivalent when BMDCs lacking antigenic peptide were added, demonstrating that BMDCs mediate rescue independently of their ability to generate strong TCR signals. However, supernatant from competent BMDC-T cell cultures, added at 20%, was unable to restore division, suggesting that cell-cell contact was primarily responsible. In addition, we found that resting B cells were unable to support cell division in *Sept7*cKO $CD8^+$ OT-I T cells whereas lipopolysaccharide (LPS)-activated B cells facilitated enhanced proliferation (**Figure 3.6B, Figure 3.8B**), though still not to the same extent as BMDCs (**Figure 3.6A**). That BMDCs and LPS-treated B cells supported *Sept7*cKO OT-I T cell division suggested that this rescue was mediated by cellular properties unique to highly activated APCs.

In addition to TCR signals, APCs provide numerous accessory cues for T cells and we investigated many of these. In doing so, we found that signaling from co-stimulatory molecules to CD28 and from ICAM adhesion molecules to integrin LFA-1 represented a prominent portion of the rescue; antigen-free BMDCs restored cell division to *Sept7*cKO OT-I cells and this was partially inhibited with blocking antibodies to CD80 and CD86 or antibodies to LFA-1 (**Figure 3.6C, Figure 3.7B**). This block was even more profound when anti-CD80/86 was combined with anti-LFA-1. Surprisingly, blockade mediated by these antibodies was nearly as effective when added 24 h after the initial stimulation with PMA and ionomycin plus BMDCs. This finding suggested that rescue of cell division was mediated by BMDCs in cell-cell contacts that take place well after the initiation of TCR signals.

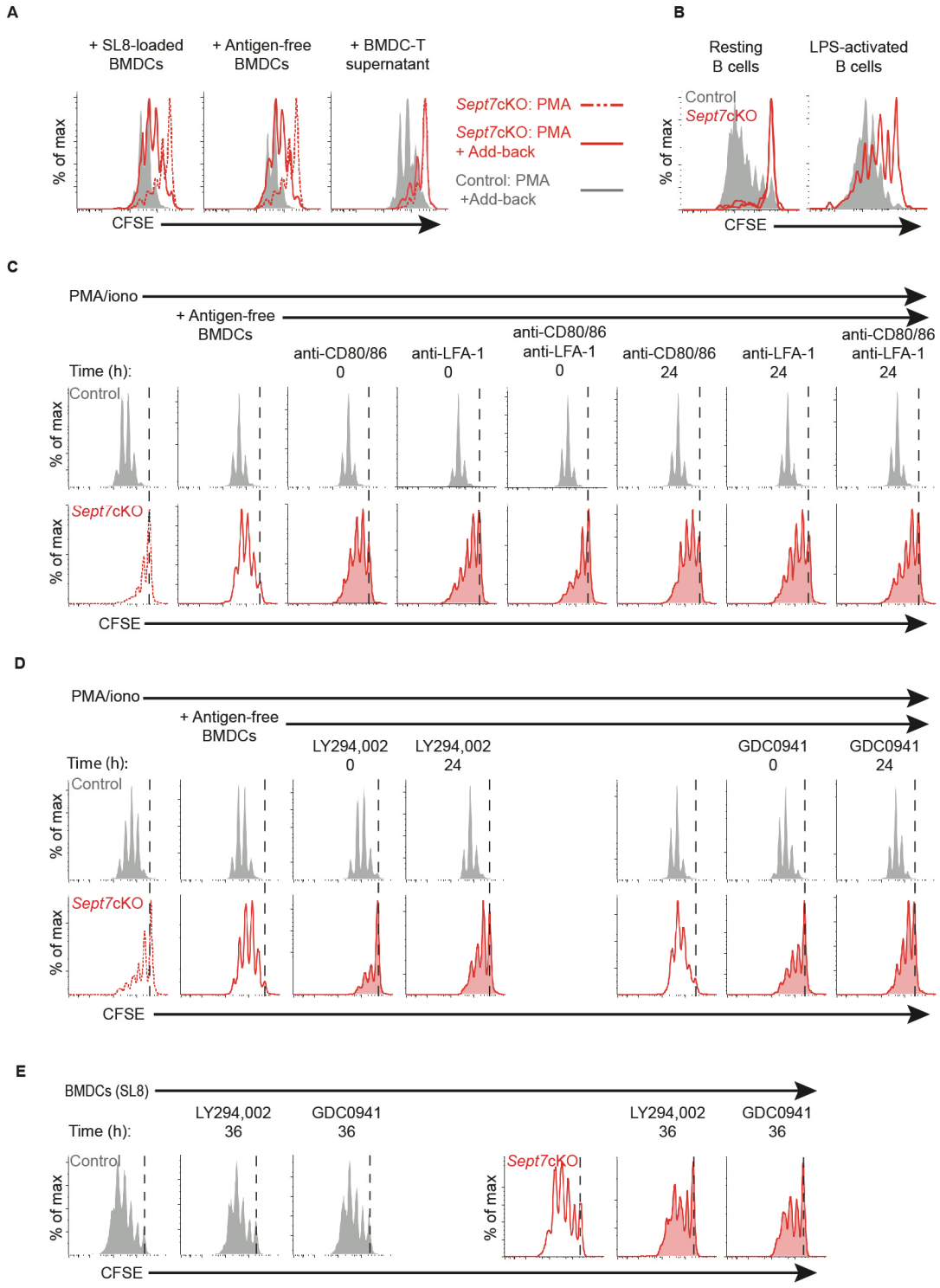
A
+ SL8-loaded BMDCs
+ Antigen-free BMDCs
+ BMDC-T supernatant
% of max
CFSE
Sept7cKO: PMA
Sept7cKO: PMA + Add-back
Control: PMA +Add-back
B
Resting B cells
LPS-activated B cells
Control
Sept7cKO
% of max
CFSE
C
PMA/iono
+ Antigen-free BMDCs
Time (h):
anti-CD80/86 0
anti-LFA-1 0
anti-CD80/86 anti-LFA-1 0
anti-CD80/86 24
anti-LFA-1 24
anti-CD80/86 anti-LFA-1 24
Control
Sept7cKO
% of max
CFSE
D
PMA/iono
+ Antigen-free BMDCs
Time (h):
LY294,002 0
LY294,002 24
GDC0941 0
GDC0941 24
Control
Sept7cKO
% of max
CFSE
E
BMDCs (SL8)
Time (h):
LY294,002 36
GDC0941 36
LY294,002 36
GDC0941 36
Control
Sept7cKO
% of max
CFSE

Figure 3.6 APCs mediate rescue of septin-null $CD8^+$ T cell cytokinetic defect through co-stimulatory PI(3)K signaling.
(**A**) CFSE dilution of live Sept7cKO or control $CD8^+$ OT-I T cells stimulated with PMA and ionomycin and co-cultured at the time of plating with SL8-pulsed (100ng/ml) BMDCs (**left**), unpulsed BMDCs (**middle**), or 20% supernatant generated from wild-type BMDC-T cell cultures (**right**). (**B**) CFSE dilution of live Sept7cKO or control $CD8^+$ OT-I T cells following 72h of co-culture with resting or LPS-treated SL8-pulsed splenic B cells. (**C, D**) CFSE dilution of live Sept7cKO or control $CD8^+$ OT-I T cells that were stimulated with PMA and ionomycin, co-cultured with unpulsed BMDCs, and subsequently treated with blocking antibodies against CD80, CD86, and/or LFA-1 (**C**), or PI(3)K inhibitors LY294,002 (10uM) or GDC-0941 (10uM) (**D**) at the designated time after initial plating. (**E**) CFSE dilution of Sept7cKO or control $CD8^+$ OT-I live blasted T cells that were co-cultured with SL8-pulsed (1-100ng/ml) BMDCs and treated with PI(3)K inhibitors LY294,002 (10uM) or GDC-0941 (10uM) 36h after plating. Data is representative of at least three (**A, E**), four (**B**), or five (**C, D**) independent experiments.

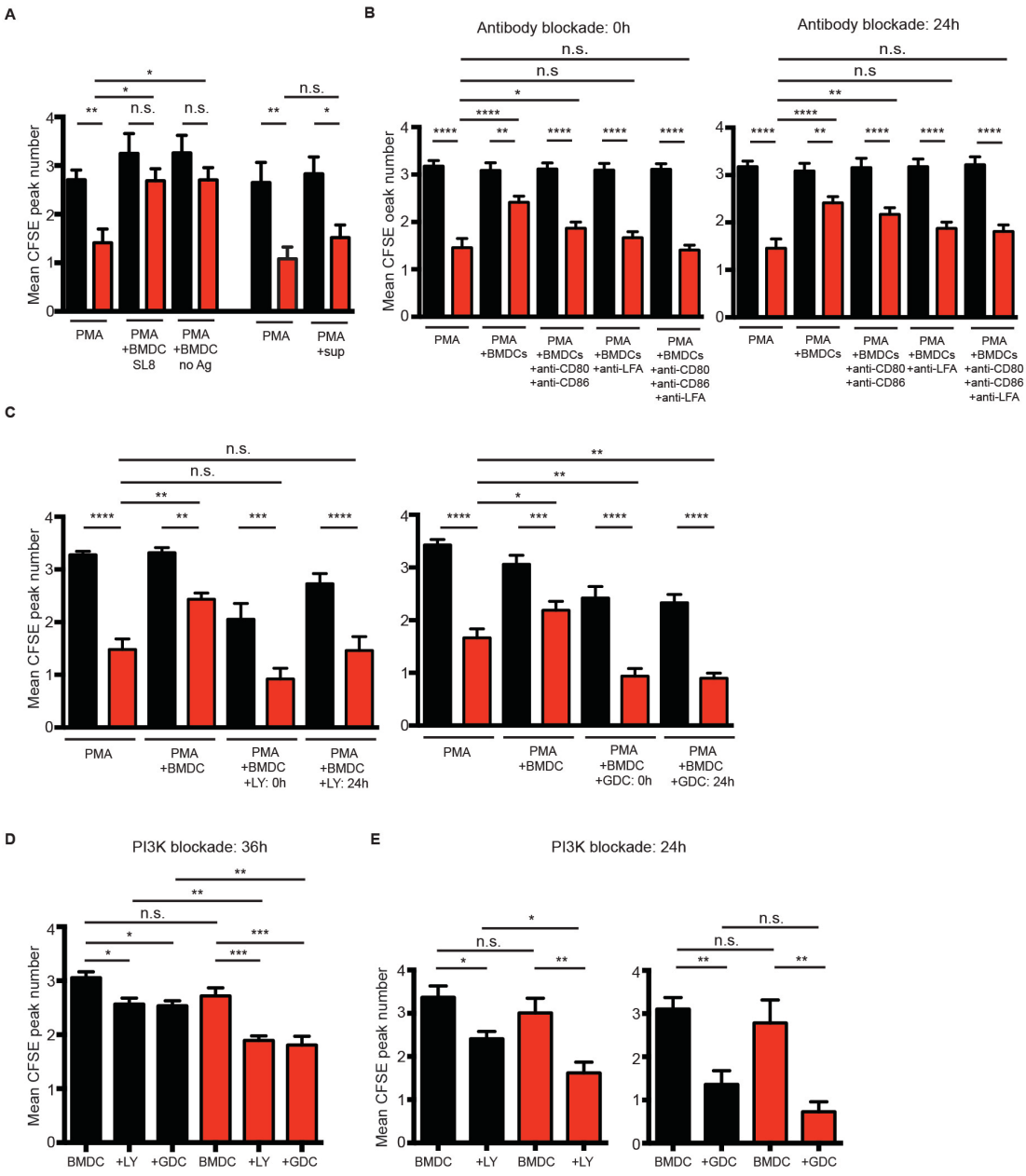
A
B
C
D
E
Mean CFSE peak number
Mean CFSE oeak number
Antibody blockade: 0h
Antibody blockade: 24h
PMA
PMA +BMDC SL8
PMA +BMDC no Ag
PMA +sup
PMA +BMDCs
PMA +BMDCs +anti-CD80 +anti-CD86
PMA +BMDCs +anti-LFA
PMA +BMDCs +anti-CD80 +anti-CD86 +anti-LFA
PMA +BMDC +LY: 0h
PMA +BMDC +LY: 24h
PMA +BMDC +GDC: 0h
PMA +BMDC +GDC: 24h
PI3K blockade: 36h
PI3K blockade: 24h
BMDC
+LY
+GDC
n.s.
n.s

Figure 3.7 BMDCs mediate septin-deficient T cell division through PI(3)K co-stimulatory signaling.
(**A-E**) Sept7cKO (**red**) and control (**black**) OT-I live cell mean CFSE dilution peak number was calculated following *in vitro* activation. Quantification of T cell CFSE dilution 72h following PMA/iono activation with addition of unpulsed or SL8-pulsed (100ng/ml) BMDCs, or supernatant from BMDC-T cell culture (**A**), 72h following PMA/iono activation with addition of unpulsed BMDCs and designated blocking antibody 0h (**left**) or 24h (**right**) after plating (**B**), 72h following PMA/iono activation with addition of unpulsed BMDCs and PI3K inhibitor LY294,002 (10μM) (**left**) or GDC-0941 (10μM) (**right**) (**C**), or 72h following activation with SL8-pulsed (1-100ng/ml) BMDCs with addition of PI3K inhibitor LY244,022 (10μM) or GDC-0941 (10μM) 36h (**D**) or 24h (**E**) after plating. The average of technical duplicate samples was calculated and graphed. Small horizontal bars denote the SEM. Data is pooled from at least three (**A, D, E**) or five (**B, C**) independent experiments. *P< 0.05, **<P 0.01, ***P< 0.001, ****P <0.0001 with data analyzed with an unmatched one-way ANOVA test with Fisher's LSD post-test.

To test whether these interactions were purely adhesive or resulted from signaling, we repeated the BMDC add-back experiments using several inhibitors that target phosphatidylinositol-3-OH kinase (PI(3)K), a key downstream signal transduction molecule in CD28 and LFA-1 pathways. We found that pan-PI(3)K inhibitor compounds LY294,002 and GDC-0941 blocked the BMDC-mediated rescue of *Sept7*cKO OT-I cell division with a modest reduction in control T cell proliferation (**Figure 3.6D, Figure 3.7C**). Wild-type cell viability, however, was not grossly impacted at the dose used (data not shown). Notably, blockade of PI(3)K signaling reduced septin-null OT-I T cell proliferation, whether added 24 h after BMDC addition, or at the onset of culture. To extend these findings to a more physiological setting, we similarly inhibited PI(3)K signaling 36 h after co-culturing *Sept7*cKO and control OT-I T cells with SL8-pulsed BMDCs and found that treatment reduced *Sept7*cKO T cell proliferation (**Figure 3.6 E, Figure 3.7D**). Interestingly, control T cell proliferation was again modestly inhibited, with a more substantial loss in proliferation if PI(3)K was inhibited 24 h after initial co-culture with BMDCs (**Figure 3.7E**). While the magnitude of this effect was larger for septin-null T cells, this implies that ongoing PI(3)K activity is required for maximal proliferation, even in wild-type T cells.

Consistent with these results, the differential capacity of resting or LPS-treated B cells in facilitating *Sept7*cKO OT-I T cell division was not due to differences in proximal T cell activation as assessed by CD69 up-regulation (**Figure 3.8A**). Rather, LPS-treated B cell-driven T cell division was similarly mediated through prolonged signaling via CD28 and LFA-1 and dependent upon PI(3)K (**Figure 3.8B, C**). Together these findings support a model whereby APCs establish a niche of cell-cell contact interactions characterized by PI(3)K signaling that complements or compensates for septin function in $CD8^+$ T cell division.

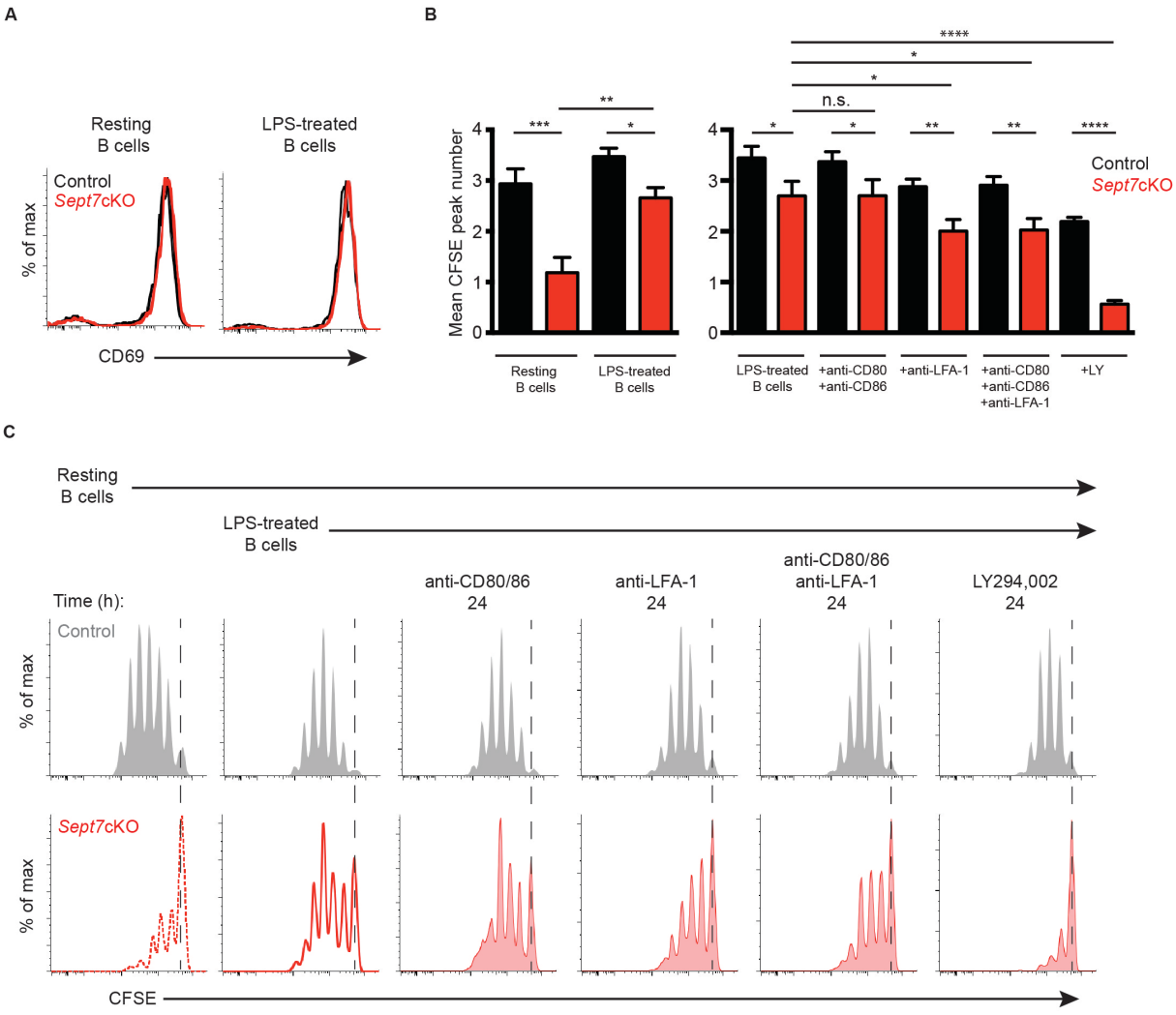
A
Resting
B cells
LPS-treated
B cells
Control
Sept7cKO
% of max
CD69
B
Mean CFSE peak number
Resting
B cells
LPS-treated
B cells
LPS-treated
B cells
+anti-CD80
+anti-CD86
+anti-LFA-1
+anti-CD80
+anti-CD86
+anti-LFA-1
+LY
Control
Sept7cKO
n.s.
C
Resting
B cells
LPS-treated
B cells
Time (h):
anti-CD80/86
24
anti-LFA-1
24
anti-CD80/86
anti-LFA-1
24
LY294,002
24
Control
Sept7cKO
% of max
CFSE

Figure 3.8 LPS-treated B cells enhance septin-null $CD8^+$ T cell division through co-stimulatory PI(3)K signaling.
(**A**) Cell surface expression of CD69 by Sept7cKO or control $CD8^+$ OT-I T cells following 24h of co-culture with SL8-pulsed (100ng/ml) resting or LPS-treated B cells. (**B**) Quantification of Sept7cKO and control OT-I live cell mean CFSE peak number 72h following *in vitro* co-culture with resting or LPS-treated B cells and addition of blocking antibodies against CD80, CD86, and/or LFA-1, or PI3K inhibitor LY294,002 (10μM). The average of technical duplicate samples was calculated and graphed. Small horizontal bars denote the SEM. (**C**) CFSE dilution of Sept7cKO or control $CD8^+$ OT-I T cells 72h after *in vitro* activation by resting or LPS-treated B cells and addition of denoted blocking antibodies, or PI3K inhibitor LY294,002 (10μM). Data is representative of at least three experiments. *P< 0.05, **P< 0.01, ***P< 0.001, ****P <0.0001 with data analyzed with an unmatched one-way ANOVA test with Fisher's LSD post-test (**B**).

Polarized Contacts Support *Sept7*cKO T cell Division

BMDCs bearing CD80, CD86, and ICAM-1 represent a likely polarized surface during cell division and we sought to address whether that feature was sufficient to complement septin deficiency. To address this, we cultured PMA-activated OT-I T cells on wells coated with adhesive molecules including ICAM-1, fibronectin, and antibodies against CD44 and CD28. Of these, ICAM-1 and anti-CD28 were uniquely capable of enhancing septin-null $CD8^+$ T cell division (**Figure 3.9A, Figure 3.5C**). These findings suggest that BMDCs facilitate septin-null division through specific signaling, not merely through general adhesion and cellular contact**.** Furthermore, by selectively plating OT-I T cells on ICAM-1 at various times during the stimulation, we determined that rescue was taking place at least 24 h after initial activation, but not at the time of initial stimulation (**Figure 3.9B, Figure 3.5D**). T cells begin dividing at least 24 h after activation[29] and so this temporal window coincided with the kinetics of T cell entry into the cell cycle and ongoing division.

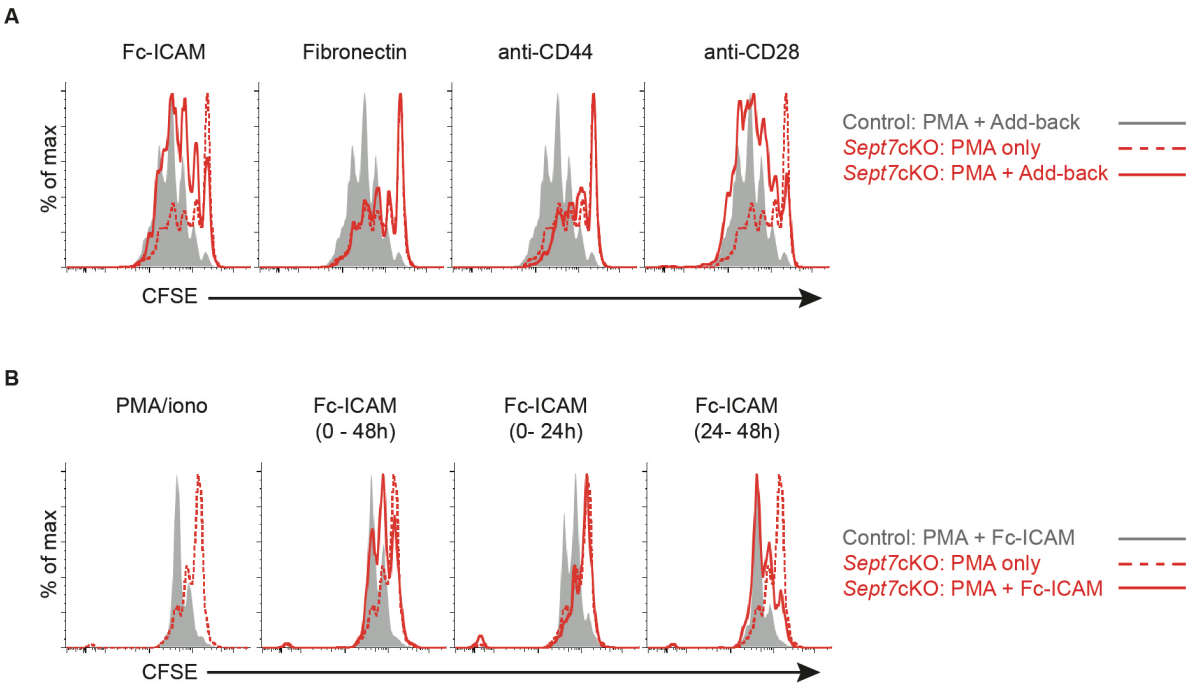
A
Fc-ICAM
Fibronectin
anti-CD44
anti-CD28
% of max
CFSE
Control: PMA + Add-back
Sept7cKO: PMA only
Sept7cKO: PMA + Add-back
B
PMA/iono
Fc-ICAM (0 - 48h)
Fc-ICAM (0- 24h)
Fc-ICAM (24- 48h)
% of max
CFSE
Control: PMA + Fc-ICAM
Sept7cKO: PMA only
Sept7cKO: PMA + Fc-ICAM

Figure 3.9 Co-stimulatory signaling is sufficient to enhance septin-null $CD8^+$ T cell division. (**A**) CFSE dilution of live Sept7cKO or control $CD8^+$ OT-I T cells stimulated with PMA and ionomycin and cultured on plate-bound Fc-ICAM, fibronectin, anti-CD44, or anti-CD28 for 72h. (**B**) CFSE dilution of live Sept7cKO or control $CD8^+$ OT-I T cells stimulated with PMA and ionomycin for 48h and cultured on plate-bound Fc-ICAM for a designated interval of time following initial plating. Data is representative of at least three independent experiments.

Septin Dependence Separates Proliferation Drivers *in vivo*

Our *in vitro* findings suggested that the requirement for septins in T cell division distinguishes cell division that is driven by the presence or absence of specific contacts or niches. We therefore compared different activating stimuli *in vivo*. Using the Dec-OVA model of antigen delivery to load antigens onto lymph node resident DCs[319] we found that adoptively transferred septin-null $CD8^+$ OT-I T cells expanded similarly to their co-transferred wild-type counterparts (**Figure 3.10A**). To test whether *Sept7*cKO T cells continue to require the presence of antigen-loaded APCs after initial activation, CFSE-labeled *Sept7*cKO and control $CD8^+$ OT-I T cells were co-cultured *in vitro* with SL8-pulsed BMDCs for 36 h, at which point the T cells were isolated. *Sept7*cKO and control T cells were then re-plated *in vitro* or co-transferred to antigen-free mice. When the T cells were cultured *in vitro*, *Sept7*cKO T cells exhibited notable cell division defects (**Figure 3.10B**, top). *Sept7*cKO T cells, however, were able to divide proficiently compared to control T cells when transferred to antigen-free host mice (**Figure 3.10B**, bottom). These findings suggest that while *Sept7*cKO T cells do not require antigen-bearing APCs during cell division, endogenous interactions *in vivo* that are absent from the T cell-only culture are sufficient to support successful cell division.

In contrast, when anti-IL-2 complexes were delivered to generate cytokine mediated proliferation in the absence of overt APC involvement, expansion of adoptively transferred septin-null OT-I T cells was significantly reduced compared to that of control cells (**Figure 3.10C).** As an additional cytokine-mediated *in vivo* challenge, we transferred polyclonal wild-type and *Sept7*cKO cells into sub-lethally irradiated mice. In these mice, T cells typically undergo a slow form of lymphopenic-induced proliferation, which is thought to mimic an acute form of homeostatic expansion[184]. Again, septin-null $CD8^+$ T cells were impaired in their overall expansion (**Figure 3.10D**). These findings support a context-dependent requirement for septins in T cell division and extend our model to critical *in vivo* processes.

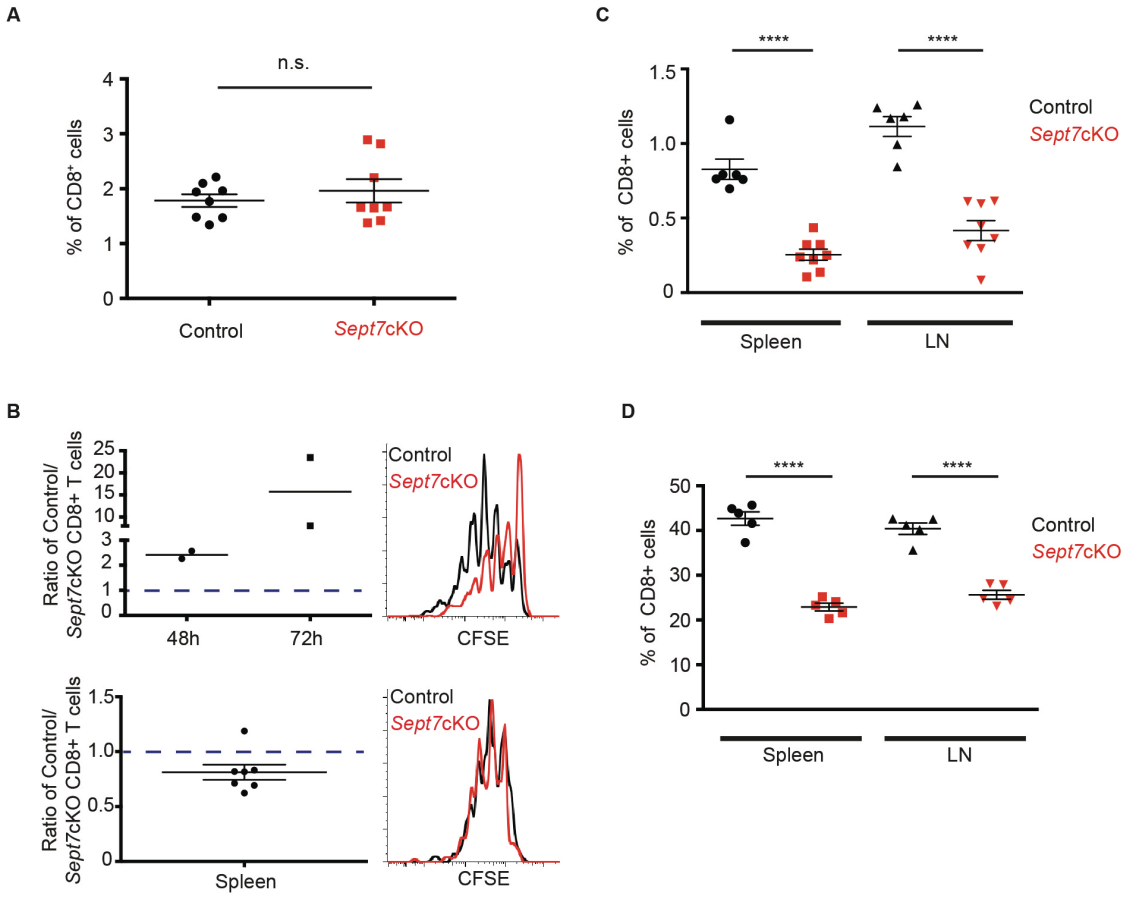
A
n.s.
% of CD8+ cells
Control
Sept7cKO
C
****
****
% of CD8+ cells
Control
Sept7cKO
Spleen
LN
B
Ratio of Control/ Sept7cKO CD8+ T cells
48h
72h
Control
Sept7cKO
CFSE
Ratio of Control/ Sept7cKO CD8+ T cells
Spleen
Control
Sept7cKO
CFSE
D
****
****
% of CD8+ cells
Control
Sept7cKO
Spleen
LN

Figure 3.10 Septin deficiency differentiates APC- and cytokine-driven division *in vivo*.
(**A**) Frequency of co-transferred control or Sept7cKO $CD8^+$ OT-I T cells that expanded in draining inguinal lymph nodes of host mice that had been immunized subcutaneously with Dec205-OVA and anti-CD40 6d prior. (**B**) Naïve Sept7cKO and control $CD8^+$ OT-I T cells were co-cultured with SL8-pulsed (100ng/ml) BMDCs *in vitro*, isolated 36h later, and either co-cultured *in vitro* with low-dose IL-2 (10U/ml) (**top**) or co-transferred to antigen-free host mice (**bottom**). Ratio of control to Sept7cKO live T cells 48h or 72h following *in vitro* culture, along with a representative CFSE dilution profile 48h after T cell isolation (**top**). Ratio of control to Sept7cKO T cells recovered from host mouse spleen 48h after co-transfer, as well as CFSE dilution of cells (**bottom**). *P value = 0.0351 with data analyzed with 1-sample *t*-test comparing distribution to theoretical mean of 1. (**C**) Frequency of $CD45.2^+$ $CD8^+$ OT-I T cells that expanded in the spleen and inguinal lymph nodes of $CD45.1^+$ host mice following IL-2 complex delivery i.p.daily for 7 days. (**D**) Frequency of co-transferred Sept7cKO and control polyclonal $CD8^+$ T cells in the spleen and skin-draining lymph nodes of sub-lethally irradiated mice.
Each symbol represents an inguinal lymph node (left or right flank) from host mice (**A**), individual host mice (**B**-**D**), or an *in vitro* culture sample (**B**). Small horizontal lines demarcate the SEM. Data is representative of at least three independent experiments with n = 3-5 mice (**A, D**), or pooled from at least two (**B; top**) or three experiments with total n = 7 (**B; bottom**) or 8 mice (**C**). *P < 0.05, **P < 0.01, ***P < 0.001, ****P < 0.0001 with data analyzed with paired (**A, D**), or unpaired (**C**) *t*-test.

Septin Requirement for CD8$^+$ T cell Homeostasis

We found evidence for defects in steady-state homeostatic maintenance of naïve and memory CD8$^+$ *Sept7*cKO T cells, which is in agreement with findings that Septin 7 is required for cytokine-driven proliferation. Although peripheral CD8 compartments were comparable between *Sept7*cKO and control OT-I mice at 6–8 weeks of age, the frequency of CD8$^+$ T cells declined after 6 months (**Figure 3.11A,** left, middle). In addition, we found that this was accompanied by a significant loss of phenotypically naïve CD44$^{low/med}$ CD8$^+$ T cells in aged *Sept7*cKO OT-I mice. Of the CD8$^+$ T cells that remained in aged *Sept7*cKO mice, CD8$^+$ T cells were broadly CD44^{hi} as compared to bimodal expression in control mice (**Figure 3.11A**, right), suggesting a lymphopenic environment in which these surviving *Sept7*cKO CD8$^+$ T cells may be responding to antigen[320,321]. Given that memory CD8$^+$ T cell homeostasis also relies on cytokines, we examined maintenance of memory CD8$^+$ *Sept7*cKO T cells. Naïve *Sept7*cKO and wild-type CD8$^+$ OT-I T cells were co-transferred to host mice that were immunized i.v. with DecOVA. *Sept7*cKO T cells were detected 14 days later at similar frequency in the spleen (**Figure 3.11B,** left), although slightly reduced in number in lymph nodes (**Figure 3.12A**), and highly expressed memory precursor cell (MPEC) markers CD44 and CD62L (**Figure 3.12B**). These *Sept7*cKO and wild-type OT-I T cells were then sorted from the spleen and lymph nodes and co-transferred to antigen-free mice. The frequency of *Sept7*cKO and control T cells was determined 8 weeks later as previous studies have demonstrated that multiple rounds of homeostatic turnover occurs over this period of time[322]. Indeed when quantified, the frequency of *Sept7*cKO T cells was significantly lower than control T cells in antigen-free host spleens (**Figure 3.11B,** right), indicating a role for septins in facilitating memory T cell homeostasis. In contrast, while we noted a trend toward preferential wild-type T cell maintenance in the lymph node, it was not as severe as in the spleen (**Figure 3.12C**). This observation may speak to intriguingly different milieus between the two organs that support homeostatic division, but

remains an area of future investigation. Altogether, this data demonstrates that a lack of septins impedes T cell division in a stimulus-dependent manner *in vivo*.

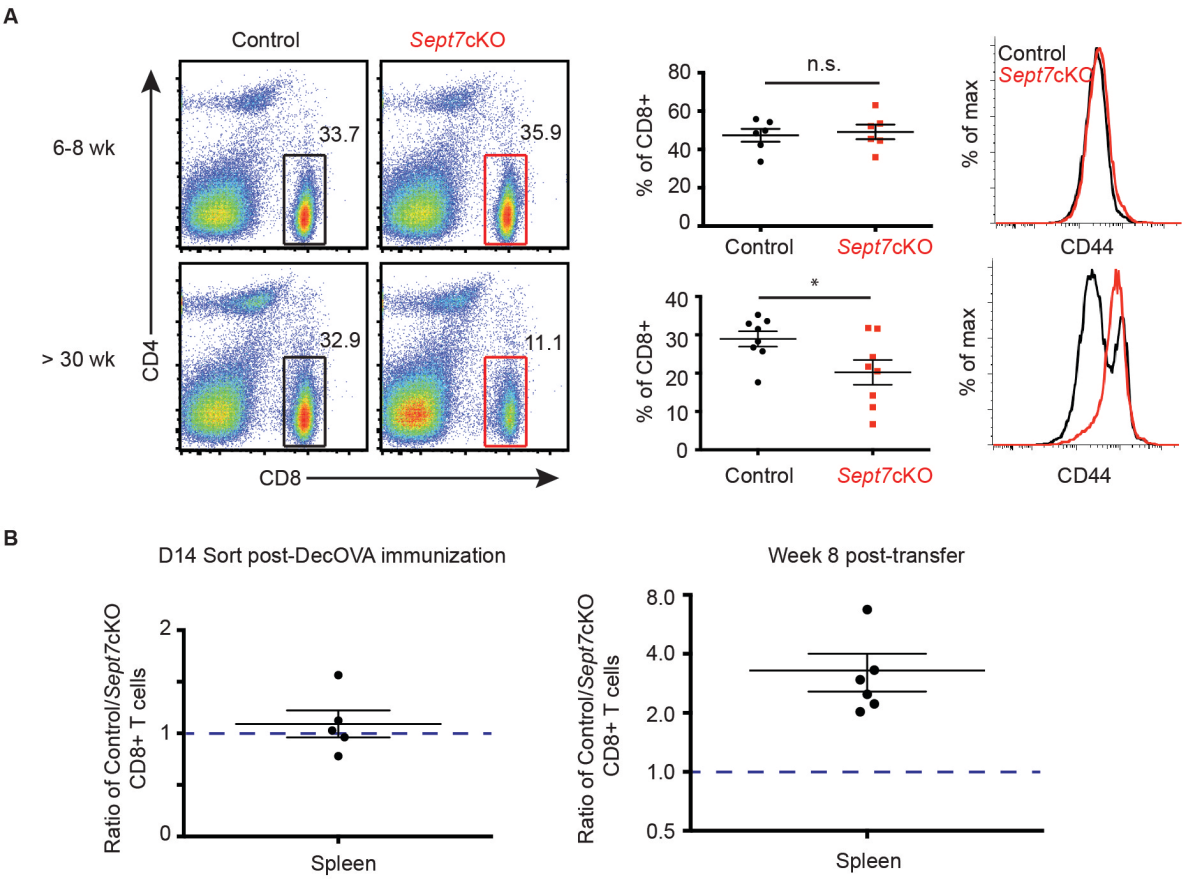
A
Control
Sept7cKO
6-8 wk
> 30 wk
CD4
CD8
33.7
35.9
32.9
11.1
n.s.
% of CD8+
Control
Sept7cKO
*
% of max
CD44
B
D14 Sort post-DecOVA immunization
Week 8 post-transfer
Ratio of Control/Sept7cKO CD8+ T cells
Spleen

Figure 3.11 Septins are required for homeostatic maintenance of naïve and memory $CD8^+$ T cells *in vivo*.
(**A**) Frequency of $CD8^+$ T cell population (**left**) and $CD8^+$ T cell CD44 surface expression (**right**) in pooled lymph nodes of 6-8 week-old (**top**) or 6-month-old (**bottom**) OT-I mice. (**B**) Sept7cKO and control OT-I T cells were transferred to mice which were then immunized i.v. with DecOVA. OT-I T cells were sorted from immunized mouse spleen and lymph nodes 14d later, and co-transferred to antigen-free host mice. Ratio of control to Sept7cKO cells sorted from spleen 14d post-DecOVA immunization (**left**). Ratio of control to Sept7cKO T cells recovered from spleens of antigen-free host mice 8 weeks after transfer (**right**). Non-significant P value (> 0.05) (**left**) and *P value = 0.0243 (**right**) with data analyzed with 1-sample *t*-test comparing distribution to theoretical mean of 1 (**B**). Each symbol represents an individual mouse (**A, B; right**) or an independent experiment (**B; left**). Small horizontal lines denote the SEM. Data is pooled from at least four independent experiments with total n = 8 (**A**), 5 (**B; left**), or 6 (**B; right**). *P <0.05 with data analyzed with unpaired *t*-test (**A**).

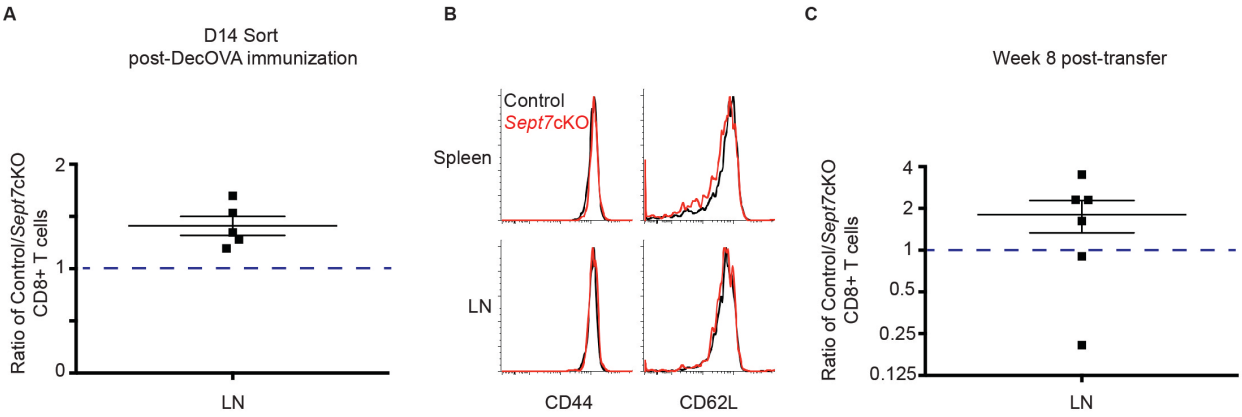
A
D14 Sort
post-DecOVA immunization
Ratio of Control/Sept7cKO
CD8+ T cells
2
1
0
LN
B
Control
Sept7cKO
Spleen
LN
CD44
CD62L
C
Week 8 post-transfer
Ratio of Control/Sept7cKO
CD8+ T cells
4
2
1
0.5
0.25
0.125
LN

Figure 3.12 Homeostatic maintenance of septin-deficient and control $CD8^+$ memory T cells in the lymph node.
(**A-C**) Sept7cKO and control OT-I T cells were transferred to DecOVA-immunized mice, sorted from the spleen and lymph nodes 14d later, and co-transferred to antigen-free host mice. Ratio of control to Sept7cKO OT-I T cells sorted from lymph nodes 14d post-DecOVA immunization. *P value = 0.0107 with data analyzed with 1-sample *t*-test comparing distribution to theoretical mean of 1 (**A**). Surface expression of CD44 and CD62L on Sept7cKO and control OT-I T cells sorted from pooled spleen and lymph nodes 14d post-DecOVA immunization (**B**). Ratio of control to Sept7cKO OT-I T cells recovered from pooled skin-draining lymph nodes 8 weeks following co-transfer to antigen-free hosts. Non-significant P value (> 0.05) with data analyzed with 1-sample *t*-test comparing distribution to theoretical mean of 1 (**C**). Each symbol represents an individual experiment (**A**) or mouse (**C**). Small horizontal lines demarcate the SEM. Data is pooled from at least four independent experiments (**A, C**) or representative of two independent experiments (**B**).

III. DISCUSSION

The significance of these results is that we have identified a situation and mechanism that differentiates APC/niche-driven proliferation from niche-independent division. This suggests that specific types of T cell division might be differentially targeted in the future, for example with cytoskeletal inhibitors. This is of particular importance since homeostatic expansion arising from lymphopenic conditions can result in organ transplant rejection or possibly autoimmunity, and is not responsive to co-stimulatory blockade[323,324,325,326,327]. In fact, a preponderance of clinical immunosuppressive agents are actually directed against antigen-specific T cell expansion, typically targeting pathways downstream of T cell activation such as mTOR or calcineurin[324]. Drugs that are available to restrict homeostatic division such as MMF target non-specific processes like DNA synthesis[328] that are characteristic of all forms of T cell division, and thus leave patients ill-equipped to face pathogen challenge. Our work suggests that targeting septins and the pathways they use might yield better therapeutic strategies in these cases.

Previous to this work, it had been found that T cells, amongst a select few eukaryotic cells, did not appear to require septins to complete cell division[208,210]. Now, we understand that the T cell exception reflects, not a cell-type, but a context-dependent role of septins in cell division. In the case of T cells, the context that rescues T cell division is the presence of a highly adhesive and activated surface or cell type. Previous *in vivo* lymph node imaging studies of proliferating T cells demonstrate antigen-specific T cells dividing independently of contact with labeled APCs[309], though division following DC contact has also been noted[329]. Our findings that APCs or surfaces high in specific co-stimulatory molecules and integrins rescue septin-null T cell cytokinetic defects *in vitro* and *in vivo* provide support that a niche, in which T cells engage in contact interactions during the temporal window of division, serves a functional role. We observed a spectrum of septin-null T cell proliferative competence across the conditions PMA/ionomycin, anti-TCR/anti-CD28, or antigen-pulsed APCs, an effect that thus corresponds to the degree of PI(3)K signaling expected to be generated by these stimuli. It may thus be that

a threshold of total PI(3)K signaling must be reached for T cells to divide in the absence of septins. Yet, cytokines like IL-7 and IL-2 generate PI(3)K activity through their receptors as well, and we did not find partial or full rescue of the cytokinesis defect in these conditions. Distinctions in how and when PI(3)K is active likely underlie this, and it is also possible that the activating PI(3)K cue could be counterbalanced by additional cell-cell cues. Based on the data, we favor a model in which APCs can mediate septin-null cell division by providing a highly polarized source of PI(3)K signaling and/or stabilized cell cortex, given at or near the time of cell division.

As septins have been described to establish polarity in yeast and reinforce local membrane compartmentalization by serving as a diffusion barrier[279,242,330], it is tempting to speculate that septins and PI(3)K may cooperate or act redundantly to ensure that proper polarity is maintained while T cells undergo cell division. Notably, compartmentalization of phospholipids has been described as important during cytokinesis as the cytokinetic furrow is enriched for phosphatidylinositol-(4,5)-bisphosphate (PtdIns(4,5)P_2)[331,332]. While previous studies have found PI(3)K signaling within the first 8 h of T cell activation to be the most critical in impacting eventual proliferation[333], our data using PI(3)K inhibitors suggests that PI(3)K signaling even 24 h post-T cell activation continue to regulate wild-type T cell proliferative potential and kinetics. Indeed, one area where a dual PI(3)K–septin pharmacological inhibition might prove selective would be in blocking antigen-independent proliferation of leukemic cells while sparing the proliferation of antigen-dependent host T cells.

One surprising result of our data in this paper and previous is that T cell signaling, even at a synapse, is independent of septins. In fact, our original impetus for studying these proteins was that they assemble more densely as a ring around the immune synapse (IS) (J.G. and M.F.K., unpublished). To this extent, our collective data is at odds with recent studies which used shRNA approaches to implicate septins in efficient STIM1 and ORAI co-localization and subsequent calcium flux in HeLa, Jurkat, and HEK cells[253,334]. We, in contrast, did not find that

differences in septin-deficient T cell division capacity stemmed from defects in TCR signaling processes. One possible reason for this difference would be some form of compensation in our cells for this specific septin function. The presence of cell division defects argues against ubiquitous compensation, and the idea of signaling-specific compensation is not supported by data in which normal calcium flux was observed despite Cre transfection of *Sept7*$^{flox/flox}$ T cell blasts (A.M.M. and M.F.K., unpublished). An alternative explanation for the apparent septin defect reported in cell lines may be that these cells are experiencing cytokinetic failure, and thus defective signaling is relatively distal to septin deficiency. At present, although we cannot support that there is a requirement of septins for T cell calcium signaling, further work may be needed to determine how and when our findings align with previous signaling studies.

Why were we ever able to isolate T cells from the periphery of conditional knockout mice if cell division is possibly compromised? One answer is that while the *Cd4*-Cre allele depletes septins in the pre-DP window, T cells post-DP stage typically do not divide again unless called upon to do so for homeostatic expansion. Additionally, with respect to homeostatic processes, although septin-null cells are clearly defective in expanding *in vivo* when transferred to a sub-lethally irradiated mouse, the effect was not as profound as the division defect to pure cytokines *in vitro*. It may be that some maintenance, if not expansion, of T cells in developing mice can involve synaptic cell-cell encounters that are septin-independent. For example, IL-15 is trans-presented to CD8$^+$ T cells by another cell bearing the alpha chain[335]. Additionally, T cells at steady-state engage in cellular contact with APCs presenting self-pMHC and/or fibroblastic reticular cells (FRCs) that produce homeostatic cytokines like IL-7[5].

What is the breadth of this requirement? Septin-null T cells did appear to selectively lose CD44$^-$CD8$^+$ populations in lymph nodes[320,321] and we also observed defective homeostasis of memory CD8$^+$ OT-I *Sept7*cKO T cells in the spleen. In light of the trend in septin requirement, these findings suggest that endogenous cell-cell contacts in these settings do not mediate *Sept7*cKO T cell division like endogenous cell-cell contacts do for activated T cells. Although

we found no specific defects in septin-deficient T cells for effector generation as assessed by surface markers or interferon-g at day 6 post-immunization (A.M.M, J.G. and M.F.K., unpublished), late-stage cellular contacts such as those during asymmetric cell division or in late-stage T-T interactions[31,32]may supply an additional higher degree of complexity in T cell effector and memory development, as well as clonal burst size and sustained survival. In sum, septin-dependent versus -independent immune cell cytokinesis indicates the possibilities for enhanced selective targeting of proliferative processes.

IV. METHODS

Mice

*Sept7*cKO *Sept7*$^{flox/flox}$ mice[210] were crossed to *Cd4*-Cre transgenic mice[317] to deplete Septin 7 in T cells. These mice were bred to Ovalbumin (OVA)-specific TCR transgenic OT-I mice[336] and/or mTmG mice[316] (The Jackson Laboratory). Cells designated as experimental controls were generated from *Sept7*$^{flox/flox}$ *Cd4*-Cre^{-} or *Sept7*$^{flox/-}$ *Cd4*-Cre^{+} mice. These mice, along with C57BL/6 (The Jackson Laboratory and Simonsen) and CD45.1^{+} mice, were housed and bred under specific pathogen-free conditions at the University of California Animal Barrier Facility. All experiments using mice were approved by the Institutional Animal Care and Use Committee of the University of California.

Cell isolation

CD8^{+} polyclonal or OT-I T cells were isolated from lymph nodes of 6–8-week-old mice using EasySep CD8 negative selection kits (STEMCELL Technologies). B cells were isolated from spleens of 6–8-week-old mice using EasySep B cell negative selection kits (STEMCELL Technologies). In specified experiments, B cells were treated with 1 mg/ml LPS (Sigma-Aldrich) for 5 h before use. BMDCs were generated from treating cultured bone marrow cells with GM-CSF (granulocyte-macrophage colony-stimulating factor) for 7–11 days. IL-4 was added for the last 2 days with 1 mg/ml LPS stimulation 6–24 h before use. BMDCs and B cells were incubated with 1–100 ng/ml SL8 OVA peptide (SIINFEKL) (Anaspec), or variant peptides N4, T4, Q4H7, V4 (gift from E. Palmer and D. Zehn) for at least 30 min at 37°C and washed 3 times.

Immunoblot

Naïve CD8^{+} T cells were isolated from 6 week-old *Sept7*cKO and littermate control OT-I mice. 10^{6} cells per sample were lysed in PBS containing 1% Triton X-100 in the presence of a cocktail of protease and phosphatase inhibitors (2 mg/ml aprotinin, 2 mg/ml leupeptin, 2 mM

phenylmethyl sulfonyl fluoride (PMSF), 10 mM sodium fluoride, 10 mM iodoacetamide and 1 mM sodium orthovanadate). After 15 min lysis on ice, lysates were spun at high speed for 10 min to remove insoluble material and protein concentration in the supernatant was quantified by the Bio-Rad detergent-compatible protein assay to ensure equal loading. Samples were resolved by SDS-PAGE, and immunoblot analysis was performed using rabbit polyclonal primary antibodies against Sept1, Sept6C, Sept9^{241}, Sept7 (IBL-America, Inc.), and HRP-Conjugated Goat anti-Rabbit secondary antibody (Jackson ImmunoResearch) Relative protein abundance was quantified using ImageJ software (NIH).

***In vitro* T cell activation assays**

Isolated T cells were labeled with 0.5–5 mM CFSE (carboxyfluorescein diacetate succinimidyl ester; Invitrogen) or CellTrace Proliferation Dye (BD Biosciences) for 15 min at 37 °C, cultured in 96-well plates at a density of 0.1 × 10^6/ml in complete RPMI and harvested for analysis 72 h later unless noted otherwise. $CD8^+$ T cells were cultured on plate-bound anti-CD3 (2C11; UCSF Hybridoma Core) or anti-TCRb (H57-597; produced in our lab) with addition of soluble anti-CD28 at 2 mg/ml (PV-1; UCSF Hybridoma Core). Alternatively, T cells were stimulated with 100–1000 ng/ml PMA (phorbol 12-myristate 13-acetate) and 125 ng/ml ionomycin. In specified experiments 10–20 U/ml of recombinant human IL-2 (NIH AIDS Reagent Program) or 20% supernatant harvested from previous wild-type BMDC-T cell cultures was added at time of plating. For other indicated experiments, 96-well plates were coated with the following antibodies or proteins: 10 mg/ml anti-CD44 (IM7, eBiosciences), 10 mg/ml anti-CD28 (PV-1; UCSF Hybridoma Core), 5 mg/ml recombinant mouse ICAM-1 Fc Chimera protein (R&D Systems), or 10 mg/ml fibronectin, bovine plasma (EMD Millipore). In some experiments, cells were moved to or removed from plates containing ICAM-1 Fc Chimera protein, prepared as detailed above.

In co-culture experiments, OT-I T cells were plated with activated BMDCs at a 10:1 ratio in flat-bottom wells, or with isolated B cells at a 1:1 ratio in round-bottom wells. In specified experiments, 10 mM of PI(3)K inhibitors LY-294,002 (Sigma-Aldrich) or GDC-0941 (gift from J. Roose) was added to culture 24 h or 36 h after plating. For BMDC rescue assays, T cells were stimulated with PMA and ionomycin, and mature activated BMDCs were added at time of plating. To block co-stimulatory signaling, 10 mg/ml anti-CD80 (16-10A1; UCSF Hybridoma Core) and 10 mg/ml anti-CD86 (GL-1; UCSF Hybridoma Core) and/or anti-CD11a (M17/4; UCSF Hybridoma Core) was added to culture 0 or 24 h after plating. Alternatively, 10 mM of LY-294,002 or 10 mM GDC-0941 was added 0 or 24 h after plating. In other experiments, T cells were plated with activated BMDCs at a 5:1 ratio, isolated with a CD8 negative selection kit, and re-plated with 10 U/ml of human recombinant IL-2.

Cytokine exposure

Isolated $CD8^+$ OT-I T cells were cultured in 96-well plates at a density of 0.1×10^6/ml. 5000 U/ml of human recombinant IL-2, or murine recombinant 5 ng/ml IL-7 (Peprotech) and 100 ng/ml IL-15 (Peprotech) were added to media at time of plating, with cells harvested for analysis 5 days later.

Surface and intracellular flow cytometry staining

Cells were harvested from lymph nodes, spleens, or *in vitro* culture, washed with PBS and non-specific binding blocked with flow cytometry buffer (PBS, 2% FCS) and anti-CD16/32 (2.4G2; UCSF Hybridoma Core). Surface proteins on cells were stained with the following antibodies for 25 min at 4 °C: anti-CD69 (H1.2F3; eBiosciences), anti-CD25 (PC61.5; eBiosciences), anti-CD71 (C2, BD Pharmingen), anti-CD8a (53-6.7 eBiosciences), anti-CD4 (RM4-5; BioLegend), anti-CD44 (IM7; eBiosciences), anti-CD45.1(A20; eBiosciences), or anti-CD45.2 (104;

BioLegend). Cells were again washed and resuspended with flow cytometry buffer before data collection, with addition of black latex beads to samples to quantify cellular number.

For intracellular stains, cells were washed with PBS, incubated with Zombie NIR fixable viability dye (BioLegend) at 4 °C for 30 min to demarcate dead cells. Cells were next washed and fixed with 4% PFA for 15 min at 20 °C. Lastly, cells were washed and stained in flow cytometry buffer with 0.2% saponin, along with anti-Septin 7[241] or phalloidin probe (Invitrogen) for 30 min before a final wash and resuspension in flow cytometry buffer. Alternatively, fixed cells were treated with cold (-20°C) MeOH for 30 min at 4°C. Cells were then stained for 1 h at 20 °C in staining buffer (PBS, 1% BSA) containing anti-c-Myc (D84C12; Cell Signaling Technology), washed, and stained with fluorescently labeled donkey F(ab')2 anti-rabbit (Abcam) for 30 min at 20 °C.

For assessing cellular DNA content with Hoechst dye, harvested cells were washed with PBS, fixed in 70% EtOH for 30 min on ice, and washed twice again with PBS. Cells were then incubated with PBS containing 0.1% Triton-X-100, 0.1 mM EDTA, 100 mg/ml RNAse A (Thermo Scientific), and 5 mg/ml Hoechst dye (Thermo Scientific). Cells were again washed and resuspended in flow cytometry buffer.

STAT5 phosphorylation assay

Isolated $CD8^+$ OT-I T cells were cultured in 96-well plates and activated through PMA and ionomycin stimulation or co-culture with SL8-pulsed activated BMDCs. Anti-mouse IL-2 (15 mg/ml, JES6-1A12) was added to cultures at time of plating to restrict IL-2 delivery. After 24 h, recombinant human IL-2 (0.1-100 U/ml) was added to wells for 20 min at 37 °C. Cells were washed, fixed with 4% PFA for 15 min at 20 °C,and washed. Cells were resuspended with cold (-20 °C) MeOH and washed with flow cytometry buffer 4 times. To stain, cells were incubated in

PBS containing 2% BSA and anti-phospho-STAT5 (C71E5; Cell Signaling Technology) before a final wash and resuspension in flow cytometry buffer.

Calcium flux signalling

Isolated $CD8^+$ OT-I cells were labeled with 1 mM ratiomeric calcium-binding dye Indo-1, AM (Life Technologies) in PBS for 15 min at 37 °C. Cells were washed twice with complete RPMI, and incubated at 37 °C for 15 min to allow for complete de-esterification. Cells were coated with 5 mg/ml anti-CD3 (2C11; UCSF Hybridoma Core) on ice, washed, and transferred to 37 °C 10 min prior to data collection. To induce CD3 cross-linking, 10 mg/ml of anti-Armenian hamster (BioLegend) was added to CD3-coated cells after 1 min of sample collection. Alternatively, 1 mM of thapsigargin (Sigma-Aldrich) was added to uncoated cells. Cell samples were kept in a heating chamber (37 °C) during data collection by flow cytometry.

***In vivo* cell transfer and Dec-OVA immunization**

Isolated $CD8^+$ T cells were resuspended in PBS and adoptively transferred by retro-orbital or tail-vein injection to recipient mice. 0.5×10^6 CFSE-labeled wild-type and *Sept7*cKO polyclonal T cells were co-transferred to host mice that had been sub-lethally irradiated. Inguinal lymph nodes and spleen were harvested and analyzed 14 days following transfer. $0.5–1 \times 10^6$ CFSE-labeled wild-type and *Sept7*cKO $CD8^+$ OT-I T cells that had been co-cultured *in vitro* with SL8-pulsed BMDCs were isolated and co-transferred to antigen-free host mice. Spleens were harvested and analyzed 48 h later.

Alternatively, 2.5×10^3 wild-type and *Sept7*cKO OT-I T cells were co-transferred to congenic wild-type mice, respectively. Dec-OVA complexes were generated in-house from conjugation of anti-Dec205 (NLDC-145) to OVA. 1 mg of Dec-OVA, along with 10 mg of anti-CD40 (1C10;

eBiosciences), was injected subcutaneously in the left and right flanks of host mice. Inguinal lymph nodes were harvested and analyzed 6 or 7 days later.

For memory homeostasis experiments, 2.5 × 10^6 naïve $CD8^+$ OT-I wild-type and *Sept7*cKO T cells were co-transferred to host mice that were immunized i.v. with 10 mg DecOVA and 50 mg anti-CD40. Transferred T cells were sorted from pooled spleens and lymph nodes of these mice 14 days later, counted, and 0.5–1 × 10^6 wild-type and *Sept7*cKO cells were co-transferred to antigen-free mice. Spleens and lymph nodes were harvested and analyzed 8 weeks later.

***In vivo* cell transfer and IL-2 complex delivery**

1 × 10^6 isolated *Sept7*cKO or control OT-I $CD8^+$ T cells were adoptively transferred by retro-orbital injection to congenic recipient mice. IL-2 complexes were formed by incubating 1 mg of recombinant murine IL-2 peptide (Peprotech) with 5 mg murine anti-IL-2 (S4B6-1; BioXCell) for 1 h at 20 °C. PBS was added and the solution administered by intra-peritoneal injections. IL-2 complexes were freshly made and injected daily, with harvesting and analysis of inguinal lymph nodes and spleen after 7 days.

T cell morphology analysis

T cells were activated, and imaged on ICAM-coated coverslips with 0.25% low-melt agarose for morphological analysis. Cell length was measured using Metamorph software's *Integrated Morphometry Analysis* (IMA) measurement tool. Images were acquired on a modified ZeissAxiovert 200M microscope with a plan-neofluor 63× objective (Carl Zeiss) using Metamorph imaging software (MDS Analytical Tech).

Confocal microscopy

Isolated $CD8^+$ T cells were stimulated with PMA and ionomycin, and cultured for 48 h. Cells were then transferred to poly-L-Lysine coated chamber slides. Once adherent, cells were washed twice with PBS, fixed with 4% PFA (PBS) for 15 min at 20 °C and washed. Cells were permeabilized with 0.1% Triton-X-100 (PBS) for 5 min, and washed twice with 1% BSA (PBS). Cells were then stained with DAPI (Invitrogen) before a final wash and application of a cover slip. Images of cells were generated using an inverted Yokogawa CSU-10 spinning-disk confocal microscope (Zeiss) with Micro-Manager imaging software (www.micro-manager.org).

CFSE quantification

A mean CFSE peak number was quantified for each *in vitro* proliferation experiment with CFSE-labeled T cells. For a given sample's CFSE profile of live cells, each CFSE peak was gated, and the percentage of cells populating the peak was generated. A weighted mean of the number of CFSE peaks diluted was then calculated.

Statistics

Comparisons between groups were analyzed with Student's *t*-test as indicated with GraphPrism software. Data was denoted as significant if *P*-values were 0.05 or less.

CHAPTER 4: DENDRITIC CELLS IN CANCER

Originally identified by Ralph Steinman based on their distinctive dendritic morphology, dendritic cells (DCs) encompass a group of professional antigen-presenting cells (APCs) that present self- and foreign- antigen to T cells through MHC-I and MHC-II, and are uniquely positioned to initiate T cell activation[337]. Responsive to environmental stimuli, be it homeostatic, infectious, or noxious, mature DCs also express a constellation of additional cues like co-stimulatory molecules or cytokines that inform T cell proliferation and differentiation. As a vital link between innate and adaptive immunity, DCs serve as the crux and cellular driver of the 'cancer immunity cycle' that generates antigen-specific anti-tumor T cell responses[338,339]. Briefly, this model outlines the process by which tumor DCs first phagocytose tumor cell antigen. A subset of these DCs traffic to the tumor-draining lymph node (LN) to present tumor antigen and prime tumor antigen-specific T cells. Other DCs present in the tumor microenvironment (TME) can reactivate these effector T cells upon entry. Although activation of DCs leads to migration to the LN[22], it remains unclear which DCs are relegated to either migration or re-activation of T cells entering the TME. Speaking to the central role of DCs in directing cancer immunity, however, high mature DC density is associated with T cell activation and improved cancer patient outcome[340,341,342]. Furthermore, in human melanoma samples, *Ccr7* expression is associated with higher T cell count as well as improved overall survival, reinforcing the role of migratory DCs in initiating T cell responses systemically as well as locally[343]

Yet while an anti-tumor immune response would ideally lead to the clearance of aberrant cancer cells, immunosuppressive factors can stymie a potent anti-tumor immune response. Such factors may include: lack of neo-antigens, lack of stimuli to activate DCs, low tumor DC density, dysfunctional or tolerogenic tumor DCs, and exclusion or immunosuppression of effector T cells at the tumor site[344]. Recent advances in immunotherapy enable modulation of dysfunctional T cells through 'checkpoint blockade' of inhibitory receptors like CTLA-4 and/or

PD-1[345,346,347]. Yet while these modalities have demonstrated clear clinical value across several cancer indications, a substantial portion of patients do not respond or acquire resistance[348,349]. In these settings, it may be that the anti-tumor T cells are not responsive to targeting, or that immunosuppressive factors continue to promote T cell dysfunction. In these settings, it may prove beneficial to boost anti-tumor activity in innate immune cells that can partner with anti-tumor T cells. Indeed, therapeutic augmentation of tumor DCs can improve tumor growth control or synergize when in combination with checkpoint blockade[350,351,352]. As such, a better understanding of DC subset specialization, the signals that trigger maturation and antigen processing in the TME, and the mechanisms by which tumor DCs drive T cell responses will help to guide ongoing development of myeloid-oriented therapies.

I. TUMOR MYELOID COMPARTMENT

Dendritic cells. Classical DCs (cDCs) in mice and humans refer to DCs that emerge from a restricted pre-cDC-derived lineage and exhibit exceptional antigen-presentation and T cell activation capacity[353]. cDCs are segmented into two separate lineage classifications (cDC1 and cDC2) that correspond to differential transcription factor requirements and functional specialization across tissue systems[354,355,356]. Both cDC1s and cDC2s can be found in mouse and human tumors[342,350,357,358] and a better understanding of subset populations and their distinct functionality will inform development of DC-targeted therapies.

cDC1s excel at cross-presentation of antigen and are critical for initiating $CD8^+$ T cell responses across a number of immunological settings[13,359,360,361,362]. cDC1s include lymphoid tissue resident $CD8a^+$ DCs and non-lymphoid tissue (NLT) migratory $CD103^+$ DCs, which are strikingly similar transcriptionally and share expression of the chemokine receptor XCR1[363,364]. Together cDC1s depend on IRF8[365,366] , BATF3[361,363], ID2[367], and NFIL3[368] for development, although there may be differences in strict requirements between the subsets[369,370]. Notably, in humans, $BDCA3^+$ ($CD141^+$) $XCR1^+$ $CLEC9A^+$ cells are found in blood, lymphoid, and NLT, and

closely resemble cDC1s in transcriptional signature and enhanced cross-presentation ability[371,372].

In contrast, cDC2s preferentially activate $CD4^+$ T cells through MHC-II[337,353], express SIRPα, and are dependent on the transcription factor IRF-4[356,373,374]. Additional development requirements include ZEB2[375], NOTCH2[376], RELB[377], and TRAF6[378]. Despite this overarching classification, cDC2s encapsulate a great degree of heterogeneity that likely represents diverse biological function[364,379]. While historically cDC2s have largely been identified as $CD11b^+$ DCs[354], dermal cDC2s at least include a $CD11b^{hi}$ and $CD11b^{lo}$ KLF4-dependent population[380], and highlights the advantage of using SIRPα instead of CD11b as a defining marker. Another complicating feature of cDC2s is that they share many surface markers with monocytes and macrophages (e.g. CD11b, CD11c, SIRPα, CX3CR1, CCR2). This overlap in commonly used markers has made it difficult to precisely define and isolate cDC2 cells and assess functionality, although CD64, MERTK, and Ly6c have been proposed as markers to selectively identify macrophages and monocytes[381]. In humans, cDC2s are best aligned with the $CD1c^+$ ($BDCA1^+$) subset found in the blood and various tissues[372,382,383] and include at least two subset populations as revealed by recent single-cell RNA-sequencing analysis[384]. Although much progress has been made in better defining cDC populations, recent advances in single-cell profiling by RNA-seq and CyTOF in both mouse and human will help to further resolve their heterogeneity.

With regard to ontogeny, cDCs arise from pre-cDCs, which are defined as $Lineage^-$ $CD11c^+$ $MHC\text{-}II^-$ $FLT\text{-}3^+$ $SIRP\alpha^-$ in mice[385] and as Lin^- $HLA\text{-}DR^+$ $FLT\text{-}3^+$ $CD117^+$ $CD116^+$ $CD123^+$ $CD33^+$ $CD45RA^+$ in humans[386,387]. Originating in the bone marrow, pre-cDCs migrate through the blood and can be found in lymphoid tissue as well as NLT like the lung, kidney, or liver[388,366]. Pre-cDCs notably commit early to cDC1 or cDC2 lineages and pre-cDC1 or pre-cDC2s can be identified in the bone marrow, blood and lymphoid tissue[385,386]**.** Both pre-cDCs and cDCs express FLT-3, and FLT-3L is required for cDC development and for *in situ* proliferation in the

periphery[389,366]. In addition, CSF-2R is expressed by cDC1s and cDC2s and, while GM-CSF does not appear to be required for resident cDC populations in lymphoid tissue development[390], it is required for DC survival in peripheral tissue[391] and induces CD103 expression[392]. While both cytokines influence DC biology, there does appear to be selective responsiveness, as FLT3-ligand (FLT-3L) preferentially increases $CD103^+$ DCs while GM-CSF expands $CD11b^+$ DCs[342].

Pre-cDCs can be found in the tumor microenvironment (TME), and in some instances up-regulation of CCL3 by the tumor can recruit pre-DCs[393]. Although this particular study found that pre-DCs matured into functional cDCs in the tumor (albeit with slightly decreased MHC-II levels), extensive characterization of tumor pre-cDC populations across tumor indications and classes has yet to be completed. It thus remains to be determined whether cDC differentiation is altered or impaired in the TME. It will be of interest to test if poor cDC1 infiltration, which is associated with decreased survival rates[342], results from a shift in differentiation or exclusion of pre-DCs from the TME.

Plasmacytoid DCs. Plasmacytoid DCs (pDCs) develop from the common DC progenitor (CDP), but are independent of the cDC lineage[354]. In tumors they have often been associated with poor outcome as high numbers of $CD123^+$ pDCs in early-stage breast cancer and melanoma correlate with decreased survival[394,395]. Despite their tolerogenic properties, some studies have found potent anti-tumor activity in pDCs upon therapeutic stimulation[396]. It is important to note, however, that a recent study has identified human pre-cDCs to be $CD123^+$ $CD303^+$ and to exhibit substantial overlap in additional surface markers with pDCs[387]. Although CD33 expression can separate pre-cDCs from pDCs, previous studies of pDCs may be contaminated with pre-cDCs and conclusions drawn may warrant reevaluation.

Monocytes & Inflammatory DCs. Although cDCs are tautologically pre-cDC-derived, monocytes can be recruited to sites of inflammation and differentiate into monocyte-derived

DCs (moDCs), or, inflammatory DCs[397]. Monocyte ontogeny is primarily demarcated by CCR2-dependency, and differential surface markers aim to identify inflammatory DCs across tissue systems such as ESAM-lo CD11b moDCs in the spleen[376], $CD11b^+$ CD103- moDCs in the intestine[398,399], $CCR2^+$ $CD64^+$ moDCs in the dermis[381] or $CD64^+$ $FcyRI^+$ moDCs in the muscle[400]. These inflammatory DCs have also been reported in response to a number of infectious or adjuvant agents such as influenza[401], HSV-2[402], *Leishmania major*[403], *Listeria monocytogenes*[404] LPS[405], or alum[406]. Transcriptional profiling of populations from the skin reveals that inflammatory DCs exhibit a similar gene signature to $CD11b^+$ cDCs[381], and in some cases, inflammatory DCs may substitute for cDC functionality[406] or shape T cell differentiation[403,407]. As with cDCs, inflammatory DCs have been described in humans across various disease conditions and are thought to express HLA-DR, CD11c, CD11b, CD14, CD1c (BDCA1), CD1a, CD206, Sirpa, and FceRI[397]. Furthermore, inflammatory DCs have also been identified in the TME of mice[408] and human tumor ascites[409], and may also contribute to anti-tumor immunity. Indeed, anthracycline chemotherapy can prompt massive recruitment and differentiation of monocytes. Here in this model the therapeutic benefit of chemotherapy relied on $CD11b^+$ cells[410], suggesting that these inflammatory DCs may exhibit anti-tumor activity in pro-inflammatory conditions.

Many questions remain as to how inflammatory DCs develop, if inflammatory DC populations from these studies share common transcriptional programs, and how they are functionally distinct from peer cDCs. Some of the murkiness regarding function stems from a dearth of markers that cleanly and consistently separates inflammatory DCs from cDC2s or macrophages. Practical limitations have also restricted use of monocyte transfers to demonstrate ontogeny and instead have relied on CSF-1- or CCR2-dependency. There is evidence, however, for heterogeneity within the umbrella of 'inflammatory DCs.' *Listeria monocytogenes* infection results in a TNFα- and iNOS-producing inflammatory DC population (TipDCs) in the spleen[404] while LPS injection leads to DC-SIGN $(CD209)^+$ $CD206^+$ inflammatory

DCs in LNs[405]. Despite their originally proposed monocyte origin, DC-SIGN$^+$ CD206$^+$ cells were found later to express the cDC-specific transcription factor Zbtb46 and to be FLT-3L-dependent[10], while Zbtb46 expression is absent in TipDCs[411]. This discrepancy suggests that the LPS-induced DC-SIGN$^+$ cells may instead be cDC- and not monocyte-derived, or, alternatively, opens the possibility that Zbtb46 can be up-regulated during moDC development. In contrast, TipDCs are dependent on CSF-1 but not GM-CSF[391] and may simply represent an inflammatory monocyte. As evident, further functional analysis and discussion is needed to determine the threshold that a monocyte-derived cell must meet to be considered a DC. A similar predicament exists in human studies as well, in which promiscuous expression of myeloid surface markers and a lack of rigorous lineage tracing may lead to inappropriate labeling of DCs and cells of monocyte origin. While seemingly semantic, clarity on ontogeny and functional specification will allow for more consistent comparisons across models and shed light on the myeloid populations that contribute to anti-tumor responses.

Macrophages. Like DCs, tissue macrophages have heterogeneous ontogeny, but tumor-associated macrophages (TAMs) are largely monocyte-derived[412] and far out-number cDCs in the TME[342]. Functionally they are thought to be largely pro-tumor through production of immunosuppressive cytokines and surface markers like IL-10, TGF-β, and PDL-1, and factors that facilitate tissue remodeling, angiogenesis, and tumor cell growth and migration[413,414]. Macrophages have been described as more efficient at phagocytosis than DCs but far more inefficient at antigen cross-presentation[14,415]. As such, TAMs are incapable of supporting T cell proliferation[342,357,416,417], and hence represent a functional counterpoint to cDCs. High frequencies of TAMs are generally associated with poor prognosis of a wide variety of cancer indications, although correlations between high TAM density and improved survival have emerged[418]. Like their myeloid brethren, macrophages are not uniform and take on distinct activation states, often characterized from *in vitro* studies as classical (M1) or alternative (M2)

activation based on initial stimulus[419]. Although likely more reductionist than what occurs *in vivo,* these two cellular profiles represent polarized transcriptional and secretory programs that may explain conflicting correlations in patient outcome[413]. For example, the M2 profile tends to be anti-inflammatory and promote wound-healing processes. In line with this functional divergence, a M2 signature is associated with a worse prognosis than a M1 signature[420,421]. Finer resolution of these populations *in vivo* will likely yield insight into TAM function as well as their impact on tumor development and responsiveness to immunotherapy.

II. ROLE OF DCs IN DRIVING T CELL RESPONSES

cDC1s. cDC1s are exceptional at cross-presenting endocytosed antigen on MHC-I, and unlike $CD11b^+$ DCs, do not require activation to do so[422]. To ensure cross-presentation of antigen, cDCs restrict degradation of endocytosed peptides in phagosomes by limiting early recruitment of proteases, maintaining a neutral phagosomal pH, and facilitating export of antigen to cytosol[14]. DCs express an ER- and lipid body- resident GTPase Igtp that is required for lipid body accumulation following stimulation. Loss of Igtp or a lipid body coat component was accompanied by defective phagosomal maturation and $CD8^+$ T cell cross-priming, which suggests an intriguing role for lipid bodies in regulation of cross-presentation[423]. In addition, cDC1s maintain a higher pH through Rac2-mediated Nox2 assembly and ROS production in phagosomes[424]. In line with these findings, our group has similarly observed that tumor $CD103^+$ DCs have a higher vesicular pH than tumor $CD11b^+$ DCs[342] and although all DCs contain fluorescent antigen in the TME, only $CD103^+$ DCs contain detectable fluorescent protein antigen following CCR7-dependent migration to the tumor-draining LN[350,343].

With such specialization in cross-presentation, cDC1s are uniquely well equipped to initiate $CD8^+$ T cell responses[425,426], and a number of studies have demonstrated their critical role across a variety of models[13,359,360,361,362]. Indeed, while naïve antigen-specific $CD8^+$ T cells can proliferate and differentiate into cytotoxic T cells (CTLs) in tumor-draining LNs of

spontaneous and ectopic tumor models[427], anti-tumor $CD8^+$ T cell responses are greatly diminished with loss of Batf3-dependent cDC1s[361]. Although this could implicate $CD8^+$ resident lymphoid DCs or tissue migratory $CD103^+$ DCs, use of mixed bone marrow chimeras highlighted the critical role of $CCR7^+$ $CD103^+$ DCs specifically for initiating $CD8^+$ T cells responses[343]. Moreover, loading of a pH-stable tumor antigen across resident DCs in the tumor-draining LN was CCR7-dependent, arguing that $CCR7^+$ DCs from the tumor are the primary source of antigen in the LN and that antigen handoff occurs between $CCR7^+$ and LN resident populations[343]. The relationship between resident and migratory DC populations in the tumor-draining LN is unclear, but $CD8^+$ T cells preferentially interact with migratory DC populations[428] and XCR-1^+ DC1s have been visualized engaging in stable contacts with tumor-specific $CD8^+$ T cells[343,429]. Notably, $CD103^+$ DCs take up antigen early in primary and metastatic tumor development[343,429] and thus are poised to set the stage for the subsequent anti-tumor $CD8^+$ T cell response.

In addition to priming $CD8^+$ T cells in the LN, $CD103^+$ DCs are also central T cell partners in the TME. Although $CD103^+$ DCs are an extremely rare population in the tumor, their anti-tumor activity can be potent[342]. Numbers of $CD103^+$ DCs and tumor-infiltrating $CD8^+$ T cells are correlated[350], and $CD103^+$ DCs can recruit activated T cells into the tumor through production of CXCL9 and CXCL10[430]. Analysis of human melanoma tumors confirmed a positive correlation between *Batf3*-expressing DCs and *Cxcl9* or *Cxcl10* expression, as well as with $CD8^+$ T cells[430]. $CD103^+$ DCs present in the TME have been found to be uniquely capable of supporting $CD8^+$ T cell proliferation and are important for re-stimulating activated $CD8^+$ T cells upon arrival to the tumor[342]. Although the mechanistic requirements of re-activation by DCs in the TME is still not well understood, the presence of $CD103^+$ DCs in the TME may promote higher T cell motility and contact with cancer cells[430]. In addition to outrivaling other cells at cross-presentation and activating $CD8^+$ T cells, cDC1s are a primary producer of IL-12[342,431,431], which helps to drive $CD8^+$ T cell proliferation and effector function[432]. The benefit of IL-12 is

supported by the finding that higher *Il12a* expression levels are associated with $CD8^+$ T cell effector genes and higher rates of responsiveness to chemotherapy[434].

As suspected from their outsized role in driving $CD8^+$ T cell responses, higher tumor $CD103^+$ DC numbers correspond to survival across multiple indications[342]. Even more indicative of their pro-stimulatory potential, immunotherapeutic benefit may rest on $CD103^+$ DCs. In murine tumor models $CD103^+$ DCs are required for the recruitment and local re-activation of $CD8^+$ T cells that enables successful adoptive cellular therapy (ACT) with CTLs[342,430]. They are also necessary for anti-tumor effects of anti-PD1, -PDL1, or -CD137 therapy[433], as well as vaccine approaches with FLT-3L and Poly:IC[350], or inactivated vaccinia virus[434].

cDC2s. cDC2s contain an unresolved degree of heterogeneity, but were first described to be predominantly responsible for initiating and supporting $CD4^+$ T cell activation and proliferation[12,13,]. Although population definitions have not been consistent, cDC2s broadly have been attributed to driving $CD4^+$ T cell helper subset differentiation toward Th1[435], Th2[380,436,437], Th17[376,438], as well as T follicular helper cell[439] fate across a variety of immunological models. Some specialization of skewing capacity appears to be in place as $Mgl2^+$ ($CD301b^+$) $CD11b^+$ DCs were identified as critical for mediating Th2 but not Th1 responses[437]. Given the heterogeneity present in the cDC2 compartment, the requirements and coordination for initial $CD4^+$ T cell activation and later differentiation in the LN and tissue are not well understood and likely complex. Sequential interactions with multiple DC populations has been documented in the LN[440] and these multicellular dynamics may also shape a given $CD4^+$ T cell's early differentiation program after initial priming. For example, in some scenarios cDC1s contribute to Th1 skewing[441], and other LN DC subsets may similarly influence $CD4^+$ T cell fate. While cDC2s are present in the TME, their role in anti-tumor immunity has not yet been fully defined. Notably a recent study using LLC-tumors observed $CD4^+$ T cell proliferation when co-cultured with $CD11b^+$ tumor and LN cDC2s and, interestingly, found that these cDC2s skewed $CD4^+$ T cells

toward a Th17 phenotype primarily *in vitro*[408]. From this finding, it will be valuable to determine whether there is a functional significance of generating anti-tumor Th17 cells and to test how cDC2s function in $CD4^+$ T cell activation and differentiation across different indications with an eye to the heterogeneity in that compartment.

The requirements for $CD4^+$ T cells can differ across types of immunological challenges[442]. Although it remains unclear the extent to which $CD4^+$ T cells provide 'help' to $CD8^+$ T cells during an anti-tumor response, there is precedent for $CD4^+$ T cells to 'license' LN APCs with CD40L and boost T cell responses to apoptotic cell antigens. In doing so, $CD4^+$ T cells can bolster the quality of $CD8^+$ T cell priming by shifting the $CD8^+$ T cell response one of tolerance to CTL generation[443,444,445,446,447]. $CD4^+$ T cells also contribute to robust T cell memory programming and maintenance[448,449,450]. Later in the TME $CD4^+$ T cells can promote $CD8^+$ T cell infiltration and effector function in the tumor[451,452].

Going forward, it will be of interest to determine how DCs organize $CD4^+$ T cell responses in different tumor models, and whether therapeutic targeting of $CD4^+$ T cell function can effectively promote anti-tumor immunity. A combinatorial immunotherapeutic approach with allogeneic tumor-binding antibodies, anti-CD40, and IFNγ induced systemic expansion of an effector $CD4^+$ T cell population that protected against new tumors, and a similar population was observed in patients undergoing immunotherapy[453]. These findings are similarly supported by the demonstration that ACT with $CD4^+$ T cells can be effective in some models[454,455,456,457]. It remains to be determined whether $CD4^+$ T cells play an outsized role in certain tumor models or therapeutic approaches, and whether cDC2s mediate these responses. Vaccination with cDC2s was more protective against a mouse model of LLC tumor growth than vaccination with cDC1s. Interestingly, the converse was true for B16 growth, suggesting that cDC2 profiles or $CD4^+$ T cell contribution may vary between the two models[408]. Lastly, although cDC2s are thought to primarily drive $CD4^+$ T cell responses and display sub-optimal cross-presentation, delivery of antigen with stimuli like immune complexes or TLR7 agonists can substantially boost cDC2

ability to cross-present antigen to $CD8^+$ T cells[422,130]. Neither tumor nor LN $CD11b^+$ DCs were capable of activating $CD8^+$ T cells to the same extent as $CD103^+$ DCs in a B16 model[342,343] although it remains to be tested whether therapeutic modalities could improve $CD8^+$ T cell function via cDC2s as well as cDC1s.

III. DENDRITIC CELLS: ARBITER OF TOLERANCE VS. ACTIVATION

In the steady-state DCs are tasked with maintaining systemic tolerance. Cross-presentation of antigen or apoptotic cells by cDC1s results in tolerant or suppressive $CD8^+$ T cells[458,459,460,461,462]. cDC1 presentation of self-antigen can also support Treg expansion[463]. Transcriptional profiling of steady-state migratory DCs reveals a gene signature that includes genes like *Socs2*, *Tmem176a*, and *Tmem176b* that that could function to dampen DC activation[11]. Widespread loss of DCs with a CD11c-Cre-DTA model thus results in tissue infiltration of $CD4^+$ T cells and onset of autoimmunity[464]. Similarly, Ikkβ-deficient DCs are unable to migrate from the skin to the draining LN, and this leads to a loss of Treg generation and severe autoimmunity[465].

Immunological challenges such as infection may present themselves, however, and host survival will require a shift from tolerance to robust effector adaptive immunity. To distinguish between 'self' and 'non-self' DCs express an assortment of pattern-recognition receptors (PRRs) including Toll-like receptors (TLRs) that bind to a diverse set pathogen-specific ligands[20]. This model was later broadened to account for danger associated molecular patterns (DAMPs) that signal tissue damage and cell death and that can also trigger DCs to take action[21]. Detection of pathogen or DAMP ligands activates DCs and enables them to alert the adaptive immune system through up-regulation of co-stimulatory molecules and inflammatory cytokines and migration to a draining LN[466]. While efficient antigen presentation by DCs is necessary to initiate T cell priming, these additional signals are required to drive effector T cell responses and robust anti-tumor immunity. In addition to antigen (Signal 1), co-stimulatory

molecules like CD80, CD86, or CD70 (Signal 2) increase T cell capacity to proliferate and produce cytokines[467,468] and inflammatory cytokines like IL-12, IL-27, or type I interferon are critical for T cell effector differentiation[130,131,469]. As a regulatory measure to ensure that a DC has been directly exposed to a stimulus of immunological concern, cell-intrinsic TLR signaling is required to support robust T cell expansion and Th1 generation[470].

Many patients with cancer do have tumor-specific T cells in circulation and within the TME[471,472], indicating that mature tumor DCs are initiating an antigen-specific response. Transfer of naïve tumor-specific T cells in mouse tumor models results in priming and expansion in the tumor, again confirming that spontaneous anti-tumor responses are underway but insufficient to clear the tumor[343]. Given the requirement for DCs laden with Signal 1 (antigen), 2 (co-stimulatory molecules), and 3 (inflammatory cytokines) to tip the balance away from tolerance, investigation of both antigen uptake processes and DC-activation cues in the TME have been an important and active area of research.

Tumor antigen recognition and uptake. DCs recognize and ingest tumor antigen through a variety of mechanisms. Tumor cell death occurs regularly and dying cells release 'find me' signals like lysophosphatidylcholine[473], ATP[474], or HMGB1[475] that recruit myeloid cells to the site of cell death. Upon arrival, 'eat me' signals such as phosphatidylserine (PS) or calreticulin on the dying cell surface, as well as intermediate-binding partners, can be recognized by a variety of myeloid surface receptors[476] allowing phagocytic cells like DCs to clear that dead cells[477]. These receptors include CD36, αvβ5 integrin, MERTK, CD91, or C-type lectin receptors which bind to the dead cell material and facilitate phagocytosis[415,478,479]. Tumor antigen immune complexes or opsonized dead cells can also be detected and cleared through complement, scavenger, or Fc receptors on DCs[477]. In addition to endocytosis of dead cells, DCs can obtain tumor antigen from living tumor cells through 'nibbling' with scavenger receptors[480] or acquisition of tumor-derived exosomes[481]. Transfer of antigen between DCs *in vitro* has been reported as

well, suggesting that tumor antigen may be dispersed throughout the myeloid network regardless of proximal intimacy with tumor cells[482].

Immunogenic tumor cell death. Although DCs can capture tumor antigen through multiple sources, the signals that result from tumor cell death have been characterized extensively[483]. Dying tumor cells can act dually as a source of antigen and as a stimulatory DAMP, and robust generation of both $CD8^+$ and $CD4^+$ effector T cell responses requires 1) immunogenic cell death and 2) processing of cellular antigens through the cross-presentation pathway[484].

Apoptotic cell uptake was historically thought to be primarily immunosuppressive as apoptotic cell presentation results in 'helpless' $CD8^+$ T cells[459]. Ingestion of apoptotic cells can prompt down-regulation of MHC-II and co-stimulatory molecules on DCs[485], as well as a reduction in IL-12[486]. Macrophages and monocytes also phagocytose apoptotic cells, and uptake can increase production of IL-10, TGFβ, prostaglandin E2, and platelet-activating factor (PAF) alongside a reduction in pro-inflammatory cytokines such as IL-1β, IL8, GM-CSF, or TNFα[487]. Indeed suppressive signaling is initiated in DCs when apoptotic cells are ingested via a number of receptors such as complement receptor 3[485,488], Mer-TK[489], and inhibitory Fc receptors[490]. In addition to influencing DC-intrinsic signaling, apoptotic cells can prevent initial immune recognition of 'danger' signals. HMGB1 is a well-characterized alarmin that, when released from dying cells, activates myeloid cells through RAGE and TLRs[491]. In apoptotic cells caspase activation deacetylates the chromatin, which allows for HMGB1 binding and prevents its release and detection[492]. Caspase activation also leads to mitochrondrial production of reactive oxygen species (ROS). This ROS oxidizes the alarmin HMGB1 and neutralizes its activity so that it goes undetected[493]. Conversely, inhibition of ROS or sites of HMGB1 oxidation results in stimulatory apoptotic cells that break tolerance in a delayed type hypersensitivity model. Lastly, in some scenarios of apoptosis, caspases inhibit mitochondrial DNA from activating the DNA-sensing STING pathway and downstream type I interferon[494,495].

Originally considered to be a foil to apoptotic cells, necrotic or necroptotic cells are highly immunogenic[496] and trigger innate immune cell activation and recruitment through a number of pathways. Necrotic cells release a number of intracellular alarmin factors that initiate pro-inflammatory cascades. The multi-functional alarmin HMGB1 forms complexes with nucleic acids and facilitates their localization and detection in endosomes to trigger myeloid PRR signaling[497]. HMGB1 leads to DC maturation and $CD4^+$ Th1 skewing[498], and can be presented on DC surface CD24 to directly co-stimulate T cells[499]. Intracellular uric acid released from necrotic cells similarly stimulates DC maturation and enhances T cell responses when used as an adjuvant[500]. Accordingly, an anti-tumor vaccination with necroptotic cancer cells can offer protection against tumor growth[501].

This dichotomy between apoptosis and necrosis, however, has become more complex with further experimentation. First, apoptosis can also be immunogenic in some settings[502]. Cross-presentation of infected cells in influenza is key to drive T cell immunity[503] and presentation of apoptotic cells drives diabetes autoimmunity[504]. Although there have been varying results, injection of apoptotic cells can prevent tumor growth upon inoculation[505]. Moreover, irradiated- and UV light-induced apoptosis[506] as well as doxorubicin-induced tumor cell death[507] resulted in immunogenicity. Levels of autophagy may also influence immunogenicity given that ATP release from chemotherapy-induced tumor cell death requires autophagy[508] and stimulation of autophagy leads to HMGB1 release[509]. With these findings in conflict with those that find apoptosis to immunologically silent, it may be that immunogenicity of apoptotic cells is dependent on an activation or stress status.

APCs can sense DNA from dying cells[510] as DNA binds to cyclic GMP-AMP synthase (cGAS), a sensor that catalyzes synthesis of the secondary messenger cyclic GMP-AMP (cGAMP) that activates STING, and this event in turn provokes a downstream type-I interferon production through the transcription factor IRF3[511]. Although $CD11c^+$ immune cells in the tumor ingest tumor DNA[512], it is still unclear in which cell types cGas pathway is active and how tumor

DNA obtains access to the cytosol. It is well established, however, that type-I IFN is critical for anti-tumor responses. Although type-I IFN is expressed $CD11c^+$ immune cells in tumor and draining-LNs[512], type-I IFN is also sensed by tumor cDC1s and this pathway required for $CD8^+$ T cell infiltration in the tumor[513,514]. STING and components of the signaling pathway are thus critical for spontaneous or basal anti-tumor T cell responses[512].

Therapeutic approaches to promote immunogenic cell death. Although the presence of an ongoing anti-tumor T cell responses in patients suggests that immunogenic cell death (ICD) and antigen processing are already occurring, therapeutic strategies like chemotherapy, radiation therapy (RT), or immunotherapy often depend on and/or boost these ICD recognition processes. For example, basal STING signaling from dsDNA recognition in mouse models is required for anti-CTLA4/PD1[512] or anti-PDL1[351] therapeutic efficacy, as well as RT benefits[515]. In a poorly immunogenic mouse model of metastatic mammary carcinoma, anti-CTLA4 alone did not improve growth or survival, but combination with RT resulted in increased survival[516]. Although more experimentation is required to determine the mechanism and kinetics of the immune response, this model may represent 'cold' tumors with little spontaneous T cell infiltration and highlight the value in initiating flow of immunogenic antigen into the myeloid compartment to kick-start the adaptive immune response.

Chemotherapies like oxaliplatin or anthracycline result in immunogenic cell death through TLR4 detection of HMGB1. This response is beneficial as breast cancer patients with loss-of-function alleles of TLR4 relapsed at a faster rate and advanced CRC patients experienced reduced survival[517,518], although conflicting findings have been reported in non-small cell lung cancer[519]. Anthracyclines trigger pre-apoptotic translocation of calreticulin to the cell surface, which enhances DC-mediated phagocytosis and T cell responses[520]. Chemotherapy can also amplify immunogenicity of tumor cells by triggering ATP release as apoptosis progresses[521]. This ATP acts on DC purinergic receptors like P2RX7 to activate the

NLRP3 inflammasome and IL-1β secretion[522] and can elicit myeloid cell recruitment and monocyte differentiation into inflammatory DCs[410]. A study of anthracycline-treated breast cancer patients observed that loss-of-function of P2RX7 corresponded to a worse prognosis[522]. With multiple factors and processes at play to signal and recognize ICD, the weighted role of any given pathway likely varies across cancer indication, sub-class, and therapeutic modality. For example, as highlighted by several studies already cited, TLR4 can be protective through ICD detection following chemotherapy[517,518]. In contrast, other studies found that TLRs are not required for spontaneous anti-tumor T cell responses[512], and RT benefits were instead dependent on STING signaling[515]. Overall, more research is needed to better clarify when and why certain pathways participate in tumor recognition and clearance and how therapeutic approaches can be more appropriately tailored to a given tumor class.

Cross-presentation of tumor antigen. Effective cross-presentation drives robust $CD8^+$ T cell priming and requires coordinated regulation of antigen uptake and processing. In addition to facilitating endocytosis by binding to the DAMP F-actin[523,524], CLEC9A on cDC1s directs cell material into the endosomal compartment for cross-presentation[525,526]. DAMPs like heat shock proteins can be immunogenic and mature DCs through CD91[527], but they also chaperone peptide antigen to enable cross-presentation[528]. At least in some situations chemotherapy promotes ICD cross-presentation as $CD8^+$ T cell priming is reduced with loss of key pathways like NLRP3, caspase-1, or IL-1R[522]. Conversely, although immunogenic forms of apoptotic or necrotic cells mature DCs, sensing of DAMPs does not guarantee that cross-presentation of antigen occurs. Intriguingly, a recent study found that cross-presentation required RIPK1-dependent NF-κβ signaling within the dying cell before phagocytosis[529]. Both necroptosis and apoptosis relied on this pathway for immunogenicity and cross-presentation, and inhibition within dying cells results in a reduction in anti-tumor $CD8^+$ T cell responses. Thus, a more

comprehensive understanding of cross-priming requirements could help to predict therapeutic efficacy of engaging these signaling pathways.

IV. SUPPRESSION OF TUMOR DCs

cDC density and differentiation. While the TME may be a site chock-full with antigen and endogenous DAMPs capable of activating DCs, a network of immunosuppressive factors can stave off DCs and subdue their anti-tumor capacity. Higher cDC numbers are associated with better patient outcome[341,342]. Yet, cDCs may only be a rare population across a number of cancers in patients and mice[342,530], which may be due to suboptimal recruitment, differentiation, or longevity. In mice, tumors with active β-catenin signaling express less CCL3, CCL4, CXCL1, and CXCL2. These tumors exhibit a substantial reduction of cDC1 infiltration in particular, and this results in decreased $CD8^+$ T cell infiltration, impaired contact between CTLs and cancer cells, and magnified tumor outgrowth[531]. Perturbations in the cDC compartment may occur early in tumor development as the frequency of $CD141^+$ cDC1s was already selectively reduced in early lung adenocarcinomas compared to healthy lung tissue[358]. Indeed, a decrease in, or loss of, DC infiltration may aid in early tumor evasion from immune detection and hinder the swift anti-tumor detection that has been observed in a mouse model of metastatic lung cancer[429].

The TME may also curb DC development and differentiation. VEGF, a tumor-derived factor, can interfere with FLT-3L activity[532] and negatively impact DC differentiation *in vitro*[533] while, conversely, blockade of VEGF increases the number of mature tumor DCs[534]. DC maturation and survival, as well as differentiation to inflammatory DCs may also be inhibited by a number of tumor-derived factors such as gangliosides, prostanoids, polyamines, lactic acid, and neuropeptides[535]. Beyond soluble factors, tumor cells can also shed microvesicles or exosomes that contain bioactive messengers in the form of proteins, lipids, or microRNA[535,536]. Evidence suggests that uptake of these vesicular bodies restricts differentiation of inflammatory DCs from monocytes[537] and alters DC activity through MHC-II down-regulation[538] and T cell

skewing potential[539,540]. *In vivo* imaging of newly arriving metastatic cells in the lung revealed formation and shedding of cytoplasmic blebs, or cytoplasts, that were ingested by first-responder immune cells like monocytes[429]. Although the bioactive components of the cytoplasts remain to be determined, these early interactions between tumor material and phagocytes may afford pioneering tumor cells the opportunity to tune immune responses and establish their niche.

Handling of tumor antigen. Suppression of tumor DC antigen detection and processing pathways curtails ensuing effector T cell responses. Tumor DCs express higher levels of Tim3, which prevents ICD recognition by binding to HMGB1 and limiting recruitment of nucleic acids into endosomes[541]. This expression of Tim3 also inhibits DC maturation and reduces responsiveness to chemotherapy. Tumor DC cross-presentation function also appears to be compromised by the tumor. A recent study demonstrated that lipid peroxidation products in tumor DCs cause ER stress. Constitutive activation of the stress sensor IRE1a and downstream XBP1 signaling leads to lipid accumulation and impairs DC ability to activate T cells[542]. As further evidence of metabolic perturbations in tumor DCs, DCs from tumor-bearing mice and patients exhibit a high density of triglycerides and tumor extract increased levels of scavenger receptors that increase uptake of extracellular lipids[543]. Although these lipid-laden DCs expressed similar MHC-I levels, they could not process antigen as well and were defective in activating T cells. In addition, oxidized lipids specifically appear to block antigen cross-presentation[544].

DC-mediated T cell responses. Factors in the TME also influence DC phenotype and function in shaping T cell responses. Tumor-derived versican can induce IL-10R expression on DCs enabling exposure to IL-10, which can limit their ability to activate $CD4^+$ and $CD8^+$ T cells[545,546,547,548]. Indeed, TAM-derived IL-10 inhibits DC production of the pro-inflammatory

cytokine IL-12, a T cell effector-skewing cytokine[552]. IL-4 may also inhibit IL-12, as well as MHC-II levels[549]. Other tumor-derived factors like PGE2 and TGFβ can up-regulate PD-L1 on DCs and thus influence T cell activation and exhaustion[550].

As a prominent tumor-infiltrating cell population with immunosuppressive function, Tregs can contribute to impairment of DC activity and effector T cell activation through secretion of IL-10 and modulation of co-stimulatory molecule expression[551]**.** Recent evidence suggests that Tregs can also engage in particularly strong cellular contacts with DCs to perturb their cytoskeleton and reduce motility and T cell priming[552]. Tregs are notably increased in blood, LNs, the TME, and metastatic lesions in a variety of different tumor types, and appear to be functionally immunosuppressive based on IL-10 production and *in vitro* contact suppression assays[553,554]. In some cases Tregs can be recruited to the tumor cells or TAMs via CCL22 in ovarian cancer[555] or CCL2 in melanoma[556]. Depletion of Tregs in mouse models leads to tumor rejection[557] and a higher ratio of $CD8^+$ T cells to Tregs correlates with improved patient outcome[558].

As a DC becomes tolerogenic, it becomes more likely to generate regulatory T cells instead of effector T cells, thus contributing to a pro-tumor feedback loop. DCs can produce factors like TGFβ that skews $CD4^+$ T cells toward Treg differentiation[559,560] and even traffic to the thymus to partake in T cell clonal selection[561] and generation of central Tregs[562]. In general, DC function may also dynamically adjust with tumor development and growth. Phenotypic changes in tumor DCs have been observed during tumor progression whereby DCs down-regulate MHC-II and but up-regulate inhibitory molecules like PD-L1[550]. In these cases, DC function may be beneficial (though insufficient) during early tumor growth, but become deleterious with tumor outgrowth.

V. THERAPEUTIC STRATEGIES TO HARNESS DC FUNCTIONALITY

Many cancer patients have an ongoing and active anti-tumor immune response as detected by tumor-reactive T cells in their blood[471,472]., but this response is insufficient to control growth in instances of tumor progression. Within patients tumors with higher mutational burdens and neo-antigen loads respond better to T cell checkpoint blockade with anti-CTLA4 or anti-PD-1 therapy[563,564,565]. In contrast, other tumors appear to be ignored by the adaptive immune system and have limited lymphocyte infiltration such that T cell modulation may have little benefit[566]. Targeting of DCs, especially in the context of checkpoint blockade, ideally will improve T cell activation to broaden the clonal diversity, increase T cell infiltration, and re-activate pre-existing tumor-specific T cells. This strategy also holds the potential of boosting immunogenicity of tumors that may otherwise have not initiated a robust adaptive immune response. Suppression anti-tumor immunity can occur in the tumor-draining LN as well as the local TME, and while different cancer settings may require either systemic or local tuning[410,453,567], targeting both may widen overall patient responsiveness to immunotherapy. Lastly, although cDC1 activity is critical for anti-tumor immunity in some mouse models, it remains to be determined if it is sufficient in patients, or whether synergy between cDC1s and cDC2s will confer broader or more durable clinical benefit. cDC1s and cDC2s have different growth factor sensitivities, antigen processing pathways, and TLR profiles, and these differences will be important to note as therapeutic avenues are designed and compared[353].

Strategies to augment DC function. Injection or over-expression of Flt3L prompts expansion of DCs, though preferentially cDC1s, in mice and humans[568,569,570]. Other efforts to expand and activate DCs in the setting of checkpoint blockade include transferring irradiated GM-CSF- or FLT-3L-producing cells with checkpoint blockade[352,571]. In cases where a DC legion is in place to stimulate T cells but cannot overcome the immunosuppressive milieu of the TME, DC activation and reprogramming may need to be the priority. Paired expansion and stimulation of DCs has

had preclinical success with synergy observed following co-treatment with systemic Flt3L and intratumoral poly:IC and anti-PD-1/anti-4-1BB[350]. STING agonists have shown promising results as injection of cGAS ligands alone or with checkpoint blockade improve murine anti-tumor responses[351,572], as has anti-CD40 with anti-PD-L1[573]. In addition to activating DCs, others have tried to also heighten productive antigen uptake and processing through therapeutic delivery of allogeneic IgG-coated tumor cells in combination with anti-CD40[574]. Inhibition of phosphatases like SHP-1 and those that regulate Akt can also increase immune complex uptake and maturation profile of tumor DCs[575]. Intriguingly, TLR or PRR signaling independently of tumor antigen may also boost DC function and indirectly confer improved anti-tumor activity. Recent studies found that anti-CTLA4 immunotherapy required microbiota species like B. fragilis and this contribution was partially mediated through TLR2[576]. Complementary to this finding, administration of Bifidobacterium synergized with anti-PDL1 treatment whereby tumor DC profiling revealed an increase in genes associated with anti-tumor immunity[577].

As the biological bona vide vaccine, there has been great interest in harnessing DC biology to develop therapeutic cancer vaccines and has been reviewed extensively[578,579,580]. Briefly, this area of research covers several distinct strategies including adoptive transfer of antigen-bearing DCs, direct targeting of antigen to endogenous DCs, or injection of emulsified peptides, or recombinant viral or bacterial vectors. Cellular therapy with DCs generated *ex vivo* has been a tempting strategy as *ex vivo* culture enables robust activation, and there has been early success with personalized therapy based on neo-antigens present in a patient's cancer[581]. Pre-sensitization of the vaccine site with a recall antigen like tetanus/diphtheria toxoid can improve DC migration to the LN and potency[582], but a more comprehensive understanding of the factors that determine efficacy is needed. While promising, challenges certainly persist as the antigens to use for loading DCs remains to be determined and it remains unclear how responses will adapt to cancer cell immunoediting. The goal of course for neo-antigen delivery and presentation is to promote effector T cell responses. These T cells, however, will still be

susceptible to immunosuppression and dysfunction from tumor antigen-specific Tregs, tolerogenic endogenous DCs, and the TME milieu at large. These prevailing dynamics suggest that vaccination efforts may need to be paired with therapeutic reprogramming of the TME.

Strategies to disable immunosuppressive APCs. TAMs are often the immune population with the greatest frequency in the TME and take on a number of pro-tumor functions through secretion and surface expression of factors that directly support tumor cell survival, growth, and metastasis, as well as those that directly inhibit DCs and effector T cells[413]. Although high densities of TAMs has been linked to poor prognosis, there are a number of studies with conflicting findings. This may be due to differences in markers used or analysis performed but there can also be heterogeneity within TAMs and a mix of pro- and anti-tumor profiles[418]. Refined analysis with markers that more specifically correspond to an immunosuppressive phenotype, however, correlates with worse outcomes across several tumor types[420,421]**.** Depletion of or repolarization of immunosuppressive TAMs has thus emerged as an appealing therapeutic strategy with the goal to shifting the balance toward DC-mediated T cell activity. TAMs are dependent on CSF-1 and neutralization of CSF-1 results in lower frequencies of TAMs in conjunction with higher frequencies of cDC1s and cDC2s in a mammary tumor mouse model[587]. Indeed, blockade of CSF-1R in patients can reduce $F480^+$ TAMs with increased $CD8^+/CD4^+$ T cell ratios[583]. This inhibition approach has benefitted anti-tumor responses across a number of pre-clinical studies where it also synergizes with other therapies like chemotherapy, ACT, or checkpoint blockade, and a number of antibody and small molecule agents are currently being tested in clinical trials[418]. It has yet to be determined, however, whether depletion or reprogramming of TAMs is more advantageous and whether the benefits of a given strategy may vary based on the cancer type. Efforts to convert immunosuppressive TAMs with an 'alternatively activated' M2 phenotype are also yielding preclinical success, and include PI3Ky[584] and class IIa HDAC inhibitors[585]. PI3Ky inhibition did not change the number of $CD11b^+$ $F480^+$

cells, but the authors observed a shift in their phenotype, noting a decrease in TGFβ, arginase, and IDO concurrent with an increase in IL-12 and iNOS[584]. The Class IIa HDAC inhibitor TMP195 actually led to an increase in $CD11b^+$ and $F480^+$ cells, but macrophages exhibited dramatic shifts in gene expression and took on pro-tumor function as evidenced by their critical role in TMP195's anti-tumor therapeutic effects[585].

CHAPTER 5: ROLE OF CD11B$^+$ DCS IN ANTI-TUMOR CD4$^+$ T CELL RESPONSES

I. INTRODUCTION

The importance of an adaptive T cell response and its critical role in controlling tumor growth and/or regression has been well established. An absence of T cells has negative ramifications for immune control of tumor development[586,587] while adoptive cell transfer (ACT) of CD8 T cells has shown promise in treating human cancer[588]. While the TME often exerts immunosuppressive pressure to prevent productive CTL recruitment, infiltration, or tumor cell elimination, the first-generation of immunotherapy has appreciated clinical success by boosting anti-tumor T cell activity through blockade of inhibitory checkpoint molecules like CTLA-4 and PD-1[589,590]. As expected, tumor rejection in mouse models of checkpoint blockade is contingent on improved T cell function[591].

Generation of this cohort of anti-tumor T cells in the tumor microenvironment (TME), however, prototypically first requires activation in secondary lymphoid organs (SLOs) that drain the tumor. Such priming of anti-tumor T cells in the lymph node (LN) notably enables the migration and infiltration of tumor antigen-specific T cells into the tumor mass, and may be a tipping point that dictates early tumor recognition or escape from immunological control. While some treatment modalities, such as combination therapy of anti-CTLA-4 and anti-PD-1, primarily depends on re-activation of T cells in the local TME, T cell priming in the LN during early stages of tumor growth is still required[567].

Although CD8 T cells are equipped to exert potent anti-tumor activity, CD4 T cells too are important in mounting a robust anti-tumor response. In immunogenic settings, CD4 T cells provide notable support in augmenting immune cell function through licensing of DCs[592], stimulation of pro-inflammatory myeloid programs[593,594,595], as well as direct effects on CTL recruitment and activity in the TME[451]. Adoptive therapy of CD4 T cells too has exhibited potential for therapeutic use[454,596], and in some settings CD4$^+$ T cells can even exhibit cytotoxic

capacity[597]. Notably, some therapeutic modalities such as anti-CTLA4[598] or combinations of anti-CD40, anti-PD1, and allogeneic-IgG immune complexes[453] coincide with an emergence of a robust $CD4^+$ effector T cell response.

As professional APCs, antigen-bearing dendritic cells (DCs) are tasked with stimulating cognate T cells and producing an antigen-specific effector response. It has been appreciated that, as with prototypical immunological models, distinct tumor antigen-bearing DC subset populations carry out specialized roles in preferentially priming $CD8^+$ or $CD4^+$ T cells in SLOs[343,408] as well re-activating T cells in the TME[342]. These specialized features may result from a variety of factors such as differential antigen acquisition, differential ability to present different forms of antigen through MHC-I or MHC-II, or spatial localization relative to T cell populations. In the example of skin melanoma, our group and others have observed that migratory DCs emigrate from the TME to the draining LN and serve as the primary source of tumor antigen[343]. Migratory $CD103^+$ DC1s in particular have been identified as a pivotal myeloid partner for CD8 T cells as they are required for spontaneous anti-tumor CD8 T cell responses and are also thought to mediate anti-tumor responses following immunotherapeutic checkpoint blockade[343,433].

In contrast to $CD103^+$ DC1s, DC2s have been identified as important in driving $CD4^+$ T cell responses in a variety of models, although a number of myeloid cell populations may have outsized roles in a given helper T cell differentiation program[380,437, 438,441,599,]. In anti-tumor responses, $CD11b^+$ DCs generally have been demonstrated to drive $CD4^+$ T cell responses and skew T cells toward a Th17 fate[357]. Yet, evidence that DC2s contain substantial and further heterogeneity[437,380] complicates the conclusion of this study, and it remains unclear which myeloid cell population(s) participate in anti-tumor responses, and which predominantly support anti-tumor CD4 T cell activation and effector cell differentiation. Indeed the diversity of DC populations that are present in the lymph node and TME, and how they collectively shape a given immune response is still not fully understood. For these reasons, we set out to better

characterize the DC populations that participate in anti-tumor responses and coordinate CD8 and CD4 T cell responses.

II. RESULTS

Single-cell RNA-sequencing reveals diversity in myeloid populations within the LN

Flow cytometry has enabled considerable strides in distinguishing a number of distinct DC populations by surface marker expression and this biological segregation has revealed specialized immunological functionality. Yet, defining cell populations by a limited set of surface markers can mask additional heterogeneity within a given population, introduce an arbitrary hand in grouping of cell populations, or create difficulty in concluding cell identity and function when inconsistently applied across studies. We thus aimed to define LN myeloid populations based on a core transcriptional identity independent of surface marker delineation with single-cell RNA sequencing. To do so, we sorted non-lymphocyte (CD90- B220- NK1.1-) myeloid ($CD11c^+$ or $CD11b^+$) cells from B16 tumor-draining LNs and processed them for single-cell RNA-sequencing with the 10x Genomics platform. We used the R software package Seurat to filter for cells that expressed more than 200 genes and genes that were expressed by at least 3 cells. To minimize the degree to which cell cycle status influenced cell clustering, we removed cells with more than 5% reads associated with cell cycle and scaled count data to correct for remaining cell cycle contribution. We next used Seurat to identify a set of highly variable genes to drive principal component (PC) analysis and unguided graph-based clustering. A *t*-SNE plot analysis of the cell clustering generated 10 population clusters (**Figure 5.1A**). Clusters 0-4 and 6-7 expressed canonical cDC genes such as the cDC-restricted transcription factor *Zbtb46*[10] or the *Flt3* receptor for the growth factor FLT-3L[389,366] (**Figure 5.1B**) and we reasoned these cells represented LN cDCs. In contrast, Cluster 5 exclusively expressed prototypical monocyte and/or macrophage marker genes such as *Ly6c2*, *Fcgr1*, *Apoe*, and *Mertk* (**Figure 5.1B**). With differential expression analysis between all clusters we found Cluster 8 and 9 to be lymphocyte and stroma cell contamination, respectively (**Figure 5.2A**). While cluster marker genes emerged from this analysis and helped to distinguish these clusters as populations, visualization of the

top 10 markers did demonstrate there was a substantial degree of shared identity across populations. Such unifying programs likely reflect these cells' common myeloid origin and/or function.

Within cDCs we were able to distinguish migratory DCs from resident DCs based on elevated gene expression of markers whose protein expression is restricted to migratory DCs such as *Ccr7* and *Slamf1* (**Figure 5.1C**). We combined cells from migratory DC clusters (Clusters 0,1,2,4,6) or resident DC clusters (Clusters 3, 7) and performed differential expression analysis between these cluster groups to generate a general migratory DC and resident DC gene signature (**Figure 5.3A**). Expression of each of the signatures was largely uniform across each of the previously identified migratory or resident DCs, suggesting that these cell populations do indeed share a common set of gene markers based on this categorization. The exception was Cluster 6, which appeared to express the resident DC signature to a stronger degree than the migratory one. Closer examination of the *Ccr7* expression distribution on the *t*-SNE plot revealed segregated expression of this gene (**Figure 5.1C**), indicating additional heterogeneity. Cluster 6 may contain a mix of migratory and resident DCs and will require further attention. Overall, the migratory DC signature contained a number of gene markers, such as *Ccr7*, *Fscn1*, *Socs2*, *Nudt17*, *Anxa3*, *Cacnb3*, *Samsn1*, and *Tmem123*, which were identified in previous studies of LN migratory myeloid populations[364,600]. These similarities confirmed these cells' migratory origin, and demonstrated consistency in signature across studies and models. In contrast, the resident DC signature consisted of enriched expression of MHC-II and MHC-II-processing genes such as *H2-Ab1, H2-DMa, H2-DMb1, H2-DMb2, H2-Aa, H2-Eb1, and Cd74*. As migratory DCs express higher cell surface protein levels of MHC-II, it is unclear whether the increased expression of MHC-II genes in resident DCs reflects differences in translation rates or limitations in sequencing depth.

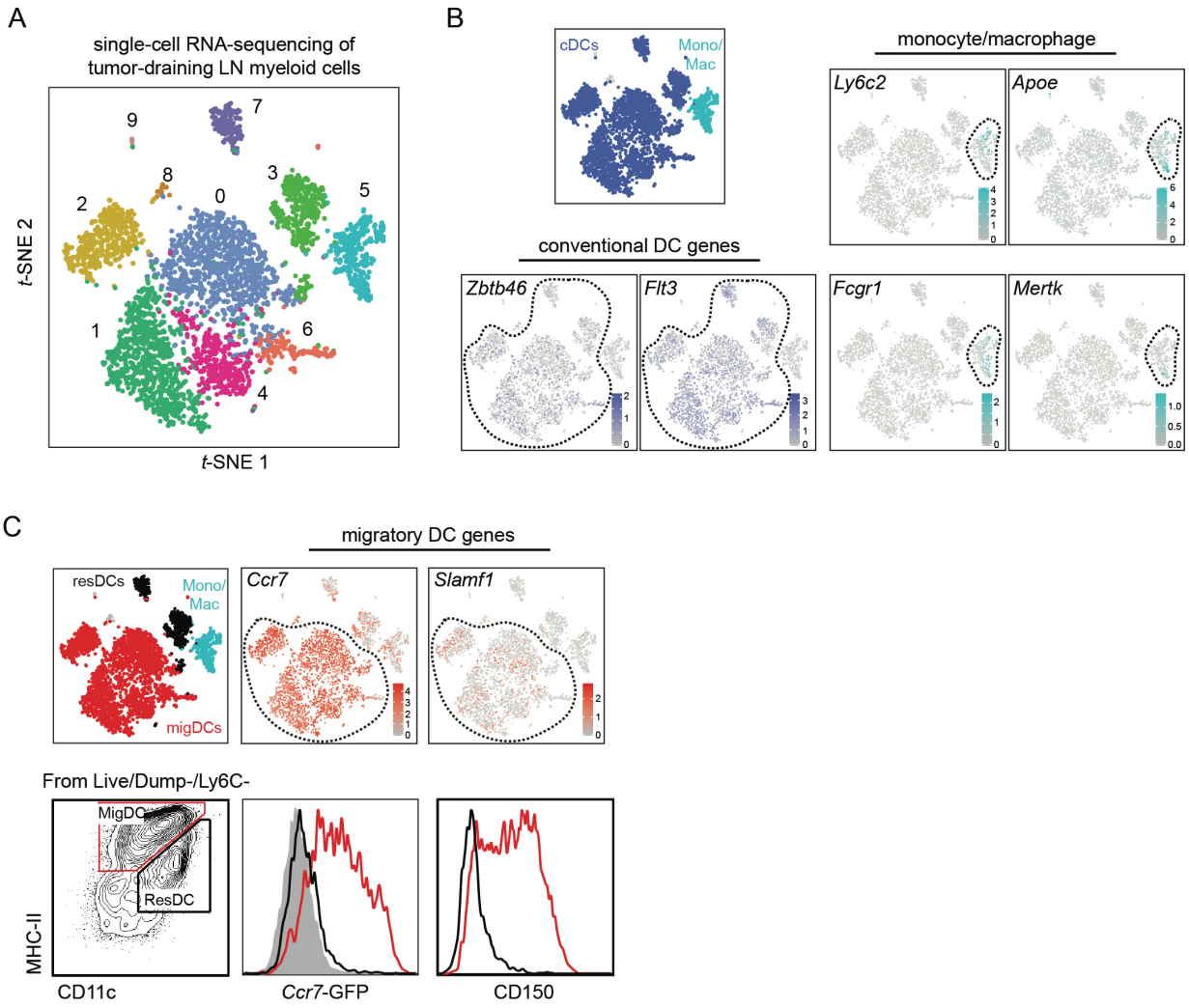
A
single-cell RNA-sequencing of
tumor-draining LN myeloid cells
t-SNE 2
t-SNE 1
0
1
2
3
4
5
6
7
8
9
B
cDCs
Mono/
Mac
monocyte/macrophage
Ly6c2
Apoe
conventional DC genes
Zbtb46
Flt3
Fcgr1
Mertk
C
migratory DC genes
resDCs
Mono/
Mac
migDCs
Ccr7
Slamf1
From Live/Dump-/Ly6C-
MigDC
ResDC
MHC-II
CD11c
Ccr7-GFP
CD150

Figure 5.1 Identification of tumor-draining lymph node myeloid cells by single-cell RNA-sequencing analysis.
(**A**) t-SNE analysis of live CD90- B220- NK1.1- $CD11b^+$ and/or $CD11c^+$ myeloid cells sorted from B16 tumor-draining LNs and processed for single-cell RNA-sequencing. Each individual dot represents a single cell. (**B**) Distribution of expression of canonical cDC genes (**left**) or monocyte and/or macrophage genes **(right**) on t-SNE plot of LN myeloid cells. (**C**) Distribution of gene expression of Ccr7 and Slamf1 on t-SNE plot of
LN myeloid cells (**top**), and GFP and CD150 protein expression by migratory (red) and resident (black) DCs with isotype control (gray) (**bottom**) in tumor-bearing Ccr7gfp reporter or wild-type mice, respectively.

A

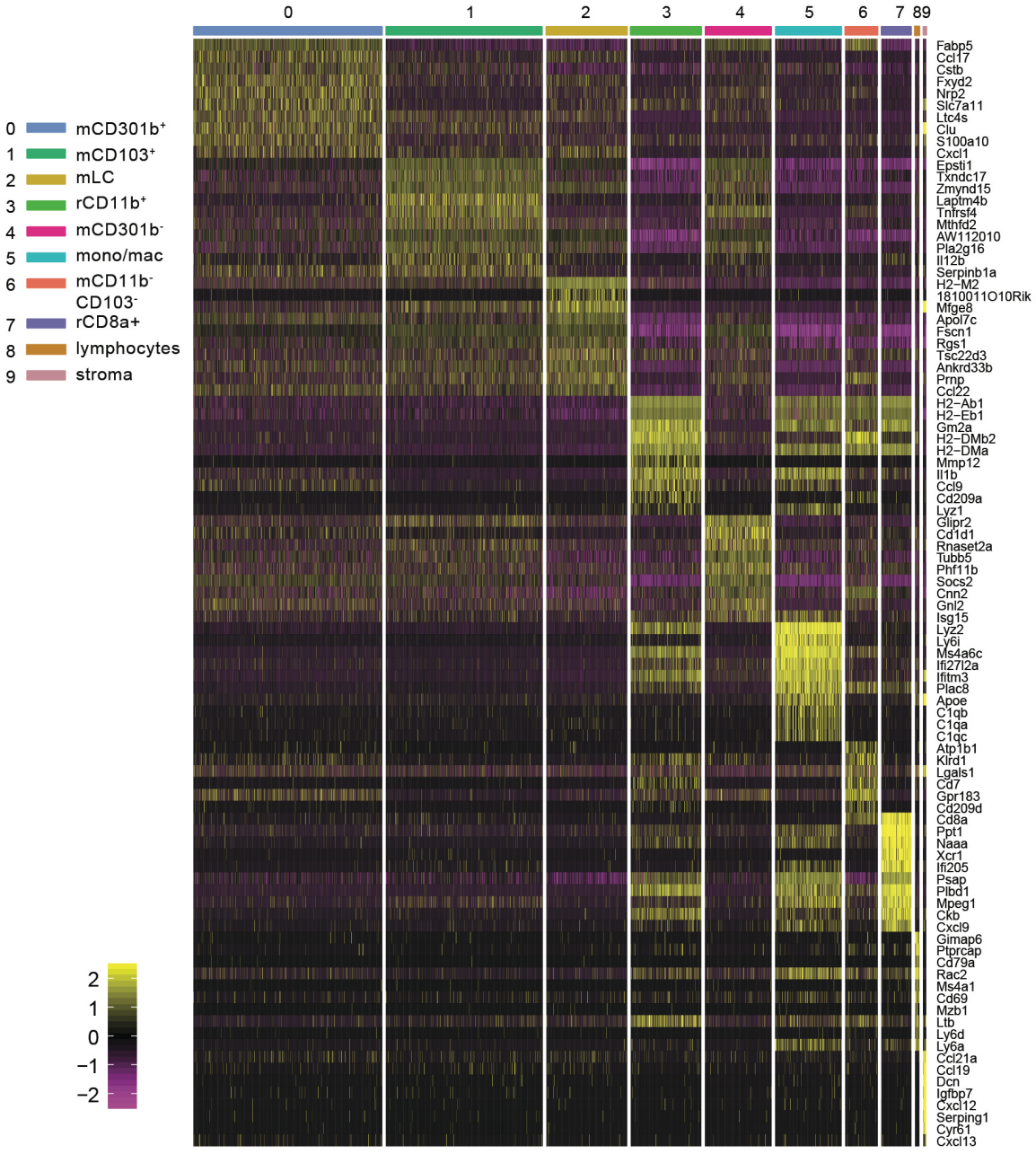
0 mCD301b+
1 mCD103+
2 mLC
3 rCD11b+
4 mCD301b-
5 mono/mac
6 mCD11b- CD103-
7 rCD8a+
8 lymphocytes
9 stroma
0 1 2 3 4 5 6 7 8 9
Fabp5
Ccl17
Cstb
Fxyd2
Nrp2
Slc7a11
Ltc4s
Clu
S100a10
Cxcl1
Epsti1
Txndc17
Zmynd15
Laptm4b
Tnfrsf4
Mthfd2
AW112010
Pla2g16
Il12b
Serpinb1a
H2-M2
1810011O10Rik
Mfge8
Apol7c
Fscn1
Rgs1
Tsc22d3
Ankrd33b
Prnp
Ccl22
H2-Ab1
H2-Eb1
Gm2a
H2-DMb2
H2-DMa
Mmp12
Il1b
Ccl9
Cd209a
Lyz1
Glipr2
Cd1d1
Rnaset2a
Tubb5
Phf11b
Socs2
Cnn2
Gnl2
Isg15
Lyz2
Ly6i
Ms4a6c
Ifi27l2a
Ifitm3
Plac8
Apoe
C1qb
C1qa
C1qc
Atp1b1
Klrd1
Lgals1
Cd7
Gpr183
Cd209d
Cd8a
Ppt1
Naaa
Xcr1
Ifi205
Psap
Plbd1
Mpeg1
Ckb
Cxcl9
Gimap6
Ptprcap
Cd79a
Rac2
Ms4a1
Cd69
Mzb1
Ltb
Ly6d
Ly6a
Ccl21a
Ccl19
Dcn
Igfbp7
Cxcl12
Serping1
Cyr61
Cxcl13
2
1
0
−1
−2

Figure 5.2 Tumor-draining LN myeloid cell population gene signatures.
(**A**) Heat map of cluster marker genes (log*N*fold change>0.5, expressed in ≥25% of all cells within cluster of interest) for each cluster as defined in **Figure 2.1**.

A

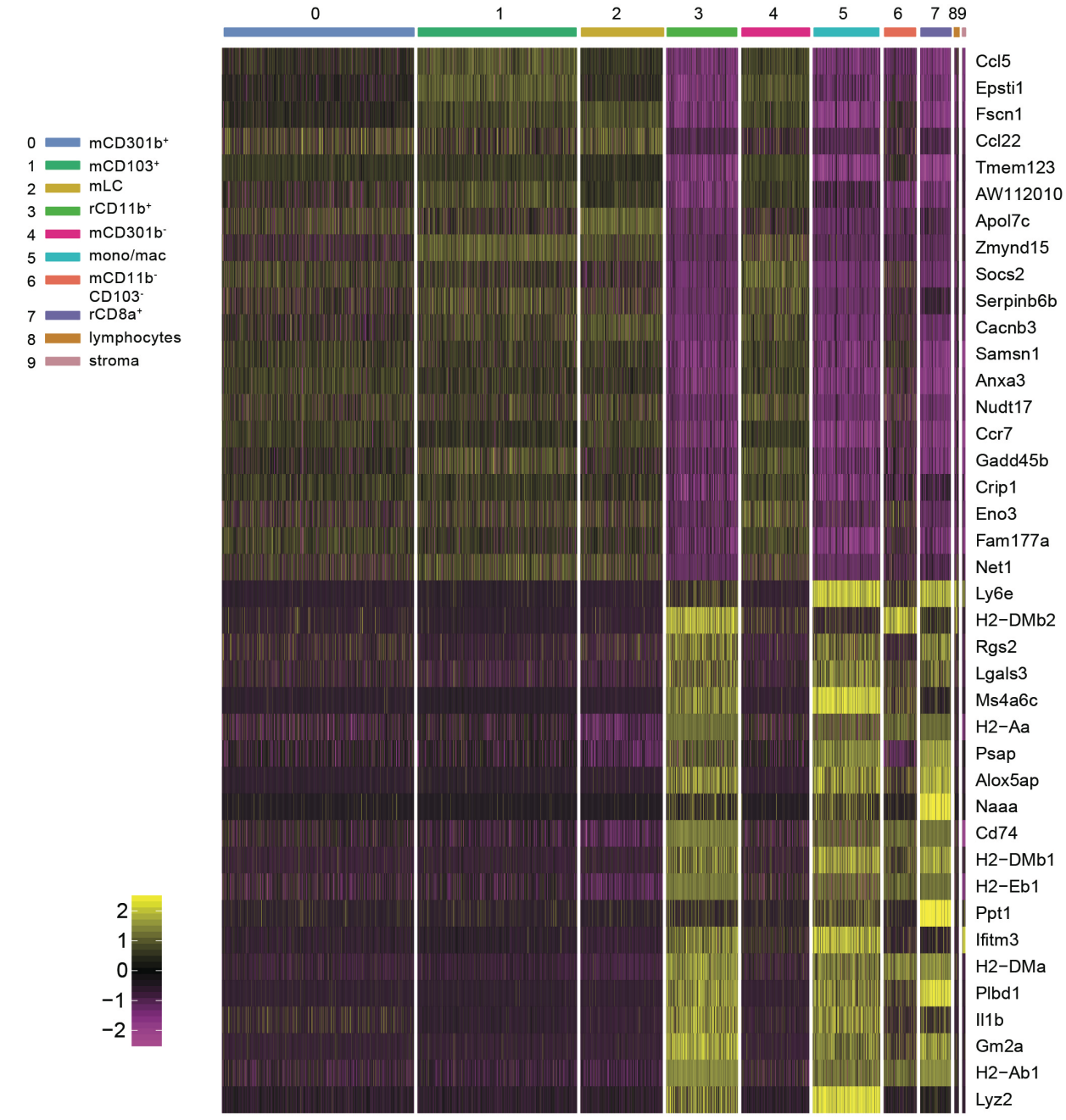
0
1
2
3
4
5
6
7
8
9
mCD301b+
mCD103+
mLC
rCD11b+
mCD301b-
mono/mac
mCD11b- CD103-
rCD8a+
lymphocytes
stroma
0 1 2 3 4 5 6 7 89
Ccl5
Epsti1
Fscn1
Ccl22
Tmem123
AW112010
Apol7c
Zmynd15
Socs2
Serpinb6b
Cacnb3
Samsn1
Anxa3
Nudt17
Ccr7
Gadd45b
Crip1
Eno3
Fam177a
Net1
Ly6e
H2−DMb2
Rgs2
Lgals3
Ms4a6c
H2−Aa
Psap
Alox5ap
Naaa
Cd74
H2−DMb1
H2−Eb1
Ppt1
Ifitm3
H2−DMa
Plbd1
Il1b
Gm2a
H2−Ab1
Lyz2
2
1
0
−1
−2

Figure 5.3 Gene signatures of tumor-draining LN migratory and resident DCs.
(**A**) Migratory (Cluster 0, 1, 2, 4, 6) and resident (Cluster 3, 7) DC clusters were each combined into group clusters and differential expression analysis between the two groups was performed. Heat map of scaled expression of genes (log*N*fold change>0.5, expressed in ≥50% of cells within the group cluster) across individual clusters.

To more specifically delineate individual cell population identity, we generated gene signatures from myeloid cell samples available from the Immunological Genome Project (ImmGen) database and plotted expression of these signatures on the LN *t*-SNE plot (**Figure 5.4A**). This approach allowed us to confirm monocytes as Cluster 5, and separate resident DCs into CD11b$^+$ DCs (rCD11b$^+$) as Cluster 3 and CD8a$^+$ DCs (rCD8a$^+$) as Cluster 7. The migratory CD103 DC1 (mCD103$^+$) signature was enriched in Cluster 1, and migratory Langerhans cells (mLCs) was localized to Cluster 2. As noted previously, recent studies have revealed considerable diversity within DC2s. Although DC2s are commonly defined as IRF4-dependent SIRPa$^+$ CD11b$^+$ DCs[356], heterogeneity in surface protein expression like CD301b (Mgl2) or PDL-2 has been observed[436,437]. In addition, IRF4-dependency has been attributed both to CD11b$^+$ populations as well as a CD11b- CD24- population[380]. Reflective of this heterogeneity, the migratory CD11b$^+$ DC signature was primarily expressed across both Cluster 0 and 4. The CD11b-CD103- signature localized to Cluster 6, although we did note spillover expression in Cluster 0 as well. From this analysis, we hypothesized that these three clusters represented LN DC2 populations, and each expressed genes such as *Gpr183* and *Zeb2* (**Figure 5.4B**), which have been previously shown to be expressed by DC2s[375,601]. Although Immgen database sample populations did not provide further resolution of CD11b$^+$ DCs, we hypothesized based on prior literature that Cluster 0 and 4 contained CD11b$^+$ CD301b$^+$ (mCD301b$^+$) and CD301b- (mCD301b-) DCs as these CD11b$^+$ DCs have been identified to exhibit distinct biological function[436,437]. Although *Mgl2* expression was present in a subset of resident DCs, it was absent in migratory DCs (**Figure 5.4C**) and thus prevented us from identifying CD301b$^+$ DCs in our data set. Surprisingly, when we looked by single-cell RNA-sequencing analysis at these DC populations in the tumor tissue itself, down-regulation of *Mgl2* expression was concurrent with *Ccr7* up-regulation within CD301b$^+$ DCs (data not shown) and this relationship seems to explain the lack of *Mgl2* expression detected in migratory LN DCs.

A

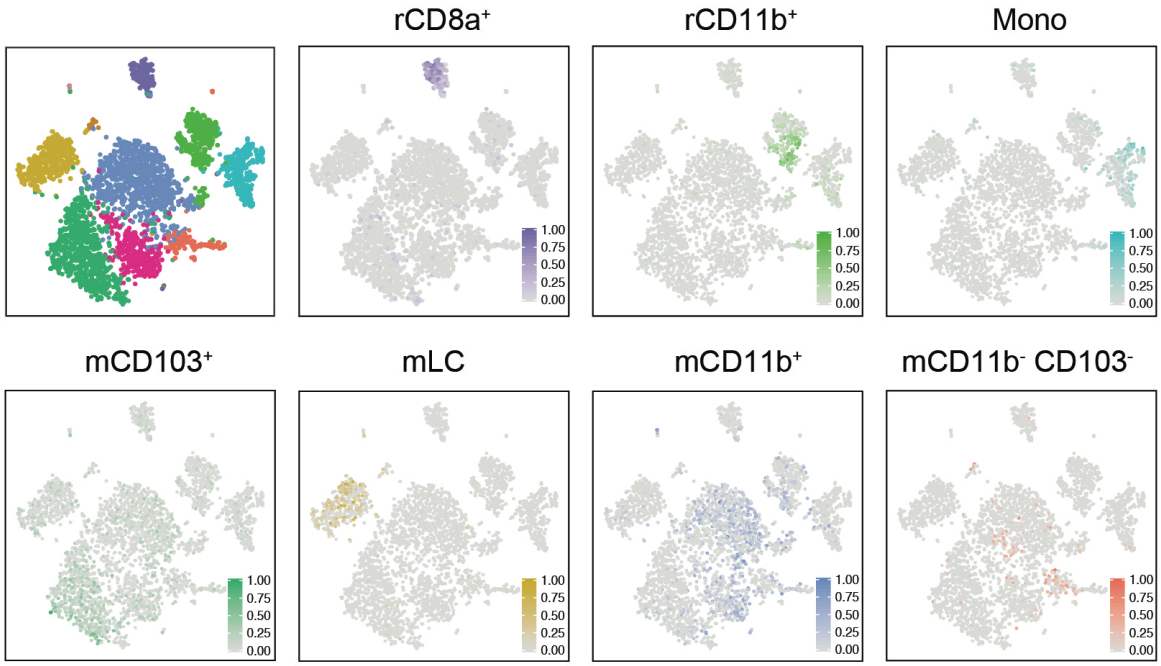
rCD8a+
rCD11b+
Mono
mCD103+
mLC
mCD11b+
mCD11b- CD103-
1.00
0.75
0.50
0.25
0.00

B

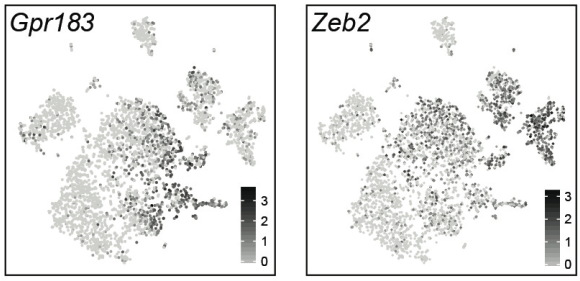
Gpr183
Zeb2
3
2
1
0

C

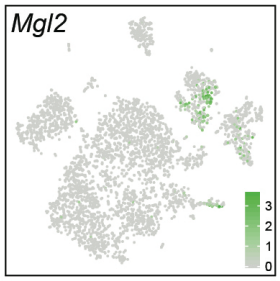
Mgl2
3
2
1
0

Figure 5.4 Identification of myeloid cluster populations generated by single-cell RNA-sequencing analysis.
(**A**) Expression of Immgen.org gene signatures distributed across t-SNE plot of tumor-draining LN. (**B, C**) Expression of *Gpr183* and *Zeb2* (**B**), and *Mgl2* (**C**) plotted on t-SNE of LN myeloid cells.

Given our inability to evaluate whether these DCs separate based on CD301b$^+$ expression, we performed differential expression between Cluster 0 and 4 (**Figure 5.5A**). In addition to mitochondrial genes, Cluster 0 expressed higher levels of chemotactic genes like *Ccl17*, *Cxcl1*, *Ccl22*, *Cxcl22*, and leukotriene C4 synthase gene *Ltc4s*. In contrast, Cluster 4, exhibited higher levels of genes that have been associated with type I interferon signaling like *Glipr2*[602], *Ifitm3*[603], and *Isg15*[604], as well as antigen processing genes like the transport protein genes *Tap1*, *Tap2*, the immunoproteasome element *Psmb2*, and the negative regulator of autophagy *Glipr2*[605]. Of the candidate surface marker genes that emerged from this analysis, only CD9, but not CD134 (*Tnfrsf4*) or CD1d, appeared to sub-divide migratory non-Langerhans CD24lo CD11b$^+$ DCs (**Figure 5.6A**). Indeed, CD9 surface expression also corresponded with CD301b surface expression, suggesting that CD11b$^+$ DCs largely contain populations of CD301b$^+$ CD9$^+$ and CD301b$^-$ CD9$^-$ cells (**Figure 5.6B**). Further validation of this CD9/CD301b delineation is required, however, and we intend to sort migratory CD11b DCs based on surface expression of CD301b$^+$ or CD9. We can then test gene expression of candidate gene markers that differentiate Cluster 0 and 4 to determine if this relationship is recapitulated with these sorting strategies. For the time being, these analyses largely confirmed FACS-based separation of LN DC populations and, in particular, provided support for reports of increased DC2 heterogeneity and the presence of three populations distinct in genomic identity.

A

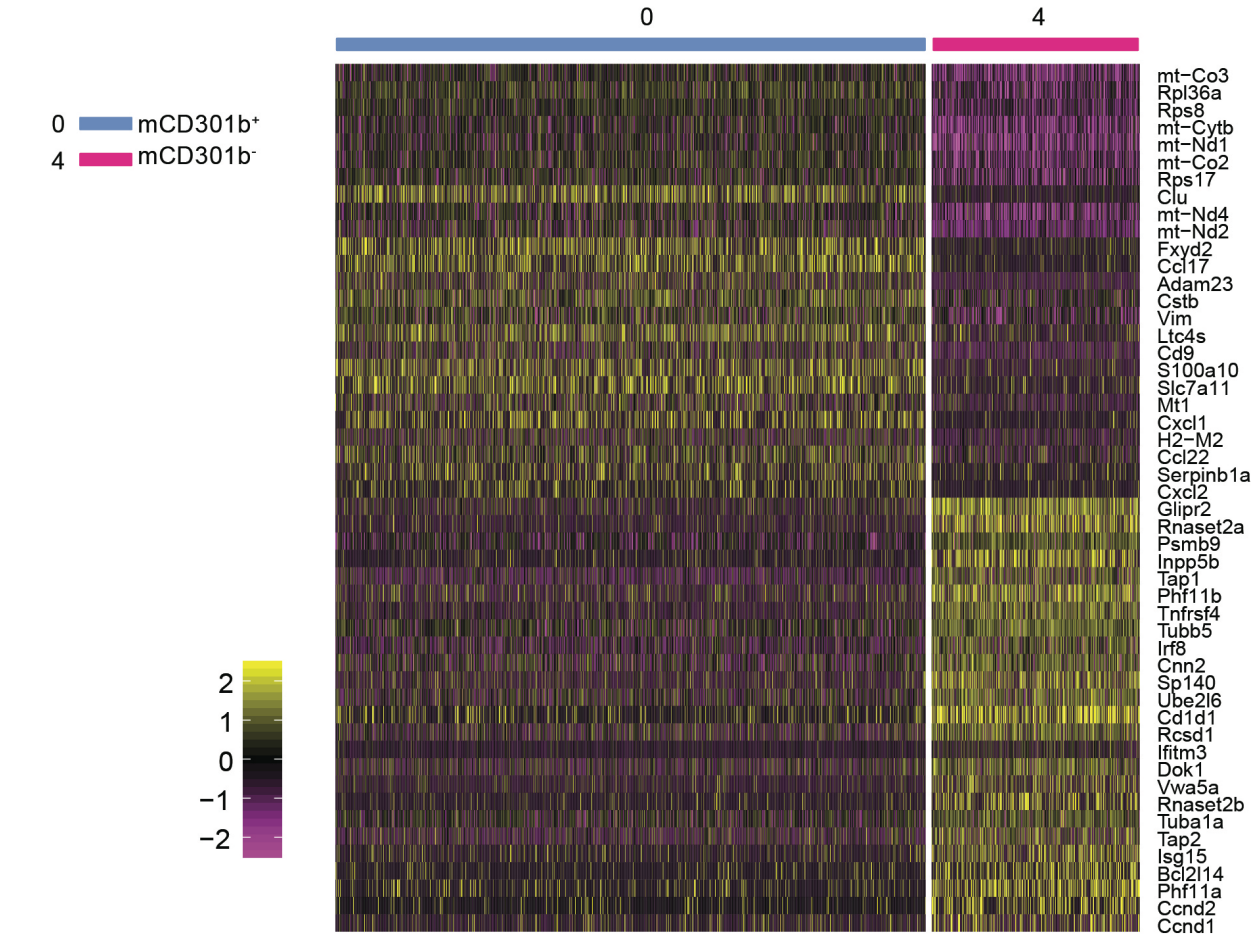
0
4
0 mCD301b+
4 mCD301b-
2
1
0
−1
−2
mt−Co3
Rpl36a
Rps8
mt−Cytb
mt−Nd1
mt−Co2
Rps17
Clu
mt−Nd4
mt−Nd2
Fxyd2
Ccl17
Adam23
Cstb
Vim
Ltc4s
Cd9
S100a10
Slc7a11
Mt1
Cxcl1
H2−M2
Ccl22
Serpinb1a
Cxcl2
Glipr2
Rnaset2a
Psmb9
Inpp5b
Tap1
Phf11b
Tnfrsf4
Tubb5
Irf8
Cnn2
Sp140
Ube2l6
Cd1d1
Rcsd1
Ifitm3
Dok1
Vwa5a
Rnaset2b
Tuba1a
Tap2
Isg15
Bcl2l14
Phf11a
Ccnd2
Ccnd1

Figure 5.5 Gene signatures for tumor-draining LN migratory CD11b^{+} DC populations. (**A**) Differential analysis was performed between Cluster 0 and 4. Heat map of scaled expression of cluster marker genes (log*N*fold change>0.5, expressed in ≥25% of cells within the cluster of interest).

A

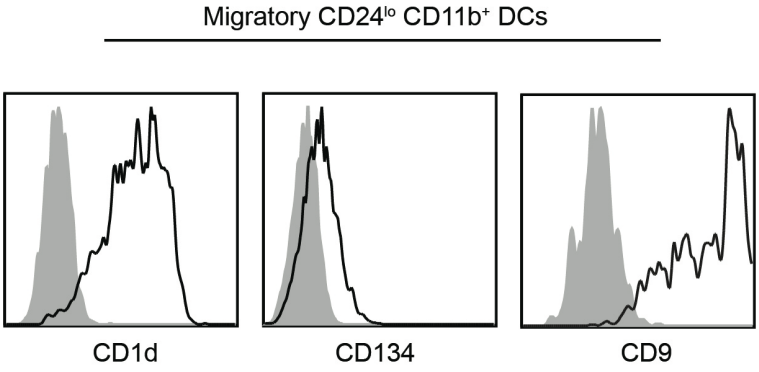
Migratory CD24lo CD11b+ DCs
CD1d
CD134
CD9

B

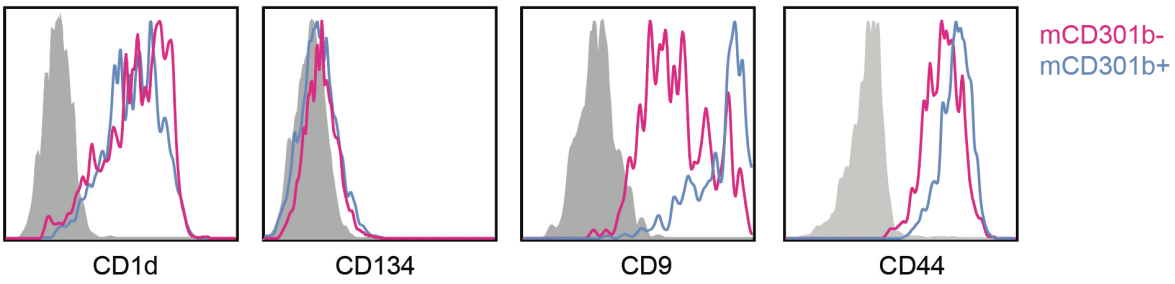
CD1d
CD134
CD9
CD44
mCD301b-
mCD301b+

Figure 5.6 Migratory CD11b$^+$ DCs can be divided based on CD9 and CD301b expression. (**A**) Surface protein expression of CD1d, CD134, or CD9 on migratory CD24lo CD11b$^+$ DCs (black) with isotype control (gray) (**B**) Surface expression of CD1d, CD134, CD9, and CD44 on migratory CD11b$^+$ CD301b- (pink) or CD301b$^+$ (blue) cells with isotype control (gray).

We thus focused on the myeloid populations identified in the single-cell RNA-sequencing analysis and sought to characterize whether and how these different DC cells participated in anti-tumor T cell responses. For downstream experimentation we treated populations as specified by flow cytometry gating strategy whereby we could define monocytes (**Figure 5.7A**), resident $CD8a^+$ and $CD11b^+$ DCs (**Figure 5.7B**), and migratory $CD103^+$, $CD11b^+$ CD24hi Langerhans, $CD11b^+$ CD24lo CD301b-, $CD11b^+$ CD24lo $CD301b^+$, or CD11b- CD103- DCs (**Figure 5.7C**). For CD11b- CD103- DCs, given that Cluster 6 already contained noted heterogeneity and a negative gating strategy had the potential for contamination from other populations, we enriched for $CD24^+$ expression within this population (**Figure 5.7D**). The majority of CD11b- CD103- DCs were $CD24^{hi}$ compared to $CD11b^+$ DC2s and this difference was reflected in the gene distribution of *Cd24a* in Cluster 6.

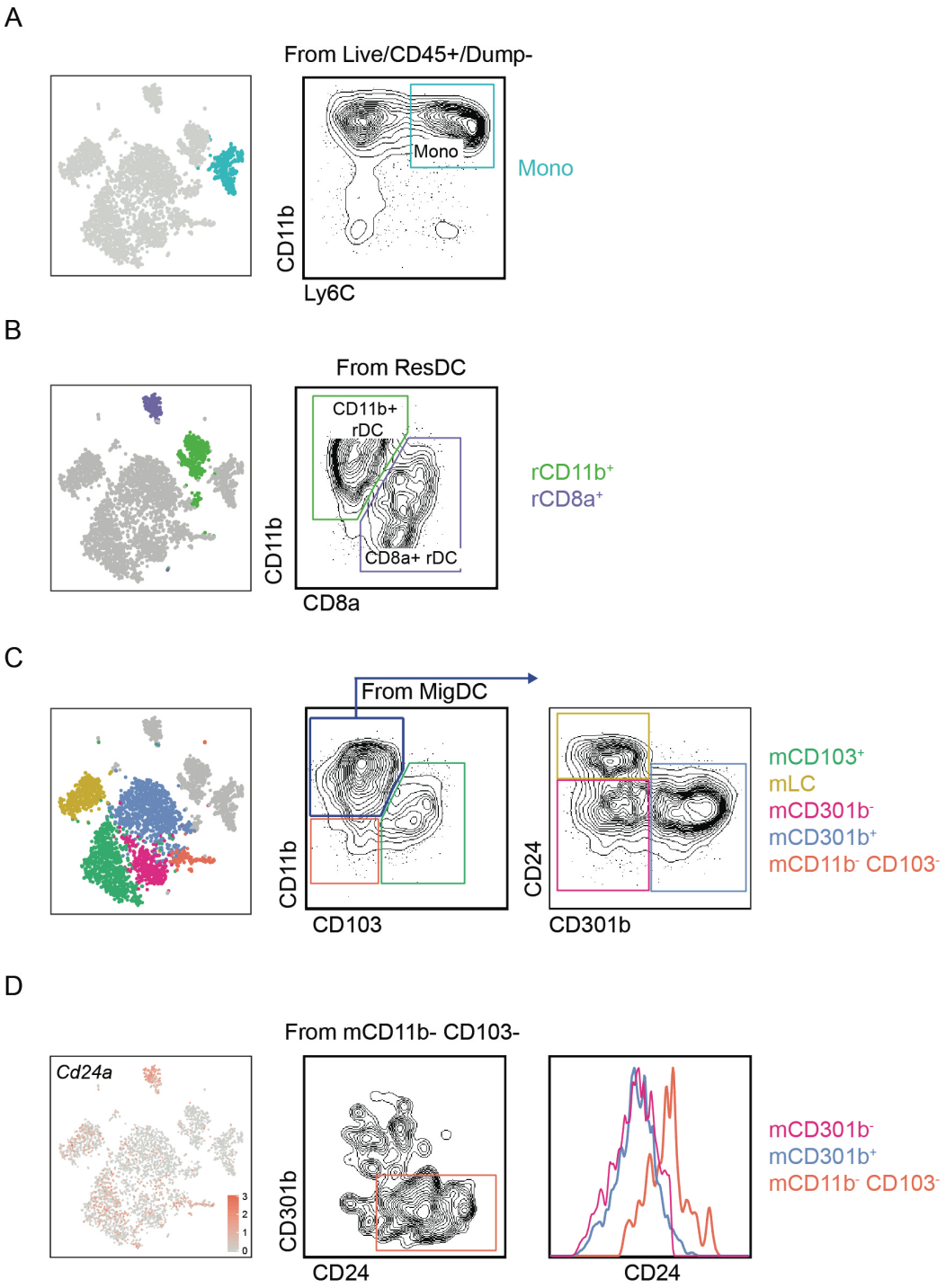
A
From Live/CD45+/Dump-
Mono
Mono
CD11b
Ly6C
B
From ResDC
CD11b+
rDC
CD8a+ rDC
rCD11b+
rCD8a+
CD11b
CD8a
C
From MigDC
mCD103+
mLC
mCD301b-
mCD301b+
mCD11b- CD103-
CD11b
CD103
CD24
CD301b
D
From mCD11b- CD103-
Cd24a
3
2
1
0
mCD301b-
mCD301b+
mCD11b- CD103-
CD301b
CD24
CD24

Figure 5.7 Dissection of LN myeloid populations by flow cytometric surface marker identification.
(**A**) Identification of monocyte cells on t-SNE plot (**left**) and by flow cytometry (**right**). (**B**) Identification of resident CD8a$^+$ and CD11b$^+$ DCs on t-SNE plot (**left**) and by flow cytometry (**right**). (**C**) Identification of the following migratory DCs on t-SNE plot (**left**) and by flow cytometry (**right**): CD103$^+$ DCs, CD11b$^+$ CD24hi Langerhans cells, CD11b$^+$ CD24lo CD301b- DCs, CD11b$^+$ CD24lo CD301b$^+$ DCs, and CD11b- CD103- DCs. (**D**) Expression of *Cd24a* by LN myeloid cells (**left**) and surface expression of CD24 by migratory CD11b- CD103- DCs (**middle**) compared to migratory LN CD11b$^+$ DCs (**right**).

Migratory cells from the tumor are required for antigen loading of myeloid populations in the lymph node and anti-tumor CD4 T cell activation

LN DC populations were verified to be DCs based on high levels of GFP expression relative to monocytes in tumor-draining LNs of B16-tumor-bearing *Zbtb46*^{gfp} reporter mice (**Figure 5.8A**). Using a B16 cell line that expresses the pH-stable fluorophore ZsGreen[343], we tracked antigen uptake and observed loading of tumor ZsGreen antigen in all DC and monocyte populations (**Figure 5.8B, C**), which was consistent with previously published reports[343]. While monocytes exhibited the highest frequency of antigen uptake, migratory CD11b$^+$ CD301b$^+$ DCs were the population amongst DCs with the highest degree of loading. Although a previous study from our lab did not find migratory CD11b$^+$ DCs to contain such a relatively high degree of ZsGreen antigen[343], at the time, F4/80$^+$ cells were treated as macrophages and not DCs. Upon further analysis, however, migratory CD11b$^+$ DCs appear to have the highest levels of F4/80$^+$ amongst migratory DCs (**Figure 5.8D**), and thus would have been excluded from analysis. We believe our updated gating strategy better represents DC populations, and that improved resolution of CD11b$^+$ DCs will yield insight into their specific roles in anti-tumor immunity.

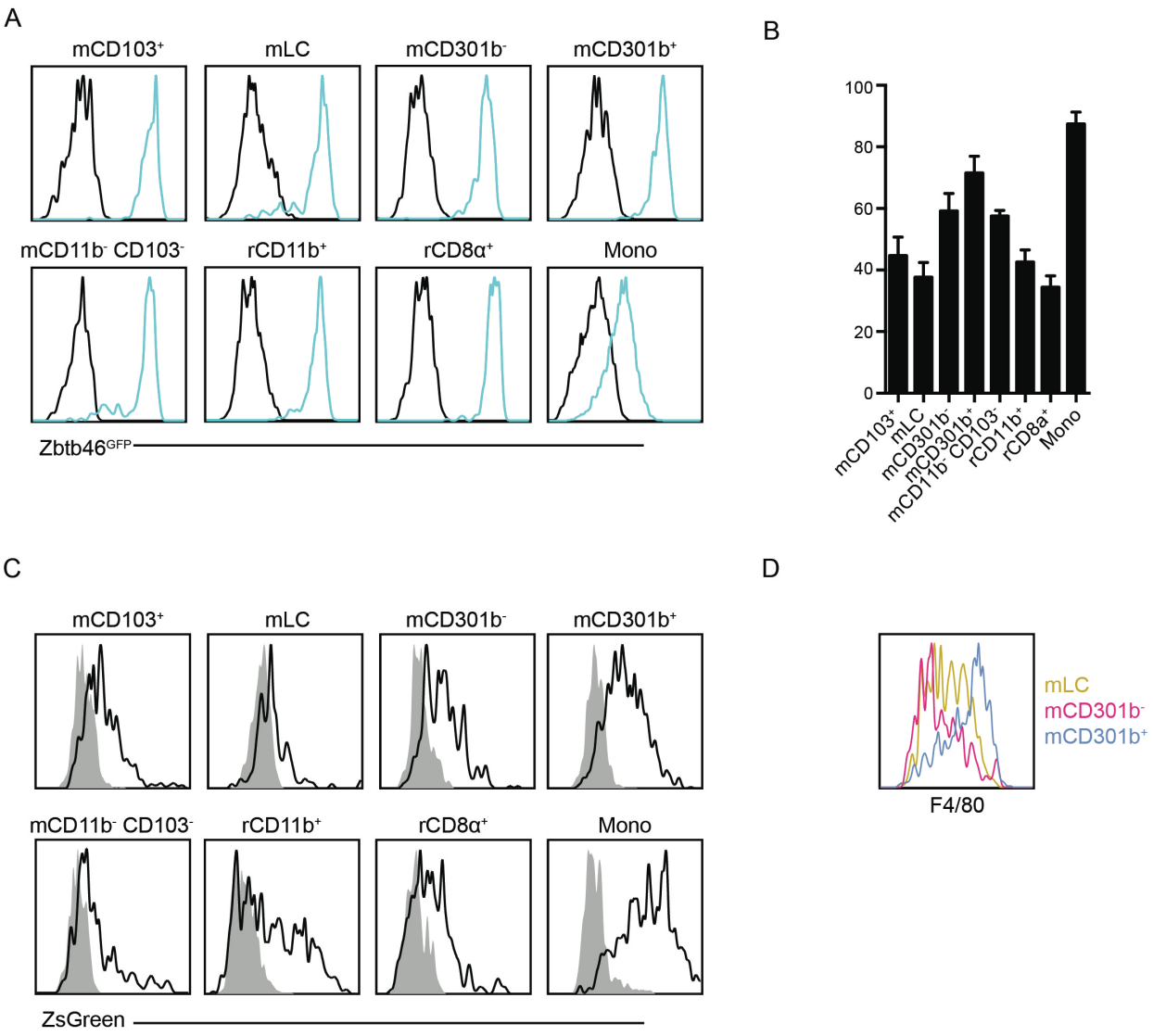
A
mCD103+
mLC
mCD301b-
mCD301b+
mCD11b- CD103-
rCD11b+
rCD8α+
Mono
Zbtb46GFP
B
100
80
60
40
20
0
mCD103+
mLC
mCD301b-
mCD301b+
mCD11b- CD103-
rCD11b+
rCD8α+
Mono
C
mCD103+
mLC
mCD301b-
mCD301b+
mCD11b- CD103-
rCD11b+
rCD8α+
Mono
ZsGreen
D
mLC
mCD301b-
mCD301b+
F4/80

Figure 5.8 Composition of and antigen uptake by myeloid populations in B16-tumor-draining LNs.
B16 tumor cells were injected in wild-type mice, and tumor-draining LNs were harvested and pooled for analysis. (**A**) GFP expression levels of myeloid populations in tumor-draining LNs of B16-tumor-bearing *Zbtb*^{gfp} mice (blue) or wild-type control mice (black). (**B,C**) Tumor-draining LNs were collected from B16-ZsGreen tumor bearing mice. (**B**) Frequency of LN myeloid populations labeled with ZsGreen tumor antigen and (**C**) ZsGreen levels in myeloid populations (black) with naive non-tumor bearing controls (gray). (**D**) Expression levels of F4/80 on tumor-draining LN migratory CD11b^{+} CD301b-, CD11b^{+} CD301b^{+}, and Langerhans cells. Data is representative of at least three independent experiments. Small horizontal bars denote the SEM.

In addition to the LN, we were able to also identify migratory DCs in the TME. As previously reported, $CD103^+$ and $CD11b^+$ DCs are present in the tumor[342], as are CD103-CD11b- DCs[350](**Figure 5.9A**). As in the LN, we could further divide $CD11b^+$ DCs into those expressing CD301b or not. Given the subcutaneous tumor model used we did not observe a population of migratory $CD24^{hi}$ $CD207^+$ $CD11b^+$ Langerhans cells (data not shown). We again verified our use of tumor DC nomenclature by confirming that these DC populations expressed high levels of GFP in *Zbtb46*-GFP mice (**Figure 5.9B**), but, as reported historically, are far outnumbered by monocytes and TAMs in B16 tumors (**Figure 5.8C**). While it should be noted that our lab has previously gated on tumor DCs as $CD24^{hi}$ [342], with more experimentation we have observed variable CD24 levels on tumor DCs. In experiments that produce a greater range in CD24 expression, we find $CD11b^+$ DCs to be $CD24^{lo}$ (**Figure 5.9D**). We thus recommend simply gating on $F4/80^-$ cells amongst MHC-II^+ $CD90^-$ $B220^-$ $NK1.1^-$ Ly-$6G^-$ cells to include all DCs. Lastly, each DC population contained a $CCR7^+$ subset of cells, indicating potential to migrate from the tumor to the tumor-draining LN (**Figure 5.9E**).

With our updated gating strategy we confirmed that each of the LN DC populations we deemed to be migratory indeed expressed CCR7 unlike resident DC populations (**Figure 5.10A**). These migratory LN DC populations were specifically reduced in CCR7-deficient tumor-bearing mice (**Figure 5.10B**), and, consistent with our lab's previous findings, tumor ZsGreen antigen was reduced across all DC populations in CCR7-deficient mice (**Figure 5.10C**). Our lab previously demonstrated that migration of tumor DCs to tumor-draining LNs is critical for transport of antigen to the LN and initiation of anti-tumor $CD8^+$ T cell responses[343]. Since anti-tumor $CD4^+$ T cell activation is not as well understood, we tested whether $CD4^+$ T cell activation had the same requirements. Indeed, when transferred into tumor-bearing CCR7-deficient hosts, $CD4^+$ OT-II T cells did not proliferate to the same extent as those transferred to wild-type hosts (**Figure 5.10, E**).

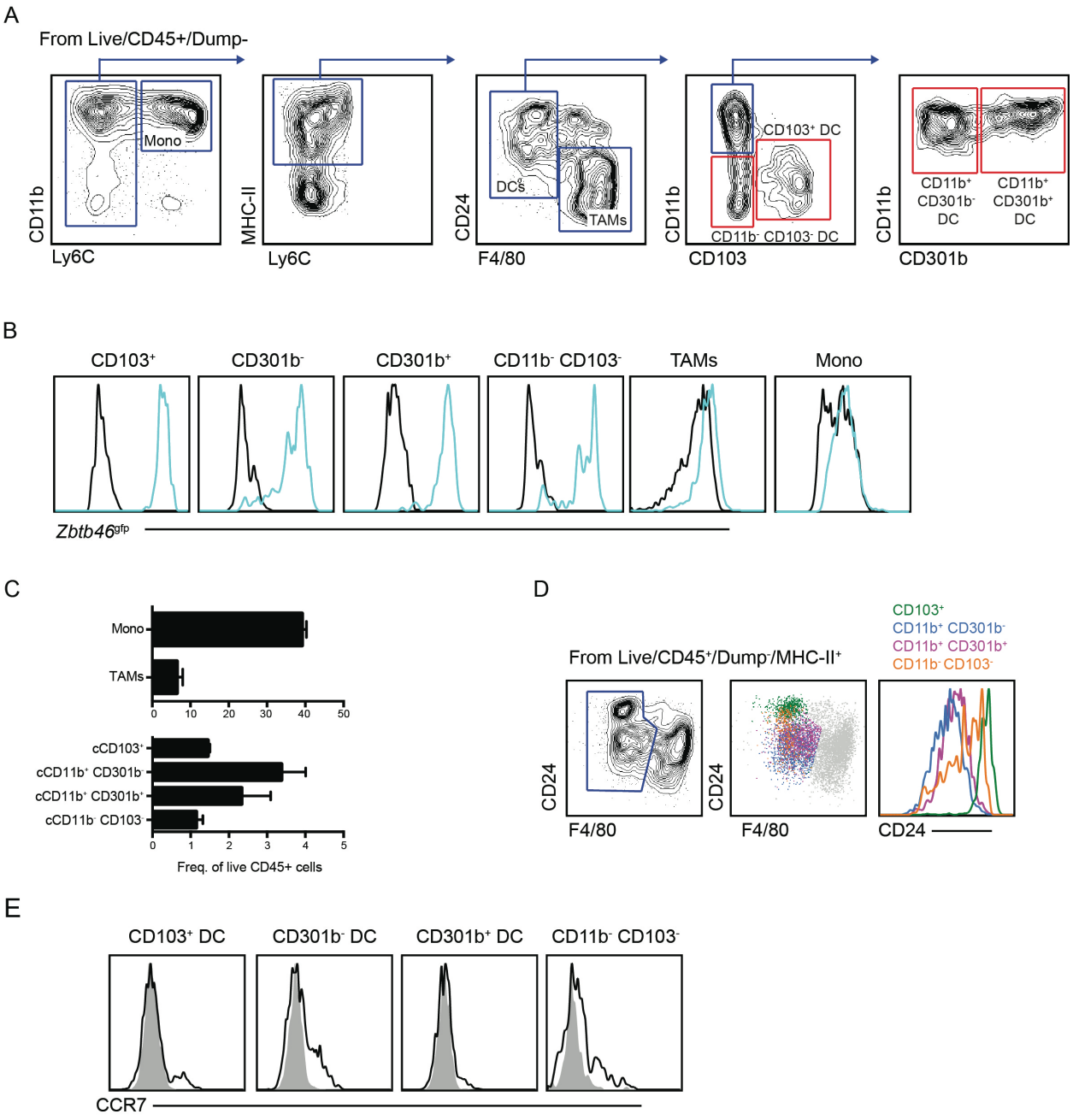
A
From Live/CD45+/Dump-
Mono
CD11b
Ly6C
MHC-II
Ly6C
CD24
DCs
TAMs
F4/80
CD103+ DC
CD11b- CD103- DC
CD11b
CD103
CD11b+ CD301b- DC
CD11b+ CD301b+ DC
CD11b
CD301b
B
CD103+
CD301b-
CD301b+
CD11b- CD103-
TAMs
Mono
Zbtb46gfp
C
Mono
TAMs
0 10 20 30 40 50
cCD103+
cCD11b+ CD301b-
cCD11b+ CD301b+
cCD11b- CD103-
0 1 2 3 4 5
Freq. of live CD45+ cells
D
CD103+
CD11b+ CD301b-
CD11b+ CD301b+
CD11b- CD103-
From Live/CD45+/Dump-/MHC-II+
CD24
F4/80
CD24
F4/80
CD24
E
CD103+ DC
CD301b- DC
CD301b+ DC
CD11b- CD103-
CCR7

Figure 5.9 Composition of myeloid populations in primary B16 melanoma tumor.
(**A**) Flow cytometric gating strategy for myeloid populations in primary B16 tumors with cDC subset populations denoted in red. Dump refers to CD90.2, B220, NK1.1, Ly-6G. (**B**) Expression of GFP in tumor myeloid populations in tumor-bearing Zbtb^{gfp} mice (blue) or wild-type control mice (black). (**C**) Frequency of myeloid populations of live CD45^{+} cells in B16 tumors. (**D**) Flow cytometric gating example of cDCs (blue) in B16 tumors (**left**) with overlay of CD103^{+}, CD11b^{+} CD301b-, CD11b^{+} CD301b-, and CD11b- CD103- cDC subsets on live CD45^{+} Dump- MHC-II^{+} cells (**middle**), and their surface expression of CD24 (**righ**t). (**E**) Surface CCR7 levels (black) on tumor DC populations with isotype control (gray). Data is representative of at least three experiments (**A,B,D**) or pooled average values from three independent experiments (**C**). Small horizontal bars denote the SEM.

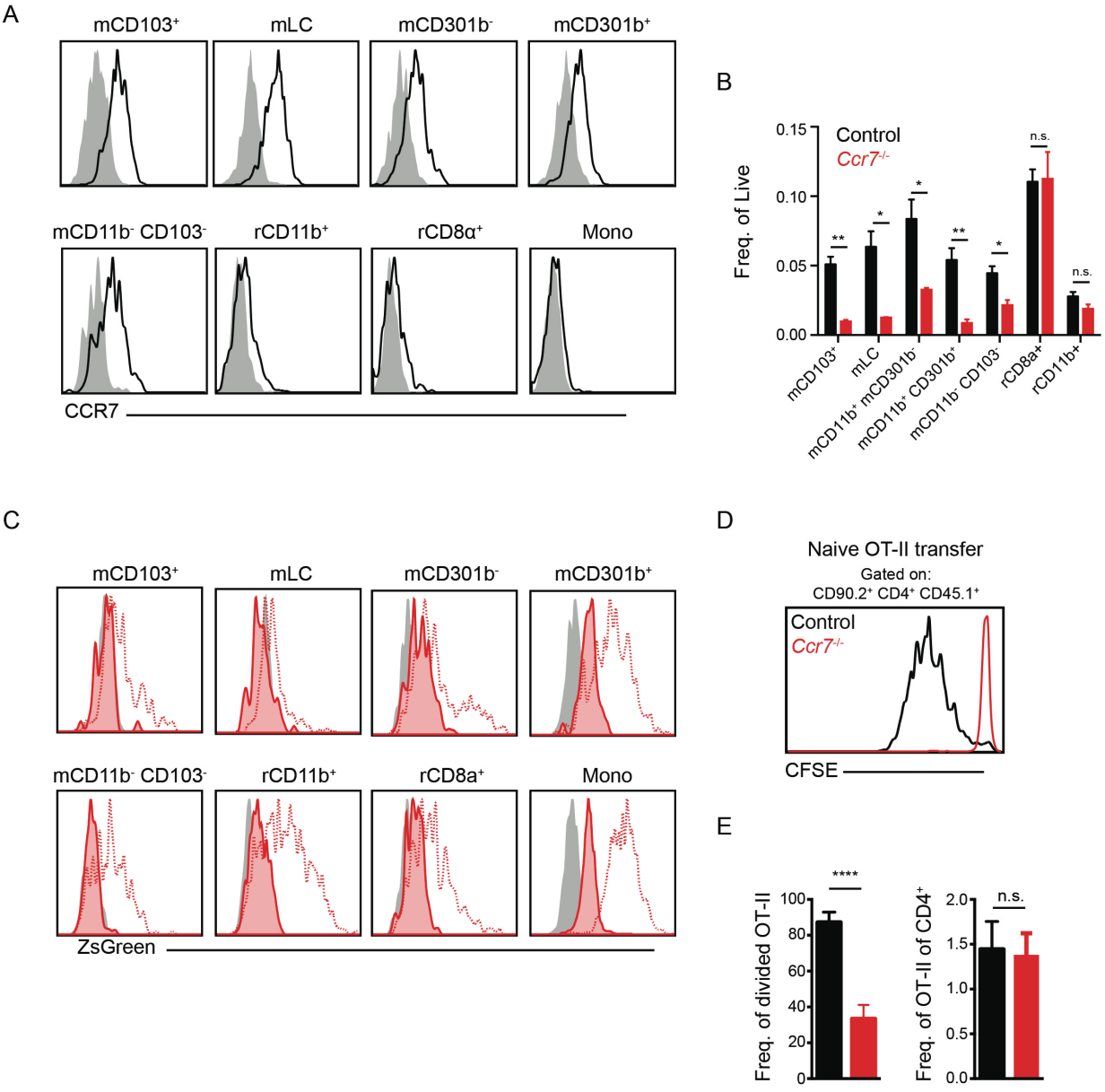
A
mCD103+
mLC
mCD301b-
mCD301b+
mCD11b- CD103-
rCD11b+
rCD8α+
Mono
CCR7
B
Control
Ccr7-/-
Freq. of Live
0.15
0.10
0.05
0.00
n.s.
mCD103+
mLC
mCD11b+ mCD301b-
mCD11b+ CD301b+
mCD11b- CD103-
rCD8a+
rCD11b+
C
mCD103+
mLC
mCD301b-
mCD301b+
mCD11b- CD103-
rCD11b+
rCD8a+
Mono
ZsGreen
D
Naive OT-II transfer
Gated on:
CD90.2+ CD4+ CD45.1+
Control
Ccr7-/-
CFSE
E
****
Freq. of divided OT-II
100
80
60
40
20
0
Freq. of OT-II of CD4+
2.0
1.5
1.0
0.5
0.0
n.s.

Figure 5.10 Migratory DCs are required for tumor antigen trafficking to the LN and anti-tumor $CD4^+$ T cell priming.
(**A**) CCR7 surface expression on migratory DCs identified in B16 tumor-draining LNs. (**B**) Frequency of LN DC populations in wild-type or *Ccr7*$^{-/-}$ tumor-bearing mice. (**C**) ZsGreen levels in LN myeloid populations from B16-ZsGreen tumor-bearing wild-type (red, open) or *Ccr7*-/- (red, filled) mice. Naive wild-type control displayed in gray. (**D**) CFSE dilution of $CD45.1^+$ OT-II $CD4^+$ T cells 3d after adoptive transfer into *Ccr7*$^{-/-}$ or control B16-chOVA tumor-bearing animals. (**E**) Frequency of $CD45.1^+$ OT-II T cells that had undergone division (**left**) and their frequency of endogenous $CD4^+$ T cells (**right**). Data is representative of at least two (**A-C**) or three (**D**) independent experiments, or pooled from three independent experiments (E). Small horizontal bars denote the SEM (**B, E**). *P <0.05, **P<0.01, ****P<0.0001 with data analyzed with unpaired *t*-test (**B, E**).

Migratory CD24^{lo} CD11b^{+} DCs are uniquely required for initiating anti-tumor CD4^{+} T cell responses

Multiple studies have demonstrated the unique capacity of migratory CD103^{+} DCs to cross-present antigen and prime CD8^{+} T cells across a number of models, including tumor responses[343,350]. The DC population(s) that is charged with activating CD4^{+} T cells in settings of tumor immunity, however, is not as well characterized, especially given the population heterogeneity that our single-cell sequencing experiment reinforced. To determine which myeloid population predominantly contributes, we sorted each of the demarcated LN myeloid populations from mice that had been injected with OVA-expressing B16 (B16-chOVA) tumors. We then co-cultured these myeloid cells with naïve CD4^{+} OT-II T cells and tested which population was capable of initiating CD4^{+} T cell activation and proliferation. We found that migratory CD24^{lo} CD11b^{+} DCs, whether they be CD301b^{+} or CD301b^{-}, supported the greatest amount of CD4^{+} OT-II T cell expansion based on absolute cell number (**Figure 5.11A**) and frequency of cells undergoing cell division (**Figure 5.11B**). This superior ability in stimulating CD4^{+} T cell activation was likely not due to differential DC viability or ability to interact with CD4 T cells as addition of exogenous OVA peptide at the time of plating resulted in comparable CD4 activation and proliferation across DC populations (**Figure 5.11C, D**).

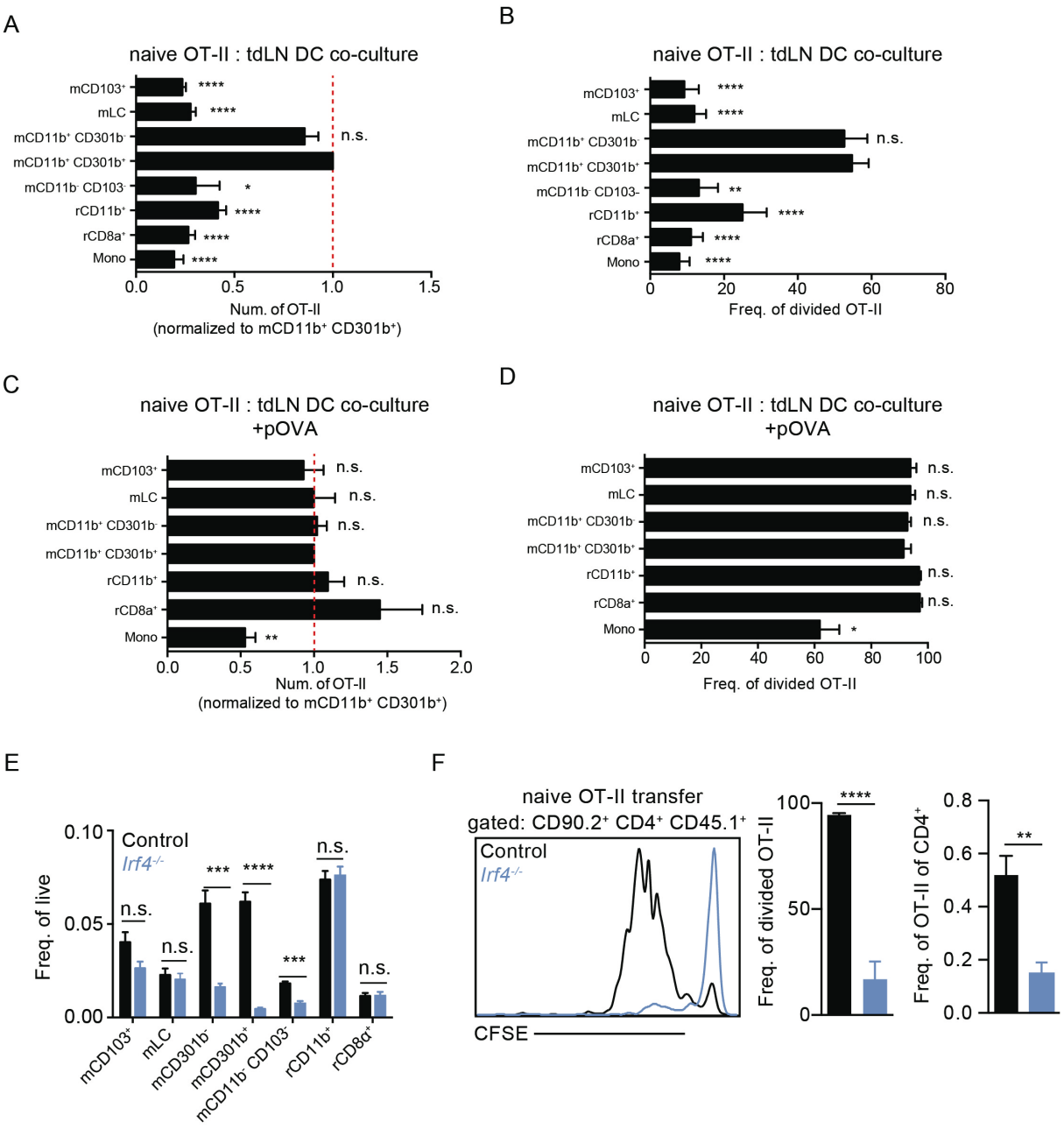
A
naive OT-II : tdLN DC co-culture
mCD103+
mLC
mCD11b+ CD301b-
mCD11b+ CD301b+
mCD11b- CD103-
rCD11b+
rCD8a+
Mono
****
n.s.
*
0.0
0.5
1.0
1.5
Num. of OT-II
(normalized to mCD11b+ CD301b+)
B
naive OT-II : tdLN DC co-culture
**
0
20
40
60
80
Freq. of divided OT-II
C
naive OT-II : tdLN DC co-culture
+pOVA
2.0
D
naive OT-II : tdLN DC co-culture
+pOVA
100
E
Freq. of live
0.10
0.05
0.00
Control
Irf4-/-
***
mCD103+
mLC
mCD301b-
mCD301b+
mCD11b- CD103-
rCD11b+
rCD8a+
F
naive OT-II transfer
gated: CD90.2+ CD4+ CD45.1+
CFSE
Freq. of divided OT-II
Freq. of OT-II of CD4+

Figure 5.11 Migratory $CD24^{lo}$ $CD11b^{+}$ DCs are required for anti-tumor $CD4^{+}$ T cell priming. (**A-D**) LN myeloid populations were sorted from B16-chOVA-tumor-draining LNs and co-cultured ex vivo with naive $CD4^{+}$ OT-II T cells, either alone (**A, B**) or with the addition of exogenous OVA peptide (323-339) (**C, D**). (**A, C**) Absolute number of live OT-II T cells recovered from culture 3d after plating, normalized and statistically compared to number of live OT-II T cells recovered following culture with migratory $CD11b^{+}$ $CD301b^{+}$ DCs. (**B, D**) Frequency of recovered OT-II T cells that had undergone division. Samples statistically compared to migratory $CD11b^{+}$ $CD301b^{+}$ DC condition. (**E**) Frequency of LN DC populations in wild-type or *Irf4*$^{-/-}$ tumor-bearing mice. (**F**) $CD45.1^{+}$ $CD4^{+}$ OT-II T cells were adoptively transferred into wild-type or *Irf4*$^{-/-}$ B78-chOVA-tumor-bearing mice and recovered 3d later for analysis of CFSE dilution (**left**), the frequency of recovered cells that were dividing (**middle**), and the frequency of endogenous $CD4^{+}$ T cells (**right**). Data is representative of at least three independent experiments (**E, F**), or pooled average values from at least three independent experiments (**A-D**). Small horizontal bars denote the SEM. *P <0.05, **P<0.01, ***P<0.001, ****P<0.0001 with data analyzed with paired (**A-D**) or unpaired (**E, F**) *t*-test.

To next test whether migratory CD11b$^+$ DC2s were required for *in vivo* CD4$^+$ T cell anti-tumor responses, we adoptively transferred CD4$^+$ OT-II T cells into IRF4-deficient B16chOVA-tumor-bearing mice. These mice have been demonstrated to lack LN DC2s[356,380], and we similarly observed a loss in CD11b$^+$ CD301b$^+$, CD11b$^+$ CD301b$^-$, and CD11b$^-$ CD103$^-$ DCs (**Figure 5.11E**). In the absence of these DC2s, we observed reduced proliferation of transferred CD4$^+$ OT-II T cells based on CFSE proliferation and quantification of dividing cells (**Figure 5.11F**). While we cannot formally exclude that CD11b$^-$ CD103$^-$ DCs may contribute to CD4$^+$ T cell activation, the superior capacity of CD11b$^+$ DCs to prime CD4$^+$ T cells *ex vivo* suggests that they are the more potent partners for CD4$^+$ T cells. Notably, although we observed a reduction in DC2 populations in the IRF4-deficient mice, we did not find a statistical decrease in any of the LN migratory DC2s when IRF4 deficiency was restricted to CD11c-expressing cells (**Figure 5.12A**), nor a change in OT-II proliferation (**Figure 5.12B**). Different *CD11c*-Cre constructs have been reported to exhibit differential penetration in expression patterns[606], and we intend to test whether a *CD11c*-Cre with earlier expression will perturb these DC2 populations in a DC-specific manner, and whether defects in OT-II expansion will occur. Overall these findings suggest that, as with other models, anti-tumor CD4$^+$ T cells depend on CD11b$^+$ DCs for activation.

Although both migratory CD11b$^+$ DCs exhibited comparable ability in priming CD4 T cells *ex vivo*, acute depletion of CD301b$^+$ DCs in tumor-bearing Mgl2-DTR mice did not affect early CD4$^+$ T cell activation and expansion (**Figure 5.12C, D**). This suggested that CD301b$^+$ DCs were not uniquely required for CD4$^+$ T cell priming, and that other DCs such as CD11b$^+$ CD301b$^-$ DCs, could compensate. Acute administration of DT, however, did appear to reduce other migratory DC populations. Given this broad reduction in migratory DCs, it was puzzling that OT-II T cell proliferation was unaffected. Although more experimentation is necessary to determine the discrepancy, it may be that acute DT administration allowed for compensation by remaining antigen-bearing cells, whereas longer-term depletion would affect antigen trafficking

altogether, such as is observed in the CCR7-deficient mice. Indeed, preliminary experiments in which DT was administered to Mgl2-DTR mice throughout the course of tumor growth resulted in reduced OT-II expansion (data not shown).

Lastly, as expected from the *in vitro* priming of OT-II T cells, loss of migratory $CD103^+$ and resident $CD8a^+$ DCs in *Xcr1*-DTR mice did not impact early OT-II activation and proliferation, although initial recruitment of OT-II T cells into the ongoing anti-tumor immune response was reduced (**Figure 5.12E, F**). Similarly, we found that resident $CD11b^+$ DCs were specifically depleted in *Cd11c*-Cre x *Cx3cr1*-DTR tumor-bearing mice, and loss did not affect priming of transferred $CD4^+$ OT-II T cells (**Figure 5.12G, H**).

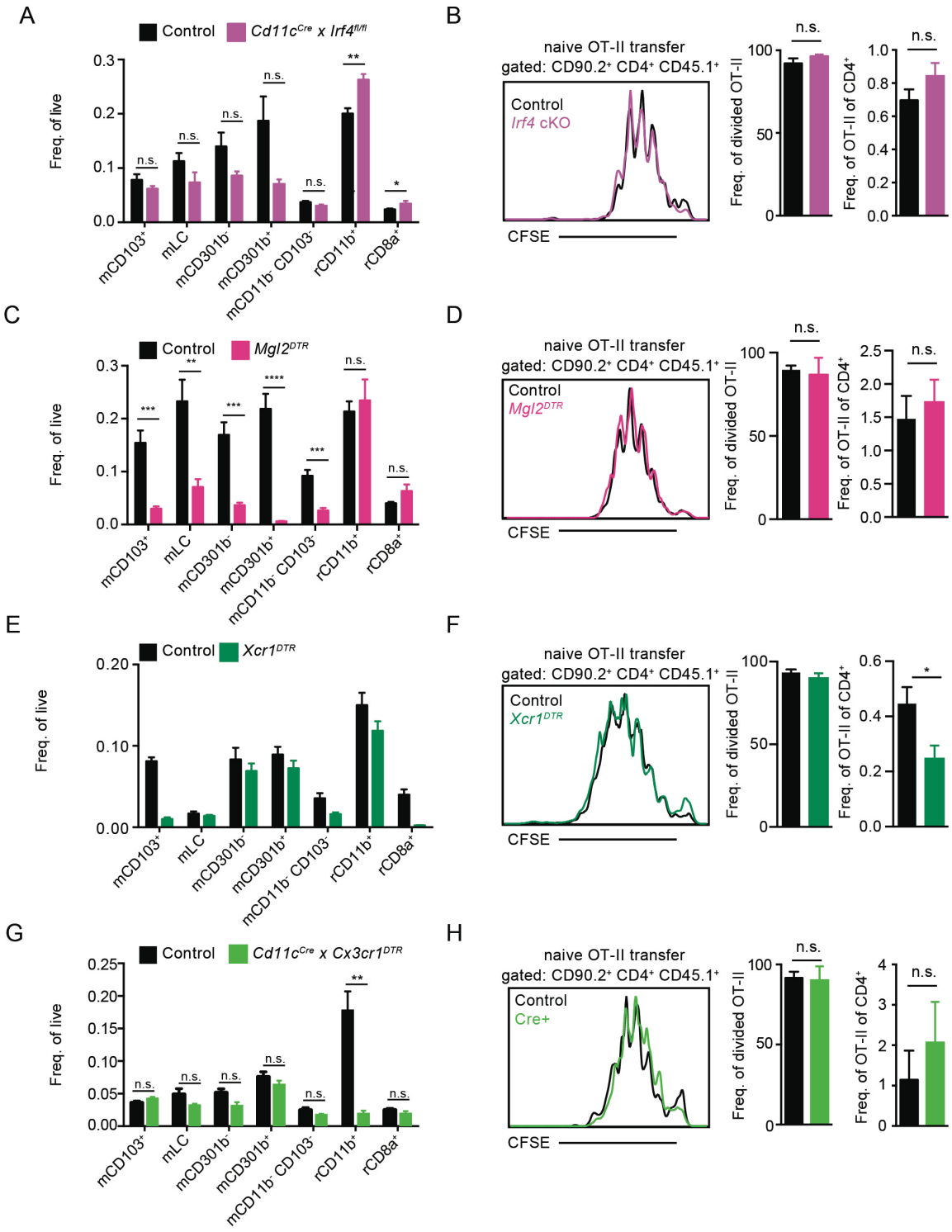
A
Control
Cd11c^Cre x Irf4^fl/fl
Freq. of live
mCD103+
mLC
mCD301b-
mCD301b+
mCD11b- CD103-
rCD11b+
rCD8a+
B
naive OT-II transfer
gated: CD90.2+ CD4+ CD45.1+
Control
Irf4 cKO
CFSE
Freq. of divided OT-II
Freq. of OT-II of CD4+
n.s.
C
Control
Mgl2^DTR
D
E
Control
Xcr1^DTR
F
G
Control
Cd11c^Cre x Cx3cr1^DTR
H
Control
Cre+

Figure 5.12 Depletion of migratory CD301b$^+$, XCR1$^+$, or resident CD11b$^+$ DCs does not impair anti-tumor CD4$^+$ T cell priming.
Frequency of LN myeloid populations in Irf4fl/fl x Cd11cCre (**A**), Mgl2DTR (**C**) Xcr1DTR (**E**), or Cx3cr1DTR x CD11cCre (**G**) tumor-bearing mice. (**B,D,F,H**) Naive CD45.1$^+$ CD4$^+$ OT-II T cells were adoptively transferred into tumor-bearing mice and tumor-draining LNs were harvested 3d later for analysis of CFSE dilution (**left**), frequency of OT-II T cells that were dividing (**middle)**, and the frequency of OT-II T cells amongst endogenous CD4$^+$ T cells (**right**). In DTR models, diptheria toxin was administered i.p. 1d prior to T cell transfer and continued daily for the remainder of the experiment (**C-H**). Data is representative of at least three (**C-F**), two (**G, H**), or one (**A, B**) independent experiments. Small horizontal bars denote the SEM. *P <0.05, **P<0.01, ***P<0.001, ****P<0.0001 with data analyzed with unpaired *t*-test.

Migratory CD24^{lo} CD11b^{+} DCs support Th17 and not Th1 differentiation of anti-tumor CD4^{+} T cells

Although activation of CD4^{+} T cells is of course critical for the mounting of a CD4 T cell response, downstream CD4^{+} T cell differentiation into T helper subsets shapes the overall T cell response. Different DC subsets have been found to contribute to CD4^{+} T cell differentiation across a variety of models, with conflicting findings at times[437,380,441,599,438,357]. We thus sought to test how different LN DC populations could shape CD4^{+} T cell differentiation by again sorting DC subsets from B16-chOVA-tumor-draining LNs and co-culturing them with naïve CD4^{+} OT-II T cells. To ensure that OT-II T cells were similarly activated, we added exogenous antigen to the wells. We then collected supernatant three days later and tested for a panel of cytokines by ELISA (**Figure 5.13A**). Of the cytokines that were detected, we statistically compared levels across conditions. At this time point, migratory CD11b^{+} CD24^{lo} DCs notably supported lower levels of IFNy compared to other DC populations. IL-2, TNF-a, IL-17A, and IL-22 were also detected in the supernatant samples, but these cytokines were produced at comparable levels across DC conditions.

To confirm our findings via an alternative method, we again co-cultured naïve CD4^{+} OT-II T cells with different DC populations, and now re-stimulated the cells with PMA and ionomycin 3 or 5 days post-plating (**Figure 5.13B, C**). Again, migratory CD11b^{+} CD24^{lo} DCs were incapable of supporting, or actively suppressed, early CD4^{+} T cell IFNy production. By 5 days post-plating, however, the frequency of IFNy^{+} cells had decreased across all DC populations, perhaps indicating a lack of sustained Th1 differentiation. In contrast, few IL-17A^{+} cells were observed 3 days post-plating with the exception of those stimulated with CD11b^{+} CD301b^{+} DCs. Indeed, migratory CD11b^{+} CD24^{lo} DCs were unique in their ability to drive IL-17A-producing CD4^{+} T cells. This Th17 programming was not an artifact of excessive or non-physiological antigen levels, as we observed similar skewing results when we cultured naïve CD4^{+} OT-II T cells with each LN migratory CD11b^{+} CD24^{lo} DC subset with no addition of antigen (**Figure 5.13D**). These

results confirm a recent study that also found that $CD11b^+$ DCs primarily promote Th17 skewing in LLC-tumor $CD4^+$ T cell responses[408].

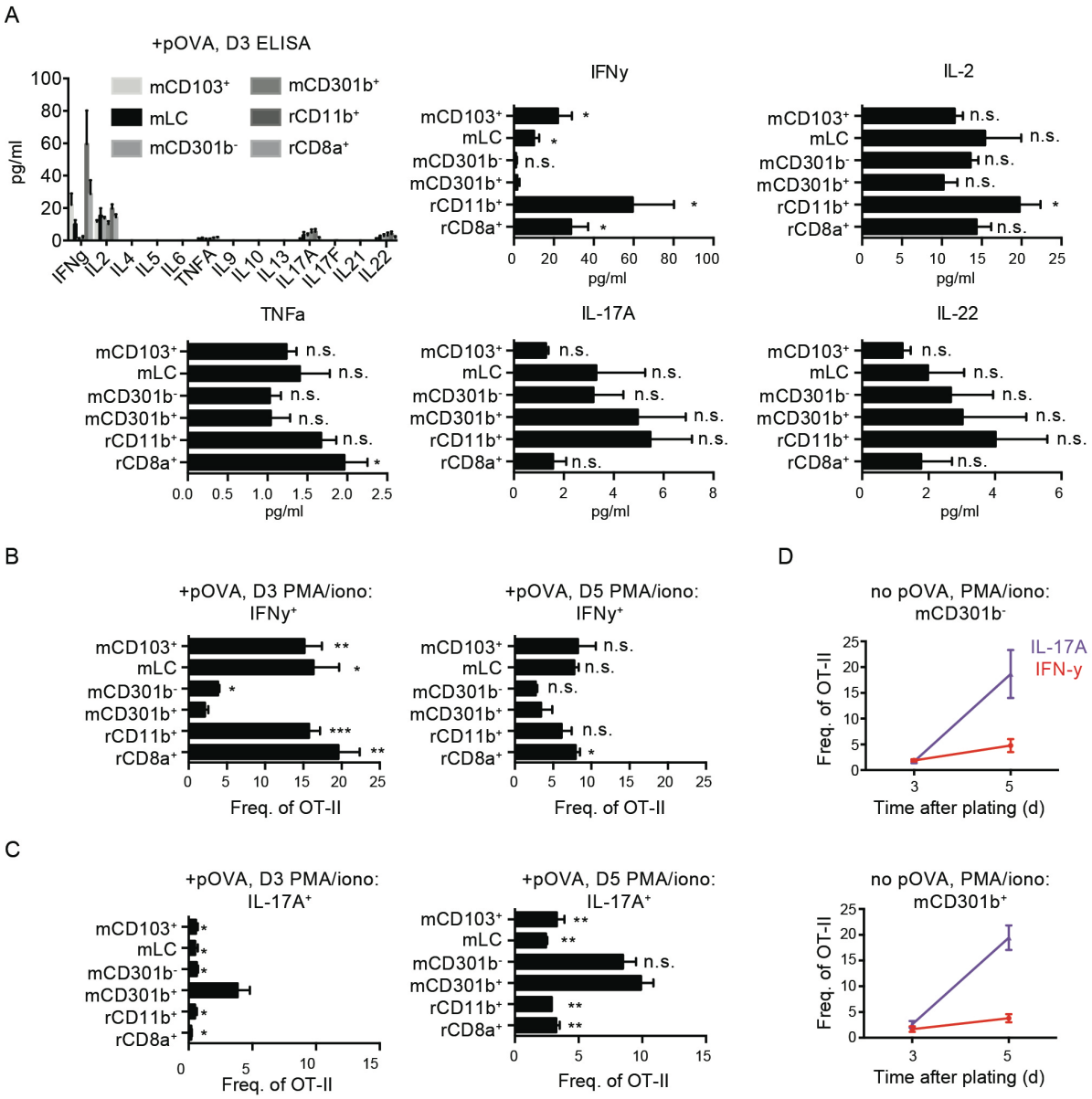
A
+pOVA, D3 ELISA
pg/ml
mCD103+
mLC
mCD301b-
mCD301b+
rCD11b+
rCD8a+
IFNg
IL2
IL4
IL5
IL6
TNFA
IL9
IL10
IL13
IL17A
IL17F
IL21
IL22
IFNy
IL-2
TNFa
IL-17A
IL-22
n.s.
B
+pOVA, D3 PMA/iono: IFNy+
+pOVA, D5 PMA/iono: IFNy+
Freq. of OT-II
C
+pOVA, D3 PMA/iono: IL-17A+
+pOVA, D5 PMA/iono: IL-17A+
D
no pOVA, PMA/iono: mCD301b-
IL-17A
IFN-y
Freq. of OT-II
Time after plating (d)
no pOVA, PMA/iono: mCD301b+

Figure 5.13 Migratory $CD24^{lo}$ $CD11b^{+}$ DCs support $CD4^{+}$ OT-II T cell production of IL-17A *ex vivo*.
LN myeloid populations were sorted from B16-chOVA tumor-draining LNs and co-cultured with naive $CD4^{+}$ OT-II T cells. Cells were cultured with exogenous OVA peptide (pOVA) (323-339) (**A-C**) or alone (**D**). Culture well supernatant (**A**) or cells (**B-D**) were collected 3 or 5d later. (**A**) Concentration of cytokines detected by ELISA of DC-T cell supernatant. For cytokines detected, protein concentrations were individually graphed. Negative concentration values were converted to 0. (**B**) Frequency of IFN-y^{+} OT-II T cells detected following re-stimulation 3d (**left**) or 5d (**right**) after co-culture with a given DC population and pOVA. (**C**) Frequency of IL-$17A^{+}$ OT-II cells detected following re-stimulation 3d (**left**) or 5d (**right**) after co-culture with a given DC population and pOVA. (**D**) Frequency of IFN-y^{+} and IL-$17A^{+}$ OT-II T cells detected following re-stimulation 3d (**left**) or 5d (**right**) after co-culture with migratory $CD11b^{+}$ DC populations. Data is pooled from two independent experiments, each with two technical replicates (**A**), or is representative of at least two experiments with 2-3 technical replicates (**B-D**). Small horizontal bars denote the SEM. Statistical analysis was performed between the $mCD301b^{+}$ DC condition with an unpaired *t*-test (A-C). *P <0.05, **P<0.01, ***P<0.001, ****P<0.0001.

Although CD11b$^+$ DCs initiate anti-tumor CD4$^+$ T cell responses and can drive Th17 differentiation, it is unclear to what extent this capacity unfolds *in vivo*. In contrast to our *ex vivo* observations, adoptive transfer of OT-II T cells into B16-chOVA-tumor-bearing mice did not result in a strong T helper subset profile in tumor-draining LNs. A relatively low frequency of OT-II T cells produced IFNy upon re-stimulation, and we observed even less IL-17A production (**Figure 5.14A**). Nor did we observe up-regulation of FoxP3 (data not shown). In the TME, however, the majority of CD44$^+$ FoxP3$^-$ conventional CD4$^+$ T cells produced IFNy following re-stimulation with minimal IL-17A production (**Figure 5.14B**). Given that these tumor-infiltrating CD4$^+$ T cells exhibit a Th1 profile, it is unclear whether the Th17 skewing by CD11b$^+$ DCs *ex vivo* represents an artificial situation where migratory CD11b$^+$ DCs are isolated from physiological environmental cues, or if other myeloid populations dominate in advancing their CD4$^+$ T cell programs *in vivo*.

A previously published RNA-sequencing database revealed that tumor CD11b$^+$ DCs express *Tlr7* at greater levels than CD103$^+$ DCs[342]. A preliminary experiment in which TLR7 agonists Gardiquimod, Imiquimod, or Resiquimod were injected intratumorally resulted in a decrease in the frequency of Tregs in the tumor and a shift in conventional CD4$^+$ T cells from a Th1 to a Th17 profile (**Figure 5.14C**). While other myeloid cells do express TLR7 and thus could be responsible for these changes in the CD4$^+$ T cell compartment, it would be intriguing to test whether DCs are required for this improved effector T cell profile, and whether specific stimulation of CD11b$^+$ DCs could unleash their potential for Th17 skewing.

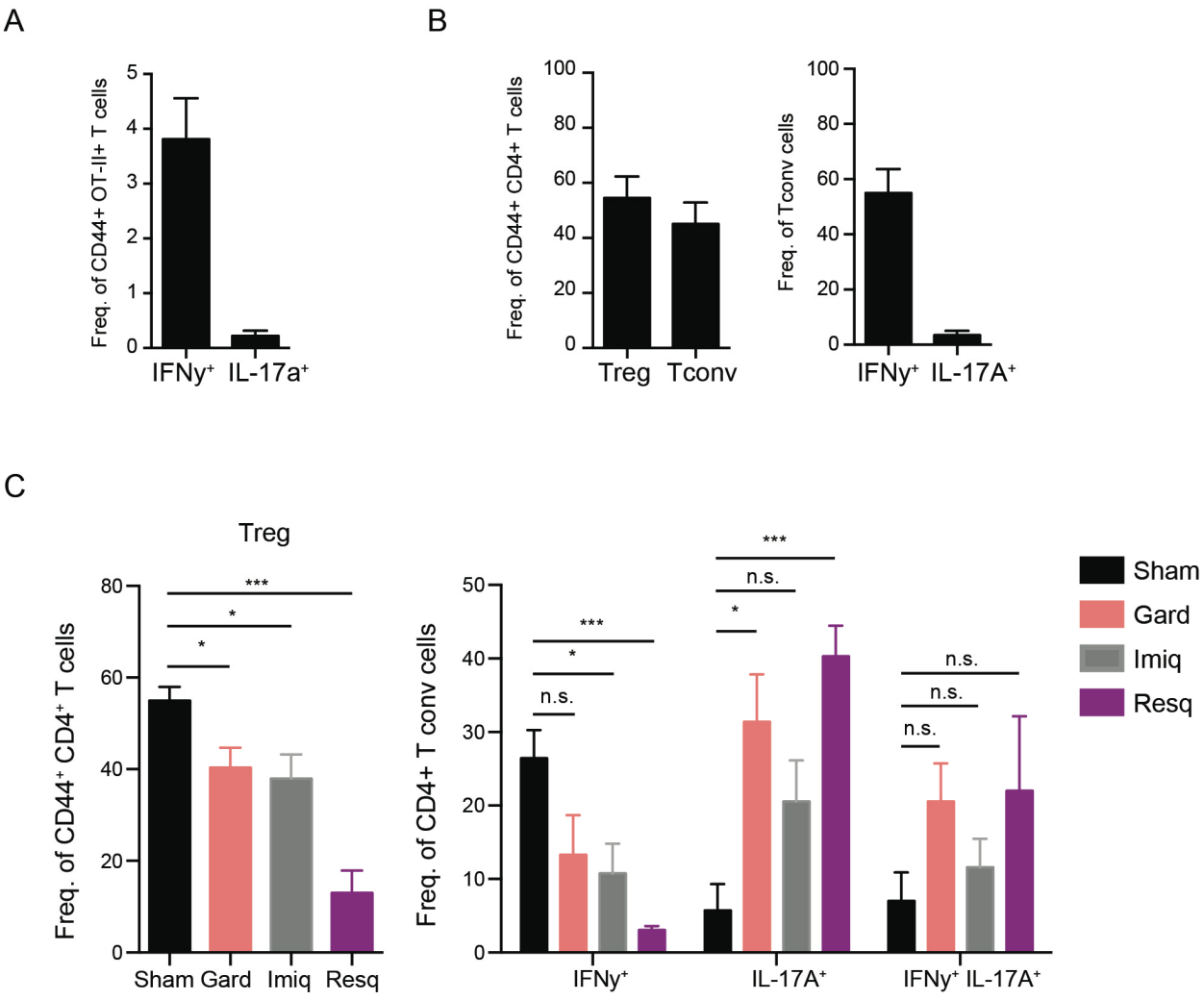
A
Freq. of CD44+ OT-II+ T cells
IFNγ+ IL-17a+
B
Freq. of CD44+ CD4+ T cells
Treg Tconv
Freq. of Tconv cells
IFNγ+ IL-17A+
C
Treg
Freq. of CD44+ CD4+ T cells
Sham Gard Imiq Resq
Freq. of CD4+ T conv cells
IFNγ+ IL-17A+ IFNγ+ IL-17A+
n.s.
Sham
Gard
Imiq
Resq

Figure 5.14 TLR7 agonism induces a Th17 phenotype in B16 tumor infiltrating conventional $CD4^+$ T cells.
(**A**) Frequency of $CD4^+$ OT-II T cells in tumor-draining LNs that were $IFNy^+$ or $IL\text{-}17A^+$ following ex vivo re-stimulation 7 days after transfer into B16-chOVA-tumor-bearing animals. (**B**) Frequency of $FoxP3^+$ $CD4^+$ regulatory T cells of B16 tumor-infiltrating $CD44^+$ $CD4^+$ $CD90^+$ T cells (**left**) and frequency of conventional FoxP3- $CD4^+$ T cells that produced IFNy or IL-17A (**right**) following re-stimulation ex vivo. (**C**) B16-tumor-bearing mice were administered intratumoral injections of Gardiquimod, Imiquimod, or Resiquimod, and tumors were harvested for ex vivo re-stimulation. Frequency of $FoxP3^+$ $CD4^+$ regulatory T cells of tumor-infiltrating $CD44^+$ $CD4^+$ $CD90^+$ T cells (**left**), and frequency of conventional $CD44^+$ $CD4^+$ T cells that were $IFNy^+$, $IL\text{-}17A^+$, or $IFNy^+$ $IL\text{-}17A^+$ (**right**). Data was pooled from two independent experiments (**A, B**) or representative of one experiment (**C**). Small horizontal bars denote the SEM. *P <0.05, ***P<0.001 with data analyzed with unpaired *t*-test.

CD301b$^+$ and CD301b$^-$ migratory CD11b$^+$ DCs express different surface markers and respond differentially to growth factors

Although CD301b$^+$ DCs in particular have been linked to driving Th2 but not Th1 responses, we were surprised to find that migratory CD301b$^+$ and CD301b$^-$ CD11b$^+$ DCs behaved so similarly across the assays we performed here. In addition to the single-cell RNA-sequencing analysis, they do appear to represent distinct cell populations, or at least distinct cell states. Although the two populations express similar levels of FLT-3 and SIRP-a, thereby reinforcing their identity as DC2s, CD301b$^+$ DCs express a number of surface markers typically associated with monocytes or macrophages (**Figure 5.15A**). In addition to PDL-2, which has been reported previously[436,437], CD301b$^+$ DCs express elevated levels of CD14, CD16/32, CD200R, and CD206. We also tested the effects of heightened systemic levels of DC growth factors like FLT-3 or GM-CSF by injecting *Flt3l*- or *Gmcsf*- over-expressing B16 tumor cells into wild-type mice. While all DC subsets expanded with increased levels of FLT-3L, CD301b$^-$ CD11b$^+$ DCs preferentially expanded relative to CD301b$^+$ DCs (**Figure 5.15B**). In contrast, CD301b$^+$ CD11b$^+$ expanded at a greater rate with increased levels of GM-CSF (**Figure 5.15C**). While this further supports these two DC subsets as functionally distinct, there does exist the caveat that these factors may affect levels of CD301b itself as has been reported for CD103[607], which would confound demarcation of these very populations.

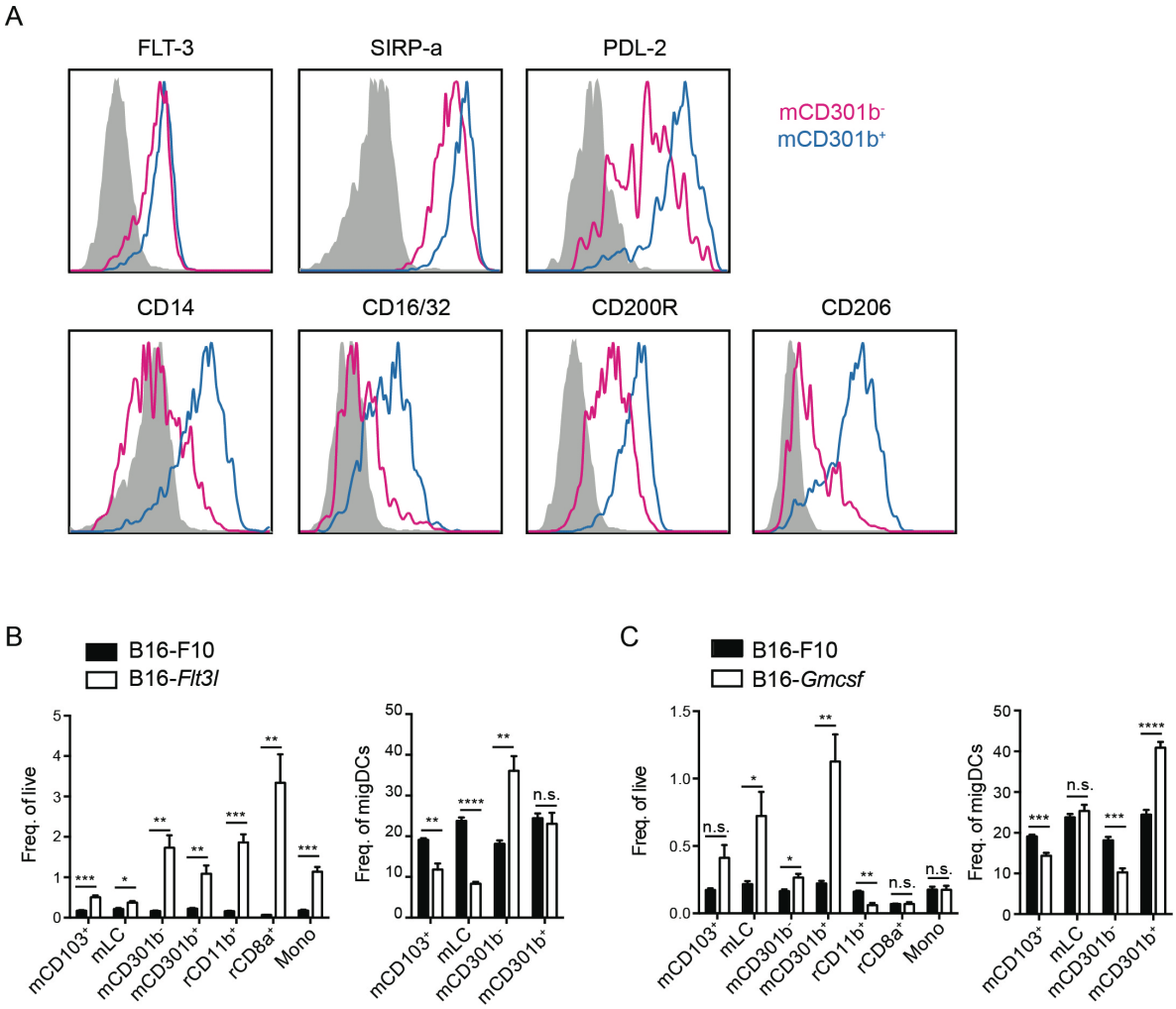
A
FLT-3
SIRP-a
PDL-2
mCD301b-
mCD301b+
CD14
CD16/32
CD200R
CD206
B
B16-F10
B16-Flt3l
Freq. of live
Freq. of migDCs
mCD103+
mLC
mCD301b-
mCD301b+
rCD11b+
rCD8a+
Mono
C
B16-F10
B16-Gmcsf
n.s.

Figure 5.15 Migratory CD11b$^+$ CD301b- and CD301b$^+$ DCs are distinct in surface marker expression and responsiveness to FLT-3 and GM-CSF.
(**A**) Surface marker expression of denoted proteins byB16-tumor-draining LN migratory CD11b$^+$ CD301b- or CD301b$^+$ DCs with isotype antibody control (gray). (**B,C**) Wild-type mice were injected s.c. with *Flt3l*- (**B**) or *Gmcsf*- (**C**) over-expressing B16 tumor cell lines and tumor-draining LNs were harvested 14d later for analysis by flow cytometry. Frequency of LN myeloid populations was quantified as a proportion of live cells (**left**) or of migratory DCs **(right**).

Migratory CD11b$^+$ DCs can prime CD8$^+$ as well as CD4$^+$ T cells, but are inferior in supporting effector T cell development

The current dogma is that cDC1s are specialized in cross-presentation and they are thus well positioned to initiate CD8 T cell priming[362,426]. There are indications, however, that CD103$^-$ or CD11b$^+$ DCs have the potential of cross-presentation and can stimulate CD8$^+$ T cells[130,422]. With our gating strategy that dissects migratory CD11b$^+$ DCs with higher granularity, we investigated whether these subsets were capable of contributing to CD8$^+$ as well as CD4$^+$ T cell responses. We again sorted tumor-draining LN DC populations and co-cultured them with naïve CD8$^+$ OT-I T cells. To our surprise, we found that CD11b$^+$ CD301b$^+$ DCs supported equivalent, if not increased, CD8$^+$ T cell expansion *ex vivo* as migratory CD103$^+$ DCs (**Figure 5.16A**). Although our group along with others has reported superior priming from migratory CD103$^+$ DCs [343,433], migratory CD11b$^+$ DCs were sorted according to a different strategy and were likely dominated by Langerhans cells, which provided little stimulation here. Migratory CD11b$^+$ CD301b$^-$ and CD11b$^-$ CD103$^-$ DCs also supported some CD8$^+$ T cell expansion, though levels were reduced compared to migratory CD103$^+$ DCs (**Figure 5.16A)**.
Intriguingly, however, the CD8$^+$ T cells that were cultured with migratory CD11b$^+$ DCs expressed lower levels of CD44, suggesting that their activation may not have been as robust (**Figure 5.16B**). When we tested whether T cell effector function was affected by different DC subsets, we found that, as with CD4$^+$ T cells, migratory CD11b$^+$ DCs were incapable of supporting comparable IFN-γ production (**Figure 5.16C**). This reduction did not appear to be a gross reduction in cytokine production as TNF-α levels were consistent across DC conditions. Migratory CD11b$^+$ CD301b$^+$ DCs in particular primed CD8$^+$ T cells with lower levels of transcription factors Eomes and T-bet, indicating that early T cell activation programs may be altered in the absence of CD103$^+$ DCs. As T cell priming does not occur in isolation, we next investigated whether migratory CD11b$^+$ DCs could actively suppress IFNγ production when migratory CD103$^+$ DCs were present. To test this, we co-cultured naïve CD8$^+$ T cells with

migratory CD103$^+$ DCs alone, or with each migratory CD11b$^+$ DC population. Here again we observed a reduction in the frequency of IFNy$^+$ OT-I T cells when CD11b$^+$ DCs were in culture (**Figure 5.16D**). While each CD11b$^+$ DC population led to similar IFNy levels in each experiment, CD301b$^+$ appeared to be more potent at limiting Eomes and T-bet expression in both experiments, a discrepancy that will require further exploration.

Although CD11b$^+$ DCs are able to prime CD8$^+$ T cells *ex vivo*, it is unclear whether they exercise this capacity *in vivo*. Acute depletion of XCR1$^+$ CD103$^+$ DCs with *Xcr1*-DTR mice surprisingly did not impact initial activation and proliferation of transferred CD8$^+$ OT-I T cells (**Figure 5.16E**). Previous work has demonstrated that specific loss of migratory CD103$^+$ DCs resulted in a reduction of transferred OT-I T cells over a period of 14 days[343] and we too observe this (data not shown). We are thus interested in testing whether CD8$^+$ T cell activation can initially occur in the absence of CD103$^+$ DCs, but whether the quality or survival of effector T cells is impaired. Further experimentation is of course needed to explore whether migratory CD11b$^+$ DCs can actively contribute to the priming of anti-tumor CD8$^+$ T cells, and it will be informative to first test whether CD301b$^+$ DCs are spatially positioned to interact with CD8$^+$ T cells.

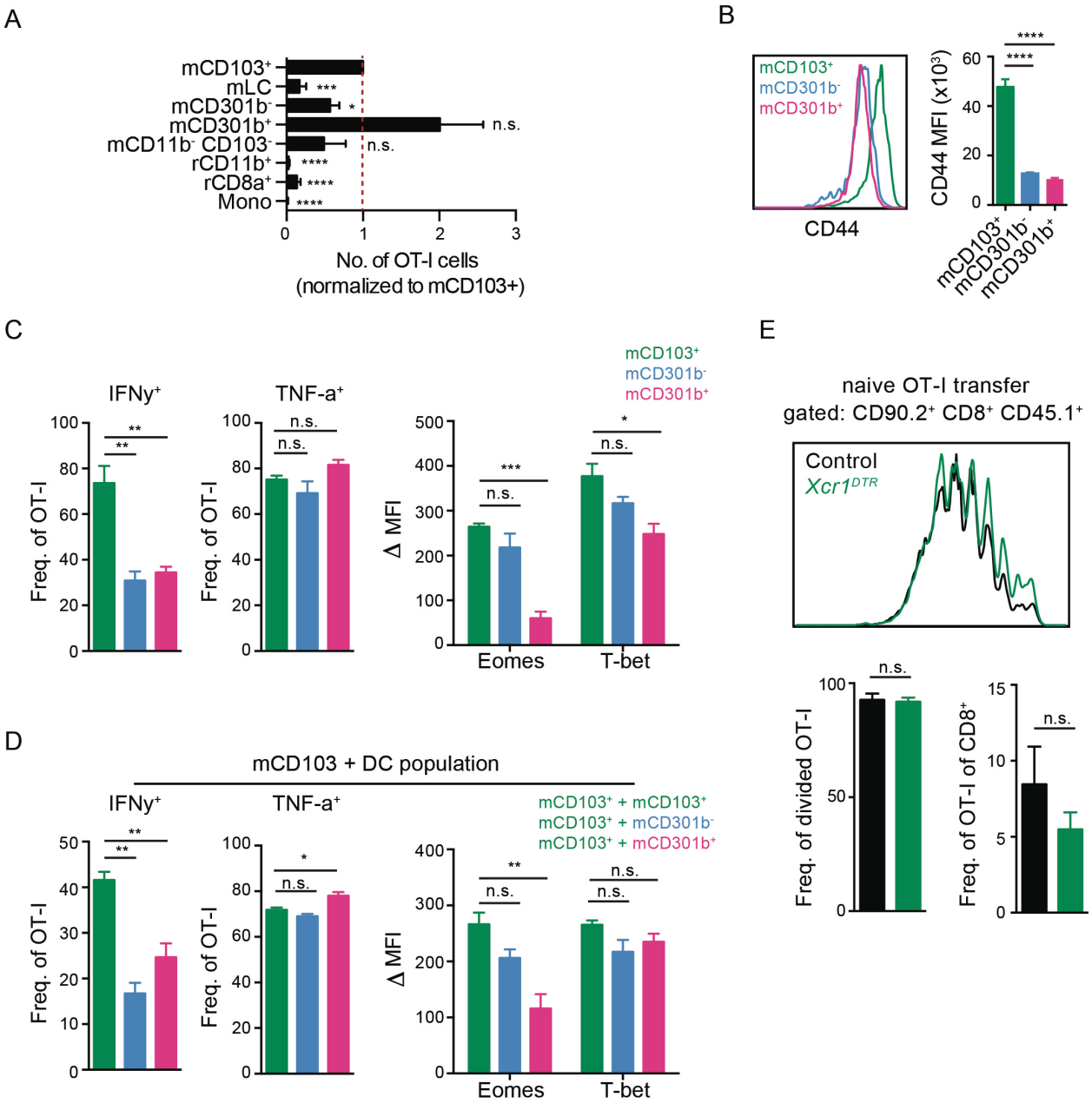
A
mCD103+
mLC
mCD301b-
mCD301b+
mCD11b- CD103-
rCD11b+
rCD8a+
Mono
***
*
n.s.
n.s.
****
****
****
0
1
2
3
No. of OT-I cells
(normalized to mCD103+)
B
mCD103+
mCD301b-
mCD301b+
CD44
CD44 MFI (x10³)
****
****
mCD103+
mCD301b-
mCD301b+
C
mCD103+
mCD301b-
mCD301b+
IFNγ+
TNF-a+
Freq. of OT-I
Δ MFI
Eomes
T-bet
D
mCD103 + DC population
mCD103+ + mCD103+
mCD103+ + mCD301b-
mCD103+ + mCD301b+
E
naive OT-I transfer
gated: CD90.2+ CD8+ CD45.1+
Control
Xcr1DTR
Freq. of divided OT-I
Freq. of OT-I of CD8+
n.s.

Figure 5.16 Migratory XCR1$^-$ DC populations are capable of anti-tumor CD8$^+$ T cell priming. (**A-D**) Myeloid populations were sorted from B16-chOVA tumor-draining LNs and co-cultured with naive CD8$^+$ OT-I T cells ex vivo for 3d. (**A**) Absolute number of live OT-1 T cells recovered from culture, with cell number normalized and statistically compared to those cultured with migratory CD103$^+$ DCs. (**B**) CD44 surface expression (**left**) and quantification of MFI (**right**) of OT-I T cells that were co-cultured with a given DC population. (**C**) OT-I T cells that had been co-cultured with the designated DC population were re-stimulated and analyzed for IFNy (**left**), TNF-a (**middle**), and Eomes and T-bet expression (**right**). (**D**) OT-I T cells were co-cultured with a mix of migratory CD103$^+$ DCs and specified DC population. Frequency of IFNy$^+$ (**left**) and TNF-a$^+$ (**middle**) OT-I T cells, along with Eomes and T-bet MFI expression levels (**right**). (**D**) Naive CD45.1$^+$ CD8$^+$ OT-I T cells were adoptively transferred into *Xcr1*-DTR or wild-type B16-chOVA-tumor-bearing mice, and tumor-draining LNs were harvested 3d later. CFSE dilution of transferred OT-I T cells (**top**), frequency of OT-I T cells that had divided (**bottom, left**), and frequency of OT-I T cells of endogenous CD8$^+$ T cells (**bottom, right**). Data is pooled from five (**A**) or two (**B**) independent experiments, is representative of at least two experiments (**C, D**), or is displayed as a preliminary experiment (**E**). Delta MFI refers to the change in MFI from unstained control (**C, D**). Small horizontal bars denote the SEM. *P <0.05, **P<0.01, ***P<0.001, ****P<0.0001 with data analyzed with a paired (**A**) or unpaired (**B-E**) *t*-test.

Therapeutic targeting of migratory DCs with anti-CD40 may improve T cell priming

Given the critical role for DCs in stimulating effector anti-tumor T cell responses, efforts have been made to increase DC number and functionality. For example, treatment with FLT-3L and agonists that stimulate TLRs expressed on migratory $CD103^+$ DCs like poly I:C has been tested to boost $CD8^+$ T cell activity[350]. As migratory $CD11b^+$ DCs are responsible for $CD4^+$ T cell priming and may contribute to $CD8^+$ T cell priming, we sought to test therapeutic modalities that could stimulate $CD11b^+$ DCs as well as $CD103^+$ DCs. We found that anti-CD40 agonism led to a substantial increase in migratory $CD11b^+$ DC, as well as monocyte, representation in tumor-draining LNs (**Figure 5.17A**). A preliminary experiment with anti-CD40 treatment resulted in an increase in transferred $IFNy^+$ $CD4^+$ OT-II T cells that produced IFNy in the LN (**Figure 5.17B**). We also observed up-regulation of surface co-stimulatory molecules such as CD80, CD86, and CD70 (**Figure 5.17C**). Migratory DC populations appeared to be those primarily targeted by anti-CD40 treatment, with $CD301b^+$ DCs exhibiting the greatest changes in surface levels of these markers. We also noted that while CD70 was absent on DCs in control tumor-draining LNs, it was up-regulated with anti-CD40 treatment. Given its role in Th1 and effector T cell differentiation[608,609] it will be interesting to test whether CD70 along with other co-stimulatory molecules plays a critical role in re-shaping T cell responses following anti-CD40 treatment. As expected, anti-CD40 treatment leads to slower B16 tumor growth (**Figure 5.18A**). Yet, although anti-CD40 treatment improves Th1 skewing and has been linked to improved systemic $CD4^+$ T cell responses[453], primary tumor control with anti-CD40 treatment appears to be mediated through $CD8^+$ and not $CD4^+$ T cells (**Figure 5.18A**). It may be that anti-CD40 stimulation bypasses the utility of $CD4^+$ T cell help in controlling a primary tumor, but that improved $CD4^+$ T cell priming is beneficial for protection against tumor metastasis or tumor re-growth. In either or both scenarios, it will be of interest to test whether anti-CD40 treatment requires DC populations for improved T cell functionality, and whether $CD103^+$ DCs and/or $CD11b^+$ DCs are responsible.

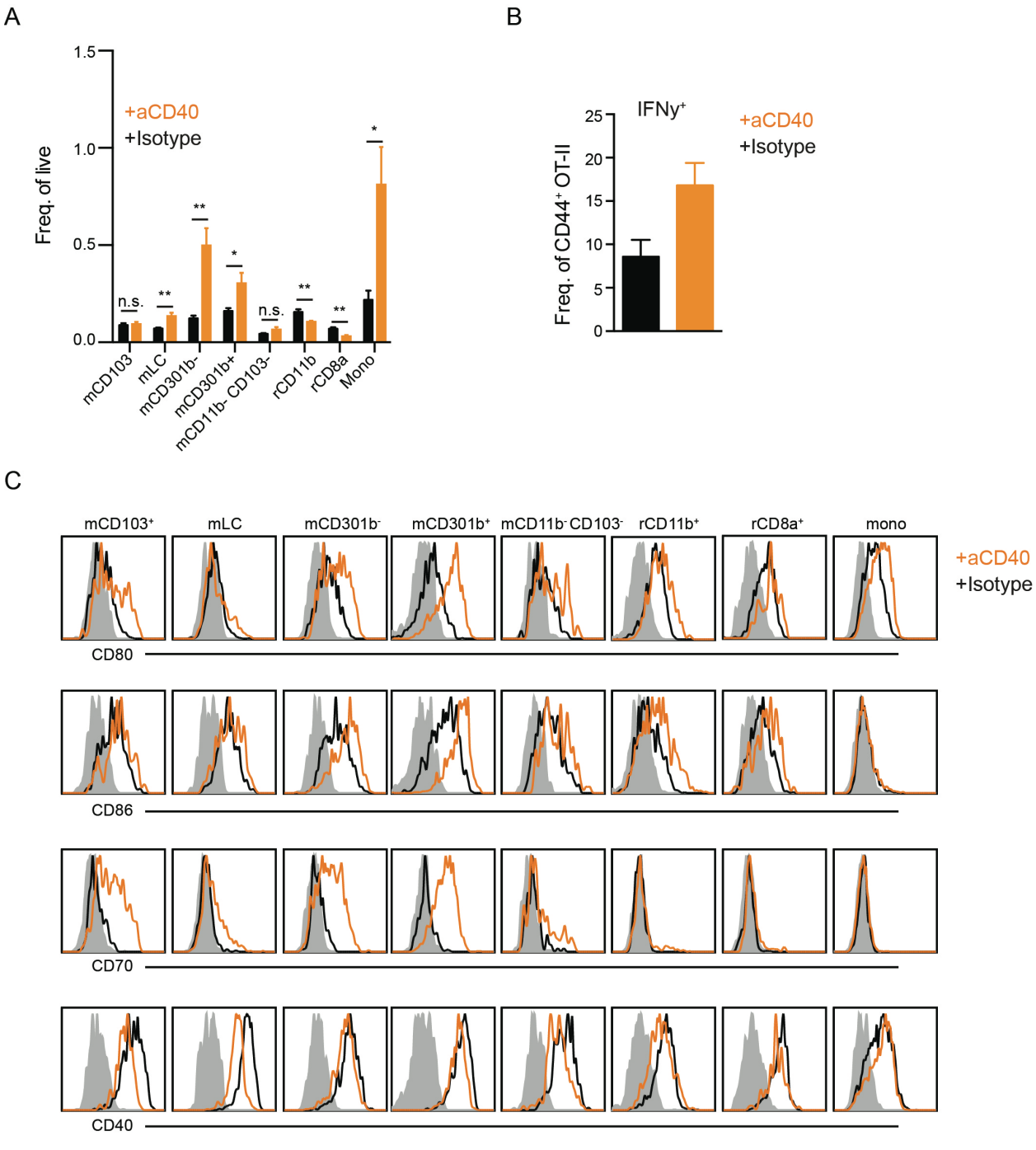
A
Freq. of live
1.5
1.0
0.5
0.0
+aCD40
+Isotype
n.s.
**
**
*
n.s.
**
**
*
mCD103
mLC
mCD301b-
mCD301b+
mCD11b- CD103-
rCD11b
rCD8a
Mono
B
IFNγ+
Freq. of CD44+ OT-II
25
20
15
10
5
0
+aCD40
+Isotype
C
mCD103+
mLC
mCD301b-
mCD301b+
mCD11b- CD103-
rCD11b+
rCD8a+
mono
+aCD40
+Isotype
CD80
CD86
CD70
CD40

Figure 5.17 Anti-CD40 agonist treatment induces migratory CD11b^{+} DC expansion and increased expression of co-stimulatory surface molecules.
(**A**) Frequency of myeloid populations in LNs harvested from B16-tumor-bearing wild-type mice that were treated with anti-CD40 or isotype antibody. (**B**) Naive OT-II T cells were adoptively transferred into B16-chOVA tumor-bearing mice that underwent anti-CD40 or isotype antibody treatment. IFNy production was analyzed by harvesting and re-stimulating tumor-draining LNs 7d following T cell transfer. (**C**) Surface expression of CD80, CD86, CD70, or CD40 on B16-tumor-draining LN myeloid populations following anti-CD40 or isotype antibody treatment. Antibody treatment was administered every 2 days for 4 days before LNs were harvested.

A

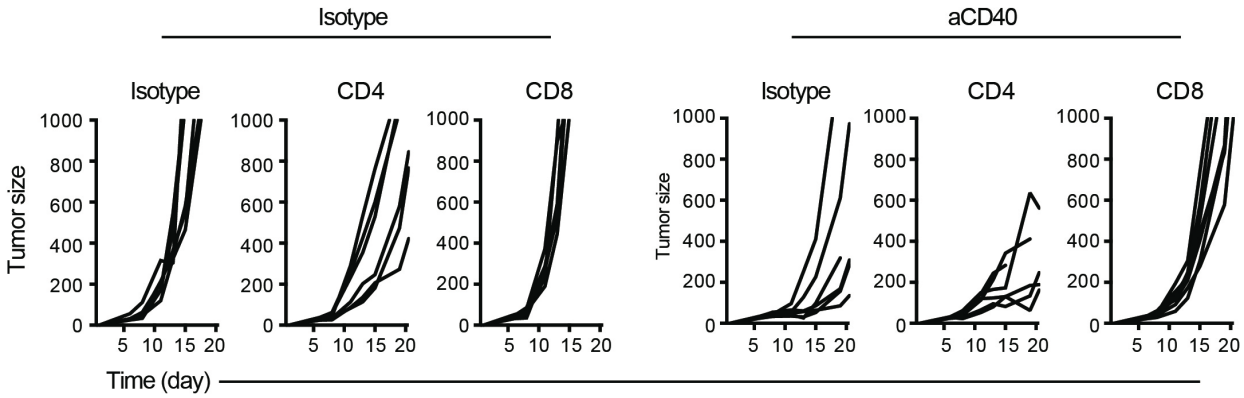
Isotype
aCD40
Isotype
CD4
CD8
Isotype
CD4
CD8
Tumor size
Tumor size
1000
800
600
400
200
0
5 10 15 20
Time (day)

Figure 5.18 $CD8^+$ T cells are required to mediate the anti-tumor benefits of anti-CD40 therapeutic delivery.
(**A**) Wild-type B16-tumor-bearing mice were treated with anti-CD40 or isotype antibody i.p.in conjunction with CD4- or CD8- depleting antibodies, and tumor size was measured. Data is representing one preliminary experiment.

III. DISCUSSION

Here we demonstrate that while single-cell RNA-sequencing analysis of tumor-draining LN myeloid cells largely reflects populations defined by flow cytometric approaches, higher resolution of DC2 subsets is critical for dissecting their function in anti-tumor responses. Amongst identified DC2 populations, migratory CD11b^{+} CD24^{lo} CD301b^{-} and CD301b^{+} DCs are those primarily capable of initiating anti-tumor CD4^{+} T cell responses *ex vivo* and required *in vivo* for CD4^{+} T cell expansion. While CD11b^{+} DCs have been thought to be the canonical population to drive CD4^{+} T cell activation, the role of these DCs in light of their heterogeneity has varied across models. More specifically, the contribution by each DC2 population in anti-tumor immune responses has not yet been characterized, and this finding brings increased clarity as to which populations we should target to improve the CD4^{+} T cell arm of anti-tumor immunity.

In addition to activating CD4^{+} T cells, these migratory CD11b^{+} DCs were uniquely capable in supporting Th17 cell differentiation *ex vivo*. This finding reaffirms a similar observation from another group studying CD11b^{+} DC function in anti-tumor CD4^{+} T cell responses[357]. Yet if migratory CD11b^{+} DCs are primarily responsible for CD4^{+} T cell activation and preferentially support Th17 skewing, it remains curious that little IL-17A production is observed *in vivo*. Greater clarification is required for this discrepancy, but it may be CD11b^{+} DCs are unable to promote Th17 responses *in vivo* or other myeloid populations contribute more heavily toward T helper cell differentiation programming and outweigh the influence of CD11b^{+} DCs. Regulatory T cells are also a substantial, and often dominant, T cell subset within the tumor and it remains unclear which myeloid population predominantly supports their generation and/or expansion in the tumor microenvironment.

Other studies have demonstrated a critical role for CD301b^{+} DCs in particular for driving Th2 responses[437]. In immunization models with adjuvants that led to Th2 skewing like papain, CD301b^{+} DCs were specifically required for such CD4^{+} T cell Th2 differentiation[437]. Highlighting

their unique features, CD301b$^+$ DCs exhibit a notably distinct surface marker phenotype from CD301b$^-$ DCs. Given these findings, we had expected to observe divergence in CD301b$^-$ and CD301b$^+$ DC functionality. We were surprised, however, that both appeared to equivalently initiate naïve CD4$^+$ OT-II T cell expansion in B16-tumor responses, and both DC subsets skewed T cells toward a similar Th17 fate *ex vivo*. As discussed previously, B16 tumors appear to provoke a Th1-skewed immune response *in vivo*. Given this Th1 profile, it may be that the B16-tumor model captures how CD11b$^+$ CD301b$^-$ and CD301b$^+$ DCs function in a Th1 setting. For example, in Th1-dominated responses following challenge with CpG or HSV-1, loss of CD11b$^+$ CD301b$^+$ DCs did not impact CD4$^+$ T cell activation or differentiation[437]. Similarly, we observed normal CD4$^+$ OT-II T cell activation and proliferation when cells were transferred into CD301b$^+$ DC-depleted tumor-bearing animals. Although still an open question, perhaps the CD11b$^+$ CD301b- and CD301b$^+$ DCs play similar roles in anti-tumor immunity, but CD301b$^+$ DCs are uniquely capable of undertaking Th2- specific functionality when stimulated appropriately.

In addition to initiating CD4$^+$ T cell activation, we also found that migratory CD11b$^+$ DCs have the capacity of initiating CD8$^+$ T cell activation *ex vivo*, with CD301b$^+$ DCs in particular capable of supporting comparable expansion as CD103$^+$ DCs. Yet, as with CD4$^+$ T cells, of CD8$^+$ T cells that had been primed with CD11b$^+$ DCs, fewer produced IFNy. These CD8$^+$ T cells also expressed lower levels of transcription factors such as Eomes and T-bet that are a part of T activation programs and contribute to robust effector and memory T cell development. More work must be done to determine the extent to which these CD11b$^+$ DCs contribute to CD8$^+$ T cell priming *in vivo*, but this situation may reflect the benefits of therapeutically tilting DC number toward DC1s instead of DC2s. Alternatively, this relationship may call for the design of therapeutic strategies that improve CD11b$^+$ DC functionality in addition to that of CD103$^+$ DCs. We are currently exploring whether anti-CD40 stimulation could broadly reprogram migratory

DCs and thus boost anti-tumor $CD8^+$ and $CD4^+$ T cell effector and protective responses simultaneously.

IV. METHODS

Mice

All mice were maintained under specific pathogen-free conditions and treated in accordance with the regulatory standards of the National Institutes of Health and American Association of Laboratory Animal Care, and are consisted with the UCSF Institution of Animal Care and Use Committee. The following mice were purchased for acute use or maintained under specific pathogen-free conditions at the University of California, San Francisco Animal Barrier Facility: C57BL/6J (The Jackson Laboratory, stock 000664), CD45.1 (The Jackson Laboratory, stock 002014) OT-I[336] (The Jackson Laboratory, stock 003831), OT-II[610] (The Jackson Laboratory, stock 004194), *Xcr1*-DTR[611](generious gift from Tsuneyasu Kaisho, Osaka University), *Mgl2*-DTR[437] (The Jackson Laboratory, stock 023822), *Cd11c*-Cre[612] (The Jackson Laboratory, stock 008068), *Cx3cr1-lsl*-DTR[613] (The Jackson Laboratory, stock 025629), germline-deficient *Irf4*$^{fl/fl}$ [614](gift from Shomi Sanjabi, UCSF) and confirmed germline deficiency by PCR[614], *Ccr7*$^{-/-}$[615] (The Jackson Laboratory, stock 006621), *Ccr7*^{gfp} [616](The Jackson Laboratory, stock 027913), *Cd11c*-Cre[617] crossed with *Irf4*$^{fl/fl}$ (generous gift from Anne Sperling, University of Chicago), *Zbtb46*^{gfp} [411] (The Jackson Laboratory, stock 027618). All experiments in which mice were used were approved by the Institutional Animal Care and Use Committee of the University of California.

Tumor cell lines

B16F10 (ATCC, CRL-6475) and E.G7-OVA (ATCC, CRL-2133) were purchased. B16-ChOVA, a derivative of B16F10, was transfected with an mCherry-OVA (ChOVA) fusion construct identical to that used in previous studies in our lab[343,427]. B16-ZsGreen (B16ZsGr) was

previously generated in our laboratory as described[429]. B16-GMCSF[618] and B16-FLT3L[619] were generously provided by Lawrence Fong, UC San Francisco. Adherent cell lines were cultured at 37°C in 5% CO_2 in DMEM (Invitrogen), 10% FCS (Benchmark), Pen/Strep/Glut (Invitrogen). Suspension cell lines were cultured in RPMI-1640 (Invitrogen), 10% FCS, Pen/Strep/Glut and beta-mercaptoethanol.

Single-cell RNA sequencing

Live CD90- B220- Ly6G- NK1.1- $CD11b^+$ and/or $CD11c^+$ cells were sorted from B16 tumor-draining LNs with a BD FACSAria Fusion. $5x10^4$ cells were re-suspended in 0.04%BSA (PBS) and loaded onto 10X Genomics' Chromium Controller. Samples were processed for single-cell encapsulation and cDNA library generation using 10x Genomics Chromium using Single Cell 3' v2 Reagent Kits. The library was subsequently sequenced on an Illumina HiSeq 4000.

Single-cell RNA sequencing analyses

Sequencing data was processed using 10X Genomics Cell Ranger V1.2 pipeline. The Cell Ranger subroutine *mkfastq* aggregated reads on a per-cellular barcode basis and passed this data onto the Cell Ranger *count,* which aligned each cell's reads against UCSC mm10 genome using the aligner STAR[620]. After assigning each read to its unique molecular identifier (UMI), *count* generated a final gene-cellular barcode matrix.

This matrix was passed to the R software package Seurat[621] (http://satijalab.org/seurat) (v2.0) for all downstream analyses. We then filtered on cells that expressed a minimum of 200 genes and required that all genes be expressed in at least 3 cells. We also removed cells that contained > 5% reads associated with cell cycle genes[622,623]. Count data was then log2 transformed and scaled using each cell's proportion of cell cycle genes as a nuisance factor to correct for any remaining cell cycle effect in downstream clustering and differential expression analyses. For each sample,

principal component (PC) analysis was performed on a set of highly variable genes defined by Seurat's FindVariableGenes function. Genes associated with the resulting PCs (chosen by visual inspection of scree plots) were then used for graph-based cluster identification and subsequent dimensionality reduction using t distributed stochastic neighbor embedding (tSNE). Cluster-based marker identification and differential expression was performed using Seurat's FindAllMarkers for all between-cluster comparisons, using only genes that were expressed in a minimum of at least 25% of all cells in one of the two relevant groups and had an absolute log2 fold change of at least 0.5.

To generate a priori signatures for the myeloid cell types that we expected to find in the tumor-draining lymph node sample, we downloaded microarray based transcriptional profiles from the Immunological Genome Project data Phase 1[624] (GSE15907) for the following samples:

IMMGEN population	**Analysis ID**	**Replicates**
DC.8^{+}.SLN	rCD8a	3
DC.4^{+}.SLN	rCD11b	3
DC.IIhilang-103-11blo.SLN	mCD11b^{-} CD103^{-}	3
DC.IIhilang^{+}103^{+}11blo.SLN	mCD103^{+}	3
DC.IIhilang^{+}103-11b^{+}.SLN	mLC	3
DC.IIhilang-103-11b^{+}.SLN	mCD11b^{+}	3
Mo.6C^{+}II-.Bl	Mono	5
Mo.6C^{+}II^{+}.Bl		

For each IMMGEN population, we performed differential expression analysis comparing samples from the population of interest to the aggregate of the remaining 6 groups using the R package limma[625]. We cross-referenced the 20 genes with minimal FDR[626] values with those genes expressed in the various single cell data sets and ordered the resulting pool by fold

change. The single-cell expression profile top 5-10 genes were median normalized and aggregated to create a single “signature gene” for each cell type. These signature genes were 0-1 scaled and plotted in the context of the TSNE dimensionality reduction to show cellular location.

Surface and intracellular protein staining for flow cytometry

Tumor and LN tissues were harvested and enzymatically digested with 0.2 mg/ml DNAse I (Sigma-Aldrich), 100 U/ml Collagenase I (Worthington Biochemical), and 500 U/ml Collagenase Type IV (Worthington Biochemical) for 30-45 minutes at 37 °C. Tumor samples were subjected to consistent agitation during this time and LN samples were rapidly pipetted at the half-point time. Samples were filtered to generate a single-cell suspension and washed with stain media (PBS, 2% FCS).

Cells harvested from these tissues or *in vitro* culture were washed with PBS and stained with Zombie NIR fixable viability dye (BioLegend) for 30 minutes at 4°C to distinguish live and dead cells. Cells were then washed with stain media and non-specific binding was blocked with anti-CD16/32 (2.4G2, UCSF Hybridoma Core), and 2% normal rat (Invitrogen) and Armenian hamster (Innovative Research) serum. The following antibodies were used to stain for cell surface proteins at 4°C for 25 minutes: anti-CD11c (N418, BioLegend), anti-CD11b (M1/70, BioLegend), anti-CD103 (2E7, BioLegend), anti-Ly-6C (HK1.4, BioLegend), anti-CD90.2 (30-H12, BioLegend), anti-B220 (RA3-6B2, BioLegend), anti-Ly-6G (1A8, BioLegend), anti-NK1.1 (PK136, BioLegend), anti-CD24 (M1/69, BioLegend), anti-CD8a (53-6.7, BioLegend), anti-CD301b (URA-1, BioLegend), anti-MHC-II (M5/114.15.2, BioLegend), anti-F4/80 (BM8, BioLegend), anti-CCR7 (4B12, BioLegend), anti-CD150 (TC15-12F12.2, BioLegend), anti-XCR1 (ZET, BioLegend), anti-SIRPα, (P84, BioLegend), anti-CD326 (G8.8, BioLegend), anti-CD207 (4C7, BioLegend), anti-CD80 (16-10A1, BioLegend), anti-CD86 (PO3, BioLegend), anti-CD70 (FR70, BioLegend), anti-CD40 (3/23, BioLegend), anti-CD45.1 (A20, BioLegend), anti-CD4

(RM4-5, BioLegend), anti-CD69 (H1.2F3, ThermoFisher Scientific), anti-CD44 (IM7, BioLegend), anti-FLT3 (A2F10, BioLegend), anti-CD26 (H194-112, BioLegend), anti-PDL2 (TY25, BioLegend), anti-CD14 (Sa14-2, BioLegend), anti-CD206 (C068C2, BioLegend), anti-CD200R (OX-110, BioLegend), anti-CD16/32 (93, BioLegend). Cells were washed again and re-suspended with stain media prior to collection and analysis on a BD Fortesssa or LSR-II flow cytometer. When applicable, black latex beads were added to the sample for quantification of absolute cell number.

For intracellular stains, cells were fixed and permeabilized with the FoxP3/Transcription Factor Staining Buffer Set (ThermoFisher Scientific) after surface marker staining. The following antibodies were used to stain for intracellular cell proteins at 25 °C for 30-60 minutes: anti-IFN-γ (XMG1.2, BioLegend), anti-IL-17A (TC11-18H10.1, BioLegend), anti-FoxP3 (150D, Biolegend), Eomes (Dan11mag, eBioscience), and anti-T-bet (4B10, Biolegend).

T cell isolation

OT-I or OT-II T cells were isolated from LNs of CD45.1$^+$ OT-I or OT-II transgenic mice using EasySep CD8 or CD4 negative-selection kits (STEMCELL Technologies), respectively.

***In vivo* T cell adoptive transfer and proliferation**

Isolated CD45.1$^+$ OT-I or OT-II T cells were labeled with Cell Proliferation Dye eFluor670 (ThermoFisher Scientific) and 5x10^5 cells were adoptively transferred to CD45.2$^+$ mice that had been injected with a subcutaneous tumor 14 days previously. LNs from tumor-bearing mice were harvested for analysis 3 days later. When applicable, 500ng of diphtheria toxin was administered intraperitoneally the day before transferring T cells, and continued daily for the remainder of the experiment.

APC-T cell *in vitro* co-culture assays

APC populations were sorted from tumor-draining LNs using a BD FACSAria Fusion and co-cultured with $2x10^4$ isolated eFluor670-labeled OT-I or OT-II T cells at a 1:5 ratio in complete RPMI. Cells or culture supernatant were harvested for analysis 3 or 5 days later.

T cell cytokine analysis

To analyze DC-T cell *in vitro* cultures, cells were collected 3 or 5 days after initial plating. For adoptive T cell transfer experiments, $1x10^5$ naïve $CD4^+$ OT-II T cells were transferred to tumor-bearing mice 7-10 days after tumor injections. Tumor-draining LNs were harvested 7 days following the T cell transfer and re-stimulated *ex vivo*. For tumor-infiltrating T cell experiments, tumors were harvested 12-18 days after injection and $8\text{-}16x10^6$ cells were used for re-stimulation. Single cell suspensions that were re-stimulated were incubated with 50 ng/ml PMA (Sigma-Aldrich), 500 ng/ml ionomycin (Invitrogen), 3 µg/ml brefeldin A (Cayman Chemical Company), and 2µM monensin (ThermoFisher Scientific) for 5-6 hours in complete RPMI and stained for surface and intracellular proteins.

Alternatively, 3 days post-initiation of DC-T cell co-cultures, cells were pelleted and the supernatant was collected and stored at -20C for later use. A bead-based assay was then used to quantify the concentration for pan-T helper cytokines present in the co-culture supernatant (LEGENDplex Mouse Th Cytokine, Biolegend, Cat #740001), as per the manufacturer's instructions.

Antibody or therapeutic treatment *in vivo*

To assess CD4/CD8 T cell dependency for anti-CD40-mediated anti-tumor response, 100 µg of anti-CD40 (Clone: FGK4.5, BioXCell) or isotype (Clone: 2A3, BioXCell) was injected on days 8, 11, and 14. 250 ug of isotype (Clone: LTF-2, BioXCell), anti-CD4 (Clone: GK1.5, BioXCell) or anti-CD8a (Clone: 2.43, BioXCell) was injected at days 7, 10 and 13. To assess changes in cell

surface markers following anti-CD40 treatment, mice were injected with 100 ug of either isotype or anti-CD40 on days 10 and 12 and euthanized at day 14.

To stimulate TLR7 *in vivo*, 25µg Gardiquimod (Invivogen), Imiquimod (Invivogen), or Resiquimod (Invivogen) was injected intratumorally on days 7, 9, 11, and 13.

Statistical analysis

Data groups were compared and analyzed with Student's *t*-test using GraphPrism or Microsoft Excel software. Significance was established if a P value was ≤0.05. Experimental group assignment was determined by genotype or, if all wild-type mice, by random designation. Investigators were not blinded to group assignment during experimental procedures or analysis.

REFERENCES

1. Smith, K. A. Toward a molecular understanding of adaptive immunity: a chronology - part II. *Front Immunol* **3,** 364 (2012).

2. Koch, U. & Radtke, F. Mechanisms of T cell development and transformation. *Annu. Rev. Cell Dev. Biol.* **27,** 539–562 (2011).

3. Klein, L., Hinterberger, M., Wirnsberger, G. & Kyewski, B. Antigen presentation in the thymus for positive selection and central tolerance induction. *Nature Reviews Immunology* **9,** 833–844 (2009).

4. Masopust, D. & Schenkel, J. M. The integration of T cell migration, differentiation and function. *Nature Reviews Immunology* **13,** 309–320 (2013).

5. Takada, K. & Jameson, S. C. Naive T cell homeostasis: from awareness of space to a sense of place. *Nat. Rev. Immunol.* **9,** 823–832 (2009).

6. Steinman, R. M. & Cohn, Z. A. Identification of a novel cell type in peripheral lymphoid organs of mice. I. Morphology, quantitation, tissue distribution. *J. Exp. Med.* **137,** 1142–1162 (1973).

7. Steinman, R. M. & Witmer, M. D. Lymphoid dendritic cells are potent stimulators of the primary mixed leukocyte reaction in mice. *Proc. Natl. Acad. Sci. U.S.A.* **75,** 5132–5136 (1978).

8. Nussenzweig, M. C., Steinman, R. M., Gutchinov, B. & Cohn, Z. A. Dendritic cells are accessory cells for the development of anti-trinitrophenyl cytotoxic T lymphocytes. *J. Exp. Med.* **152,** 1070–1084 (1980).

9. Jung, S. *et al. In vivo* depletion of $CD11c^+$ dendritic cells abrogates priming of $CD8^+$ T cells by exogenous cell-associated antigens. *Immunity* **17,** 211–220 (2002).

10. Meredith, M. M. *et al.* Expression of the zinc finger transcription factor zDC (Zbtb46, Btbd4) defines the classical dendritic cell lineage. *Journal of Experimental Medicine* **209,** 1153–1165 (2012).

11. Anandasabapathy, N. *et al.* Classical Flt3L-dependent dendritic cells control immunity to protein vaccine. *Journal of Experimental Medicine* jem.20131397 (2014). doi:10.1084/jem.20131397

12. Kamphorst, A. O., Guermonprez, P., Dudziak, D. & Nussenzweig, M. C. Route of antigen uptake differentially impacts presentation by dendritic cells and activated monocytes. *The Journal of Immunology* **185,** 3426–3435 (2010).

13. Dudziak, D. *et al.* Differential antigen processing by dendritic cell subsets *in vivo*. *Science* **315,** 107–111 (2007).

14. Savina, A. & Amigorena, S. Phagocytosis and antigen presentation in dendritic cells. *Immunol. Rev.* **219,** 143–156 (2007).

15. Trombetta, E. S. & Mellman, I. Cell biology of antigen processing *in vitro* and *in vivo*. *Annu. Rev. Immunol.* **23,** 975–1028 (2005).

16. Zehner, M. *et al.* The translocon protein Sec61 mediates antigen transport from endosomes in the cytosol for cross-presentation to CD8($^+$) T cells. *Immunity* **42,** 850–863 (2015).

17. Blum, J. S., Wearsch, P. A. & Cresswell, P. Pathways of antigen processing. *Annu. Rev. Immunol.* **31,** 443–473 (2013).

18. Paludan, C. *et al.* Endogenous MHC class II processing of a viral nuclear antigen after autophagy. *Science* **307,** 593–596 (2005).

19. Lee, H. K. *et al. In vivo* Requirement for Atg5 in Antigen Presentation by Dendritic Cells. *Immunity* **32,** 227–239 (2010).

20. Medzhitov, R. & Janeway, C. A. Decoding the patterns of self and nonself by the innate immune system. *Science* **296,** 298–300 (2002).

21. Matzinger, P. Tolerance, danger, and the extended family. *Annu. Rev. Immunol.* **12,** 991–1045 (1994).

22. Alvarez, D., Vollmann, E. H. & Andrian, von, U. H. Mechanisms and consequences of dendritic cell migration. *Immunity* **29,** 325–342 (2008).

23. Tal, O. *et al.* DC mobilization from the skin requires docking to immobilized CCL21 on lymphatic endothelium and intralymphatic crawling. *Journal of Experimental Medicine* **208,** 2141–2153 (2011).

24. Braun, A. *et al.* Afferent lymph-derived T cells and DCs use different chemokine receptor CCR7-dependent routes for entry into the lymph node and intranodal migration. *Nat Immunol* **12,** 879–887 (2011).

25. Ulvmar, M. H. *et al.* The atypical chemokine receptor CCRL1 shapes functional CCL21 gradients in lymph nodes. *Nat Immunol* **15,** 623–630 (2014).

26. Krummel, M. F., Bartumeus, F. & Gérard, A. T cell migration, search strategies and mechanisms. *Nature Reviews Immunology* **16,** 193–201 (2016).

27. Gérard, A. *et al.* Detection of rare antigen-presenting cells through T cell-intrinsic meandering motility, mediated by Myo1g. *Cell* **158,** 492–505 (2014).

28. Castellino, F. *et al.* Chemokines enhance immunity by guiding naive CD8$^+$ T cells to sites of CD4$^+$ T cell-dendritic cell interaction. *Nature* **440,** 890–895 (2006).

29. Mempel, T. R., Henrickson, S. E. & Andrian, von, U. H. T-cell priming by dendritic cells in lymph nodes occurs in three distinct phases. *Nature* **427,** 154–159 (2004).

30. Cyster, J. G. & Schwab, S. R. Sphingosine-1-phosphate and lymphocyte egress from lymphoid organs. *Annu. Rev. Immunol.* **30,** 69–94 (2012).

31. Chang, J. T. *et al.* Asymmetric T lymphocyte division in the initiation of adaptive immune responses. *Science* **315,** 1687–1691 (2007).

32. Gérard, A. *et al.* Secondary T cell-T cell synaptic interactions drive the differentiation of protective $CD8^+$ T cells. *Nat Immunol* **14,** 356–363 (2013).

33. Zhu, J., Yamane, H. & Paul, W. E. Differentiation of effector CD4 T cell populations. *Annu. Rev. Immunol.* **28,** 445–489 (2010).

34. Kupfer, A., Singer, S. J., Janeway, C. A. & Swain, S. L. Coclustering of CD4 (L3T4) molecule with the T-cell receptor is induced by specific direct interaction of helper T cells and antigen-presenting cells. *Proc. Natl. Acad. Sci. U.S.A.* **84,** 5888–5892 (1987).

35. Kupfer, A. & Singer, S. J. The specific interaction of helper T cells and antigen-presenting B cells. IV. Membrane and cytoskeletal reorganizations in the bound T cell as a function of antigen dose. *J. Exp. Med.* **170,** 1697–1713 (1989).

36. Monks, C. R., Kupfer, H., Tamir, I., Barlow, A. & Kupfer, A. Selective modulation of protein kinase C-theta during T-cell activation. *Nature* **385,** 83–86 (1997).

37. Monks, C. R., Freiberg, B. A., Kupfer, H., Sciaky, N. & Kupfer, A. Three-dimensional segregation of supramolecular activation clusters in T cells. *Nature* **395,** 82–86 (1998).

38. Freiberg, B. A. *et al.* Staging and resetting T cell activation in SMACs. *Nat Immunol* **3,** 911–917 (2002).

39. Dustin, M. L. & Choudhuri, K. Signaling and Polarized Communication Across the T Cell Immunological Synapse. *Annu. Rev. Cell Dev. Biol.* **32,** 303–325 (2016).

40. Dustin, M. L. *et al.* A novel adaptor protein orchestrates receptor patterning and cytoskeletal polarity in T-cell contacts. *Cell* **94,** 667–677 (1998).

41. Grakoui, A. *et al.* The immunological synapse: a molecular machine controlling T cell activation. *Science* **285,** 221–227 (1999).

42. Brossard, C. *et al.* Multifocal structure of the T cell - dendritic cell synapse. *Eur. J. Immunol.* **35,** 1741–1753 (2005).

43. Mossman, K. D., Campi, G., Groves, J. T. & Dustin, M. L. Altered TCR signaling from geometrically repatterned immunological synapses. *Science* **310,** 1191–1193 (2005).

44. Dustin, M. L., Tseng, S.-Y., Varma, R. & Campi, G. T cell-dendritic cell immunological synapses. *Curr. Opin. Immunol.* **18,** 512–516 (2006).

45. Gunzer, M. *et al.* Antigen presentation in extracellular matrix: interactions of T cells with dendritic cells are dynamic, short lived, and sequential. *Immunity* **13,** 323–332 (2000).

46. Miller, M. J., Wei, S. H., Parker, I. & Cahalan, M. D. Two-photon imaging of lymphocyte motility and antigen response in intact lymph node. *Science* **296,** 1869–1873 (2002).

47. Friedman, R. S., Beemiller, P., Sorensen, C. M., Jacobelli, J. & Krummel, M. F. Real-

time analysis of T cell receptors in naive cells *in vitro* and *in vivo* reveals flexibility in synapse and signaling dynamics. *Journal of Experimental Medicine* **207,** 2733–2749 (2010).

48. Skokos, D. *et al.* Peptide-MHC potency governs dynamic interactions between T cells and dendritic cells in lymph nodes. *Nat Immunol* **8,** 835–844 (2007).

49. Henrickson, S. E. *et al.* T cell sensing of antigen dose governs interactive behavior with dendritic cells and sets a threshold for T cell activation. *Nat Immunol* **9,** 282–291 (2008).

50. Sims, T. N. *et al.* Opposing Effects of PKCθ and WASp on Symmetry Breaking and Relocation of the Immunological Synapse. *Cell* **129,** 773–785 (2007).

51. Beemiller, P., Jacobelli, J. & Krummel, M. F. Integration of the movement of signaling microclusters with cellular motility in immunological synapses. *Nat Immunol* **13,** 787–795 (2012).

52. Dustin, M. L. Cell adhesion molecules and actin cytoskeleton at immune synapses and kinapses. *Curr. Opin. Cell Biol.* **19,** 529–533 (2007).

53. Gérard, A., Beemiller, P., Friedman, R. S., Jacobelli, J. & Krummel, M. F. Evolving immune circuits are generated by flexible, motile, and sequential immunological synapses. *Immunol. Rev.* **251,** 80–96 (2013).

54. Irvine, D. J., Purbhoo, M. A., Krogsgaard, M. & Davis, M. M. Direct observation of ligand recognition by T cells. *Nature* **419,** 845–849 (2002).

55. Brownlie, R. J. & Zamoyska, R. T cell receptor signalling networks: branched, diversified and bounded. *Nature Reviews Immunology* **13,** 257–269 (2013).

56. Seminario, M.-C. & Bunnell, S. C. Signal initiation in T-cell receptor microclusters. *Immunol. Rev.* **221,** 90–106 (2008).

57. Iwashima, M., Irving, B. A., van Oers, N. S., Chan, A. C. & Weiss, A. Sequential interactions of the TCR with two distinct cytoplasmic tyrosine kinases. *Science* **263,** 1136–1139 (1994).

58. Yokosuka, T. *et al.* Newly generated T cell receptor microclusters initiate and sustain T cell activation by recruitment of Zap70 and SLP-76. *Nat Immunol* **6,** 1253–1262 (2005).

59. Smith-Garvin, J. E., Koretzky, G. A. & Jordan, M. S. T cell activation. *Annu. Rev. Immunol.* **27,** 591–619 (2009).

60. Chakraborty, A. K. & Weiss, A. Insights into the initiation of TCR signaling. *Nat Immunol* **15,** 798–807 (2014).

61. Choudhuri, K., Kearney, A., Bakker, T. R. & van der Merwe, P. A. How do T cells recognize antigen? *Current Biology* **15,** R382–5 (2005).

62. Su, X. *et al.* Phase separation of signaling molecules promotes T cell receptor signal

transduction. *Science* **352,** 595–599 (2016).

63. Beddoe, T. *et al.* Antigen ligation triggers a conformational change within the constant domain of the alphabeta T cell receptor. *Immunity* **30,** 777–788 (2009).

64. Gil, D., Schamel, W. W. A., Montoya, M., Sánchez-Madrid, F. & Alarcón, B. Recruitment of Nck by CD3 epsilon reveals a ligand-induced conformational change essential for T cell receptor signaling and synapse formation. *Cell* **109,** 901–912 (2002).

65. Gil, D., Schrum, A. G., Alarcón, B. & Palmer, E. T cell receptor engagement by peptide-MHC ligands induces a conformational change in the CD3 complex of thymocytes. *J. Exp. Med.* **201,** 517–522 (2005).

66. Martínez-Martín, N. *et al.* Cooperativity between T cell receptor complexes revealed by conformational mutants of CD3epsilon. *Sci Signal* **2,** ra43–ra43 (2009).

67. Davis, S. J. & van der Merwe, P. A. The kinetic-segregation model: TCR triggering and beyond. *Nat Immunol* **7,** 803–809 (2006).

68. Choudhuri, K., Wiseman, D., Brown, M. H., Gould, K. & van der Merwe, P. A. T-cell receptor triggering is critically dependent on the dimensions of its peptide-MHC ligand. *Nature* **436,** 578–582 (2005).

69. James, J. R. & Vale, R. D. Biophysical mechanism of T-cell receptor triggering in a reconstituted system. *Nature* **487,** 64–69 (2012).

70. Chang, V. T. *et al.* Initiation of T cell signaling by CD45 segregation at 'close contacts'. *Nat Immunol* **17,** 574–582 (2016).

71. Krummel, M. F. & Macara, I. Maintenance and modulation of T cell polarity. *Nat Immunol* **7,** 1143–1149 (2006).

72. Wülfing, C. & Davis, M. M. A receptor/cytoskeletal movement triggered by costimulation during T cell activation. *Science* **282,** 2266–2269 (1998).

73. Jacobelli, J., Chmura, S. A., Buxton, D. B., Davis, M. M. & Krummel, M. F. A single class II myosin modulates T cell motility and stopping, but not synapse formation. *Nat Immunol* **5,** 531–538 (2004).

74. Krummel, M. F., Sjaastad, M. D., Wülfing, C. & Davis, M. M. Differential clustering of CD4 and CD3zeta during T cell recognition. *Science* **289,** 1349–1352 (2000).

75. Tibaldi, E. V., Salgia, R. & Reinherz, E. L. CD2 molecules redistribute to the uropod during T cell scanning: implications for cellular activation and immune surveillance. *Proc. Natl. Acad. Sci. U.S.A.* **99,** 7582–7587 (2002).

76. Serrador, J. M. *et al.* CD43 interacts with moesin and ezrin and regulates its redistribution to the uropods of T lymphocytes at the cell-cell contacts. *Blood* **91,** 4632–4644 (1998).

77. del Pozo, M. A., Sanchez-Mateos, P., Nieto, M. & Sanchez-Madrid, F. Chemokines

regulate cellular polarization and adhesion receptor redistribution during lymphocyte interaction with endothelium and extracellular matrix. Involvement of cAMP signaling pathway. *J. Cell Biol.* **131,** 495–508 (1995).

78. Negulescu, P. A., Krasieva, T. B., Khan, A., Kerschbaum, H. H. & Cahalan, M. D. Polarity of T Cell Shape, Motility, and Sensitivity to Antigen. *Immunity* **4,** 421–430 (1996).

79. Dustin, M. L., Bromley, S. K., Kan, Z., Peterson, D. A. & Unanue, E. R. Antigen receptor engagement delivers a stop signal to migrating T lymphocytes. *Proc. Natl. Acad. Sci. U.S.A.* **94,** 3909–3913 (1997).

80. Waite, J. C. *et al.* Interference with $Ca(2^+)$ release activated $Ca(2^+)$ (CRAC) channel function delays T-cell arrest *in vivo*. *Eur. J. Immunol.* **43,** 3343–3354 (2013).

81. Ludford-Menting, M. J. *et al.* A network of PDZ-containing proteins regulates T cell polarity and morphology during migration and immunological synapse formation. *Immunity* **22,** 737–748 (2005).

82. Cullinan, P., Sperling, A. I. & Burkhardt, J. K. The distal pole complex: a novel membrane domain distal to the immunological synapse. *Immunol. Rev.* **189,** 111–122 (2002).

83. Faure, S. *et al.* ERM proteins regulate cytoskeleton relaxation promoting T cell-APC conjugation. *Nat Immunol* **5,** 272–279 (2004).

84. Delon, J., Kaibuchi, K. & Germain, R. N. Exclusion of CD43 from the immunological synapse is mediated by phosphorylation-regulated relocation of the cytoskeletal adaptor moesin. *Immunity* **15,** 691–701 (2001).

85. Cairo, C. W., Mirchev, R. & Golan, D. E. Cytoskeletal regulation couples LFA-1 conformational changes to receptor lateral mobility and clustering. *Immunity* **25,** 297–308 (2006).

86. Kinashi, T. Intracellular signalling controlling integrin activation in lymphocytes. *Nat. Rev. Immunol.* **5,** 546–559 (2005).

87. Valitutti, S., Dessing, M., Aktories, K., Gallati, H. & Lanzavecchia, A. Sustained signaling leading to T cell activation results from prolonged T cell receptor occupancy. Role of T cell actin cytoskeleton. *J. Exp. Med.* **181,** 577–584 (1995).

88. Delon, J., Bercovici, N., Liblau, R. & Trautmann, A. Imaging antigen recognition by naive $CD4^+$ T cells: compulsory cytoskeletal alterations for the triggering of an intracellular calcium response. *Eur. J. Immunol.* **28,** 716–729 (1998).

89. Tskvitaria-Fuller, I., Rozelle, A. L., Yin, H. L. & Wülfing, C. Regulation of sustained actin dynamics by the TCR and costimulation as a mechanism of receptor localization. *J. Immunol.* **171,** 2287–2295 (2003).

90. Campi, G., Varma, R. & Dustin, M. L. Actin and agonist MHC-peptide complex-dependent T cell receptor microclusters as scaffolds for signaling. *J. Exp. Med.* **202,**

1031–1036 (2005).

91. Varma, R., Campi, G., Yokosuka, T., Saito, T. & Dustin, M. L. T cell receptor-proximal signals are sustained in peripheral microclusters and terminated in the central supramolecular activation cluster. *Immunity* **25,** 117–127 (2006).

92. Billadeau, D. D., Nolz, J. C. & Gomez, T. S. Regulation of T-cell activation by the cytoskeleton. *Nat. Rev. Immunol.* **7,** 131–143 (2007).

93. Sedwick, C. E. *et al.* TCR, LFA-1, and CD28 play unique and complementary roles in signaling T cell cytoskeletal reorganization. *J. Immunol.* **162,** 1367–1375 (1999).

94. Kupfer, A., Singer, S. J. & Dennert, G. On the mechanism of unidirectional killing in mixtures of two cytotoxic T lymphocytes. Unidirectional polarization of cytoplasmic organelles and the membrane-associated cytoskeleton in the effector cell. *J. Exp. Med.* **163,** 489–498 (1986).

95. Stinchcombe, J. C., Majorovits, E., Bossi, G., Fuller, S. & Griffiths, G. M. Centrosome polarization delivers secretory granules to the immunological synapse. *Nature* **443,** 462–465 (2006).

96. Tsun, A. *et al.* Centrosome docking at the immunological synapse is controlled by Lck signaling. *J. Cell Biol.* **192,** 663–674 (2011).

97. Zhao, F., Cannons, J. L., Dutta, M., Griffiths, G. M. & Schwartzberg, P. L. Positive and Negative Signaling through SLAM Receptors Regulate Synapse Organization and Thresholds of Cytolysis. *Immunity* **36,** 1003–1016 (2012).

98. Huse, M., Lillemeier, B. F., Kuhns, M. S., Chen, D. S. & Davis, M. M. T cells use two directionally distinct pathways for cytokine secretion. *Nat Immunol* **7,** 247–255 (2006).

99. Lawrence, C. W. & Braciale, T. J. Activation, differentiation, and migration of naive virus-specific $CD8^+$ T cells during pulmonary influenza virus infection. *J. Immunol.* **173,** 1209–1218 (2004).

100. Yoon, H., Legge, K. L., Sung, S.-S. J. & Braciale, T. J. Sequential activation of $CD8^+$ T cells in the draining lymph nodes in response to pulmonary virus infection. *J. Immunol.* **179,** 391–399 (2007).

101. Yoon, H., Kim, T. S. & Braciale, T. J. The cell cycle time of $CD8^+$ T cells responding *in vivo* is controlled by the type of antigenic stimulus. *PLoS ONE* **5,** e15423 (2010).

102. Blattman, J. N. *et al.* Estimating the precursor frequency of naive antigen-specific CD8 T cells. *J. Exp. Med.* **195,** 657–664 (2002).

103. Tscharke, D. C., Croft, N. P., Doherty, P. C. & La Gruta, N. L. Sizing up the key determinants of the $CD8(^+)$ T cell response. *Nature Reviews Immunology* **15,** 705–716 (2015).

104. June, C. H., Ledbetter, J. A., Gillespie, M. M., Lindsten, T. & Thompson, C. B. T-cell proliferation involving the CD28 pathway is associated with cyclosporine-resistant

interleukin 2 gene expression. *Mol. Cell. Biol.* **7,** 4472–4481 (1987).

105. Schwartz, R. H., Mueller, D. L., Jenkins, M. K. & Quill, H. T-cell clonal anergy. *Cold Spring Harb. Symp. Quant. Biol.* **54 Pt 2,** 605–610 (1989).

106. Jenkins, M. K., Chen, C. A., Jung, G., Mueller, D. L. & Schwartz, R. H. Inhibition of antigen-specific proliferation of type 1 murine T cell clones after stimulation with immobilized anti-CD3 monoclonal antibody. *J. Immunol.* **144,** 16–22 (1990).

107. Mueller, D. L., Jenkins, M. K. & Schwartz, R. H. Clonal expansion versus functional clonal inactivation: a costimulatory signalling pathway determines the outcome of T cell antigen receptor occupancy. *Annu. Rev. Immunol.* **7,** 445–480 (1989).

108. Boomer, J. S. & Green, J. M. An enigmatic tail of CD28 signaling. *Cold Spring Harb Perspect Biol* **2,** a002436 (2010).

109. Chen, L. & Flies, D. B. Molecular mechanisms of T cell co-stimulation and co-inhibition. *Nature Reviews Immunology* **13,** 227–242 (2013).

110. Yokosuka, T. & Saito, T. Dynamic regulation of T-cell costimulation through TCR-CD28 microclusters. *Immunol. Rev.* **229,** 27–40 (2009).

111. Yokosuka, T. *et al.* Spatiotemporal basis of CTLA-4 costimulatory molecule-mediated negative regulation of T cell activation. *Immunity* **33,** 326–339 (2010).

112. Sheppard, K.-A. *et al.* PD-1 inhibits T-cell receptor induced phosphorylation of the ZAP70/CD3zeta signalosome and downstream signaling to PKCtheta. *FEBS Lett.* **574,** 37–41 (2004).

113. Yokosuka, T. *et al.* Programmed cell death 1 forms negative costimulatory microclusters that directly inhibit T cell receptor signaling by recruiting phosphatase SHP2. *Journal of Experimental Medicine* **209,** 1201–1217 (2012).

114. June, C. H., Ledbetter, J. A., Linsley, P. S. & Thompson, C. B. Role of the CD28 receptor in T-cell activation. *Immunol. Today* **11,** 211–216 (1990).

115. Nolte, M. A., van Olffen, R. W., van Gisbergen, K. P. J. M. & van Lier, R. A. W. Timing and tuning of CD27-CD70 interactions: the impact of signal strength in setting the balance between adaptive responses and immunopathology. *Immunol. Rev.* **229,** 216–231 (2009).

116. Croft, M., So, T., Duan, W. & Soroosh, P. The significance of OX40 and OX40L to T-cell biology and immune disease. *Immunol. Rev.* **229,** 173–191 (2009).

117. Wang, C., Lin, G. H. Y., McPherson, A. J. & Watts, T. H. Immune regulation by 4-1BB and 4-1BBL: complexities and challenges. *Immunol. Rev.* **229,** 192–215 (2009).

118. Sharpe, A. H. Mechanisms of costimulation. *Immunol. Rev.* **229,** 5–11 (2009).

119. Zhu, Y., Yao, S. & Chen, L. Cell surface signaling molecules in the control of immune responses: a tide model. *Immunity* **34,** 466–478 (2011).

120. Malek, T. R. The biology of interleukin-2. *Annu. Rev. Immunol.* **26,** 453–479 (2008).

121. Vella, A. T., Dow, S., Potter, T. A., Kappler, J. & Marrack, P. Cytokine-induced survival of activated T cells *in vitro* and *in vivo*. *Proc. Natl. Acad. Sci. U.S.A.* **95,** 3810–3815 (1998).

122. Whitmire, J. K., Tan, J. T. & Whitton, J. L. Interferon-gamma acts directly on $CD8^+$ T cells to increase their abundance during virus infection. *J. Exp. Med.* **201,** 1053–1059 (2005).

123. Curtsinger, J. M., Agarwal, P., Lins, D. C. & Mescher, M. F. Autocrine IFN-γ promotes naive CD8 T cell differentiation and synergizes with IFN-α to stimulate strong function. *The Journal of Immunology* **189,** 659–668 (2012).

124. Badovinac, V. P., Tvinnereim, A. R. & Harty, J. T. Regulation of antigen-specific $CD8^+$ T cell homeostasis by perforin and interferon-gamma. *Science* **290,** 1354–1358 (2000).

125. Sercan, O., Stoycheva, D., Hämmerling, G. J., Arnold, B. & Schüler, T. IFN-gamma receptor signaling regulates memory $CD8^+$ T cell differentiation. *The Journal of Immunology* **184,** 2855–2862 (2010).

126. Curtsinger, J. M. *et al.* Inflammatory cytokines provide a third signal for activation of naive $CD4^+$ and $CD8^+$ T cells. *J. Immunol.* **162,** 3256–3262 (1999).

127. Schmidt, C. S. & Mescher, M. F. Adjuvant effect of IL-12: conversion of peptide antigen administration from tolerizing to immunizing for $CD8^+$ T cells *in vivo*. *J. Immunol.* **163,** 2561–2567 (1999).

128. Schmidt, C. S. & Mescher, M. F. Peptide antigen priming of naive, but not memory, CD8 T cells requires a third signal that can be provided by IL-12. *J. Immunol.* **168,** 5521–5529 (2002).

129. Pennock, N. D., Gapin, L. & Kedl, R. M. IL-27 is required for shaping the magnitude, affinity distribution, and memory of T cells responding to subunit immunization. *Proceedings of the National Academy of Sciences* **111,** 16472–16477 (2014).

130. Desch, A. N. *et al.* Dendritic cell subsets require cis-activation for cytotoxic CD8 T-cell induction. *Nat Commun* **5,** 4674 (2014).

131. Curtsinger, J. M., Valenzuela, J. O., Agarwal, P., Lins, D. & Mescher, M. F. Type I IFNs provide a third signal to CD8 T cells to stimulate clonal expansion and differentiation. *J. Immunol.* **174,** 4465–4469 (2005).

132. Aichele, P. *et al.* CD8 T cells specific for lymphocytic choriomeningitis virus require type I IFN receptor for clonal expansion. *J. Immunol.* **176,** 4525–4529 (2006).

133. Kolumam, G. A., Thomas, S., Thompson, L. J., Sprent, J. & Murali-Krishna, K. Type I interferons act directly on CD8 T cells to allow clonal expansion and memory formation in response to viral infection. *J. Exp. Med.* **202,** 637–650 (2005).

134. Haring, J. S., Badovinac, V. P. & Harty, J. T. Inflaming the $CD8^+$ T cell response. *Immunity* **25,** 19–29 (2006).

135. Opata, M. M. & Stephens, R. Early Decision: Effector and Effector Memory T Cell Differentiation in Chronic Infection. *Curr Immunol Rev* **9,** 190–206 (2013).

136. Rohr, J. C., Gerlach, C., Kok, L. & Schumacher, T. N. Single cell behavior in T cell differentiation. *Trends Immunol.* **35,** 170–177 (2014).

137. Kaech, S. M. *et al.* Selective expression of the interleukin 7 receptor identifies effector CD8 T cells that give rise to long-lived memory cells. *Nat Immunol* **4,** 1191–1198 (2003).

138. Kalia, V. *et al.* Prolonged interleukin-2Ralpha expression on virus-specific $CD8^+$ T cells favors terminal-effector differentiation *in vivo*. *Immunity* **32,** 91–103 (2010).

139. Obar, J. J. & Lefrançois, L. Early events governing memory $CD8^+$ T-cell differentiation. *Int. Immunol.* **22,** 619–625 (2010).

140. van Oers, N. S., Killeen, N. & Weiss, A. ZAP-70 is constitutively associated with tyrosine-phosphorylated TCR zeta in murine thymocytes and lymph node T cells. *Immunity* **1,** 675–685 (1994).

141. Dorfman, J. R., Stefanová, I., Yasutomo, K. & Germain, R. N. $CD4^+$ T cell survival is not directly linked to self-MHC-induced TCR signaling. *Nat Immunol* **1,** 329–335 (2000).

142. Witherden, D. *et al.* Tetracycline-controllable selection of $CD4(^+)$ T cells: half-life and survival signals in the absence of major histocompatibility complex class II molecules. *J. Exp. Med.* **191,** 355–364 (2000).

143. Nesić, D. & Vukmanović, S. MHC class I is required for peripheral accumulation of $CD8^+$ thymic emigrants. *J. Immunol.* **160,** 3705–3712 (1998).

144. Markiewicz, M. A., Brown, I. & Gajewski, T. F. Death of peripheral $CD8^+$ T cells in the absence of MHC class I is Fas-dependent and not blocked by Bcl-xL. *Eur. J. Immunol.* **33,** 2917–2926 (2003).

145. Tanchot, C., Lemonnier, F. A., Pérarnau, B., Freitas, A. A. & Rocha, B. Differential requirements for survival and proliferation of CD8 naïve or memory T cells. *Science* **276,** 2057–2062 (1997).

146. Takada, K. & Jameson, S. C. Self-class I MHC molecules support survival of naive CD8 T cells, but depress their functional sensitivity through regulation of CD8 expression levels. *Journal of Experimental Medicine* **206,** 2253–2269 (2009).

147. Labrecque, N. *et al.* How much TCR does a T cell need? *Immunity* **15,** 71–82 (2001).

148. Polic, B., Kunkel, D., Scheffold, A. & Rajewsky, K. How alpha beta T cells deal with induced TCR alpha ablation. *Proc. Natl. Acad. Sci. U.S.A.* **98,** 8744–8749 (2001).

149. Hirosue, S. & Dubrot, J. Modes of Antigen Presentation by Lymph Node Stromal Cells

and Their Immunological Implications. *Front Immunol* **6,** 446 (2015).

150. Hochweller, K. *et al.* Dendritic cells control T cell tonic signaling required for responsiveness to foreign antigen. *Proceedings of the National Academy of Sciences* **107,** 5931–5936 (2010).

151. Kirberg, J., Berns, A. & Boehmer, von, H. Peripheral T cell survival requires continual ligation of the T cell receptor to major histocompatibility complex-encoded molecules. *J. Exp. Med.* **186,** 1269–1275 (1997).

152. Brocker, T. Survival of mature CD4 T lymphocytes is dependent on major histocompatibility complex class II-expressing dendritic cells. *J. Exp. Med.* **186,** 1223–1232 (1997).

153. Takeda, S., Rodewald, H.-R., Arakawa, H., Bluethmann, H. & Shimizu, T. MHC Class II Molecules Are Not Required for Survival of Newly Generated $CD4^+$ T Cells, but Affect Their Long-Term Life Span. *Immunity* **5,** 217–228 (1996).

154. Martin, B., Bécourt, C., Bienvenu, B. & Lucas, B. Self-recognition is crucial for maintaining the peripheral $CD4^+$ T-cell pool in a nonlymphopenic environment. *Blood* **108,** 270–277 (2006).

155. Grandjean, I. *et al.* Are major histocompatibility complex molecules involved in the survival of naive $CD4^+$ T cells? *J. Exp. Med.* **198,** 1089–1102 (2003).

156. Clarke, S. R. & Rudensky, A. Y. Survival and homeostatic proliferation of naive peripheral $CD4^+$ T cells in the absence of self peptide:MHC complexes. *J. Immunol.* **165,** 2458–2464 (2000).

157. Fischer, U. B. *et al.* MHC class II deprivation impairs CD4 T cell motility and responsiveness to antigen-bearing dendritic cells *in vivo*. *Proc. Natl. Acad. Sci. U.S.A.* **104,** 7181–7186 (2007).

158. Stefanová, I., Dorfman, J. R. & Germain, R. N. Self-recognition promotes the foreign antigen sensitivity of naive T lymphocytes. *Nature* **420,** 429–434 (2002).

159. Bhandoola, A. *et al.* Peripheral expression of self-MHC-II influences the reactivity and self-tolerance of mature $CD4(^+)$ T cells: evidence from a lymphopenic T cell model. *Immunity* **17,** 425–436 (2002).

160. Smith, K. *et al.* Sensory adaptation in naive peripheral CD4 T cells. *J. Exp. Med.* **194,** 1253–1261 (2001).

161. Azzam, H. S. *et al.* CD5 expression is developmentally regulated by T cell receptor (TCR) signals and TCR avidity. *J. Exp. Med.* **188,** 2301–2311 (1998).

162. Wong, P., Barton, G. M., Forbush, K. A. & Rudensky, A. Y. Dynamic tuning of T cell reactivity by self-peptide-major histocompatibility complex ligands. *J. Exp. Med.* **193,** 1179–1187 (2001).

163. Seddon, B. & Zamoyska, R. TCR signals mediated by Src family kinases are essential

for the survival of naive T cells. *J. Immunol.* **169,** 2997–3005 (2002).

164. Fulton, R. B. *et al.* The TCR's sensitivity to self peptide-MHC dictates the ability of naive CD8(+) T cells to respond to foreign antigens. *Nat Immunol* **16,** 107–117 (2015).

165. Mandl, J. N., Monteiro, J. P., Vrisekoop, N. & Germain, R. N. T cell-positive selection uses self-ligand binding strength to optimize repertoire recognition of foreign antigens. *Immunity* **38,** 263–274 (2013).

166. Weber, K. S. *et al.* Distinct $CD4^+$ helper T cells involved in primary and secondary responses to infection. *Proceedings of the National Academy of Sciences* **109,** 9511–9516 (2012).

167. Persaud, S. P., Parker, C. R., Lo, W.-L., Weber, K. S. & Allen, P. M. Intrinsic $CD4^+$ T cell sensitivity and response to a pathogen are set and sustained by avidity for thymic and peripheral complexes of self peptide and MHC. *Nat Immunol* **15,** 266–274 (2014).

168. Schluns, K. S., Kieper, W. C., Jameson, S. C. & Lefrançois, L. Interleukin-7 mediates the homeostasis of naïve and memory CD8 T cells *in vivo*. *Nat Immunol* **1,** 426–432 (2000).

169. Opferman, J. T. *et al.* Development and maintenance of B and T lymphocytes requires antiapoptotic MCL-1. *Nature* **426,** 671–676 (2003).

170. Jiang, Q. *et al.* Cell biology of IL-7, a key lymphotrophin. *Cytokine Growth Factor Rev.* **16,** 513–533 (2005).

171. Rathmell, J. C., Farkash, E. A., Gao, W. & Thompson, C. B. IL-7 enhances the survival and maintains the size of naive T cells. *J. Immunol.* **167,** 6869–6876 (2001).

172. Wofford, J. A., Wieman, H. L., Jacobs, S. R., Zhao, Y. & Rathmell, J. C. IL-7 promotes Glut1 trafficking and glucose uptake via STAT5-mediated activation of Akt to support T-cell survival. *Blood* **111,** 2101–2111 (2008).

173. Vivien, L., Benoist, C. & Mathis, D. T lymphocytes need IL-7 but not IL-4 or IL-6 to survive *in vivo*. *Int. Immunol.* **13,** 763–768 (2001).

174. Kondrack, R. M. *et al.* Interleukin 7 Regulates the Survival and Generation of Memory CD4 Cells. *J. Exp. Med.* **198,** 1797–1806 (2003).

175. Tan, J. T. *et al.* IL-7 is critical for homeostatic proliferation and survival of naive T cells. *Proc. Natl. Acad. Sci. U.S.A.* **98,** 8732–8737 (2001).

176. Kieper, W. C. *et al.* Overexpression of Interleukin (IL)-7 Leads to IL-15–independent Generation of Memory Phenotype $CD8^+$T Cells. *J. Exp. Med.* **195,** 1533–1539 (2002).

177. Fry, T. J. & Mackall, C. L. The many faces of IL-7: from lymphopoiesis to peripheral T cell maintenance. *J. Immunol.* **174,** 6571–6576 (2005).

178. Moses, C. T., Thorstenson, K. M., Jameson, S. C. & Khoruts, A. Competition for self ligands restrains homeostatic proliferation of naive CD4 T cells. *Proc. Natl. Acad. Sci.*

U.S.A. **100,** 1185–1190 (2003).

179. Troy, A. E. & Shen, H. Cutting edge: homeostatic proliferation of peripheral T lymphocytes is regulated by clonal competition. *J. Immunol.* **170,** 672–676 (2003).

180. Leitão, C., Freitas, A. A. & Garcia, S. The role of TCR specificity and clonal competition during reconstruction of the peripheral T cell pool. *The Journal of Immunology* **182,** 5232–5239 (2009).

181. Min, B., Yamane, H., Hu-Li, J. & Paul, W. E. Spontaneous and homeostatic proliferation of CD4 T cells are regulated by different mechanisms. *J. Immunol.* **174,** 6039–6044 (2005).

182. Ramsey, C. *et al.* The lymphopenic environment of CD132 (common gamma-chain)-deficient hosts elicits rapid homeostatic proliferation of naive T cells via IL-15. *J. Immunol.* **180,** 5320–5326 (2008).

183. Cho, J.-H. H. *et al.* An intense form of homeostatic proliferation of naive $CD8^+$ cells driven by IL-2. *Journal of Experimental Medicine* **204,** 1787–1801 (2007).

184. Sprent, C. D. S. J. Homeostasis of Naive and Memory T Cells. *Immunity* **29,** 848–862 (2008).

185. Becker, T. C. *et al.* Interleukin 15 is required for proliferative renewal of virus-specific memory CD8 T cells. *J. Exp. Med.* **195,** 1541–1548 (2002).

186. Lenz, D. C. *et al.* IL-7 regulates basal homeostatic proliferation of antiviral $CD4^+$T cell memory. *Proc. Natl. Acad. Sci. U.S.A.* **101,** 9357–9362 (2004).

187. Purton, J. F. *et al.* Antiviral $CD4^+$ memory T cells are IL-15 dependent. *J. Exp. Med.* **204,** 951–961 (2007).

188. Cui, G. *et al.* Characterization of the IL-15 niche in primary and secondary lymphoid organs *in vivo*. *Proceedings of the National Academy of Sciences* (2014). doi:10.1073/pnas.1318281111

189. Mortier, E. *et al.* Macrophage- and dendritic-cell-derived interleukin-15 receptor alpha supports homeostasis of distinct $CD8^+$ T cell subsets. *Immunity* **31,** 811–822 (2009).

190. Jung, Y. W., Kim, H. G., Perry, C. J. & Kaech, S. M. CCR7 expression alters memory CD8 T-cell homeostasis by regulating occupancy in IL-7- and IL-15-dependent niches. *Proceedings of the National Academy of Sciences* **113,** 8278–8283 (2016).

191. Mostowy, S. & Cossart, P. Septins: the fourth component of the cytoskeleton. *Nat. Rev. Mol. Cell Biol.* **13,** 183–194 (2012).

192. Hartwell, L. H. Genetic control of the cell division cycle in yeast. IV. Genes controlling bud emergence and cytokinesis. *Exp. Cell Res.* **69,** 265–276 (1971).

193. Mino, A. *et al.* Shs1p: a novel member of septin that interacts with spa2p, involved in polarized growth in saccharomyces cerevisiae. *Biochem. Biophys. Res. Commun.* **251,**

732–736 (1998).

194. Casamayor, A. & Snyder, M. Molecular dissection of a yeast septin: distinct domains are required for septin interaction, localization, and function. *Mol. Cell. Biol.* **23,** 2762–2777 (2003).

195. Zhang, J. *et al.* Phosphatidylinositol polyphosphate binding to the mammalian septin H5 is modulated by GTP. *Current Biology* **9,** 1458–1467 (1999).

196. Versele, M. *et al.* Protein-protein interactions governing septin heteropentamer assembly and septin filament organization in Saccharomyces cerevisiae. *Mol. Biol. Cell* **15,** 4568–4583 (2004).

197. Pan, F., Malmberg, R. L. & Momany, M. Analysis of septins across kingdoms reveals orthology and new motifs. *BMC Evol. Biol.* **7,** 103 (2007).

198. Weirich, C. S., Erzberger, J. P. & Barral, Y. The septin family of GTPases: architecture and dynamics. *Nat. Rev. Mol. Cell Biol.* **9,** 478–489 (2008).

199. Kinoshita, M. The septins. *Genome Biol.* **4,** 236 (2003).

200. Bertin, A. *et al.* Saccharomyces cerevisiae septins: supramolecular organization of heterooligomers and the mechanism of filament assembly. *Proceedings of the National Academy of Sciences* **105,** 8274–8279 (2008).

201. Garcia, G. *et al.* Subunit-dependent modulation of septin assembly: budding yeast septin Shs1 promotes ring and gauze formation. *J. Cell Biol.* **195,** 993–1004 (2011).

202. Kaplan, C. *et al.* Absolute Arrangement of Subunits in Cytoskeletal Septin Filaments in Cells Measured by Fluorescence Microscopy. *Nano Lett.* **15,** 3859–3864 (2015).

203. Sirajuddin, M., Farkasovsky, M., Zent, E. & Wittinghofer, A. GTP-induced conformational changes in septins and implications for function. *Proceedings of the National Academy of Sciences* **106,** 16592–16597 (2009).

204. Sellin, M. E., Sandblad, L., Stenmark, S. & Gullberg, M. Deciphering the rules governing assembly order of mammalian septin complexes. *Mol. Biol. Cell* **22,** 3152–3164 (2011).

205. Sandrock, K. *et al.* Characterization of human septin interactions. *Biol. Chem.* **392,** 751–761 (2011).

206. Kim, M. S., Froese, C. D., Xie, H. & Trimble, W. S. Uncovering principles that control septin-septin interactions. *Journal of Biological Chemistry* **287,** 30406–30413 (2012).

207. Kinoshita, M., Field, C. M., Coughlin, M. L., Straight, A. F. & Mitchison, T. J. Self- and actin-templated assembly of mammalian septins. *Dev. Cell* **3,** 791–802 (2002).

208. Tooley, A. J. *et al.* Amoeboid T lymphocytes require the septin cytoskeleton for cortical integrity and persistent motility. *Nat. Cell Biol.* **11,** 17–26 (2009).

209. Ageta-Ishihara, N. *et al.* Septins promote dendrite and axon development by negatively regulating microtubule stability via HDAC6-mediated deacetylation. *Nat Commun* **4,** 2532 (2013).

210. Menon, M. B. *et al.* Genetic deletion of SEPT7 reveals a cell type-specific role of septins in microtubule destabilization for the completion of cytokinesis. *PLoS Genet* **10,** e1004558 (2014).

211. Bertin, A. *et al.* Three-dimensional ultrastructure of the septin filament network in Saccharomyces cerevisiae. *Mol. Biol. Cell* **23,** 423–432 (2012).

212. McMurray, M. A. & Thorner, J. Septin Stability and Recycling during Dynamic Structural Transitions in Cell Division and Development. *Curr. Biol.* **18,** 1203–1208 (2008).

213. McMurray, M. A. *et al.* Septin Filament Formation Is Essential in Budding Yeast. *Dev. Cell* **20,** 540–549 (2011).

214. Leipe, D. D., Wolf, Y. I., Koonin, E. V. & Aravind, L. Classification and evolution of P-loop GTPases and related ATPases. *J. Mol. Biol.* **317,** 41–72 (2002).

215. Field, C. M. *et al.* A purified Drosophila septin complex forms filaments and exhibits GTPase activity. *J. Cell Biol.* **133,** 605–616 (1996).

216. Vrabioiu, A. M., Gerber, S. A., Gygi, S. P., Field, C. M. & Mitchison, T. J. The majority of the Saccharomyces cerevisiae septin complexes do not exchange guanine nucleotides. *J. Biol. Chem.* **279,** 3111–3118 (2004).

217. Farkasovsky, M., Herter, P., Voß, B. & Wittinghofer, A. Nucleotide binding and filament assembly of recombinant yeast septin complexes. *Biol. Chem.* **386,** 643–656 (2005).

218. Sirajuddin, M. *et al.* Structural insight into filament formation by mammalian septins. *Nature* **449,** 311–315 (2007).

219. John, C. M. *et al.* The Caenorhabditis elegans septin complex is nonpolar. *EMBO J.* **26,** 3296–3307 (2007).

220. DeMay, B. S. *et al.* Septin filaments exhibit a dynamic, paired organization that is conserved from yeast to mammals. *J. Cell Biol.* **193,** 1065–1081 (2011).

221. Hagiwara, A. *et al.* Submembranous septins as relatively stable components of actin-based membrane skeleton. *Cytoskeleton (Hoboken)* **68,** 512–525 (2011).

222. Gilden, J. K., Peck, S., Chen, Y.-C. M. & Krummel, M. F. The septin cytoskeleton facilitates membrane retraction during motility and blebbing. *J. Cell Biol.* **196,** 103–114 (2012).

223. Joo, E., Surka, M. C. & Trimble, W. S. Mammalian SEPT2 is required for scaffolding nonmuscle myosin II and its kinases. *Dev. Cell* **13,** 677–690 (2007).

224. Oegema, K., Savoian, M. S., Mitchison, T. J. & Field, C. M. Functional analysis of a human homologue of the Drosophila actin binding protein anillin suggests a role in

cytokinesis. *J. Cell Biol.* **150,** 539–552 (2000).

225. Kechad, A., Jananji, S., Ruella, Y. & Hickson, G. R. X. Anillin Acts as a Bifunctional Linker Coordinating Midbody Ring Biogenesis during Cytokinesis. *Current Biology* **22,** 197–203 (2012).

226. Founounou, N., Loyer, N. & Le Borgne, R. Septins regulate the contractility of the actomyosin ring to enable adherens junction remodeling during cytokinesis of epithelial cells. *Dev. Cell* **24,** 242–255 (2013).

227. Mostowy, S. *et al.* Entrapment of intracytosolic bacteria by septin cage-like structures. *Cell Host Microbe* **8,** 433–444 (2010).

228. Mavrakis, M. *et al.* Septins promote F-actin ring formation by crosslinking actin filaments into curved bundles. *Nat. Cell Biol.* **16,** 322–334 (2014).

229. Nagata, K.-I. *et al.* Filament formation of MSF-A, a mammalian septin, in human mammary epithelial cells depends on interactions with microtubules. *J. Biol. Chem.* **278,** 18538–18543 (2003).

230. Sellin, M. E., Holmfeldt, P., Stenmark, S. & Gullberg, M. Microtubules support a disk-like septin arrangement at the plasma membrane of mammalian cells. *Mol. Biol. Cell* **22,** 4588–4601 (2011).

231. Surka, M. C., Tsang, C. W. & Trimble, W. S. The mammalian septin MSF localizes with microtubules and is required for completion of cytokinesis. *Mol. Biol. Cell* **13,** 3532–3545 (2002).

232. Bowen, J. R., Hwang, D., Bai, X., Roy, D. & Spiliotis, E. T. Septin GTPases spatially guide microtubule organization and plus end dynamics in polarizing epithelia. *J. Cell Biol.* **194,** 187–197 (2011).

233. Kremer, B. E., Haystead, T. & Macara, I. G. Mammalian septins regulate microtubule stability through interaction with the microtubule-binding protein MAP4. *Mol. Biol. Cell* **16,** 4648–4659 (2005).

234. Bertin, A. *et al.* Phosphatidylinositol-4,5-bisphosphate promotes budding yeast septin filament assembly and organization. *J. Mol. Biol.* **404,** 711–731 (2010).

235. Tanaka-Takiguchi, Y., Kinoshita, M. & Takiguchi, K. Septin-mediated uniform bracing of phospholipid membranes. *Curr. Biol.* **19,** 140–145 (2009).

236. Bridges, A. A., Jentzsch, M. S., Oakes, P. W., Occhipinti, P. & Gladfelter, A. S. Micron-scale plasma membrane curvature is recognized by the septin cytoskeleton. *J. Cell Biol.* **213,** 23–32 (2016).

237. Lobato-Márquez, D. & Mostowy, S. Septins recognize micron-scale membrane curvature. *J. Cell Biol.* **213,** 5–6 (2016).

238. Shindo, A. & Wallingford, J. B. PCP and septins compartmentalize cortical actomyosin to direct collective cell movement. *Science* **343,** 649–652 (2014).

239. Mostowy, S. *et al.* A role for septins in the interaction between the Listeria monocytogenes INVASION PROTEIN InlB and the Met receptor. *Biophys. J.* **100,** 1949–1959 (2011).

240. Kim, S. K. *et al.* Planar cell polarity acts through septins to control collective cell movement and ciliogenesis. *Science* **329,** 1337–1340 (2010).

241. Ihara, M. *et al.* Cortical organization by the septin cytoskeleton is essential for structural and mechanical integrity of mammalian spermatozoa. *Dev. Cell* **8,** 343–352 (2005).

242. Caudron, F. & Barral, Y. Septins and the lateral compartmentalization of eukaryotic membranes. *Dev. Cell* **16,** 493–506 (2009).

243. Takizawa, P. A., DeRisi, J. L., Wilhelm, J. E. & Vale, R. D. Plasma membrane compartmentalization in yeast by messenger RNA transport and a septin diffusion barrier. *Science* **290,** 341–344 (2000).

244. Hu, Q. *et al.* A septin diffusion barrier at the base of the primary cilium maintains ciliary membrane protein distribution. *Science* **329,** 436–439 (2010).

245. Chih, B. *et al.* A ciliopathy complex at the transition zone protects the cilia as a privileged membrane domain. *Nat. Cell Biol.* **14,** 61–72 (2011).

246. Shen, Y.-R. *et al.* SEPT12 phosphorylation results in loss of the septin ring/sperm annulus, defective sperm motility and poor male fertility. *PLoS Genet* **13,** e1006631 (2017).

247. Koch, S., Acebron, S. P., Herbst, J., Hatiboglu, G. & Niehrs, C. Post-transcriptional Wnt Signaling Governs Epididymal Sperm Maturation. *Cell* **163,** 1225–1236 (2015).

248. Tada, T. *et al.* Role of Septin cytoskeleton in spine morphogenesis and dendrite development in neurons. *Current Biology* **17,** 1752–1758 (2007).

249. Xie, Y. *et al.* The GTP-binding protein Septin 7 is critical for dendrite branching and dendritic-spine morphology. *Current Biology* **17,** 1746–1751 (2007).

250. Ewers, H. *et al.* A Septin-Dependent Diffusion Barrier at Dendritic Spine Necks. *PLoS ONE* **9,** e113916 (2014).

251. Kinoshita, N. *et al.* Mammalian septin Sept2 modulates the activity of GLAST, a glutamate transporter in astrocytes. *Genes Cells* **9,** 1–14 (2004).

252. Ageta-Ishihara, N. *et al.* A CDC42EP4/septin-based perisynaptic glial scaffold facilitates glutamate clearance. *Nat Commun* **6,** 10090 (2015).

253. Sharma, S. *et al.* An siRNA screen for NFAT activation identifies septins as coordinators of store-operated $Ca2^{+}$ entry. *Nature* **499,** 238–242 (2013).

254. Ozsarac, N., Bhattacharyya, M., Dawes, I. W. & Clancy, M. J. The SPR3 gene encodes a sporulation-specific homologue of the yeast CDC3/10/11/12 family of bud neck

microfilaments and is regulated by ABFI. *Gene* **164,** 157–162 (1995).

255. De Virgilio, C., DeMarini, D. J. & Pringle, J. R. SPR28, a sixth member of the septin gene family in Saccharomyces cerevisiae that is expressed specifically in sporulating cells. *Microbiology (Reading, Engl.)* **142 (Pt 10),** 2897–2905 (1996).

256. Garcia, G. *et al.* Assembly, molecular organization, and membrane-binding properties of development-specific septins. *J. Cell Biol.* **212,** 515–529 (2016).

257. Chu, S. *et al.* The transcriptional program of sporulation in budding yeast. *Science* **282,** 699–705 (1998).

258. Gladfelter, A. S., Bose, I., Zyla, T. R., Bardes, E. S. G. & Lew, D. J. Septin ring assembly involves cycles of GTP loading and hydrolysis by Cdc42p. *J. Cell Biol.* **156,** 315–326 (2002).

259. Caviston, J. P., Longtine, M., Pringle, J. R. & Bi, E. The role of Cdc42p GTPase-activating proteins in assembly of the septin ring in yeast. *Mol. Biol. Cell* **14,** 4051–4066 (2003).

260. Iwase, M. *et al.* Role of a Cdc42p effector pathway in recruitment of the yeast septins to the presumptive bud site. *Mol. Biol. Cell* **17,** 1110–1125 (2006).

261. Vrabioiu, A. M. & Mitchison, T. J. Structural insights into yeast septin organization from polarized fluorescence microscopy. *Nature* **443,** 466–469 (2006).

262. Ong, K., Wloka, C., Okada, S., Svitkina, T. & Bi, E. Architecture and dynamic remodelling of the septin cytoskeleton during the cell cycle. *Nat Commun* **5,** 5698 (2014).

263. Glomb, O. & Gronemeyer, T. Septin Organization and Functions in Budding Yeast. *Front Cell Dev Biol* **4,** 123 (2016).

264. Gladfelter, A. S., Pringle, J. R. & Lew, D. J. The septin cortex at the yeast mother-bud neck. *Curr. Opin. Microbiol.* **4,** 681–689 (2001).

265. Kim, H. B., Haarer, B. K. & Pringle, J. R. Cellular morphogenesis in the Saccharomyces cerevisiae cell cycle: localization of the CDC3 gene product and the timing of events at the budding site. *J. Cell Biol.* **112,** 535–544 (1991).

266. Lippincott, J., Shannon, K. B., Shou, W., Deshaies, R. J. & Li, R. The Tem1 small GTPase controls actomyosin and septin dynamics during cytokinesis. *J. Cell. Sci.* **114,** 1379–1386 (2001).

267. Roh, D.-H., Bowers, B., Schmidt, M. & Cabib, E. The septation apparatus, an autonomous system in budding yeast. *Mol. Biol. Cell* **13,** 2747–2759 (2002).

268. Chant, J., Mischke, M., Mitchell, E., Herskowitz, I. & Pringle, J. R. Role of Bud3p in producing the axial budding pattern of yeast. *J. Cell Biol.* **129,** 767–778 (1995).

269. Sanders, S. L. & Herskowitz, I. The BUD4 protein of yeast, required for axial budding, is

localized to the mother/BUD neck in a cell cycle-dependent manner. *J. Cell Biol.* **134,** 413–427 (1996).

270. Orlando, K. *et al.* Exo-endocytic trafficking and the septin-based diffusion barrier are required for the maintenance of Cdc42p polarization during budding yeast asymmetric growth. *Mol. Biol. Cell* **22,** 624–633 (2011).

271. Longtine, M. S. *et al.* Septin-dependent assembly of a cell cycle-regulatory module in Saccharomyces cerevisiae. *Mol. Cell. Biol.* **20,** 4049–4061 (2000).

272. Carroll, C. W., Altman, R., Schieltz, D., Yates, J. R. & Kellogg, D. The septins are required for the mitosis-specific activation of the Gin4 kinase. *J. Cell Biol.* **143,** 709–717 (1998).

273. Barral, Y., Parra, M., Bidlingmaier, S. & Snyder, M. Nim1-related kinases coordinate cell cycle progression with the organization of the peripheral cytoskeleton in yeast. *Genes Dev.* **13,** 176–187 (1999).

274. DeMarini, D. J. *et al.* A septin-based hierarchy of proteins required for localized deposition of chitin in the Saccharomyces cerevisiae cell wall. *J. Cell Biol.* **139,** 75–93 (1997).

275. Longtine, M. S. *et al.* The septins: roles in cytokinesis and other processes. *Curr. Opin. Cell Biol.* **8,** 106–119 (1996).

276. Schneider, C., Grois, J., Renz, C., Gronemeyer, T. & Johnsson, N. Septin rings act as a template for myosin higher-order structures and inhibit redundant polarity establishment. *J. Cell. Sci.* **126,** 3390–3400 (2013).

277. Bi, E. *et al.* Involvement of an actomyosin contractile ring in Saccharomyces cerevisiae cytokinesis. *J. Cell Biol.* **142,** 1301–1312 (1998).

278. Lippincott, J. & Li, R. Sequential assembly of myosin II, an IQGAP-like protein, and filamentous actin to a ring structure involved in budding yeast cytokinesis. *J. Cell Biol.* **140,** 355–366 (1998).

279. Barral, Y., Mermall, V., Mooseker, M. S. & Snyder, M. Compartmentalization of the cell cortex by septins is required for maintenance of cell polarity in yeast. *Mol. Cell* **5,** 841–851 (2000).

280. Shcheprova, Z., Baldi, S., Frei, S. B., Gonnet, G. & Barral, Y. A mechanism for asymmetric segregation of age during yeast budding. *Nature* **454,** 728–734 (2008).

281. Neufeld, T. P. & Rubin, G. M. The Drosophila peanut gene is required for cytokinesis and encodes a protein similar to yeast putative bud neck filament proteins. *Cell* **77,** 371–379 (1994).

282. Adam, J. C., Pringle, J. R. & Peifer, M. Evidence for functional differentiation among Drosophila septins in cytokinesis and cellularization. *Mol. Biol. Cell* **11,** 3123–3135 (2000).

283. Nguyen, T. Q., Sawa, H., Okano, H. & White, J. G. The C. elegans septin genes, unc-59 and unc-61, are required for normal postembryonic cytokineses and morphogenesis but have no essential function in embryogenesis. *J. Cell. Sci.* **113 Pt 21,** 3825–3837 (2000).

284. Kinoshita, M. *et al.* Nedd5, a mammalian septin, is a novel cytoskeletal component interacting with actin-based structures. *Genes Dev.* **11,** 1535–1547 (1997).

285. Beites, C. L., Peng, X.-R. R. & Trimble, W. S. Expression and analysis of properties of septin CDCrel-1 in exocytosis. *Meth. Enzymol.* **329,** 499–510 (2001).

286. Estey, M. P., Di Ciano-Oliveira, C., Froese, C. D., Bejide, M. T. & Trimble, W. S. Distinct roles of septins in cytokinesis: SEPT9 mediates midbody abscission. *J. Cell Biol.* **191,** 741–749 (2010).

287. Amine, El, N., Kechad, A., Jananji, S. & Hickson, G. R. X. Opposing actions of septins and Sticky on Anillin promote the transition from contractile to midbody ring. *J. Cell Biol.* **203,** 487–504 (2013).

288. Spiliotis, E. T., Kinoshita, M. & Nelson, W. J. A mitotic septin scaffold required for Mammalian chromosome congression and segregation. *Science* **307,** 1781–1785 (2005).

289. Zhu, M. *et al.* Septin 7 interacts with centromere-associated protein E and is required for its kinetochore localization. *J. Biol. Chem.* **283,** 18916–18925 (2008).

290. Joo, E., Tsang, C. W. & Trimble, W. S. Septins: traffic control at the cytokinesis intersection. *Traffic* **6,** 626–634 (2005).

291. Menon, M. B. & Gaestel, M. Sep(t)arate or not – how some cells take septin-independent routes through cytokinesis. *J. Cell. Sci.* **128,** 1877–1886 (2015).

292. Bouquin, N. *et al.* Regulation of cytokinesis by the Elm1 protein kinase in Saccharomyces cerevisiae. *J. Cell. Sci.* **113 (Pt 8),** 1435–1445 (2000).

293. Gladfelter, A. S., Moskow, J. J., Zyla, T. R. & Lew, D. J. Isolation and characterization of effector-loop mutants of CDC42 in yeast. *Mol. Biol. Cell* **12,** 1239–1255 (2001).

294. Cid, V. J., Adamiková, L., Sánchez, M., Molina, M. & Nombela, C. Cell cycle control of septin ring dynamics in the budding yeast. *Microbiology (Reading, Engl.)* **147,** 1437–1450 (2001).

295. Egelhofer, T. A., Villén, J., McCusker, D., Gygi, S. P. & Kellogg, D. R. The septins function in G1 pathways that influence the pattern of cell growth in budding yeast. *PLoS ONE* **3,** e2022 (2008).

296. Dobbelaere, J., Gentry, M. S., Hallberg, R. L. & Barral, Y. Phosphorylation-dependent regulation of septin dynamics during the cell cycle. *Dev. Cell* **4,** 345–357 (2003).

297. Mortensen, E. M., McDonald, H., Yates, J. & Kellogg, D. R. Cell cycle-dependent assembly of a Gin4-septin complex. *Mol. Biol. Cell* **13,** 2091–2105 (2002).

298. Versele, M. & Thorner, J. Septin collar formation in budding yeast requires GTP binding and direct phosphorylation by the PAK, Cla4. *J. Cell Biol.* **164,** 701–715 (2004).

299. Johnson, E. S. & Blobel, G. Cell cycle-regulated attachment of the ubiquitin-related protein SUMO to the yeast septins. *J. Cell Biol.* **147,** 981–994 (1999).

300. Johnson, E. S. & Gupta, A. A. An E3-like factor that promotes SUMO conjugation to the yeast septins. *Cell* **106,** 735–744 (2001).

301. Zhang, Y. *et al.* Parkin functions as an E2-dependent ubiquitin- protein ligase and promotes the degradation of the synaptic vesicle-associated protein, CDCrel-1. *Proc. Natl. Acad. Sci. U.S.A.* **97,** 13354–13359 (2000).

302. Ageta-Ishihara, N. *et al.* Chronic overload of SEPT4, a parkin substrate that aggregates in Parkinson's disease, causes behavioral alterations but not neurodegeneration in mice. *Mol Brain* **6,** 35 (2013).

303. Joberty, G. *et al.* Borg proteins control septin organization and are negatively regulated by Cdc42. *Nat. Cell Biol.* **3,** 861–866 (2001).

304. Peterson, E. A. & Petty, E. M. Conquering the complex world of human septins: implications for health and disease. *Clin. Genet.* **77,** 511–524 (2010).

305. Angelis, D. & Spiliotis, E. T. Septin Mutations in Human Cancers. *Front Cell Dev Biol* **4,** 122 (2016).

306. Hogquist, K. A. & Jameson, S. C. The self-obsession of T cells: how TCR signaling thresholds affect fate 'decisions' and effector function. *Nat Immunol* **15,** 815–823 (2014).

307. Murali-Krishna, K. *et al. In vivo* dynamics of anti-viral CD8 T cell responses to different epitopes. An evaluation of bystander activation in primary and secondary responses to viral infection. *Adv. Exp. Med. Biol.* **452,** 123–142 (1998).

308. Zehn, D., Lee, S. Y. & Bevan, M. J. Complete but curtailed T-cell response to very low-affinity antigen. *Nature* **458,** 211–214 (2009).

309. Miller, M. J., Safrina, O., Parker, I. & Cahalan, M. D. Imaging the single cell dynamics of $CD4^+$ T cell activation by dendritic cells in lymph nodes. *J. Exp. Med.* **200,** 847–856 (2004).

310. Ehl, S., Hombach, J., Aichele, P., Hengartner, H. & Zinkernagel, R. M. Bystander activation of cytotoxic T cells: studies on the mechanism and evaluation of *in vivo* significance in a transgenic mouse model. *J. Exp. Med.* **185,** 1241–1251 (1997).

311. Nigg, E. A. Mitotic kinases as regulators of cell division and its checkpoints. *Nat. Rev. Mol. Cell Biol.* **2,** 21–32 (2001).

312. Oh, Y. & Bi, E. Septin structure and function in yeast and beyond. *Trends Cell Biol.* **21,** 141–148 (2011).

313. Estey, M. P. *et al.* Mitotic regulation of SEPT9 protein by cyclin-dependent kinase 1 (Cdk1) and Pin1 protein is important for the completion of cytokinesis. *Journal of Biological Chemistry* **288,** 30075–30086 (2013).

314. Kinoshita, M. Assembly of mammalian septins. *J. Biochem.* **134,** 491–496 (2003).

315. Rodal, A. A., Kozubowski, L., Goode, B. L., Drubin, D. G. & Hartwig, J. H. Actin and septin ultrastructures at the budding yeast cell cortex. *Mol. Biol. Cell* **16,** 372–384 (2005).

316. Muzumdar, M. D., Tasic, B., Miyamichi, K., Li, L. & Luo, L. A global double-fluorescent Cre reporter mouse. *Genesis* **45,** 593–605 (2007).

317. Lee, P. P. *et al.* A critical role for Dnmt1 and DNA methylation in T cell development, function, and survival. *Immunity* **15,** 763–774 (2001).

318. Cho, J.-H. *et al.* Unique features of naive $CD8^+$ T cell activation by IL-2. *The Journal of Immunology* **191,** 5559–5573 (2013).

319. Bonifaz, L. C. *et al. In vivo* targeting of antigens to maturing dendritic cells via the DEC-205 receptor improves T cell vaccination. *J. Exp. Med.* **199,** 815–824 (2004).

320. Kieper, W. C. & Jameson, S. C. Homeostatic expansion and phenotypic conversion of naïve T cells in response to self peptide/MHC ligands. *Proc. Natl. Acad. Sci. U.S.A.* **96,** 13306–13311 (1999).

321. Sprent, J. & Surh, C. D. Normal T cell homeostasis: the conversion of naive cells into memory-phenotype cells. *Nat Immunol* **12,** 478–484 (2011).

322. Choo, D. K., Murali-Krishna, K., Anita, R. & Ahmed, R. Homeostatic turnover of virus-specific memory CD8 T cells occurs stochastically and is independent of CD4 T cell help. *The Journal of Immunology* **185,** 3436–3444 (2010).

323. Wu, Z. *et al.* Homeostatic proliferation is a barrier to transplantation tolerance. *Nat Med* **10,** 87–92 (2004).

324. Monti, P. & Piemonti, L. Homeostatic T cell proliferation after islet transplantation. *Clin. Dev. Immunol.* **2013,** 217934 (2013).

325. Khoruts, A. & Fraser, J. M. A causal link between lymphopenia and autoimmunity. *Immunol. Lett.* **98,** 23–31 (2005).

326. Gattinoni, L. *et al.* Removal of homeostatic cytokine sinks by lymphodepletion enhances the efficacy of adoptively transferred tumor-specific $CD8^+$ T cells. *J. Exp. Med.* **202,** 907–912 (2005).

327. Tchao, N. K. & Turka, L. A. Lymphodepletion and homeostatic proliferation: implications for transplantation. *Am. J. Transplant.* **12,** 1079–1090 (2012).

328. Kitchin, J. E., Pomeranz, M. K., Pak, G., Washenik, K. & Shupack, J. L. Rediscovering

mycophenolic acid: a review of its mechanism, side effects, and potential uses. *J. Am. Acad. Dermatol.* **37,** 445–449 (1997).

329. Stoll, S., Delon, J., Brotz, T. M. & Germain, R. N. Dynamic imaging of T cell-dendritic cell interactions in lymph nodes. *Science* **296,** 1873–1876 (2002).

330. Saarikangas, J. & Barral, Y. The emerging functions of septins in metazoans. *EMBO J.* **12,** 1118–1126 (2011).

331. Field, S. J. *et al.* PtdIns(4,5)P2 functions at the cleavage furrow during cytokinesis. *Current Biology* **15,** 1407–1412 (2005).

332. Janetopoulos, C. & Devreotes, P. Phosphoinositide signaling plays a key role in cytokinesis. *J. Cell Biol.* **174,** 485–490 (2006).

333. Costello, P. S., Gallagher, M. & Cantrell, D. A. Sustained and dynamic inositol lipid metabolism inside and outside the immunological synapse. *Nat Immunol* **3,** 1082–1089 (2002).

334. Maléth, J., Choi, S., Muallem, S. & Ahuja, M. Translocation between PI(4,5)P2-poor and PI(4,5)P2-rich microdomains during store depletion determines STIM1 conformation and Orai1 gating. *Nat Commun* **5,** 5843 (2014).

335. Dubois, S., Mariner, J., Waldmann, T. A. & Tagaya, Y. IL-15Ralpha recycles and presents IL-15 In trans to neighboring cells. *Immunity* **17,** 537–547 (2002).

336. Hogquist, K. A. *et al.* T cell receptor antagonist peptides induce positive selection. *Cell* **76,** 17–27 (1994).

337. Mildner, A. & Jung, S. Development and Function of Dendritic Cell Subsets. *Immunity* **40,** 642–656 (2014).

338. Chen, D. S. & Mellman, I. Oncology Meets Immunology: The Cancer-Immunity Cycle. *Immunity* **39,** 1–10 (2013).

339. Gardner, A. & Ruffell, B. Dendritic Cells and Cancer Immunity. *Trends Immunol.* **37,** 855–865 (2016).

340. Ladányi, A. *et al.* Density of DC-LAMP($^{+}$) mature dendritic cells in combination with activated T lymphocytes infiltrating primary cutaneous melanoma is a strong independent prognostic factor. *Cancer Immunol. Immunother.* **56,** 1459–1469 (2007).

341. Iwamoto, M. *et al.* Prognostic value of tumor-infiltrating dendritic cells expressing CD83 in human breast carcinomas. *Int. J. Cancer* **104,** 92–97 (2003).

342. Broz, M. L. *et al.* Dissecting the Tumor Myeloid Compartment Reveals Rare Activating Antigen-Presenting Cells Critical for T Cell Immunity. *Cancer Cell* **26,** 638–652 (2014).

343. Roberts, E. W. *et al.* Critical Role for CD103($^{+}$)/CD141($^{+}$) Dendritic Cells Bearing CCR7 for Tumor Antigen Trafficking and Priming of T Cell Immunity in Melanoma. *Cancer Cell* **30,** 324–336 (2016).

344. Motz, G. T. & Coukos, G. Deciphering and reversing tumor immune suppression. *Immunity* **39,** 61–73 (2013).

345. Hodi, F. S. *et al.* Improved survival with ipilimumab in patients with metastatic melanoma. *N. Engl. J. Med.* **363,** 711–723 (2010).

346. Topalian, S. L. *et al.* Safety, activity, and immune correlates of anti-PD-1 antibody in cancer. *N. Engl. J. Med.* **366,** 2443–2454 (2012).

347. Wolchok, J. D. *et al.* Nivolumab plus ipilimumab in advanced melanoma. *N. Engl. J. Med.* **369,** 122–133 (2013).

348. Pitt, J. M. *et al.* Resistance Mechanisms to Immune-Checkpoint Blockade in Cancer: Tumor-Intrinsic and -Extrinsic Factors. *Immunity* **44,** 1255–1269 (2016).

349. Sharma, P., Hu-Lieskovan, S., Wargo, J. A. & Ribas, A. Primary, Adaptive, and Acquired Resistance to Cancer Immunotherapy. *Cell* **168,** 707–723 (2017).

350. Salmon, H. *et al.* Expansion and Activation of $CD103^+$ Dendritic Cell Progenitors at the Tumor Site Enhances Tumor Responses to Therapeutic PD-L1 and BRAF Inhibition. *Immunity* **44,** 924–938 (2016).

351. Wang, H. *et al.* cGAS is essential for the antitumor effect of immune checkpoint blockade. *Proceedings of the National Academy of Sciences* **114,** 1637–1642 (2017).

352. Duraiswamy, J., Kaluza, K. M., Freeman, G. J. & Coukos, G. Dual blockade of PD-1 and CTLA-4 combined with tumor vaccine effectively restores T-cell rejection function in tumors. *Cancer Res.* **73,** 3591–3603 (2013).

353. Merad, M., Sathe, P., Helft, J., Miller, J. & Mortha, A. The dendritic cell lineage: ontogeny and function of dendritic cells and their subsets in the steady state and the inflamed setting. *Annu. Rev. Immunol.* **31,** 563–604 (2013).

354. Guilliams, M. *et al.* Dendritic cells, monocytes and macrophages: a unified nomenclature based on ontogeny. *Nat. Rev. Immunol.* **14,** 571–578 (2014).

355. Murphy, T. L. *et al.* Transcriptional Control of Dendritic Cell Development. *Annu. Rev. Immunol.* **34,** 93–119 (2016).

356. Guilliams, M. *et al.* Unsupervised High-Dimensional Analysis Aligns Dendritic Cells across Tissues and Species. *Immunity* **45,** 669–684 (2016).

357. Movahedi, K. *et al.* Different tumor microenvironments contain functionally distinct subsets of macrophages derived from Ly6C(high) monocytes. *Cancer Res.* **70,** 5728–5739 (2010).

358. Lavin, Y. *et al.* Innate Immune Landscape in Early Lung Adenocarcinoma by Paired Single-Cell Analyses. *Cell* **169,** 750–765.e17 (2017).

359. Haan, den, J. M., Lehar, S. M. & Bevan, M. J. $CD8(^+)$ but not CD8(-) dendritic cells

cross-prime cytotoxic T cells *in vivo*. *J. Exp. Med.* **192,** 1685–1696 (2000).

360. Belz, G. T., Shortman, K., Bevan, M. J. & Heath, W. R. CD8alpha$^+$ dendritic cells selectively present MHC class I-restricted noncytolytic viral and intracellular bacterial antigens *in vivo*. *J. Immunol.* **175,** 196–200 (2005).

361. Hildner, K. *et al.* Batf3 deficiency reveals a critical role for CD8alpha$^+$ dendritic cells in cytotoxic T cell immunity. *Science* **322,** 1097–1100 (2008).

362. Bedoui, S. *et al.* Cross-presentation of viral and self antigens by skin-derived CD103$^+$ dendritic cells. *Nat Immunol* **10,** 488–495 (2009).

363. Edelson, B. T. *et al.* Peripheral CD103$^+$ dendritic cells form a unified subset developmentally related to CD8alpha$^+$ conventional dendritic cells. *Journal of Experimental Medicine* **207,** 823–836 (2010).

364. Miller, J. C. *et al.* Deciphering the transcriptional network of the dendritic cell lineage. *Nat Immunol* **13,** 888–899 (2012).

365. Schiavoni, G. *et al.* ICSBP is essential for the development of mouse type I interferon-producing cells and for the generation and activation of CD8alpha(+) dendritic cells. *J. Exp. Med.* **196,** 1415–1425 (2002).

366. Ginhoux, F. *et al.* The origin and development of nonlymphoid tissue CD103$^+$ DCs. *Journal of Experimental Medicine* **206,** 3115–3130 (2009).

367. Hacker, C. *et al.* Transcriptional profiling identifies Id2 function in dendritic cell development. *Nat Immunol* **4,** 380–386 (2003).

368. Kashiwada, M., Pham, N.-L. L., Pewe, L. L., Harty, J. T. & Rothman, P. B. NFIL3/E4BP4 is a key transcription factor for CD8α□ dendritic cell development. *Blood* **117,** 6193–6197 (2011).

369. Seillet, C. *et al.* CD8α$^+$ DCs can be induced in the absence of transcription factors Id2, Nfil3, and Batf3. *Blood* **121,** 1574–1583 (2013).

370. Tussiwand, R. *et al.* Compensatory dendritic cell development mediated by BATF-IRF interactions. *Nature* **490,** 502–507 (2012).

371. Bachem, A. *et al.* Superior antigen cross-presentation and XCR1 expression define human CD11c$^+$CD141$^+$ cells as homologues of mouse CD8$^+$ dendritic cells. *Journal of Experimental Medicine* **207,** 1273–1281 (2010).

372. Haniffa, M. *et al.* Human Tissues Contain CD141hi Cross-Presenting Dendritic Cells with Functional Homology to Mouse CD103$^+$ Nonlymphoid Dendritic Cells. *Immunity* **37,** 60–73 (2012).

373. Suzuki, S. *et al.* Critical roles of interferon regulatory factor 4 in CD11bhighCD8alpha-dendritic cell development. *Proc. Natl. Acad. Sci. U.S.A.* **101,** 8981–8986 (2004).

374. Tamura, T. *et al.* IFN regulatory factor-4 and -8 govern dendritic cell subset

development and their functional diversity. *J. Immunol.* **174,** 2573–2581 (2005).

375. Scott, C. L. *et al.* The transcription factor Zeb2 regulates development of conventional and plasmacytoid DCs by repressing Id2. *Journal of Experimental Medicine* **213,** 897–911 (2016).

376. Lewis, K. L. *et al.* Notch2 Receptor Signaling Controls Functional Differentiation of Dendritic Cells in the Spleen and Intestine. *Immunity* **35,** 780–791 (2011).

377. Wu, L. *et al.* RelB is essential for the development of myeloid-related CD8alpha- dendritic cells but not of lymphoid-related CD8alpha$^+$ dendritic cells. *Immunity* **9,** 839–847 (1998).

378. Kobayashi, T. *et al.* TRAF6 Is a Critical Factor for Dendritic Cell Maturation and Development. *Immunity* **19,** 353–363 (2003).

379. Jaitin, D. A. *et al.* Massively parallel single-cell RNA-seq for marker-free decomposition of tissues into cell types. *Science* **343,** 776–779 (2014).

380. Tussiwand, R. *et al.* Klf4 expression in conventional dendritic cells is required for T helper 2 cell responses. *Immunity* **42,** 916–928 (2015).

381. Tamoutounour, S. *et al.* Origins and functional specialization of macrophages and of conventional and monocyte-derived dendritic cells in mouse skin. *Immunity* **39,** 925–938 (2013).

382. Schlitzer, A. *et al.* IRF4 Transcription Factor-Dependent CD11b$^+$ Dendritic Cells in Human and Mouse Control Mucosal IL-17 Cytokine Responses. *Immunity* **38,** 970–983 (2013).

383. Granot, T. *et al.* Dendritic Cells Display Subset and Tissue-Specific Maturation Dynamics over Human Life. *Immunity* **46,** 504–515 (2017).

384. Villani, A.-C. *et al.* Single-cell RNA-seq reveals new types of human blood dendritic cells, monocytes, and progenitors. *Science* **356,** eaah4573–14 (2017).

385. Schlitzer, A. *et al.* Identification of cDC1- and cDC2-committed DC progenitors reveals early lineage priming at the common DC progenitor stage in the bone marrow. *Nat Immunol* **16,** 718–728 (2015).

386. Breton, G. *et al.* Circulating precursors of human CD1c$^+$ and CD141$^+$ dendritic cells. *Journal of Experimental Medicine* **212,** 401–413 (2015).

387. See, P. *et al.* Mapping the human DC lineage through the integration of high-dimensional techniques. *Science* **356,** (2017).

388. Liu, K. *et al. In vivo* analysis of dendritic cell development and homeostasis. *Science* **324,** 392–397 (2009).

389. Waskow, C. *et al.* The receptor tyrosine kinase Flt3 is required for dendritic cell development in peripheral lymphoid tissues. *Nature Reviews Immunology* **9,** 676–683

(2008).

390. Vremec, D. *et al.* The influence of granulocyte/macrophage colony-stimulating factor on dendritic cell levels in mouse lymphoid organs. *Eur. J. Immunol.* **27,** 40–44 (1997).

391. Greter, M. *et al.* GM-CSF Controls Nonlymphoid Tissue Dendritic Cell Homeostasis but Is Dispensable for the Differentiation of Inflammatory Dendritic Cells. *Immunity* **36,** 1031–1046 (2012).

392. Sathe, P. *et al.* The acquisition of antigen cross-presentation function by newly formed dendritic cells. *The Journal of Immunology* **186,** 5184–5192 (2011).

393. Diao, J., Zhao, J., Winter, E. & Cattral, M. S. Recruitment and differentiation of conventional dendritic cell precursors in tumors. *The Journal of Immunology* **184,** 1261–1267 (2010).

394. Jensen, T. O. *et al.* Intratumoral neutrophils and plasmacytoid dendritic cells indicate poor prognosis and are associated with pSTAT3 expression in AJCC stage I/II melanoma. *Cancer* **118,** 2476–2485 (2012).

395. Treilleux, I. *et al.* Dendritic cell infiltration and prognosis of early stage breast cancer. *Clin. Cancer Res.* **10,** 7466–7474 (2004).

396. Swiecki, M. & Colonna, M. The multifaceted biology of plasmacytoid dendritic cells. *Nat. Rev. Immunol.* **15,** 471–485 (2015).

397. Segura, E. & Amigorena, S. Inflammatory dendritic cells in mice and humans. *Trends Immunol.* **34,** 440–445 (2013).

398. Varol, C. *et al.* Intestinal Lamina Propria Dendritic Cell Subsets Have Different Origin and Functions. *Immunity* **31,** 502–512 (2009).

399. Bogunovic, M. *et al.* Origin of the Lamina Propria Dendritic Cell Network. *Immunity* **31,** 513–525 (2009).

400. Langlet, C. *et al.* CD64 expression distinguishes monocyte-derived and conventional dendritic cells and reveals their distinct role during intramuscular immunization. *The Journal of Immunology* **188,** 1751–1760 (2012).

401. Aldridge, J. R. *et al.* TNF/iNOS-producing dendritic cells are the necessary evil of lethal influenza virus infection. *Proceedings of the National Academy of Sciences* **106,** 5306–5311 (2009).

402. Iijima, N., Linehan, M. M., Saeland, S. & Iwasaki, A. Vaginal epithelial dendritic cells renew from bone marrow precursors. *Proceedings of the National Academy of Sciences* **104,** 19061–19066 (2007).

403. León, B., López-Bravo, M. & Ardavín, C. Monocyte-derived dendritic cells formed at the infection site control the induction of protective T helper 1 responses against Leishmania. *Immunity* **26,** 519–531 (2007).

404. Serbina, N. V., Salazar-Mather, T. P., Biron, C. A., Kuziel, W. A. & Pamer, E. G. TNF/iNOS-producing dendritic cells mediate innate immune defense against bacterial infection. *Immunity* **19,** 59–70 (2003).

405. Cheong, C. *et al.* Microbial stimulation fully differentiates monocytes to DC-SIGN/CD209(+) dendritic cells for immune T cell areas. *Cell* **143,** 416–429 (2010).

406. Kool, M. *et al.* Alum adjuvant boosts adaptive immunity by inducing uric acid and activating inflammatory dendritic cells. *Journal of Experimental Medicine* **205,** 869–882 (2008).

407. Nakano, H. *et al.* Blood-derived inflammatory dendritic cells in lymph nodes stimulate acute T helper type 1 immune responses. *Nature Reviews Immunology* **10,** 394–402 (2009).

408. Laoui, D. *et al.* The tumour microenvironment harbours ontogenically distinct dendritic cell populations with opposing effects on tumour immunity. *Nat Commun* **7,** 13720 (2016).

409. Segura, E. *et al.* Human inflammatory dendritic cells induce Th17 cell differentiation. *Immunity* **38,** 336–348 (2013).

410. Ma, Y. *et al.* Anticancer Chemotherapy-Induced Intratumoral Recruitment and Differentiation of Antigen-Presenting Cells. *Immunity* **38,** 729–741 (2013).

411. Satpathy, A. T. *et al.* Zbtb46 expression distinguishes classical dendritic cells and their committed progenitors from other immune lineages. *Journal of Experimental Medicine* **209,** 1135–1152 (2012).

412. Franklin, R. A. *et al.* The cellular and molecular origin of tumor-associated macrophages. *Science* **344,** 921–925 (2014).

413. Engblom, C., Pfirschke, C. & Pittet, M. J. The role of myeloid cells in cancer therapies. *Nature Reviews Immunology* **16,** 447–462 (2016).

414. Condeelis, J. & Pollard, J. W. Macrophages: obligate partners for tumor cell migration, invasion, and metastasis. *Cell* **124,** 263–266 (2006).

415. Albert, M. L. *et al.* Immature dendritic cells phagocytose apoptotic cells via alphavbeta5 and CD36, and cross-present antigens to cytotoxic T lymphocytes. *J. Exp. Med.* **188,** 1359–1368 (1998).

416. Doedens, A. L. *et al.* Macrophage expression of hypoxia-inducible factor-1 alpha suppresses T-cell function and promotes tumor progression. *Cancer Res.* **70,** 7465–7475 (2010).

417. DeNardo, D. G. *et al.* Leukocyte complexity predicts breast cancer survival and functionally regulates response to chemotherapy. *Cancer Discov* **1,** 54–67 (2011).

418. Ruffell, B. & Coussens, L. M. Macrophages and Therapeutic Resistance in Cancer. *Cancer Cell* **27,** 462–472 (2015).

419. Mantovani, A., Sozzani, S., Locati, M., Allavena, P. & Sica, A. Macrophage polarization: tumor-associated macrophages as a paradigm for polarized M2 mononuclear phagocytes. *Trends Immunol.* **23,** 549–555 (2002).

420. Komohara, Y., Jinushi, M. & Takeya, M. Clinical significance of macrophage heterogeneity in human malignant tumors. *Cancer Sci* **105,** 1–8 (2014).

421. Gentles, A. J. *et al.* The prognostic landscape of genes and infiltrating immune cells across human cancers. *Nat Med* **21,** 938–945 (2015).

422. Haan, den, J. M. M. & Bevan, M. J. Constitutive versus activation-dependent cross-presentation of immune complexes by CD8(+) and CD8(-) dendritic cells *in vivo*. *J. Exp. Med.* **196,** 817–827 (2002).

423. Bougneres, L. *et al.* A role for lipid bodies in the cross-presentation of phagocytosed antigens by MHC class I in dendritic cells. *Immunity* **31,** 232–244 (2009).

424. Savina, A. *et al.* The small GTPase Rac2 controls phagosomal alkalinization and antigen crosspresentation selectively in CD8(+) dendritic cells. *Immunity* **30,** 544–555 (2009).

425. Schnorrer, P. *et al.* The dominant role of $CD8^+$ dendritic cells in cross-presentation is not dictated by antigen capture. *Proc. Natl. Acad. Sci. U.S.A.* **103,** 10729–10734 (2006).

426. Desch, A. N. *et al.* $CD103^+$ pulmonary dendritic cells preferentially acquire and present apoptotic cell-associated antigen. *Journal of Experimental Medicine* **208,** 1789–1797 (2011).

427. Engelhardt, J. J. *et al.* Marginating Dendritic Cells of the Tumor Microenvironment Cross-Present Tumor Antigens and Stably Engage Tumor-Specific T Cells. *Cancer Cell* **21,** 402–417 (2012).

428. Kitano, M. *et al.* Imaging of the cross-presenting dendritic cell subsets in the skin-draining lymph node. *Proceedings of the National Academy of Sciences* **113,** 1044–1049 (2016).

429. Headley, M. B. *et al.* Visualization of immediate immune responses to pioneer metastatic cells in the lung. *Nature* **531,** 513–517 (2016).

430. Spranger, S., Dai, D., Horton, B. & Gajewski, T. F. Tumor-Residing Batf3 Dendritic Cells Are Required for Effector T Cell Trafficking and Adoptive T Cell Therapy. *Cancer Cell* **31,** 711–723.e4 (2017).

431. Reis e Sousa, C. *et al. In vivo* microbial stimulation induces rapid CD40 ligand-independent production of interleukin 12 by dendritic cells and their redistribution to T cell areas. *J. Exp. Med.* **186,** 1819–1829 (1997).

432. Trinchieri, G. Interleukin-12 and the regulation of innate resistance and adaptive immunity. *Nat. Rev. Immunol.* **3,** 133–146 (2003).

433. Sánchez-Paulete, A. R. *et al.* Cancer Immunotherapy with Immunomodulatory Anti-CD137 and Anti-PD-1 Monoclonal Antibodies Requires BATF3-Dependent Dendritic Cells. *Cancer Discov* **6,** 71–79 (2016).

434. Dai, P. *et al.* Intratumoral delivery of inactivated modified vaccinia virus Ankara (iMVA) induces systemic antitumor immunity via STING and Batf3-dependent dendritic cells. *Sci Immunol* **2,** (2017).

435. Zhao, X. *et al.* Vaginal submucosal dendritic cells, but not Langerhans cells, induce protective Th1 responses to herpes simplex virus-2. *J. Exp. Med.* **197,** 153–162 (2003).

436. Gao, Y. *et al.* Control of T helper 2 responses by transcription factor IRF4-dependent dendritic cells. *Immunity* **39,** 722–732 (2013).

437. Kumamoto, Y. *et al.* CD301b dermal dendritic cells drive T helper 2 cell-mediated immunity. *Immunity* **39,** 733–743 (2013).

438. Heink, S. *et al.* Trans-presentation of IL-6 by dendritic cells is required for the priming of pathogenic TH17 cells. *Nat Immunol* **18,** 74–85 (2017).

439. Li, J., Lu, E., Yi, T. & Cyster, J. G. EBI2 augments Tfh cell fate by promoting interaction with IL-2-quenching dendritic cells. *Nature* **533,** 110–114 (2016).

440. Eickhoff, S. *et al.* Robust Anti-viral Immunity Requires Multiple Distinct T Cell-Dendritic Cell Interactions. *Cell* **162,** 1322–1337 (2015).

441. Igyártó, B. Z. *et al.* Skin-resident murine dendritic cell subsets promote distinct and opposing antigen-specific T helper cell responses. *Immunity* **35,** 260–272 (2011).

442. Laidlaw, B. J., Craft, J. E. & Kaech, S. M. The multifaceted role of CD4($^+$) T cells in CD8($^+$) T cell memory. *Nature Reviews Immunology* **16,** 102–111 (2016).

443. Bennett, S. R., Carbone, F. R., Karamalis, F., Miller, J. F. A. P. & Heath, W. R. Induction of a CD8$^+$ cytotoxic T lymphocyte response by cross-priming requires cognate CD4$^+$ T cell help. *J. Exp. Med.* **186,** 65–70 (1997).

444. Albert, M. L., Jegathesan, M. & Darnell, R. B. Dendritic cell maturation is required for the cross-tolerization of CD8$^+$ T cells. *Nat Immunol* **2,** 1010–1017 (2001).

445. Bennett, S. R. *et al.* Help for cytotoxic-T-cell responses is mediated by CD40 signalling. *Nature* **393,** 478–480 (1998).

446. Schoenberger, S. P., Toes, R. E., van der Voort, E. I., Offringa, R. & Melief, C. J. T-cell help for cytotoxic T lymphocytes is mediated by CD40-CD40L interactions. *Nature* **393,** 480–483 (1998).

447. Ridge, J. P., Di Rosa, F. & Matzinger, P. A conditioned dendritic cell can be a temporal bridge between a CD4$^+$ T-helper and a T-killer cell. *Nature* **393,** 474–478 (1998).

448. Sun, J. C. & Bevan, M. J. Defective CD8 T cell memory following acute infection without

CD4 T cell help. *Science* **300,** 339–342 (2003).

449. Sun, J. C., Williams, M. A. & Bevan, M. J. $CD4^+$ T cells are required for the maintenance, not programming, of memory $CD8^+$ T cells after acute infection. *Nat Immunol* **5,** 927–933 (2004).

450. Feau, S., Arens, R., Togher, S. & Schoenberger, S. P. Autocrine IL-2 is required for secondary population expansion of CD8(+) memory T cells. *Nat Immunol* **12,** 908–913 (2011).

451. Bos, R. & Sherman, L. A. $CD4^+$ T-cell help in the tumor milieu is required for recruitment and cytolytic function of $CD8^+$ T lymphocytes. *Cancer Res.* **70,** 8368–8377 (2010).

452. Marzo, A. L. *et al.* Tumor-specific $CD4^+$ T cells have a major 'post-licensing' role in CTL mediated anti-tumor immunity. *J. Immunol.* **165,** 6047–6055 (2000).

453. Spitzer, M. H. *et al.* Systemic Immunity Is Required for Effective Cancer Immunotherapy. *Cell* **168,** 487–502.e15 (2017).

454. Muranski, P. *et al.* Tumor-specific Th17-polarized cells eradicate large established melanoma. *Blood* **112,** 362–373 (2008).

455. Xie, Y. *et al.* Naive tumor-specific CD4(+) T cells differentiated *in vivo* eradicate established melanoma. *Journal of Experimental Medicine* **207,** 651–667 (2010).

456. Tran, E. *et al.* Cancer immunotherapy based on mutation-specific $CD4^+$ T cells in a patient with epithelial cancer. *Science* **344,** 641–645 (2014).

457. Hunder, N. N. *et al.* Treatment of metastatic melanoma with autologous $CD4^+$ T cells against NY-ESO-1. *N. Engl. J. Med.* **358,** 2698–2703 (2008).

458. Belz, G. T. *et al.* The CD8alpha(+) dendritic cell is responsible for inducing peripheral self-tolerance to tissue-associated antigens. *J. Exp. Med.* **196,** 1099–1104 (2002).

459. Griffith, T. S. *et al.* Apoptotic cells induce tolerance by generating helpless $CD8^+$ T cells that produce TRAIL. *J. Immunol.* **178,** 2679–2687 (2007).

460. Kurts, C., Kosaka, H., Carbone, F. R., Miller, J. F. A. P. & Heath, W. R. Class I-restricted cross-presentation of exogenous self-antigens leads to deletion of autoreactive CD8(+) T cells. *J. Exp. Med.* **186,** 239–245 (1997).

461. Hawiger, D. *et al.* Dendritic cells induce peripheral T cell unresponsiveness under steady state conditions *in vivo*. *J. Exp. Med.* **194,** 769–779 (2001).

462. Bonifaz, L. *et al.* Efficient targeting of protein antigen to the dendritic cell receptor DEC-205 in the steady state leads to antigen presentation on major histocompatibility complex class I products and peripheral $CD8^+$ T cell tolerance. *J. Exp. Med.* **196,** 1627–1638 (2002).

463. Idoyaga, J. *et al.* Specialized role of migratory dendritic cells in peripheral tolerance induction. *J. Clin. Invest.* **123,** 844–854 (2013).

464. Ohnmacht, C. *et al.* Constitutive ablation of dendritic cells breaks self-tolerance of CD4 T cells and results in spontaneous fatal autoimmunity. *Journal of Experimental Medicine* **206,** 549–559 (2009).

465. Baratin, M. *et al.* Homeostatic NF-κB Signaling in Steady-State Migratory Dendritic Cells Regulates Immune Homeostasis and Tolerance. *Immunity* **42,** 627–639 (2015).

466. Reis e Sousa, C. Dendritic cells in a mature age. *Nat. Rev. Immunol.* **6,** 476–483 (2006).

467. Alegre, M.-L. L., Frauwirth, K. A. & Thompson, C. B. T-cell regulation by CD28 and CTLA-4. *Nat. Rev. Immunol.* **1,** 220–228 (2001).

468. Borst, J., Hendriks, J. & Xiao, Y. CD27 and CD70 in T cell and B cell activation. *Curr. Opin. Immunol.* **17,** 275–281 (2005).

469. Curtsinger, J. M., Lins, D. C. & Mescher, M. F. Signal 3 determines tolerance versus full activation of naive CD8 T cells: dissociating proliferation and development of effector function. *J. Exp. Med.* **197,** 1141–1151 (2003).

470. Spörri, R. & Reis e Sousa, C. Inflammatory mediators are insufficient for full dendritic cell activation and promote expansion of $CD4^+$ T cell populations lacking helper function. *Nat Immunol* **6,** 163–170 (2005).

471. Boon, T., Cerottini, J.-C. C., Van den Eynde, B., van der Bruggen, P. & Van Pel, A. Tumor antigens recognized by T lymphocytes. *Annu. Rev. Immunol.* **12,** 337–365 (1994).

472. Tumeh, P. C. *et al.* PD-1 blockade induces responses by inhibiting adaptive immune resistance. *Nature* **515,** 568–571 (2014).

473. Lauber, K. *et al.* Apoptotic cells induce migration of phagocytes via caspase-3-mediated release of a lipid attraction signal. *Cell* **113,** 717–730 (2003).

474. Elliott, M. R. *et al.* Nucleotides released by apoptotic cells act as a find-me signal to promote phagocytic clearance. *Nature* **461,** 282–286 (2009).

475. Schiraldi, M. *et al.* HMGB1 promotes recruitment of inflammatory cells to damaged tissues by forming a complex with CXCL12 and signaling via CXCR4. *Journal of Experimental Medicine* **209,** 551–563 (2012).

476. Poon, I. K. H., Lucas, C. D., Rossi, A. G. & Ravichandran, K. S. Apoptotic cell clearance: basic biology and therapeutic potential. *Nature Reviews Immunology* **14,** 166–180 (2014).

477. Dhodapkar, M. V., Dhodapkar, K. M. & Palucka, A. K. Interactions of tumor cells with dendritic cells: balancing immunity and tolerance. *Cell Death Differ.* **15,** 39–50 (2008).

478. Ishimoto, Y., Ohashi, K., Mizuno, K. & Nakano, T. Promotion of the uptake of PS liposomes and apoptotic cells by a product of growth arrest-specific gene, gas6. *J.*

Biochem. **127,** 411–417 (2000).

479. Ogden, C. A. *et al.* C1q and mannose binding lectin engagement of cell surface calreticulin and CD91 initiates macropinocytosis and uptake of apoptotic cells. *J. Exp. Med.* **194,** 781–795 (2001).

480. Harshyne, L. A., Zimmer, M. I., Watkins, S. C. & Barratt-Boyes, S. M. A role for class A scavenger receptor in dendritic cell nibbling from live cells. *J. Immunol.* **170,** 2302–2309 (2003).

481. Wolfers, J. *et al.* Tumor-derived exosomes are a source of shared tumor rejection antigens for CTL cross-priming. *Nat Med* **7,** 297–303 (2001).

482. Harshyne, L. A., Watkins, S. C., Gambotto, A. & Barratt-Boyes, S. M. Dendritic cells acquire antigens from live cells for cross-presentation to CTL. *J. Immunol.* **166,** 3717–3723 (2001).

483. Kroemer, G., Galluzzi, L., Kepp, O. & Zitvogel, L. Immunogenic cell death in cancer therapy. *Annu. Rev. Immunol.* **31,** 51–72 (2013).

484. Yatim, N., Cullen, S. & Albert, M. L. Dying cells actively regulate adaptive immune responses. *Nature Reviews Immunology* **17,** 262–275 (2017).

485. Verbovetski, I. *et al.* Opsonization of apoptotic cells by autologous iC3b facilitates clearance by immature dendritic cells, down-regulates DR and CD86, and up-regulates CC chemokine receptor 7. *J. Exp. Med.* **196,** 1553–1561 (2002).

486. Stuart, L. M. *et al.* Inhibitory effects of apoptotic cell ingestion upon endotoxin-driven myeloid dendritic cell maturation. *J. Immunol.* **168,** 1627–1635 (2002).

487. Fadok, V. A. *et al.* Macrophages that have ingested apoptotic cells *in vitro* inhibit proinflammatory cytokine production through autocrine/paracrine mechanisms involving TGF-beta, PGE2, and PAF. *J. Clin. Invest.* **101,** 890–898 (1998).

488. Behrens, E. M. *et al.* Complement receptor 3 ligation of dendritic cells suppresses their stimulatory capacity. *J. Immunol.* **178,** 6268–6279 (2007).

489. Sen, P. *et al.* Apoptotic cells induce Mer tyrosine kinase-dependent blockade of NF-kappaB activation in dendritic cells. *Blood* **109,** 653–660 (2007).

490. McGaha, T. L., Karlsson, M. C. I. & Ravetch, J. V. FcgammaRIIB deficiency leads to autoimmunity and a defective response to apoptosis in Mrl-MpJ mice. *J. Immunol.* **180,** 5670–5679 (2008).

491. Sims, G. P., Rowe, D. C., Rietdijk, S. T., Herbst, R. & Coyle, A. J. HMGB1 and RAGE in inflammation and cancer. *Annu. Rev. Immunol.* **28,** 367–388 (2010).

492. Scaffidi, P., Misteli, T. & Bianchi, M. E. Release of chromatin protein HMGB1 by necrotic cells triggers inflammation. *Nature* **418,** 191–195 (2002).

493. Kazama, H. *et al.* Induction of immunological tolerance by apoptotic cells requires

caspase-dependent oxidation of high-mobility group box-1 protein. *Immunity* **29,** 21–32 (2008).

494. White, M. J. *et al.* Apoptotic caspases suppress mtDNA-induced STING-mediated type I IFN production. *Cell* **159,** 1549–1562 (2014).

495. Rongvaux, A. *et al.* Apoptotic Caspases Prevent the Induction of Type I Interferons by Mitochondrial DNA. *Cell* **159,** 1563–1577 (2014).

496. Sauter, B. *et al.* Consequences of cell death: exposure to necrotic tumor cells, but not primary tissue cells or apoptotic cells, induces the maturation of immunostimulatory dendritic cells. *J. Exp. Med.* **191,** 423–434 (2000).

497. Tian, J. *et al.* Toll-like receptor 9-dependent activation by DNA-containing immune complexes is mediated by HMGB1 and RAGE. *Nat Immunol* **8,** 487–496 (2007).

498. Messmer, D. *et al.* High mobility group box protein 1: an endogenous signal for dendritic cell maturation and Th1 polarization. *J. Immunol.* **173,** 307–313 (2004).

499. Kim, T. S., Gorski, S. A., Hahn, S., Murphy, K. M. & Braciale, T. J. Distinct Dendritic Cell Subsets Dictate the Fate Decision between Effector and Memory $CD8^+$ T Cell Differentiation by a CD24-Dependent Mechanism. *Immunity* **40,** 400–413 (2014).

500. Shi, Y., Evans, J. E. & Rock, K. L. Molecular identification of a danger signal that alerts the immune system to dying cells. *Nature* **425,** 516–521 (2003).

501. Aaes, T. L. *et al.* Vaccination with Necroptotic Cancer Cells Induces Efficient Anti-tumor Immunity. *CellReports* **15,** 274–287 (2016).

502. Tesniere, A. *et al.* Molecular characteristics of immunogenic cancer cell death. *Cell Death Differ.* **15,** 3–12 (2008).

503. Albert, M. L., Sauter, B. & Bhardwaj, N. Dendritic cells acquire antigen from apoptotic cells and induce class I-restricted CTLs. *Nature* **392,** 86–89 (1998).

504. Turley, S., Poirot, L., Hattori, M., Benoist, C. & Mathis, D. Physiological beta cell death triggers priming of self-reactive T cells by dendritic cells in a type-1 diabetes model. *J. Exp. Med.* **198,** 1527–1537 (2003).

505. Scheffer, S. R. *et al.* Apoptotic, but not necrotic, tumor cell vaccines induce a potent immune response *in vivo*. *Int. J. Cancer* **103,** 205–211 (2003).

506. Obeid, M. *et al.* Calreticulin exposure is required for the immunogenicity of gamma-irradiation and UVC light-induced apoptosis. *Cell Death Differ.* **14,** 1848–1850 (2007).

507. Casares, N. *et al.* Caspase-dependent immunogenicity of doxorubicin-induced tumor cell death. *J. Exp. Med.* **202,** 1691–1701 (2005).

508. Michaud, M. *et al.* Autophagy-dependent anticancer immune responses induced by chemotherapeutic agents in mice. *Science* **334,** 1573–1577 (2011).

509. Thorburn, J. *et al.* Autophagy regulates selective HMGB1 release in tumor cells that are destined to die. *Cell Death Differ.* **16,** 175–183 (2009).

510. Ishii, K. J. *et al.* Genomic DNA released by dying cells induces the maturation of APCs. *J. Immunol.* **167,** 2602–2607 (2001).

511. Barber, G. N. STING: infection, inflammation and cancer. *Nature Reviews Immunology* **15,** 760–770 (2015).

512. Woo, S.-R. *et al.* STING-dependent cytosolic DNA sensing mediates innate immune recognition of immunogenic tumors. *Immunity* **41,** 830–842 (2014).

513. Fuertes, M. B. *et al.* Host type I IFN signals are required for antitumor $CD8^+$ T cell responses through $CD8\{alpha\}^+$ dendritic cells. *Journal of Experimental Medicine* **208,** 2005–2016 (2011).

514. Diamond, M. S. *et al.* Type I interferon is selectively required by dendritic cells for immune rejection of tumors. *Journal of Experimental Medicine* **208,** 1989–2003 (2011).

515. Deng, L. *et al.* STING-Dependent Cytosolic DNA Sensing Promotes Radiation-Induced Type I Interferon-Dependent Antitumor Immunity in Immunogenic Tumors. *Immunity* **41,** 843–852 (2014).

516. Demaria, S. *et al.* Immune-mediated inhibition of metastases after treatment with local radiation and CTLA-4 blockade in a mouse model of breast cancer. *Clin. Cancer Res.* **11,** 728–734 (2005).

517. Apetoh, L. *et al.* Toll-like receptor 4-dependent contribution of the immune system to anticancer chemotherapy and radiotherapy. *Nat Med* **13,** 1050–1059 (2007).

518. Tesniere, A. *et al.* Immunogenic death of colon cancer cells treated with oxaliplatin. *Oncogene* **29,** 482–491 (2010).

519. Vacchelli, E. *et al.* Loss-of-function alleles of P2RX7 and TLR4 fail to affect the response to chemotherapy in non-small cell lung cancer. *Oncoimmunology* **1,** 271–278 (2012).

520. Obeid, M. *et al.* Calreticulin exposure dictates the immunogenicity of cancer cell death. *Nat Med* **13,** 54–61 (2007).

521. Martins, I. *et al.* Chemotherapy induces ATP release from tumor cells. *Cell Cycle* **8,** 3723–3728 (2009).

522. Ghiringhelli, F. *et al.* Activation of the NLRP3 inflammasome in dendritic cells induces IL-1beta-dependent adaptive immunity against tumors. *Nat Med* **15,** 1170–1178 (2009).

523. Ahrens, S. *et al.* F-actin is an evolutionarily conserved damage-associated molecular pattern recognized by DNGR-1, a receptor for dead cells. *Immunity* **36,** 635–645 (2012).

524. Zhang, J.-G. *et al.* The Dendritic Cell Receptor Clec9A Binds Damaged Cells via

Exposed Actin Filaments. *Immunity* **36,** 646–657 (2012).

525. Sancho, D. *et al.* Identification of a dendritic cell receptor that couples sensing of necrosis to immunity. *Nature* **458,** 899–903 (2009).

526. Zelenay, S. *et al.* The dendritic cell receptor DNGR-1 controls endocytic handling of necrotic cell antigens to favor cross-priming of CTLs in virus-infected mice. *J. Clin. Invest.* **122,** 1615–1627 (2012).

527. Pawaria, S. & Binder, R. J. CD91-dependent programming of T-helper cell responses following heat shock protein immunization. *Nat Commun* **2,** 521 (2011).

528. Binder, R. J. & Srivastava, P. K. Peptides chaperoned by heat-shock proteins are a necessary and sufficient source of antigen in the cross-priming of $CD8^+$ T cells. *Nat Immunol* **6,** 593–599 (2005).

529. Yatim, N. *et al.* RIPK1 and NF-κB signaling in dying cells determines cross-priming of CD8 T cells. *Science* **350,** 328–334 (2015).

530. Fricke, I. & Gabrilovich, D. I. Dendritic cells and tumor microenvironment: a dangerous liaison. *Immunol. Invest.* **35,** 459–483 (2006).

531. Spranger, S., Bao, R. & Gajewski, T. F. Melanoma-intrinsic β-catenin signalling prevents anti-tumour immunity. *Nature* **523,** 231–235 (2015).

532. Ohm, J. E. *et al.* Effect of vascular endothelial growth factor and FLT3 ligand on dendritic cell generation *in vivo*. *J. Immunol.* **163,** 3260–3268 (1999).

533. Gabrilovich, D. I. *et al.* Production of vascular endothelial growth factor by human tumors inhibits the functional maturation of dendritic cells. *Nat Med* **2,** 1096–1103 (1996).

534. Roland, C. L. *et al.* Cytokine levels correlate with immune cell infiltration after anti-VEGF therapy in preclinical mouse models of breast cancer. *PLoS ONE* **4,** e7669 (2009).

535. Zong, J., Keskinov, A. A., Shurin, G. V. & Shurin, M. R. Tumor-derived factors modulating dendritic cell function. *Cancer Immunol. Immunother.* **65,** 821–833 (2016).

536. D'Souza-Schorey, C. & Clancy, J. W. Tumor-derived microvesicles: shedding light on novel microenvironment modulators and prospective cancer biomarkers. *Genes Dev.* **26,** 1287–1299 (2012).

537. Valenti, R. *et al.* Human tumor-released microvesicles promote the differentiation of myeloid cells with transforming growth factor-beta-mediated suppressive activity on T lymphocytes. *Cancer Res.* **66,** 9290–9298 (2006).

538. Ding, G. *et al.* Pancreatic cancer-derived exosomes transfer miRNAs to dendritic cells and inhibit RFXAP expression via miR-212-3p. *Oncotarget* **6,** 29877–29888 (2015).

539. Huang, S.-H., Li, Y., Zhang, J., Rong, J. & Ye, S. Epidermal growth factor receptor-containing exosomes induce tumor-specific regulatory T cells. *Cancer Invest.* **31,** 330–

335 (2013).

540. Yang, C., Kim, S.-H., Bianco, N. R. & Robbins, P. D. Tumor-derived exosomes confer antigen-specific immunosuppression in a murine delayed-type hypersensitivity model. *PLoS ONE* **6,** e22517 (2011).

541. Chiba, S. *et al.* Tumor-infiltrating DCs suppress nucleic acid-mediated innate immune responses through interactions between the receptor TIM-3 and the alarmin HMGB1. *Nat Immunol* **13,** 832–842 (2012).

542. Cubillos-Ruiz, J. R. *et al.* ER Stress Sensor XBP1 Controls Anti-tumor Immunity by Disrupting Dendritic Cell Homeostasis. *Cell* **161,** 1527–1538 (2015).

543. Herber, D. L. *et al.* Lipid accumulation and dendritic cell dysfunction in cancer. *Nat Med* **16,** 880–886 (2010).

544. Ramakrishnan, R. *et al.* Oxidized lipids block antigen cross-presentation by dendritic cells in cancer. *The Journal of Immunology* **192,** 2920–2931 (2014).

545. Tang, M. *et al.* Toll-like Receptor 2 Activation Promotes Tumor Dendritic Cell Dysfunction by Regulating IL-6 and IL-10 Receptor Signaling. *CellReports* **13,** 2851–2864 (2015).

546. Steinbrink, K., Wölfl, M., Jonuleit, H., Knop, J. & Enk, A. H. Induction of tolerance by IL-10-treated dendritic cells. *J. Immunol.* **159,** 4772–4780 (1997).

547. Sharma, S. *et al.* T cell-derived IL-10 promotes lung cancer growth by suppressing both T cell and APC function. *J. Immunol.* **163,** 5020–5028 (1999).

548. Steinbrink, K., Graulich, E., Kubsch, S., Knop, J. & Enk, A. H. CD4($^{+}$) and CD8($^{+}$) anergic T cells induced by interleukin-10-treated human dendritic cells display antigen-specific suppressor activity. *Blood* **99,** 2468–2476 (2002).

549. Koch, F. *et al.* High level IL-12 production by murine dendritic cells: upregulation via MHC class II and CD40 molecules and downregulation by IL-4 and IL-10. *J. Exp. Med.* **184,** 741–746 (1996).

550. Scarlett, U. K. *et al.* Ovarian cancer progression is controlled by phenotypic changes in dendritic cells. *Journal of Experimental Medicine* **209,** 495–506 (2012).

551. Vignali, D. A. A., Collison, L. W. & Workman, C. J. How regulatory T cells work. *Nature Reviews Immunology* **8,** 523–532 (2008).

552. Chen, J. *et al.* Strong adhesion by regulatory T cells induces dendritic cell cytoskeletal polarization and contact-dependent lethargy. *Journal of Experimental Medicine* **214,** 327–338 (2017).

553. Javia, L. R. & Rosenberg, S. A. $CD4^{+}CD25^{+}$ suppressor lymphocytes in the circulation of patients immunized against melanoma antigens. *J. Immunother.* **26,** 85–93 (2003).

554. Vence, L. *et al.* Circulating tumor antigen-specific regulatory T cells in patients with

metastatic melanoma. *Proceedings of the National Academy of Sciences* **104,** 20884–20889 (2007).

555. Curiel, T. J. *et al.* Specific recruitment of regulatory T cells in ovarian carcinoma fosters immune privilege and predicts reduced survival. *Nat Med* **10,** 942–949 (2004).

556. Kimpfler, S. *et al.* Skin melanoma development in ret transgenic mice despite the depletion of $CD25^{+}Foxp3^{+}$ regulatory T cells in lymphoid organs. *The Journal of Immunology* **183,** 6330–6337 (2009).

557. Bos, P. D., Plitas, G., Rudra, D., Lee, S. Y. & Rudensky, A. Y. Transient regulatory T cell ablation deters oncogene-driven breast cancer and enhances radiotherapy. *Journal of Experimental Medicine* **210,** 2435–2466 (2013).

558. Sato, E. *et al.* Intraepithelial $CD8^{+}$ tumor-infiltrating lymphocytes and a high $CD8^{+}$/regulatory T cell ratio are associated with favorable prognosis in ovarian cancer. *Proc. Natl. Acad. Sci. U.S.A.* **102,** 18538–18543 (2005).

559. Zhou, L. *et al.* TGF-beta-induced Foxp3 inhibits T(H)17 cell differentiation by antagonizing RORgammat function. *Nature* **453,** 236–240 (2008).

560. Marie, J. C., Letterio, J. J., Gavin, M. & Rudensky, A. Y. TGF-beta1 maintains suppressor function and Foxp3 expression in $CD4^{+}CD25^{+}$ regulatory T cells. *J. Exp. Med.* **201,** 1061–1067 (2005).

561. Bonasio, R. *et al.* Clonal deletion of thymocytes by circulating dendritic cells homing to the thymus. *Nat Immunol* **7,** 1092–1100 (2006).

562. Proietto, A. I. *et al.* Dendritic cells in the thymus contribute to T-regulatory cell induction. *Proceedings of the National Academy of Sciences* **105,** 19869–19874 (2008).

563. Rizvi, N. A. *et al.* Cancer immunology. Mutational landscape determines sensitivity to PD-1 blockade in non-small cell lung cancer. *Science* **348,** 124–128 (2015).

564. Van Allen, E. M. *et al.* Genomic correlates of response to CTLA-4 blockade in metastatic melanoma. *Science* **350,** 207–211 (2015).

565. Hugo, W. *et al.* Genomic and Transcriptomic Features of Response to Anti-PD-1 Therapy in Metastatic Melanoma. *Cell* **165,** 35–44 (2016).

566. Wargo, J. A., Reddy, S. M., Reuben, A. & Sharma, P. Monitoring immune responses in the tumor microenvironment. *Curr. Opin. Immunol.* **41,** 23–31 (2016).

567. Spranger, S. *et al.* Mechanism of tumor rejection with doublets of CTLA-4, PD-1/PD-L1, or IDO blockade involves restored IL-2 production and proliferation of $CD8(^{+})$ T cells directly within the tumor microenvironment. *J Immunother Cancer* **2,** 3 (2014).

568. Manfra, D. J. *et al.* Conditional expression of murine Flt3 ligand leads to expansion of multiple dendritic cell subsets in peripheral blood and tissues of transgenic mice. *J. Immunol.* **170,** 2843–2852 (2003).

569. Maraskovsky, E. *et al.* Dramatic increase in the numbers of functionally mature dendritic cells in Flt3 ligand-treated mice: multiple dendritic cell subpopulations identified. *J. Exp. Med.* **184,** 1953–1962 (1996).

570. Fong, L. *et al.* Altered peptide ligand vaccination with Flt3 ligand expanded dendritic cells for tumor immunotherapy. *Proc. Natl. Acad. Sci. U.S.A.* **98,** 8809–8814 (2001).

571. Curran, M. A., Montalvo, W., Yagita, H. & Allison, J. P. PD-1 and CTLA-4 combination blockade expands infiltrating T cells and reduces regulatory T and myeloid cells within B16 melanoma tumors. *Proceedings of the National Academy of Sciences* **107,** 4275–4280 (2010).

572. Ohkuri, T. *et al.* STING contributes to antiglioma immunity via triggering type I IFN signals in the tumor microenvironment. *Cancer Immunol Res* **2,** 1199–1208 (2014).

573. Zippelius, A., Schreiner, J., Herzig, P. & Müller, P. Induced PD-L1 expression mediates acquired resistance to agonistic anti-CD40 treatment. *Cancer Immunol Res* **3,** 236–244 (2015).

574. Carmi, Y. *et al.* Allogeneic IgG combined with dendritic cell stimuli induce antitumour T-cell immunity. *Nature* **521,** 99–104 (2015).

575. Carmi, Y. *et al.* Akt and SHP-1 are DC-intrinsic checkpoints for tumor immunity. *JCI Insight* **1,** e89020 (2016).

576. Vétizou, M. *et al.* Anticancer immunotherapy by CTLA-4 blockade relies on the gut microbiota. *Science* **350,** 1079–1084 (2015).

577. Sivan, A. *et al.* Commensal Bifidobacterium promotes antitumor immunity and facilitates anti-PD-L1 efficacy. *Science* **350,** 1084–1089 (2015).

578. Banchereau, J. & Palucka, A. K. Dendritic cells as therapeutic vaccines against cancer. *Nat. Rev. Immunol.* **5,** 296–306 (2005).

579. Palucka, K. & Banchereau, J. Cancer immunotherapy via dendritic cells. *Nat. Rev. Cancer* **12,** 265–277 (2012).

580. Garg, A. D., Coulie, P. G., Van den Eynde, B. J. & Agostinis, P. Integrating Next-Generation Dendritic Cell Vaccines into the Current Cancer Immunotherapy Landscape. *Trends Immunol.* (2017). doi:10.1016/j.it.2017.05.006

581. Carreno, B. M. *et al.* Cancer immunotherapy. A dendritic cell vaccine increases the breadth and diversity of melanoma neoantigen-specific T cells. *Science* **348,** 803–808 (2015).

582. Mitchell, D. A. *et al.* Tetanus toxoid and CCL3 improve dendritic cell vaccines in mice and glioblastoma patients. *Nature* **519,** 366–369 (2015).

583. Ries, C. H. *et al.* Targeting tumor-associated macrophages with anti-CSF-1R antibody reveals a strategy for cancer therapy. *Cancer Cell* **25,** 846–859 (2014).

584. De Henau, O. *et al.* Overcoming resistance to checkpoint blockade therapy by targeting PI3Kγ in myeloid cells. *Nature* **539,** 443–447 (2016).

585. Guerriero, J. L. *et al.* Class IIa HDAC inhibition reduces breast tumours and metastases through anti-tumour macrophages. *Nature* **543,** 428–432 (2017).

586. Girardi, M. *et al.* Regulation of cutaneous malignancy by gammadelta T cells. *Science* **294,** 605–609 (2001).

587. Shankaran, V. *et al.* IFNgamma and lymphocytes prevent primary tumour development and shape tumour immunogenicity. *Nature* **410,** 1107–1111 (2001).

588. Restifo, N. P., Dudley, M. E. & Rosenberg, S. A. Adoptive immunotherapy for cancer: harnessing the T cell response. *Nature Reviews Immunology* **12,** 269–281 (2012).

589. Mellman, I., Coukos, G. & Dranoff, G. Cancer immunotherapy comes of age. *Nature* **480,** 480–489 (2011).

590. Topalian, S. L., Drake, C. G. & Pardoll, D. M. Immune checkpoint blockade: a common denominator approach to cancer therapy. *Cancer Cell* **27,** 450–461 (2015).

591. Sagiv-Barfi, I. *et al.* Therapeutic antitumor immunity by checkpoint blockade is enhanced by ibrutinib, an inhibitor of both BTK and ITK. *Proceedings of the National Academy of Sciences* **112,** E966–72 (2015).

592. Behrens, G. *et al.* Helper T cells, dendritic cells and CTL Immunity. *Immunol. Cell Biol.* **82,** 84–90 (2004).

593. Knutson, K. L. & Disis, M. L. Tumor antigen-specific T helper cells in cancer immunity and immunotherapy. *Cancer Immunol. Immunother.* **54,** 721–728 (2005).

594. Corthay, A. *et al.* Primary antitumor immune response mediated by $CD4^+$ T cells. *Immunity* **22,** 371–383 (2005).

595. Haabeth, O. A. W. *et al.* Inflammation driven by tumour-specific Th1 cells protects against B-cell cancer. *Nat Commun* **2,** 240 (2011).

596. Muranski, P. & Restifo, N. P. Adoptive immunotherapy of cancer using $CD4(^+)$ T cells. *Curr. Opin. Immunol.* **21,** 200–208 (2009).

597. Quezada, S. A. *et al.* Tumor-reactive $CD4(^+)$ T cells develop cytotoxic activity and eradicate large established melanoma after transfer into lymphopenic hosts. *Journal of Experimental Medicine* **207,** 637–650 (2010).

598. Wei, S. C. *et al.* Distinct Cellular Mechanisms Underlie Anti-CTLA-4 and Anti-PD-1 Checkpoint Blockade. *Cell* **170,** 1120–1133.e17 (2017).

599. Haley, K. *et al.* Langerhans cells require MyD88-dependent signals for Candida albicans response but not for contact hypersensitivity or migration. *The Journal of Immunology* **188,** 4334–4339 (2012).

600. Nirschl, C. J. *et al.* IFNγ-Dependent Tissue-Immune Homeostasis Is Co-opted in the Tumor Microenvironment. *Cell* **170,** 127–141.e15 (2017).

601. Lu, E., Dang, E. V., McDonald, J. G. & Cyster, J. G. Distinct oxysterol requirements for positioning naïve and activated dendritic cells in the spleen. *Sci Immunol* **2,** eaal5237 (2017).

602. Zhou, Q., Hao, L., Huang, W. & Cai, Z. The Golgi-Associated Plant Pathogenesis-Related Protein GAPR-1 Enhances Type I Interferon Signaling Pathway in Response to Toll-Like Receptor 4. *Inflammation* **39,** 706–717 (2016).

603. Desai, T. M. *et al.* IFITM3 restricts influenza A virus entry by blocking the formation of fusion pores following virus-endosome hemifusion. *PLoS Pathog.* **10,** e1004048 (2014).

604. Sadler, A. J. & Williams, B. R. G. Interferon-inducible antiviral effectors. *Nature Reviews Immunology* **8,** 559–568 (2008).

605. Shoji-Kawata, S. *et al.* Identification of a candidate therapeutic autophagy-inducing peptide. *Nature* **494,** 201–206 (2013).

606. Williams, J. W. *et al.* Transcription factor IRF4 drives dendritic cells to promote Th2 differentiation. *Nat Commun* **4,** 2990 (2013).

607. Zhan, Y. *et al.* GM-CSF increases cross-presentation and CD103 expression by mouse CD8 spleen dendritic cells. *Eur. J. Immunol.* **41,** 2585–2595 (2011).

608. Soares, H. *et al.* A subset of dendritic cells induces $CD4^+$ T cells to produce IFN-gamma by an IL-12-independent but CD70-dependent mechanism *in vivo*. *J. Exp. Med.* **204,** 1095–1106 (2007).

609. Willoughby, J. E. *et al.* Differential impact of CD27 and 4-1BB costimulation on effector and memory CD8 T cell generation following peptide immunization. *The Journal of Immunology* **193,** 244–251 (2014).

610. Barnden, M. J., Allison, J., Heath, W. R. & Carbone, F. R. Defective TCR expression in transgenic mice constructed using cDNA-based alpha- and beta-chain genes under the control of heterologous regulatory elements. *Immunol. Cell Biol.* **76,** 34–40 (1998).

611. Yamazaki, C. *et al.* Critical roles of a dendritic cell subset expressing a chemokine receptor, XCR1. *The Journal of Immunology* **190,** 6071–6082 (2013).

612. Caton, M. L., Smith-Raska, M. R. & Reizis, B. Notch-RBP-J signaling controls the homeostasis of CD8- dendritic cells in the spleen. *J. Exp. Med.* **204,** 1653–1664 (2007).

613. Diehl, G. E. *et al.* Microbiota restricts trafficking of bacteria to mesenteric lymph nodes by CX(3)CR1(hi) cells. *Nature* **494,** 116–120 (2013).

614. Klein, U. *et al.* Transcription factor IRF4 controls plasma cell differentiation and class-switch recombination. *Nat Immunol* **7,** 773–782 (2006).

615. Förster, R. *et al.* CCR7 coordinates the primary immune response by establishing

functional microenvironments in secondary lymphoid organs. *Cell* **99,** 23–33 (1999).

616. Nakano, H. *et al.* Migratory properties of pulmonary dendritic cells are determined by their developmental lineage. *Mucosal Immunol* **6,** 678–691 (2013).

617. Stranges, P. B. *et al.* Elimination of antigen-presenting cells and autoreactive T cells by Fas contributes to prevention of autoimmunity. *Immunity* **26,** 629–641 (2007).

618. Dranoff, G. *et al.* Vaccination with irradiated tumor cells engineered to secrete murine granulocyte-macrophage colony-stimulating factor stimulates potent, specific, and long-lasting anti-tumor immunity. *Proc. Natl. Acad. Sci. U.S.A.* **90,** 3539–3543 (1993).

619. Curran, M. A. & Allison, J. P. Tumor vaccines expressing flt3 ligand synergize with ctla-4 blockade to reject preimplanted tumors. *Cancer Res.* **69,** 7747–7755 (2009).

620. Dobin, A. *et al.* STAR: ultrafast universal RNA-seq aligner. *Bioinformatics* **29,** 15–21 (2013).

621. Satija, R., Farrell, J. A., Gennert, D., Schier, A. F. & Regev, A. Spatial reconstruction of single-cell gene expression data. *Nat. Biotechnol.* **33,** 495–502 (2015).

622. Macosko, E. Z. *et al.* Highly Parallel Genome-wide Expression Profiling of Individual Cells Using Nanoliter Droplets. *Cell* **161,** 1202–1214 (2015).

623. Kowalczyk, M. S. *et al.* Single-cell RNA-seq reveals changes in cell cycle and differentiation programs upon aging of hematopoietic stem cells. *Genome Res.* **25,** 1860–1872 (2015).

624. Heng, T. S. P., Painter, M. W.Immunological Genome Project Consortium. The Immunological Genome Project: networks of gene expression in immune cells. *Nat Immunol* **9,** 1091–1094 (2008).

625. Ritchie, M. E. *et al.* limma powers differential expression analyses for RNA-sequencing and microarray studies. *Nucleic Acids Res.* **43,** e47 (2015).

626. Benjamini, Y. & Hochberg, Y. Controlling the false discovery rate: a practical and powerful approach to multiple testing. *Journal of the Royal Statistical Society, Series B* **57,** 289–300 (2017).

Publishing Agreement

It is the policy of the University to encourage the distribution of all theses, dissertations, and manuscripts. Copies of all UCSF theses, dissertations, and manuscripts will be routed to the library via the Graduate Division. The library will make all theses, dissertations, and manuscripts accessible to the public and will preserve these to the best of their abilities, in perpetuity.

Please sign the following statement:

I hereby grant permission to the Graduate Division of the University of California, San Francisco to release copies of my thesis, dissertation, or manuscript to the Campus Library to provide access and preservation, in whole or in part, in perpetuity.

Author Signature

12/21/17

Date